Synthetic Modification of the Natural Pyrethrins

Todd E. Markham

B. Sc. (Forensic and Analytical Science) (Honours)

A thesis submitted in fulfilment of the requirements for the degree of

Doctor of Philosophy (Ph.D.)

College of Science and Engineering

Flinders University, Australia

July 2021

Table of Contents

Summary

Pyrethrum is derived from *Tanacetum cinerariifolium* (Pyrethrum daisies) and has been used extensively as an insect control agent both domestically and agriculturally for many years. This natural extract is comprised of the Pyrethrins **5-7**, six structurally related esters that impart the concentrate with its insecticidal properties. Whilst the Pyrethrum extract has long served as an insecticidal agent for its many beneficial characteristics like broad spectrum activity, low toxicity and low environmental impact, it suffers from a lack of long term stability due to the readiness of the Pyrethrins **5-7** to undergo degradation by a number of pathways. Although there are measures in place to limit this degradation, there remains a need to further limit or prevent these degradative processes leading to pyrethrin losses. Due to this, the work described in this thesis has pursued the direct synthetic modification of the naturally derived Pyrethrins **5-7** as a potential means of stabilising the insecticidal esters whilst retaining their advantageous qualities.

Pyrethrins I **5a** and II **5b** make up over 50% of the pyrethrin content in Pyrethrum however, they are the most susceptible of the six Pyrethrins **5-7** to degradation particularly about the pentadienyl side chain. Two of the minor Pyrethrins, the jasmolins **7**, differ from the pyrethrins **5** by a single point of saturation and as such may be accessed through reduction of the terminal double bond. Chapter 2 details the exploration into the reduction chemistry of the pyrethrins **5** in a bid to elicit the transformation into their more stable jasmolin counterparts **7** (Figure 1). As a result, a number of reduced pyrethrin analogues were prepared by several common reductive pathways and the desired transformation to the jasmolins **7** was successful with their isolation as a mixture with the corresponding tetrahydropyrethrins **53**.

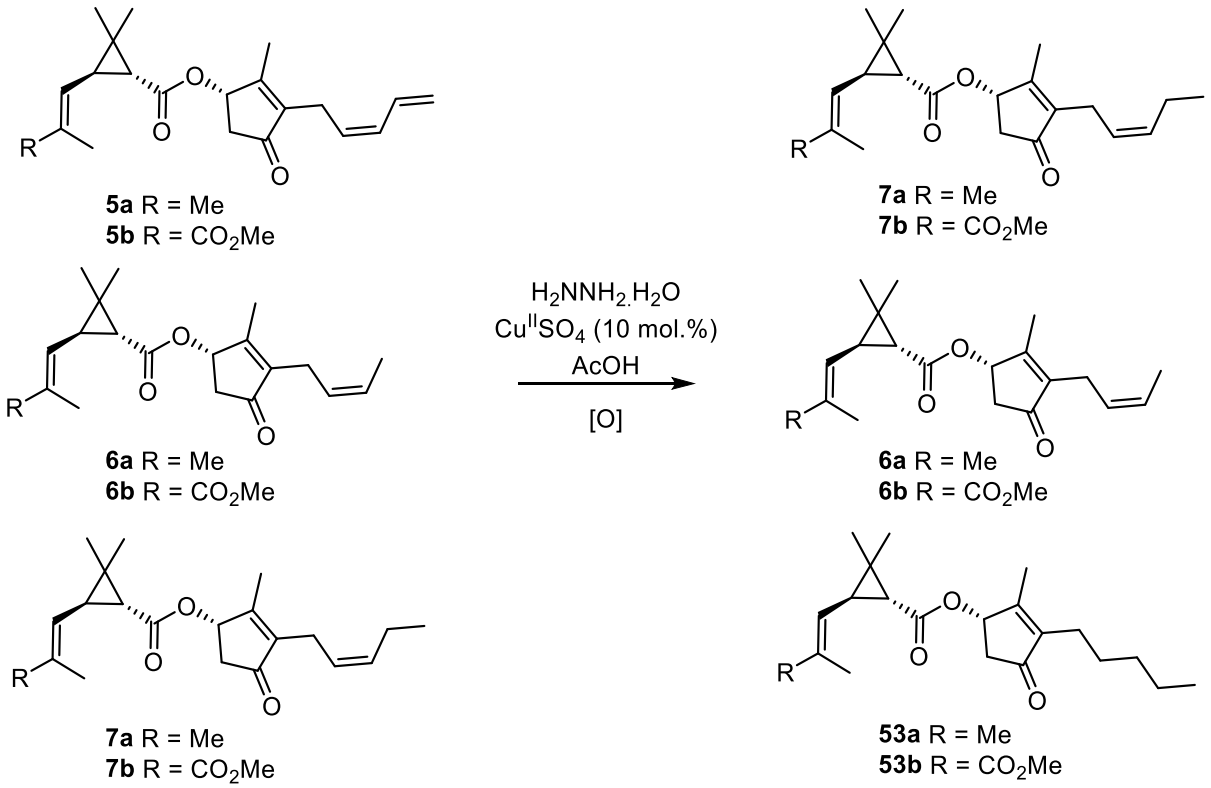

Figure 1: Selective reduction of the pyrethrins **5** in the pyrethrum concentrate to their jasmolins **7** and tetrahydropyrethrins **53** counterparts.

With the rethrolone moiety of the pyrethrins **5** containing a pentadienyl chain, its applicability in Diels-Alder cycloadditions was explored as highlighted in Chapter 3. Whilst the *cis*-geometry of the natural pyrethrins **5** was found to be inactive in the normal electron demand Diels-Alder reaction, it was found there is precedent for the *trans*-isomer **34** to take part. Alternatively, the inverse electron demand Diels-Alder reaction could be applied with the pyrethrins **5** acting as dienophile and electron-deficient tetrazines serving as dienes (Figure 2).

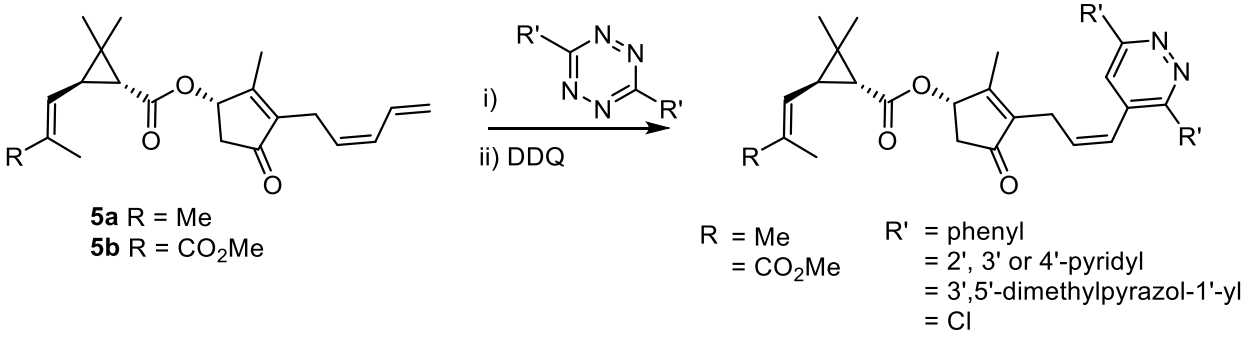

Figure 2: Inverse electron demand Diels-Alder cycloaddition reaction of the pyrethrins **5** with a range of 3,6-disubstituted-1,2,4,5-tetrazines.

In addition, the alkenes within the pyrethrin scaffold were of particular interest for application in palladium-catalysed cross coupling, specifically Heck reactions. Ultimately, a protocol was developed for the site-selective coupling of the terminal double bond in the pyrethrins **5** to aryl iodides (Figure 3), detailed in Chapter 4. The resulting products were the *E*-isomer and the migration isomer of the terminally arylated product with distribution of the two dependent on the electronic properties of the aromatic coupling partner.

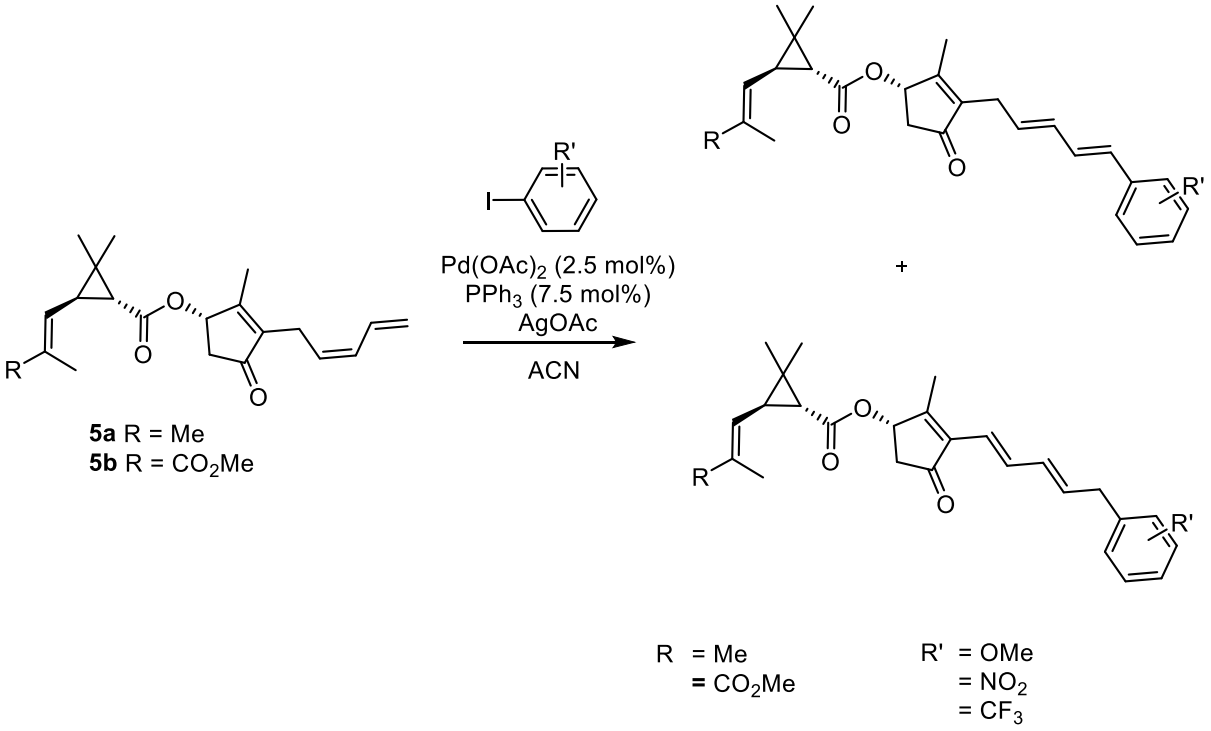

Figure 3: Terminal arylation of the pyrethrins **5** by palladium-catalysed Heck reaction with aryl iodides.

Finally, Chapter 5 details attempts to produce racemic (*Z*)-pyrethrolone **21**, the rethrolone moiety of the pyrethrins **5**, for its potential in gaining further insight into the reactivity and degradative properties of the more prominent of the Pyrethrin esters **5-7**. As a result, racemic (*Z*)-pyrethrolone **21** could be prepared as a mixture with its precursor **155** over a series of five synthetic steps in a yield of 11% as determined by ^{1}H NMR analysis (Figure 4).

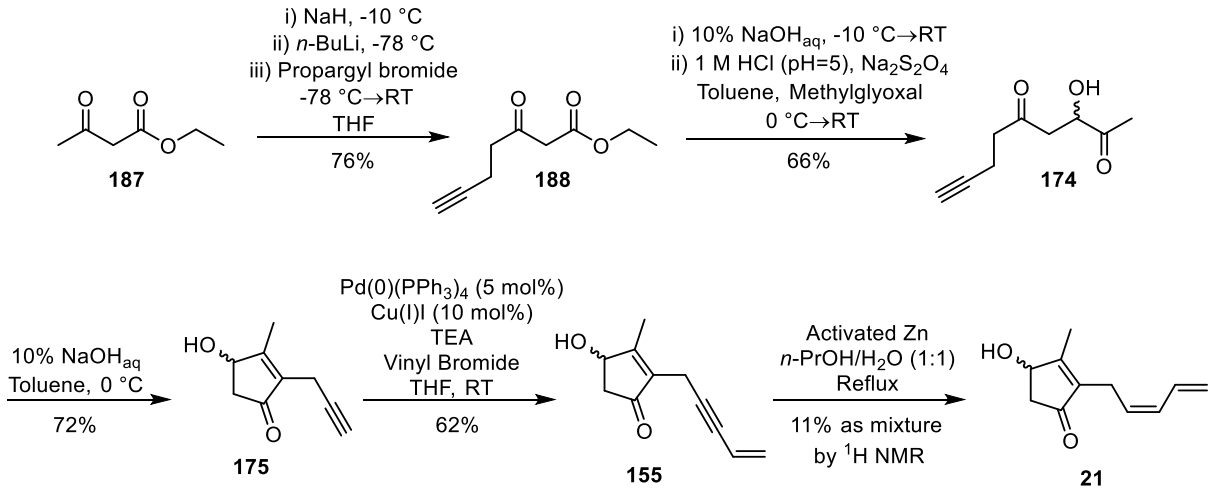

Figure 4: Synthesis of racemic (*Z*)-pyrethrolone **21** from ethyl acetoacetate **187** over five steps.

Declaration

I certify that this thesis does not incorporate without acknowledgment any material previously submitted for a degree or diploma in any university; and that to the best of my knowledge and belief it does not contain any material previously published or written by another person except where due reference is made in the text.

Todd E. Markham

18th February 2021

Publications and Presentations

Publications

1. Markham, T. E.; Kotze, A. C.; Duggan, P. J.; Johnston, M. R., Exploration of the Reduction Chemistry of Natural Pyrethrins and the Insecticidal Activity of the Isolated Reduction Products. *Aust. J. Chem*. **Online Early**. doi: 10.1071/CH20302

Presentations

1. Markham, T., Freemont, J. A., Littler, S. W., Mauger, S., Ryan, J. H., Johnston, M. & Duggan, P. J. The Oxidation and Reduction Chemistry of Pyrethrins. *Organic18.* UWA, Perth, Western Australia. 2nd-6th Dec. **2018**.
2. Markham, T., Johnston, M. R. & Duggan, P. J. Selective Modification of Natural Pyrethrins. *Organic18.* UWA, Perth, Western Australia. 2nd-6th Dec. **2018**. Poster presentation.
3. Markham, T. E.; Kotze, A. C.; Duggan, P. J.; Johnston, M. R. Exploration of the Reduction Chemistry of Natural Pyrethrins and the Insecticidal Activity of the Isolated Reduction Products. RACI Natural Products Symposium, Charles Sturt University, Wagga Wagga. 4th Oct. **2019**.
4. Markham, T. E.; Kotze, A. C.; Duggan, P. J.; Johnston, M. R. From Pyrethrin to Jasmolin: Exploring the Reduction Chemistry of the Natural Pyrethrins. SA RACI Synthesis Symposium, Flinders University, South Australia, 9th Dec. **2019**.

Acknowledgements

Firstly, I would like to thank my supervisors Martin Johnston and Peter Duggan for giving me the opportunity to work on this great but definitely challenging project. Despite the rollercoaster of trials and tribulations, I have genuinely loved the challenge that went hand in hand with this work. I am grateful for all of your input and advice along the way, without it who knows what could have happened. Martin, thank you for sharing your knowledge, particularly with the NMR, and dealing with me day to day. Peter, your input and editing has made me a better scientist.

Of course, thanks must go to the organisations and people who made this project possible. A big thanks to the CSIRO and Botanical Resources Australia (BRA) for generously providing the funding and Pyrethrins needed for this project. Both these organisations were also kind enough to allow me to visit and give research seminars. Helen Faber at BRA, thank you for bringing me over and allowing me to see the ins and outs of what goes on with pyrethrum production. My thanks must also go to Flinders University for providing me with the money to get through these last few years with the award of a Flinders University Research Scholarship.

Several people provided analyses, assistance with instruments and general insight in this project that were instrumental in getting some of this work off the ground. Andrew Kotze at CSIRO Agriculture and Food was kind enough to do all of the insecticidal activity testing of the nearly 50-odd compounds we made, thank you for all of your hard work! Thanks to Marc McEwan at CSIRO Manufacturing for running UPCC and LC-MS for some of our reduction compounds. Flinders Analytical, specifically Jason Young and Russell Fuller, for helping out with HRMS, the DSA can truly be a pain. A big thanks to Jason Smith at the University of Tasmania for insight into diimide reductions.

The greatest thanks go to the people who attempted to keep me sane throughout this wild ride. The Johnston research group: Emma Kent, Jordan Spangler, Josh Gerbhardt and James Tsoukalas. All of you made each day worth coming into the lab and we definitely kept things interesting to say the least. The “team”: Sam Pandelus, Kyle Farrell and Ruby Sims, you all kept me going with the antics and drama (of which I provided the most of).

Finally, thanks to my family and friends for being patient and understanding the huge amount of stress the whole thing put on me. You all offered the refreshing break away from all things

chemistry and always just at the right time. Special mention to my housemate and friend Janessa for being so tolerant and dealing with my regular mental breakdowns.

List of Abbreviations

[O]	Oxidation
9-BBN	9-borabicyclo[3.3.1]nonane
Ac_2O	Acetic anhydride
ACN	Acetonitrile
AcOH	Acetic acid
AgOAc	Silver(I) acetate
AOC	Allene oxide cyclase
AOS	Allene oxide synthase
APCI	Atmospheric pressure chemical ionisation
Ar	Aryl
BHT	Butylated hydroxytoluene
BRA	Botanical Resources Australia
brs	Broad singlet
CDP	Chrysanthemyl diphosphate
COSY	Correlation spectroscopy
CSIRO	Commonwealth Scientific and Industrial Research Organisation
d	Doublet
DCM	Dichloromethane
DCVC	Dry column vacuum chromatography
DDQ	2,3-dichloro-5,6-dicyano-1,4-benzoquinione
DDT	Dichlorodiphenyltrichloroethane
DDVP	2,2-dichlorovinyl dimethylphosphate
DFT	Density functional theory
DMAD	Dimethylacetylene dicarboxylate
DMAPP	Dimethylallyl pyrophosphate
DMF	*N,N*-dimethylformamide
DMSO	Dimethyl sulfoxide
dr	Diastereomeric ratio
DXP	1-deoxy-D-xylulose 5-phosphate
EDG	Electron donating group

Et	Ethyl
EtOAc	Ethyl acetate
EWG	Electron withdrawing group
eq	Equivalent
FTIR	Fourier transform infrared spectroscopy
GCMS	Gas chromatography mass spectrometry
GLIP	GDSL lipase-like protein
HAT	Hydrogen atom transfer
HDMS	High definition mass spectrometer
Hex	Hexyl
HMBC	Heteronuclear multibond correlation spectroscopy
HOMO	Highest occupied molecular orbital
HPLC	High performance liquid chromatography
HRMS	High resolution mass spectrometry
HSQC	Heteronuclear single quantum correlation spectroscopy
IC50	Half maximal Inhibitory concentration
IEDDA	Inverse electron demand Diels-Alder
J	Coupling constant
LA	Lewis acid
LC-MS	Liquid chromatography-mass spectrometry
LOX	lipoxygenase
LUMO	Lowest unoccupied molecular orbital
MeOH	Methanol
n-BuLi	*n*-butyllithium
NHOMO	Next-highest occupied molecular orbital
NMR	Nuclear magnetic resonance
nOe	Nuclear Overhauser effect
NOESY	Nuclear Overhauser effect spectroscopy
n-PrOH	*n*-propanol
OPR	*cis*-(+)-12-oxo-phytodienoic acid reductase
$Pd(PPh_3)_4$	Tetrakis(triphenylphosphine)palladium(0)

$Pd(OAc)_2$	Palladium(II) acetate
Pd/C	Palladium on carbon
Pd_2dba_3	Tris(dibenzylideneacetone)dipalladium(0)
Pd-H	Palladium hydride
PPh_3	Triphenylphosphine
PTAD	4-phenyl-1,2,4-triazole-3,5-dione
q	Quartet
quin	Quintet
RT	Room temperature
s	Singlet
SE	Standard error
SLUMO	Second-lowest unoccupied molecular orbital
t	Triplet
TCCA	Trichloroisocyanuric acid
TEA	Triethylamine
THF	Tetrahydrofuran
TLC	Thin layer chromatography
TOCSY	Total correlation spectroscopy
Ts	Tosyl
UPCC	Ultra performance convergence chromatography
UV	Ultraviolet

Chapter 1 Introduction

1.1 A brief history of insecticides

Insecticides have long been an invaluable staple in both the agricultural and domestic sectors for the control of, and protection from, a wide range of pest insect species. Pest control has been an ongoing problem for centuries with the early use of pyrethrum, a plant product with insecticidal and repellent properties, dating back to ancient China.[1] Other naturally occurring materials were popular until the 19th century, when many arsenic-containing compounds like lead arsenate ($PbHAsO_4$) and Paris Green ($Cu(AcO)_2.3Cu(AsO_2)_2$) were integrated into widespread use. Whilst effective, these materials proved to be highly toxic to humans and were found to persist within the vegetation they were applied to, including fruits and vegetables. The incredible health risk posed by these arsenical insecticides led to the development and application of alternative insecticides. Many classes of insecticide arose and continue to be used in agricultural and domestic applications, with the major classes shown below (Figure 1.1). The initial replacement of these arsenic-containing insecticides was dichlorodiphenyltrichloroethane (DDT) **1** (Figure 1.1A), the most notable member of the organochloride insecticide class.[2]

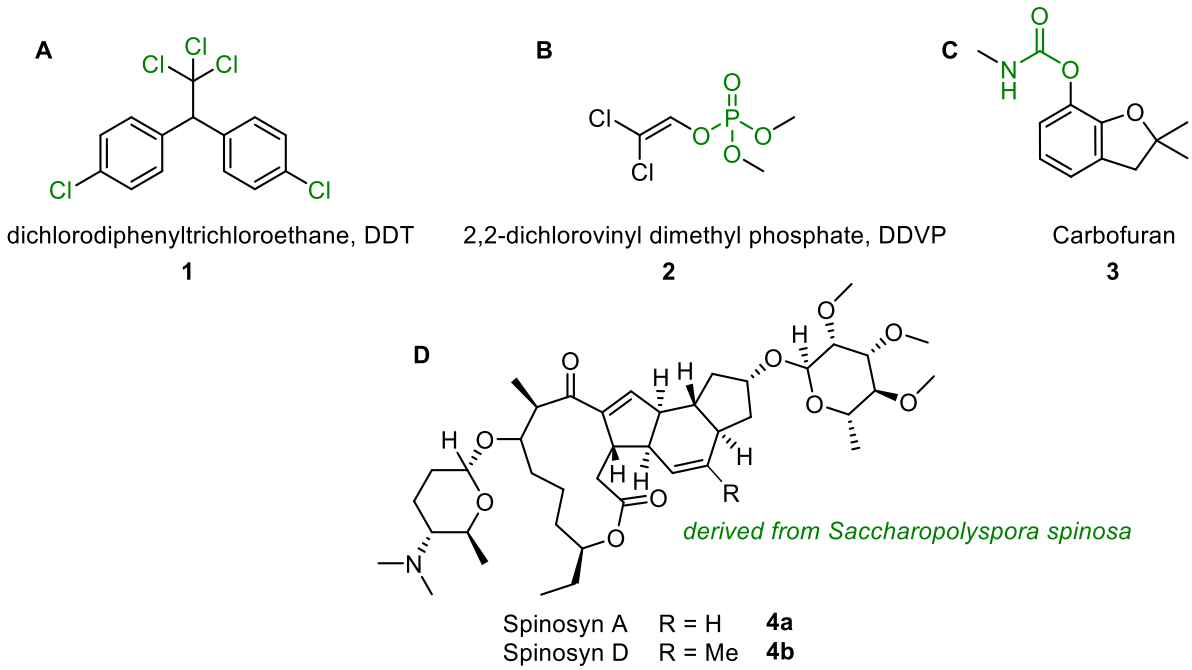

Figure 1.1: Examples of the major classes of insecticides: DDT **1**, an organochloride **(A)**; DDVP **2**, an organophosphate **(B)**; Carbofuran **3**, a carbamate **(C)**; Spinosyn A **4**, a natural product **(D)**. Main functional groups highlighted in green.

The effectiveness of DDT **1** led to its prevalent use throughout the late 19th and early 20th century but its toxicity extended beyond the insect targets into groups of non-target organisms including, but not limited to, birds and reptiles.[1, 3] Another major issue associated with DDT **1** was its ability to bioaccumulate, particularly in aquatic organisms, ultimately having a detrimental effect on organisms higher in the food chain, including humans.[4] The extreme toxicity of DDT **1** to wildlife and human health, as well as its persistence in the environment led to its worldwide ban in 2004 and prompted further development of new insecticides for its replacement in extensive pest control.[3] Organophosphates, like 2,2-dichlorovinyl dimethyl phosphate (DDVP) **2** (Figure 1.1B), and carbamates, like carbofuran **3** (Figure 1.1C), were developed in the latter half of the 1900s and still see continued use today. However, organophosphates like their organochloride equivalents have high toxicity, particularly with chronic exposure, and carbamates have been shown to affect human health through their binding to melatonin receptors.[5, 6] The adverse effect of these insecticidal agents on human health and their environmental impact causes their use to be undesirable making the naturally derived insecticides far more attractive.

Natural insecticides (Figure 1.1D) overcome the many challenges associated with the above synthetic insecticides, particularly the high toxicity and bioaccumulative effects, with botanical extracts such as neem and spinosad seeing widespread use in pest control.[7, 8] In detail, neem oil is derived from *Azadirachta indica* and contains a substantial amount of biologically active compounds. Of these compounds, the limonoids serve as the primary insecticidally active agents which present little toxicity to humans with the oil extract being used in traditional medicine and cosmetics.[7] In addition, spinosad is a mixture of two natural products, known as the spinosyns, derived from the soil bacteria *Saccaropolyspora spinosa*, in contrast to the botanical source of both neem and pyrethrum. Spinosyn A **4a** (Figure 1.1D) is the major constituent of the spinosad mixture whilst spinosyn D is the minor component. Unfortunately, the increased use of spinosad since its introduction has led to a number of cases of resistance.[8] Alternatively, a range of other naturally occurring classes of compounds have been utilised in the control of pest insect species including, but not limited to, bacterially derived macrocyclic lactones and other botanical extracts like rotenone derived from a series of tropical plant species.[1] Notably, the pyrethrum extract sees continued and more prevalent

use globally due to its broader spectrum of activity, prevailing absence of toxicity and, lack of environmental persistence.[9, 10]

1.2 Pyrethrum and its constituents

Pyrethrum has been used for centuries where dried flower heads were used as an early insect repellent with subsequent development of an insecticide made by grinding these dried flowers.[1] Importantly, the pyrethrum concentrate derives its insecticidal characteristics from six structurally-related esters commonly known as the Pyrethrins* (Figure 1.2). However, the identity of these compounds instilling the insecticidal activity to this naturally derived material were not elucidated until the early 1900s, well after its widespread use.

1.2.1 Discovery of the Pyrethrins

Early in the 20th century it was found that the activity of the pyrethrum extract was in fact due to an ester-containing compound however, the complete identity remained unknown until the mid-1920s.[11-13] In 1924, Staudinger and Ruzicka proposed that the activity was due to a mixture of two esters, pyrethrins I **5a** and II **5b** (Figure 1.2), of which they assigned structures and stereochemistry,[14] later revised to the well-known pyrethrin scaffold.[15] Notably, the stereochemical aspects were not completely assigned until the mid-1950s with final confirmation by X-ray crystallography, of their dinitrophenyhydrazone derivatives, not established until 1972.[16]

*The informal naming convention in the pyrethrin field can be confusing. Notably, the six esters as a collective are known as the Pyrethrins with two subsets known as Pyrethrins I and Pyrethrins II. In addition, two of the individual esters are also known as pyrethrins, namely pyrethrin I **5a** and pyrethrin II **5b**. As such, throughout this thesis the groups of compounds are referred to by capitals (i.e. Pyrethrins) whilst the individual esters are not (e.g. pyrethrin I).

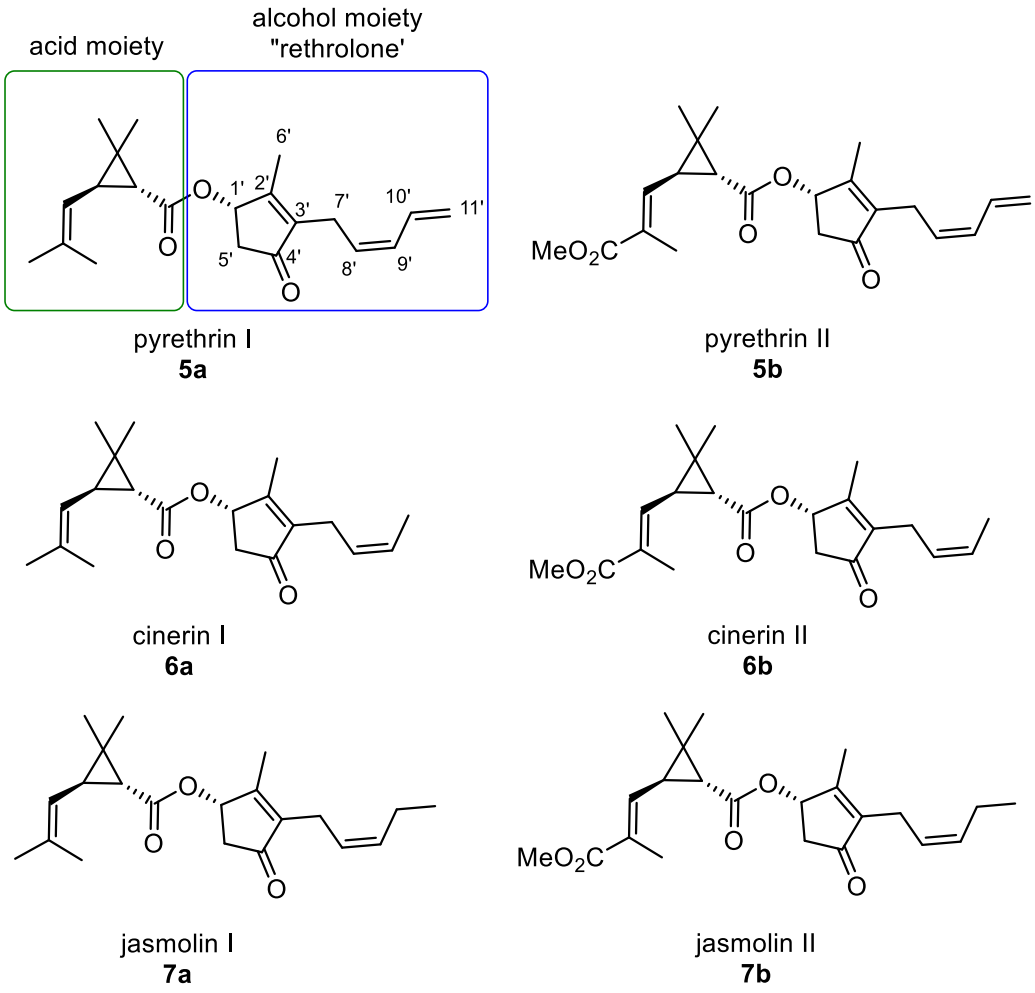

Figure 1.2: The six natural Pyrethrins **5-7** that make up the pyrethrum concentrate. Key atomic numbering of the alcohol moiety is also shown on pyrethrin I **5a**.

Ultimately, the alcohol component, more commonly referred to as the rethrolone (Figure 1.2), was isolated and characterised through its semicarbazone giving the pyrethrin structure. The underivatised rethrolone moiety itself interfered in the correct identification of these structures due to the complexity and reactivity of the enone component of these alcohols. Specifically, whilst the alkaline hydrolysis undertaken on the esters can easily liberate the acid portions of pyrethrins I **5a** and II **5b**, chrysanthemic **14a** and pyrethric **14b** acid respectively, it was found to cause the ready degradation of the alcohol moiety.[14, 15, 17, 18] Later, the extract was found to contain a further four esters contributing to its biological activity albeit in much lower proportions to the originally discovered pyrethrins **5**.

In the 1940s, LaForge and Barthel identified two of these additional esters in the pyrethrum concentrate. These were identified as cinerins I **6a** and II **6b** (Figure 1.2), where the carbon

side chain of the alcohol moiety was shorter, lacking the terminal unsaturated carbon unit.[19-21] The jasmolins **7** (Figure 1.2), the last two of the six esters, were not identified until the late 1960s by Godin as another pair of minor constituents. Much like the cinerins **6**, the difference from the pyrethrins **5** was once again a result of the alcohol side chain, where the number of carbons remained the same as the pyrethrins **5** but the terminal position was saturated.[22] Notably, all six of the Pyrethrin esters **5-7** contain a *cis*-alkene in the linear side chain with the major point of difference resulting from the terminus of this moiety.

The structural differences in these six insecticidal esters can serve as a means of categorisation with their acid moiety giving rise to two subsets namely Pyrethrins I **5a-7a** and Pyrethrins II **5b-7b**; with chrysanthemic acid **14a** giving Pyrethrins I **5a-7a** and pyrethric acid **14b** giving Pyrethrins II **5b-7b**. In conjunction, the cyclopentenone alcohol (or rethrolone) moiety defines the individual esters with; pyrethrolone **21** giving pyrethrin I **5a** and II **5b**, cinerolone **22** giving cinerin I **6a** and II **6b** and, jasmolone **20** giving jasmolin I **7a** and II **7b.**[23, 24] These subtleties in the side-chain of the rethrolone significantly alter the bioactivity, reactivity and the stability of the pyrethrin structure. Importantly, these insecticidal esters are secondary metabolites of the plants they can be extracted from, serving as a defense mechanism against herbivorous insects.

1.2.2 Biosynthesis and purpose of the Pyrethrins

The Pyrethrins **5-7** are most prominently isolated from *Tanacetum cinerariifolium*, more commonly known as pyrethrum daisies, which are farmed for the industrial extraction of pyrethrum concentrate for use in commercial insecticide formulations. As these esters are secondary metabolites of the plant, they are biosynthetically prepared through the independent synthesis of both the chrysanthemate and rethrolone moieties which then undergo an esterification to give the appropriate pyrethrin. Though many of the intricacies associated with these biosynthetic pathways have not yet been completely identified, a large number of the intermediates have been characterised and the pathways for their production proposed. The chrysanthemic acid **14** used in the construction of the Pyrethrins **5-7** is a monoterpene and as such its biosynthesis starts *via* well-known biosynthetic pathways (Scheme 1.1).

Specifically, the major pathway (Scheme 1.1A) proceeds initially by a condensation of pyruvic acid **8** with glyceraldehyde-3-phosphate **9** catalysed by 1-deoxy-D-xylulose 5-phosphate

synthase (DXP-synthase) giving 1-deoxy-D-xylulose 5-phosphate (DXP) **10**.[27] This is then used to produce a typical terpene starting material in the form of dimethylallyl pyrophosphate (DMAPP) **11** which in the presence of chrysanthemyl diphosphate (CDP) synthase can react with another equivalent of DMAPP **11** to give the cyclopropyl ring seen in the acid moiety of Pyrethrins **5-7.**[25, 27] Following dephosphorylation, the resulting chrysanthemol **13** undergoes a series of oxidations to give the appropriate chrysanthemic acid **14a**, or pyrethric acid **14b**, which can then be used in conjunction with the rethrolone equivalent **20-22** in the production of Pyrethrins **5-7**.[25, 26]

The biosynthetic pathways associated with the production of the rethrolone moieties are less understood than the acid pathway.[28] Recent literature suggests that the rethrolones are biosynthesised from (*Z*)-jasmone **19**, which originates from jasmonic acid **18** produced by the oxylipin pathway (Scheme 1.1B).[27-29] In this pathway linolenic acid **15**, produced from membrane lipids, is oxidised in the presence of lipoxygenase (LOX) to give a hydroperoxylinolenic acid **16**.[27] An allene oxide intermediate **17**, produced with allene oxide synthase (AOS), undergoes a number of transformations ultimately giving the characteristic 5-membered cyclic scaffold in the form of (*Z*)-jasmonic acid **18**.[29] The pivotal intermediate (*Z*)-jasmone **19** is then produced and subsequently hydroxylated by jasmone hydroxylase to give (*Z*)-jasmolone **20**.[29] The other rethrolones are then likely furnished through (*Z*)-jasmolone **20** and the appropriate pyrethrin produced by condensation of a coenzyme A-activated chrysanthemate **14** and the appropriate rethrolone **20-22**.[29, 30]

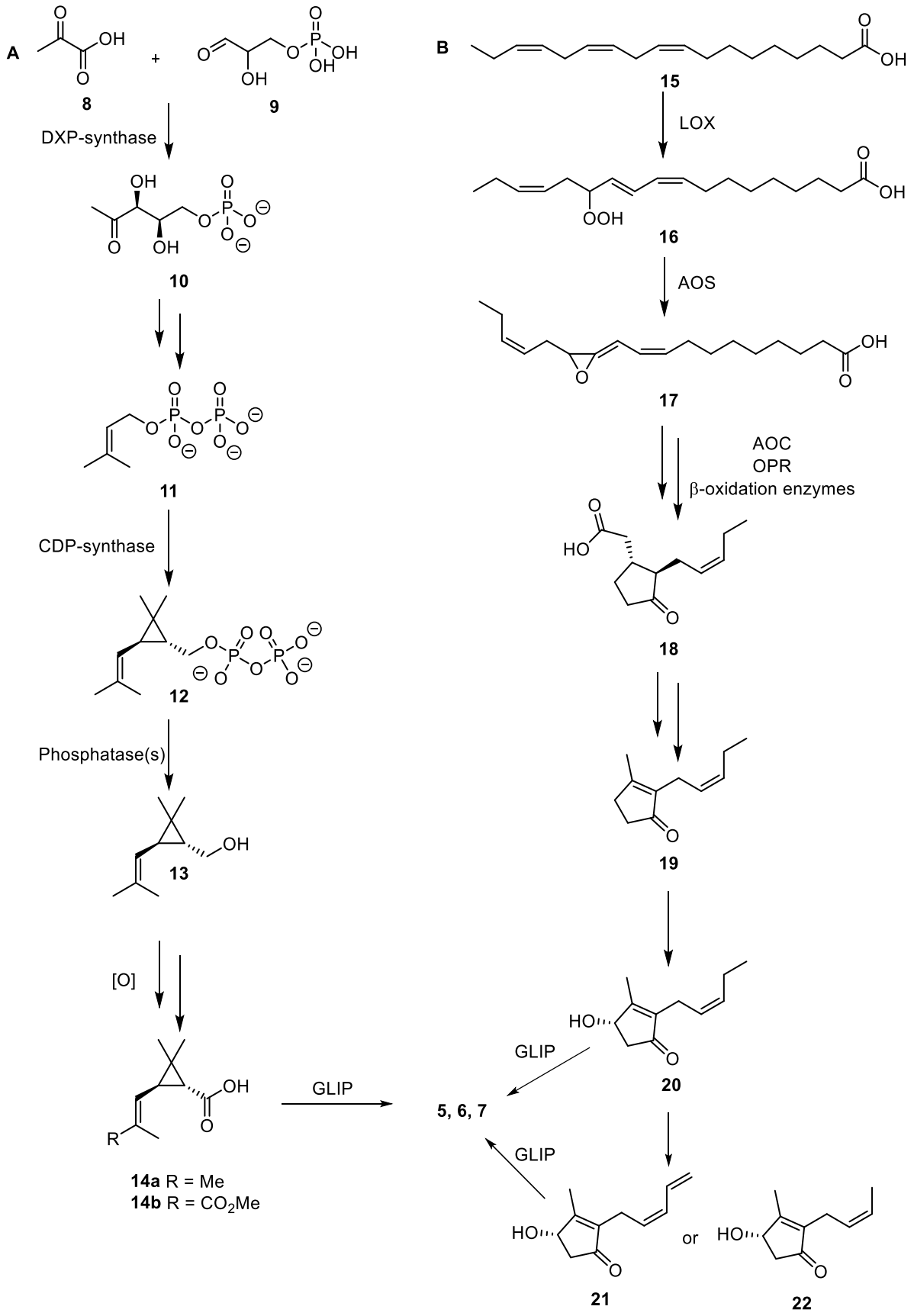

Scheme 1.1: Biosynthesis of the Pyrethrins 5-7 by independent production of the chrysanthemate (A) and rethrolone (B) moieties.

The Pyrethrins **5-7** are used by the plant primarily for the same reason as it is extracted by humans; for protection against insect pests.[27] These insecticidal esters are produced as a defense mechanism of the plant to help deter or eliminate the threat of consumption by herbivorous insects.[31, 32] A majority of the Pyrethrins **5-7** are concentrated in the flower head, in particular the seed casings, with up to 94% of the total pyrethrin content present.[33] Therefore, much of the defence lies in the protection of the seeds of the plant and as such the reproductive pathways of the pyrethrum daisy. The way in which the Pyrethrins **5-7** act, and protect the plant, is through activity on the nervous system of the insect. Specifically, the Pyrethrin esters **5-7** affect the *'para'* voltage-gated sodium ion channels (Na_v) which control the electrical pulses and transmissions through the nervous system.[34, 35] The Pyrethrins **5-7** bind to hydrophobic cavities along the sodium channel, deemed pyrethroid receptor sites, resulting in overexcitation of the nerve cell.[35] When bound in these receptor sites the Pyrethrins **5-7** promote the opening of these channels for extended time periods, through stabilisation of the open state of the sodium channel, allowing the channel to continue conducting sodium. [34, 35] This overexcitation of the nervous system through increased sodium influx results in the 'knockdown' effect where the overstimulation results in incapacitation and can ultimately cause the shutdown of the nervous system due to the inability of the nerve cells to maintain the continued activation of the sodium pump, resulting in the death of the insect.[35] Much of the work associated with the mode of action of the Pyrethrins **5-7** has been extrapolated from the action of the pyrethroids however more recently Dong, *et.al.* have highlighted the individual action of the six Pyrethrins **5-7** in support of the pyrethroid receptor site model.[34] From this, the order of activity was assigned as pyrethrin **5**> cinerin **6**> jasmolin **7** on the isolated sodium channel. In addition, they proposed structure-activity relationships associated with natural Pyrethrins **5-7** through computational docking studies with model cockroach sodium ion channels. In summary, the substantial difference in activity between pyrethrin **5** and jasmolin **7** was proposed to be due to the increased length of the jasmolin side chain and the lack of terminal π-system available for interaction in the binding pocket. This activity of the Pyrethrins **5-7** on a broad range of insect species has allowed for the effective and continued use of pyrethrum as a domestic and pre-harvest insecticide.

1.2.3 The problems with pyrethrum

Many of the beneficial qualities that the Pyrethrins **5-7** bestow upon pyrethrum-based insecticides, including its lack of environmental persistence and mammalian toxicity, stem from its ready degradation under typical environmental conditions. In particular, these esters **5-7** are sensitive to degradation through a variety of pathways particularly thermal, photochemical and oxidative routes.[24, 36, 37] However, this tendency to breakdown can adversely affect the ability to store the pyrethrum extract for extended periods of time and its long-term applicability. Due to this tendency to degrade rapidly, they have seen more prevalent use in the domestic sector for household pest control products. For large scale agriculture, storage of the pyrethrum becomes difficult because of these decomposition pathways and ensuing pyrethrin losses. As such many safeguards have been implemented to minimise the loss of material over time including storage controls and incorporation of additives. Although these measures have been put in place and have had success in slowing the decomposition of the pyrethrum, pyrethrin losses are still significant and the potential for more long-term agricultural use remains low. This has led to a myriad of studies into the mechanisms surrounding their degradation and general reactivity in an attempt to develop other solutions to minimise these degradative processes. Some of the pathways, and the resulting degradation products, will now be discussed.

1.3 Pathways resulting in pyrethrin loss

The pyrethrin scaffold possesses a number of functional groups (Figure 1.3) that are known throughout synthetic chemistry to be reactive handles for synthetic manipulation or potential sites for degradation.

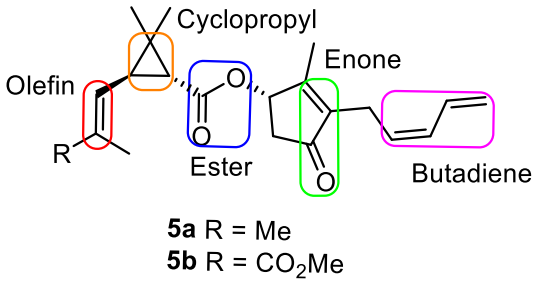

Figure 1.3: The reactive functional groups in pyrethrins **5** found to participate in a range of chemical reactions and degradative pathways.

Many of these reactive moieties contribute to the instability of the Pyrethrins **5-7** through their oxidative, photochemical, and/or thermal sensitivity. Each of these prominent degradation routes are highlighted in more detail below.

1.3.1 Oxidative degradation

There are a number of different degradation pathways that pyrethrin decomposition can occur, and one of the most common is oxidation. Oxidative reactivity is a key problem with the Pyrethrins **5-7**, particularly with the abundance of alkenes throughout the six esters **5-7.** One of the earliest studies to explore the effects of oxidation on pyrethrum was in 1933 by Gnaudinger and Corl where the concentrate and pyrethrolone analogues were exposed to the oxidant potassium permanganate ($KMnO_4$).[38] From this exposure, the pyrethrin content was significantly reduced and the pyrethrolone analogues were almost completely consumed,[38] suggesting oxidative reactivity on the rethrolone moiety. Despite this, no oxidation products were isolated and characterised leaving the fate of the Pyrethrins **5-7** unknown. Further studies by Chen and Casida, showed the production of a number of different products from the decomposition of the Pyrethrins **5-7** irradiated with a sun-lamp under aerobic conditions.[39] Whilst the individual products were again not isolated, the oxidative degradation could be readily attributed to both the acid and rethrolone portions of the scaffold by 2D TLC analysis of ^{14}C-labelled Pyrethrins **5-7**. Whilst these simulated oxidative conditions revealed insight into the potential for large pyrethrin loss and the participation from both moieties of the scaffold, the changes to the structure and its subsequent effect on biological activity remained unknown. More recent studies have been undertaken to reflect the direct action of atmospheric oxygen on stored pyrethrum crop material, elucidating some of the oxidised degradation products.[24]

A prominent degradation mechanism for the loss of pyrethrin has recently been found to be autoxidation, where molecular oxygen in the atmosphere acts upon a substrate generally by radical mechanisms. Specifically, it has been proposed that hydrogen abstraction can take place on the linear rethrolone sidechain of the Pyrethrins **5-7** (Scheme 1.2), similar to oxidative processes affecting lipids. The resulting radical is most likely formed at the 7′ methylene (Figure 1.2) due to the stability imposed by the doubly allylic character imparted by both the alkene of the enone and the conjugated diene in the sidechain.[24] Subsequent reaction with atmospheric oxygen then has the potential to form a range of oxidised products

including epoxides **23** and diols **24** (Scheme 1.2A), with some implicated in the HPLC analysis of unstabilised, stored crop.[24]

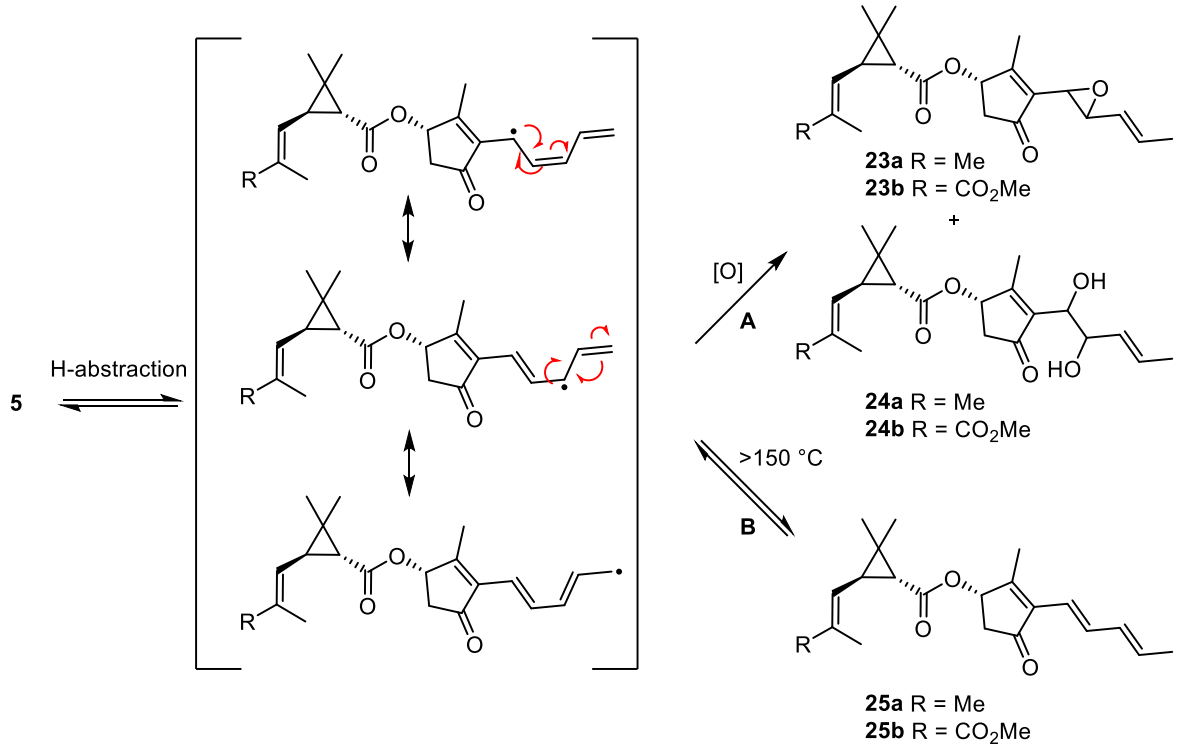

Scheme 1.2: Radical reactivity of the pentadienyl side chain of pyrethrins **5** leading to oxidation **(A)** or thermal isomerism **(B)**.

These radical procedures are more prominent in pyrethrin I **5a** and II **5b** due to stabilisation of the radical by resonance through the conjugated pentadienyl sidechain (Scheme 1.2).[24, 40] The increased stability of the radical has been linked to higher rates of decomposition of these major pyrethrum components. In conjunction, similar radical mechanisms have been implicated in the thermal isomerism of the pentadienyl unit resulting in the migration of the double bonds into conjugation with the enone (Scheme 1.2B) giving the trienyl 'isopyrethrins' **25**.[40] Mixtures and completely isomerised pyrethrin extracts have been documented to result in losses of insecticidal activity by half and knockdown activity to one quarter strength of pure pyrethrum, ultimately decreasing the applicability and effectiveness of the extract.[40]

Notably, oxidation by other means can also lead to the beneficial breakdown of the Pyrethrins **5-7**, with many metabolic pathways utilising oxidative enzymes.[41-43] Casida's exploration into mammalian oxidative metabolism identified a number of hydroxy and epoxy pyrethrin

analogues **26-29** (Figure 1.4) with reactivity taking place on both the chrysanthemate and rethrolone portions of the scaffold. [41, 43]

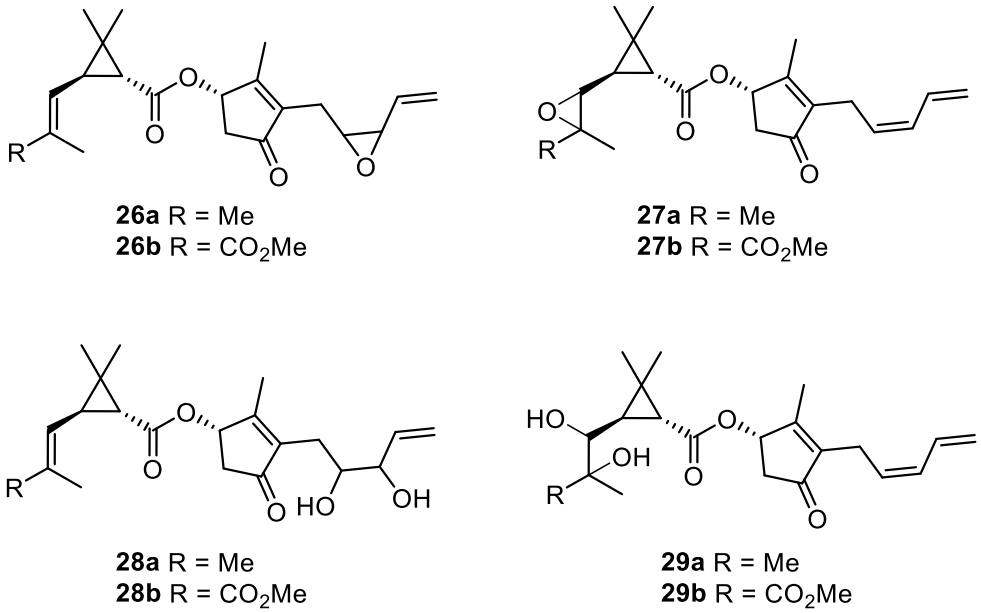

Figure 1.4: Some of the oxidative metabolites of Pyrethrins **5-7** observed in mammals.[41]

This ability to readily metabolise the Pyrethrins **5-7** through these oxidative means is a large contributor to the significant lack of toxicity of pyrethrum-based insecticides to mammalian organisms.[41] Alternatively, microorganisms have been studied for their metabolism of the Pyrethrins **5-7**,[42] however their contribution to pyrethrin degradation is negligible particularly in relation to the major degradative mechanisms.[36] Other degradative factors remain more prominent in the loss of Pyrethrins **5-7**, particularly photolytic and thermal processes.

1.3.2 Photolysis of the Pyrethrins

The photochemical degradation of the Pyrethrins **5-7** and the primary moieties that comprise them are well-documented, with a number of studies detailing the mechanisms and chemical outcomes of these routes. The photodegradation of the Pyrethrins **5-7** can result in a multitude of changes to the scaffold with reactivities such as double bond isomerism, homolytic cleavage of integral bonds and rearrangement of entire moieties taking place.[9, 44, 45] This photochemical instability makes the pyrethrum concentrate, and insecticides derived from it, sensitive to sunlight which can reduce their applicability in field use limiting the lifetime of the applied insecticide.[9, 44, 46] The acid moiety of the pyrethrin scaffold is

photolytically labile, with a number of degradative pathways possible from the homolytic cleavage of the cyclopropyl ring (Scheme 1.3).[9, 47]

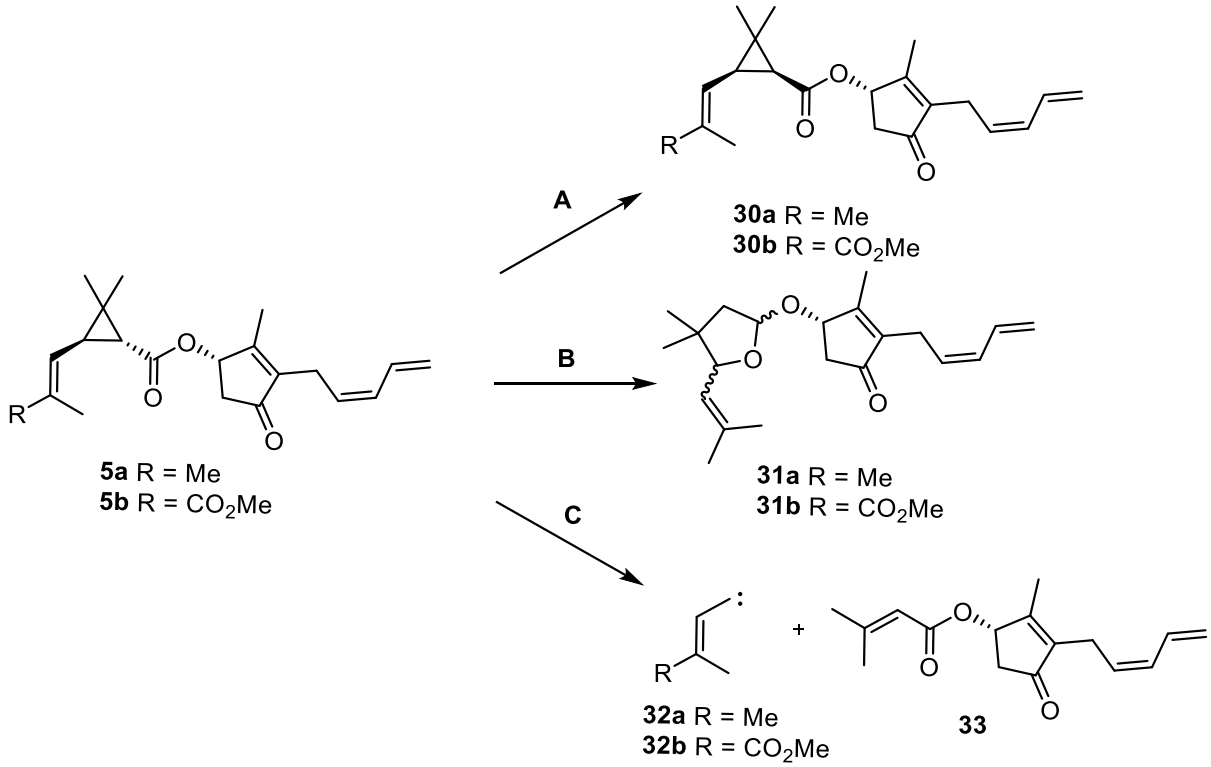

Scheme 1.3: Photolytic degradation by homolytic cleavage of the cyclopropyl moiety resulting in recombination (A), rearrangement (B) or, fragmentation (C).

This homolytic cleavage results in a diradical intermediate that can recombine regenerating the cyclopropyl ring. From this process, the natural *trans* geometry of the substitution on the cyclopropane can isomerise to the *cis*-isomer **30** (Scheme 1.3A) through free rotation of the substituents followed by the recombination of the radicals giving the 3-membered cyclic structure.[9, 45, 48] The *cis* stereochemistry of the acid moiety in Pyrethrins **5-7** has been shown to significantly decrease the insecticidal activity by up to four times the original concentrate.[9] Alternatively, the radical can delocalise onto the carbonyl of the ester (Scheme 1.3B) and subsequently recombine giving a more stable, rearranged tetrahydrofuran structure **31**.[9, 47] Finally fragmentation of the structure (Scheme 1.3C) has also been suggested as a means of decomposition, with the formation of a theorised vinyl carbene **32** and an observed isobutenyl ester **33** in studies with chrysanthemates.[9, 47] Whilst the photolysis of the chrysanthemate moiety has been well studied, the photodegradation of Pyrethrins **5-7** is not limited to this portion of the scaffold. Photochemical action on the rethrolone portion of the

Pyrethrins **5-7** occurs with alteration of the molecular configuration of the scaffold. The most prominent pathway is the *cis-trans* isomerism (Scheme 1.4) of the linear sidechain which has been documented to result in decreased biological activity.[9, 49, 50]

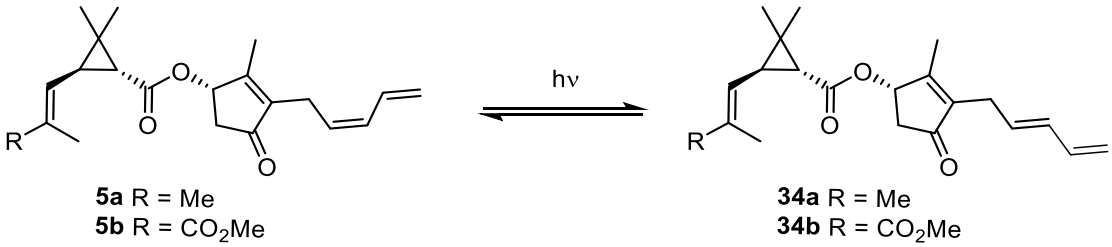

5a R = Me
5b R = CO_2Me

34a R = Me
34b R = CO_2Me

Scheme 1.4: Photochemical isomerism of the *cis*-alkene of pyrethrin **5**.

The rethrolone moiety of the Pyrethrins **5-7** is the major source of a number of other reactivities and is likely the main contributor to pyrethrin losses due to its high chemical reactivity.

1.3.3 Alternate degradation pathways

A major issue with the long-term storage of pyrethrum is the formation of polymeric material with the polymerisation of the Pyrethrins **5-7** a suggested major degradative pathway. Extracts containing polymerised material exhibit decreasing insecticidal activity with increasing polymer content.[51] Whilst the polymerisation process has been suggested to be limited to the rethrolone portion and proceed through thermal or photochemical means,[51, 52] the exact mechanism of formation and the polymer identity currently remain unknown limiting remediation of this process. Unprecedented reactivity of the Pyrethrins **5-7** has not only affected the biological activity of the insecticide but has also had significant impact in limiting their analysis. Standard quantitation methods of the Pyrethrin content in pyrethrum extracts requires the alkaline hydrolysis of the ester linkage to liberate the acid and rethrolone moieties. Whilst the chrysanthemic **14a** or pyrethric acid **14b** can be obtained intact from these hydrolytic protocols allowing for quantification of the Pyrethrins I **5a-7a** and II **5b-7b**, the rethrolone moiety reacts further preventing quantitation of the individual esters. The acidic 5' proton (Figure 1.2) leads to the rethrolone moiety undergoing an elimination reaction giving a cyclopentadienone **35** that readily dimerises by Diels-Alder cycloaddition to give the homodimers **36** and **37** (Scheme 1.5).[15]

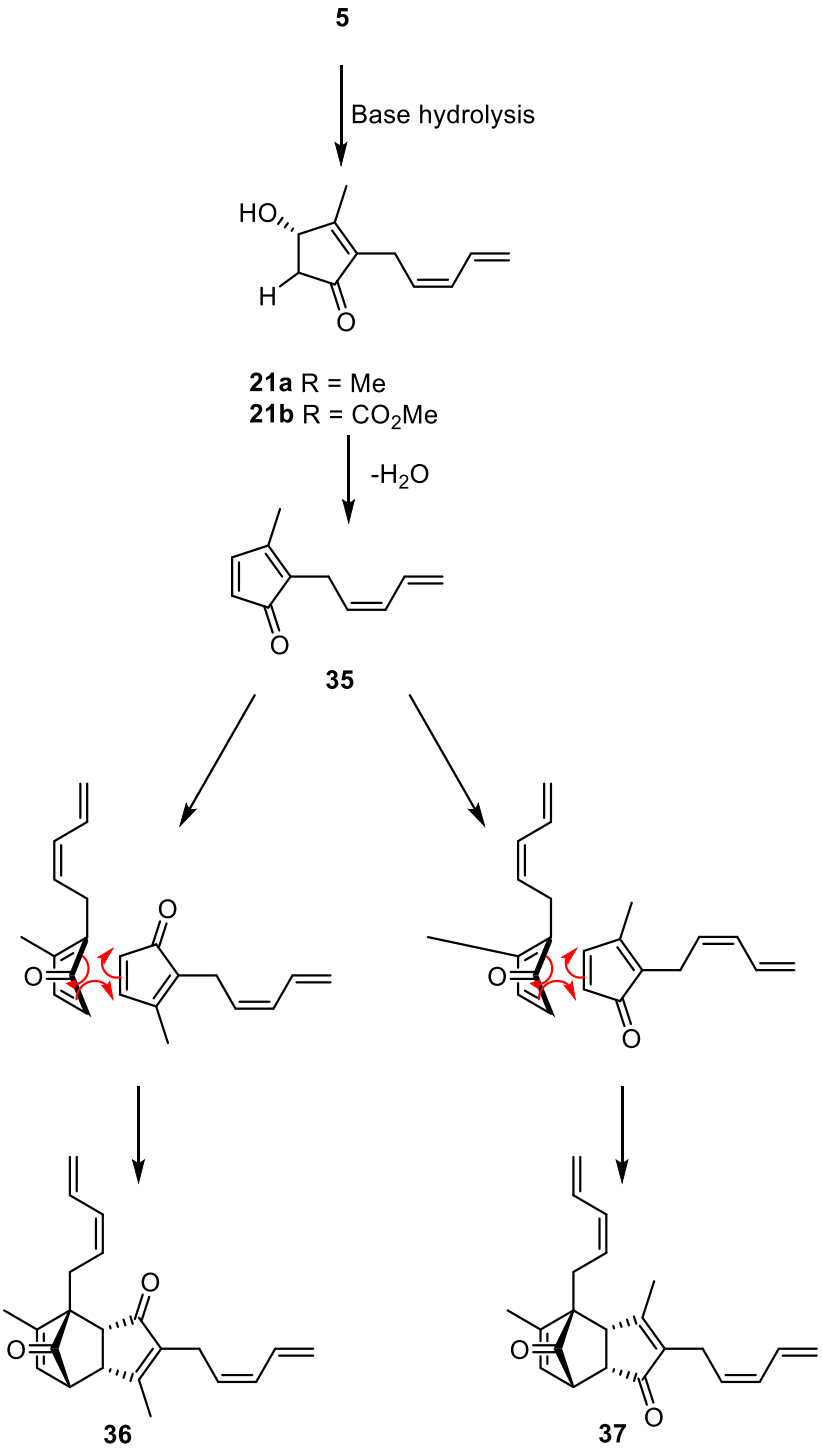

Scheme 1.5: Base-induced elimination of pyrethrin rethrolone 21 leading to Diels-Alder dimerisation of the resulting cyclopentadienone 35.[15]

Examination into the degradation of the natural Pyrethrins **5-7** has and will continue to lead to improved storage of the harvested plant material and resulting extract, with a number of countermeasures having been developed in an effort to combat these processes. Discussion

will now briefly outline current countermeasures employed to prevent loss of pyrethrin content in pyrethrum.

1.4 Current countermeasures to minimise pyrethrin loss

Currently, several strategies have been implemented to prevent or minimise the loss of Pyrethrins **5-7** from the pyrethrum crop, extract, and insecticides. Alleviating Pyrethrin losses during processing of the crop and extraction of the pyrethrum concentrate has been a priority with a number of safeguards being implemented in the storage and manufacture of the extract. [24]

1.4.1 Crop storage and processing

The loss of Pyrethrins **5-7** can occur anytime from the harvest of the plant material through to the storage of the pyrethrum concentrate and its subsequent insecticidal formulations. The earliest countermeasure is implemented directly after the dried crop is harvested. The dried plant material is stored in light-free, temperature-controlled facilities to minimise loss of Pyrethrins **5-7** from photochemical and thermal degradative pathways. Throughout the extraction process an antioxidant, e.g. butylated hydroxytoluene (BHT), is added to prevent oxidative processes affecting the pyrethrum and the pyrethrin content is closely monitored.[24] The final pyrethrum extract is typically diluted with hydrocarbon solvent and stored in dark, cool facilities with additional antioxidant added to further minimise pyrethrin loss. Countermeasures continue to be developed whether it be in the storage of the material or in the application, where longevity is desirable.

Attempts have also been made to diminish the degradation of Pyrethrins **5-7** on application of the insecticidal material, particularly in terms of photochemistry. The photochemical degradation of Pyrethrins **5-7** has been shown to be mitigated through protection in glasshouses, as displayed by the persistence of pyrethrin residues in such a setting.[49, 53] The wavelength range in which light is damaging to Pyrethrins **5-7** has been found to be 290-320 nm (UVB), with this destructive range being moderated by the glass panels employed in the greenhouse and additives like selective light absorbing materials and antioxidants added to the insecticide.[53] However, the development of fully synthetic alternatives to the Pyrethrins **5-7** has resulted in the most impact with replacement of the natural pyrethrum concentrate with pyrethroids.

1.4.2 Pyrethroids: Alternatives to the natural Pyrethrins

The instability of Pyrethrins **5-7** towards factors such as light, temperature and oxidation led to the development of more stable, fully synthetic alternatives, known as pyrethroids, as early as 1949. Pyrethroids were established as synthetic analogues of the natural Pyrethrins **5-7** in an attempt to not only potentially increase their activity towards insects but to significantly improve their stability, ultimately allowing for more widespread and long-term applicability in the agricultural sector. Early pyrethroids were developed with a similar scaffold to the natural Pyrethrins **5-7**, with minor modifications to combat the photochemical and oxidative decay observed in pyrethrum-based insecticides. Many were readily put into use as commercial insecticides for both domestic and agricultural applications with a large number of the commonly employed pyrethroids being developed in the mid-to-late 20th century. With increasing synthetic capabilities, and knowledge surrounding the action of pyrethroids, more tolerant and structurally diverse moieties have been incorporated into the pyrethroids straying from the typical pyrethrin frame. Both the chrysanthemic acid and rethrolone moieties have been the focus of alteration and have ultimately been replaced with stabilised structural motifs.

The earliest development of a pyrethroid focussed on alteration and replacement of the rethrolone sidechain due to its propensity for degradation, and as a consequence, loss of insecticidal activity, in the natural Pyrethrins **5-7**. This resulted in the first of the pyrethroids with the production of allethrins **38** (Figure 1.5), where the linear hydrocarbon sidechain of the Pyrethrins **5-7** was substituted for an allyl group.[54] Notably, both the chrysanthemic **38a** and pyrethric acid **38b** variants were developed, with each a mixture of eight possible diastereomers. This minor amendment of the pyrethrin scaffold (Figure 1.3) resulted in a drastic increase in stability compared to the natural Pyrethrins **5-7** and even increased insecticidal activity against some insect species including houseflies (*Musca domestica*).[55, 56] Despite this, allethrins **38** did not demonstrate the same broad spectrum activity of the natural Pyrethrins **5-7** and retained many of the reactive moieties of the pyrethrin scaffold requiring further development of pyrethroids with larger alteration to the rethrolone.[56]

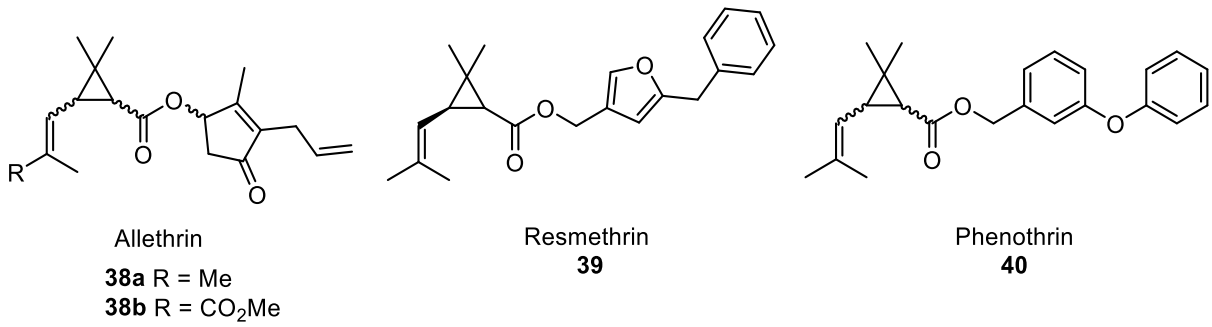

Allethrin
38a R = Me
38b R = CO_2Me

Resmethrin
39

Phenothrin
40

Figure 1.5: Early pyrethroids with alteration of the labile rethrolone moiety.

The most notable of the next generation of pyrethroids was resmethrin **39** (Figure 1.5) where the entire rethrolone moiety was redesigned. The substituted cyclopentenone of the Pyrethrins **5-7** was replaced with a benzyl furan moiety mimicking the steric qualities and high π-character of the natural rethrolone.[57] Of particular note is the lack of stereocentres in the benzyl furan replacement making industrial synthesis a more viable process without the need to produce purified stereoisomers. In conjunction, this significant modification gave the pyrethroid incredibly high activity in comparison to the natural esters and other pyrethroids on the market. Unfortunately, whilst more stable than the Pyrethrins **5-7**, resmethrin **39** was limited to domestic use due to it still being sensitive to oxidative and photochemical degradation.[10, 55] In addition, the (*R*)-configuration of the isobutenyl substituent of the chrysanthemate was necessary for high insecticidal activity.[55] Phenothrin **40** (Figure 1.5) was developed shortly after and alleviated the issues of the benzyl furan moiety of resmethrin **39** with the introduction of a 3-phenoxybenzyl group.[55] This alteration retained all the beneficial qualities of resmethrin **39** whilst increasing the resistance of the pyrethroid to photochemical and oxidative processes.[58] The remaining drawback of phenothrin **40** was the unaltered chrysanthemate and the degradative processes it could still undergo to diminish insecticidal activity.

The most stable and well-known of the classic pyrethroids were developed throughout the 1970s and 80s where the majority of the alteration to the pyrethrin scaffold shifted to the acid moiety having established a valuable rethrolone candidate. The most prominent change to the chrysanthemate was the replacement of the methyl substituents of the isobutenyl for halogens like chloride and bromide. These methyls in the isobutenyl moiety of the Pyrethrins **5-7** were established as sites for photodecomposition prompting this replacement.[39]

Permethrin **41** (Figure 1.6) was the first of the 3-phenoxybenzyl pyrethroids to introduce a dichlorovinyl substituent in place of the natural isobutenyl in Pyrethrins **5-7**.[59]

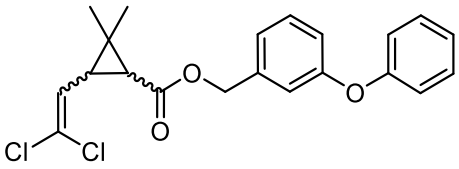

Permethrin
41

Figure 1.6: Permethrin **41**, a pyrethroid containing stabilised acid and rethrolone moieties.

This halogen incorporation about the double bond in the acid moiety was ultimately able to minimise the photosensitivity of the chrysanthemate and as such the pyrethroid as a whole preventing the radical oxidative processes that affected the pyrethrin isobutenyl group.[10, 59, 60] Having established stabilised acid and rethrolone moieties, final changes to the pyrethroid scaffold focussed on increasing insecticidal activity. Of these, cypermethrin **42** and deltamethrin **43** (Figure 1.7) were developed, introducing an α-cyano modification in the ester linkage. These two pyrethroids became the most common commercial pyrethroids in use with this continuing today. This popularity is due to their increased stability with the dihalovinyl and 3-phenoxybenzyl moieties and their high insecticidal, broad-spectrum activity increased with the α-cyano modification in the ester linkage.[10, 55, 58, 61]

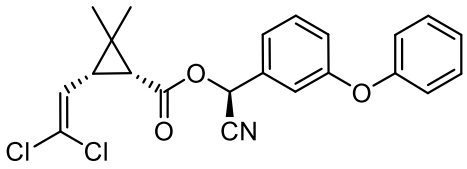

Cypermethrin
42

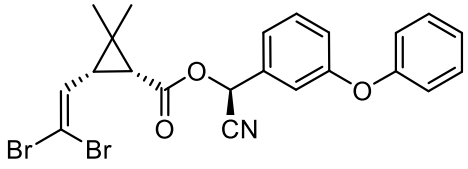

Deltamethrin
43

Figure 1.7: Commercial pyrethroids cypermethrin **42** and deltamethrin **43**.

Unfortunately, these fully synthetic alternatives to the natural Pyrethrins **5-7** suffer from their own drawbacks that can have negative impact on the environment leaving the necessity for the continued development of novel insecticidal materials.

1.4.3 Drawbacks of pyrethrin replacements

Despite the many successes the pyrethroids have accomplished, they still demonstrate a range of shortcomings that have not been fully addressed. Unfortunately, due to their

increased stability, pyrethroids exhibit extended environmental persistence, heightened mammalian toxicity and insects have demonstrated a developing resistance to a range of these heavily utilised classic pyrethroids.

Whilst the stability of the pyrethroids allows for their more widespread agricultural application, it can lead to the pyrethroids causing a detrimental impact on the environment and affecting non-target organisms.[62] The persistence of pyrethroids in soils can lead to them being transported into waterways from agricultural run-off contaminating aquatic bodies and adversely affecting aquatic life.[63, 64] Aquatic life has a well-known sensitivity to this class of insecticides as they lack many of the enzymes that mammals use to efficiently metabolise the pyrethroids. This toxicity to aquatic organisms can lead to loss of life and as such have a significant negative effect on the ecology of these environments.[65] Notably, the hydrophobicity of many of the pyrethroids can minimise their solubility in irrigation run-off however, they strongly adsorb to soil particles that move with the water run-off into these aquatic environments where detectable quantities can build up.[63, 66, 67] This negative environmental impact is not the only issue that the pyrethroids pose with the rise of resistance in many insect species.

The most prominent, ongoing issue with commercial pyrethroid insecticides, particularly those that were developed in the mid-20th century, is the emergence of resistance in a number of insect species.[68-71] A number of insect species have developed an insensitivity to the pyrethroids or are able to rapidly metabolise them minimising their affect.[68] The development of this resistance can generally be attributed to three main processes; increased metabolic ability, a decreased sensitivity at the target active site and/or decreased ability for the insecticide to penetrate the cuticle of the insect.[72] Notably, the development of resistance against one insecticide can result in cross-resistance to other similarly acting insecticide, which is particularly detrimental to the pyrethroid class. With the increasing development of resistance across several pest insect species, spikes in pest species numbers can occur and ultimately affect the production and harvest of commercially relevant crops. This ever-growing resistance to commercial pyrethroids feeds the need for ongoing research and has led to the more recent development of newer pyrethroid-like materials in an effort to replace the classic pyrethroids.

1.4.4 Current attempts to combat pyrethroid drawbacks

The focus to overcome the emerging downfalls of pyrethroids has seen the continued development of other pyrethroid-like insecticidal materials with the eventual goal of implementation in agriculture and the home. The development of these modern pyrethroids has resulted in minor amendments to the pre-existing pyrethroid scaffold, such as monohalogenated acid moieties, as seen in **44** (Figure 1.8),[73] or more significant changes that deviate further from the original pyrethroid-based skeleton.

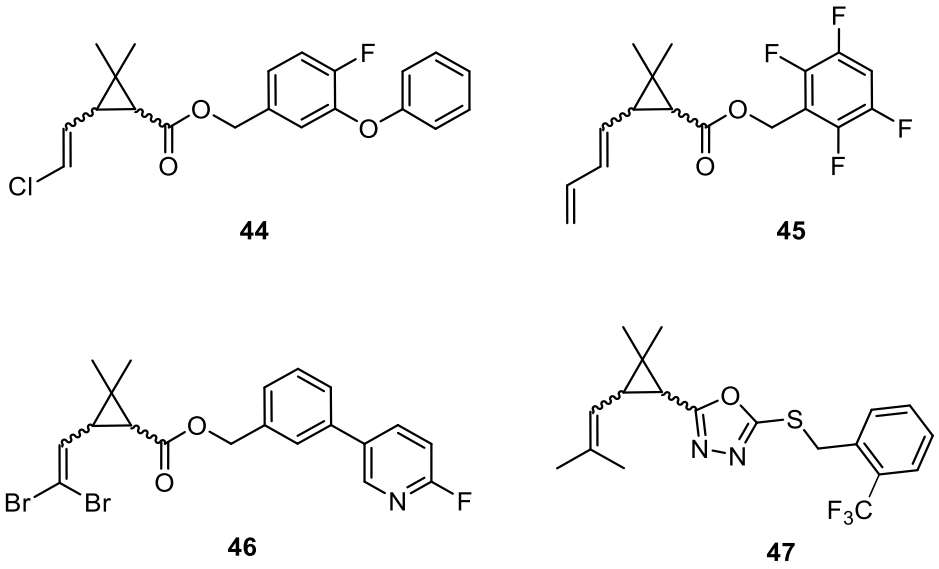

Figure 1.8: A selection of emerging pyrethroids with structures similar to the classic variants.

Whilst some of these monohalogenated acid derivatives, e.g. **44**, showed comparable activity against some pest species like aphids (*Aphis craccivora*) and armyworms (*Mythimna separata*), they were significantly less active against mosquitos (*Culex pipins pallens*) than the commercial pyrethroids cypermethrin **42** and deltamethrin **43**. Notably, with only one of the sites of the acid alkene halogenated, degradation was found to proceed much easier giving these materials potential as a middle ground between the Pyrethrins **5-7** and pyrethroids.

Use of less conventional pyrethroid alcohols, like the tetrafluorobenzyl group, with altered cyclopropyl acids has resulted in pyrethroidal materials like **45** (Figure 1.8) with broad-spectrum activity and long-term stability.[74] In conjunction, the pyrethroid **45** showed potential against a pyrethroid resistance model organism, German cockroach (*Blattela germanica*), and demonstrated minimal acute toxicity against rats. However, the high fluorine

content is likely to contribute to long-term persistence and, as such environmental impact, due to the high stability of polyfluorinated organic compounds.[75, 76]

More recently, heterocyclic components have been added to the alcohol motifs of these pyrethroid structures to alleviate the generation of toxic degradation products. Biaryl systems, like that contained in **46** (Figure 1.8), replaced the 3-phenoxybenzyl moiety of deltamethrin **43** introducing nitrogen-containing heterocycles.[77] Many of the prepared biaryl pyrethroids exhibited significant bioactivity against mosquitos and prevented the generation of toxic degradation pollutants. However, the stability and broad-spectrum capabilities of these new pyrethroids remains unknown limiting their current potential applicability. 1,3,4-Oxadiazole thioether rethrolone replacements, similar to **47** (Figure 1.8), have also recently been investigated as new pyrethroids. Many of these new analogues were able to elicit insecticidal activities comparable to those of some commercial insecticides, including cypermethrin **43**, however, the photostability and mammalian toxicity remain uncertain.[78]

The continued need for the development of novel pyrethroid insecticides is the result of the many drawbacks they present particularly in terms of their environmental impact and evolving resistance in a number of insect species. Additionally, the pyrethroids and emerging pyrethroid-like material require ground up synthesis over multiple steps which is resource and time consuming. Many of these drawbacks have potential to be remedied by the direct functionalisation of the natural Pyrethrins **5-7**.

1.5 Altering the natural pyrethrins to combat their degradation

After centuries of their use, the natural Pyrethrins **5-7** remain the ideal candidate for environmentally friendly and low toxicity insecticides due to their degradative properties and effective, broad-spectrum activity. Whilst the degradative properties of the Pyrethrins **5-7** remains beneficial from an environmental standpoint, they have been a point of concern in the long-term storage and prolonged use in agricultural settings of pyrethrum-based insecticides[24, 36, 42, 46]. Unfortunately, the many countermeasures in place to minimise this degradation do not completely alleviate the issue of pyrethrin loss in processing and storage. Alternatives like the pyrethroids have also resulted in a number of their own shortcomings. As such, a solution for both the flaws of the natural pyrethrum and the drawbacks of pyrethroid insecticides is required. A potential means of mitigating these on-going issues is to

develop new, insecticidally active analogues from the naturally derived Pyrethrins **5-7**. Specifically, this has the potential to alleviate the environmental stress and synthetic demand imposed by the pyrethroids whilst imparting stabilisation to the natural material through direct functionalisation.

1.5.1 Selective reduction of the natural pyrethrins

Of the six esters in the pyrethrum extract, pyrethrin I **5a** and II **5b** constitute the majority of the refined concentrate making up approximately 30-40% each.[79] Unfortunately, these more abundant constituents are also the most prone of the Pyrethrins **5-7** to degrade due to the pentadienyl unit.[24] The degradation of the Pyrethrins **5-7** remains a beneficial quality as it prevents the environmental persistence and minimises the development of resistance. The instability also bestows the Pyrethrins **5-7** with low mammalian toxicity. As such, a compromise between the stability of the extract for long-term storage and the beneficial degradation of the extract could be explored by means of simplifying the mixture of six esters to four. The more sensitive pyrethrins **5** differ from their jasmolin counterparts **7** solely by the saturation of the terminal bond in the penta-carbon sidechain. As such the transformation of pyrethrins **5** to jasmolins **7** could be achieved through selective reaction at this site (Scheme 1.6).

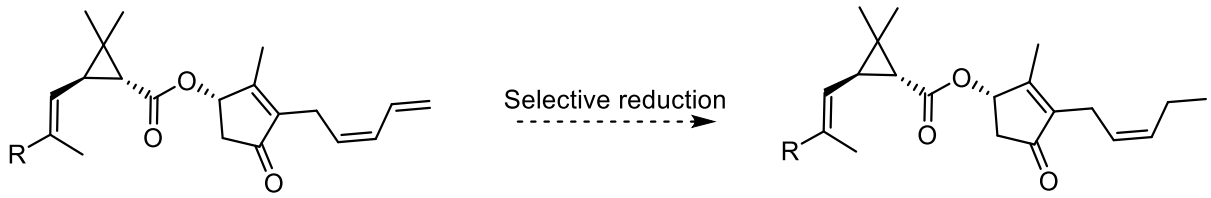

5a R = Me
5b R = CO_2Me

7a R = Me
7b R = CO_2Me

Scheme 1.6: Selective reduction of the pyrethrins **5** to the more stable jasmolins **7**.

This conversion to the more stable minor esters **7** was envisioned to be achieved through a chemo- and regio-selective reduction. Specific focus was given to implementing sterically encumbered reducing agents and/or mild conditions to minimise alternate reactivity and degradation of the pyrethrin starting material. Ultimately, such a transformation may serve to limit the degradation of the pyrethrum concentrate with long-term storage whilst retaining the beneficial qualities bestowed by the natural esters.

1.5.2 Altering the pentadienyl unit of pyrethrins I and II

The rethrolone moiety of the Pyrethrins **5-7** remains the major site of degradation, whether through oxidation or polymerisation.[24, 51] Alteration of the reactive sites on this portion of the scaffold may lead to analogues of the Pyrethrins **5-7** that exhibit an increased stability to the well-known degradation pathways. Specifically, the double bonds of the pentadienyl sidechain are responsible for this high reactivity under environmental conditions. As such, functionalisation or modification of these sites to stabilised motifs was of particular interest.

As previously highlighted, the diene of the rethrolone moiety in the pyrethrins **5** is a particularly well-established site for degradation. This pentadienyl sidechain of the major pyrethrum constituents has potential as a reactive site in Diels-Alder cycloaddition reactions. Such reactivity would allow for the production of cycloadducts of the pyrethrins **5** that no longer possess the reactive pentadienyl side chain (Scheme 1.7), potentially decreasing their propensity to decompose particularly through oxidative means.

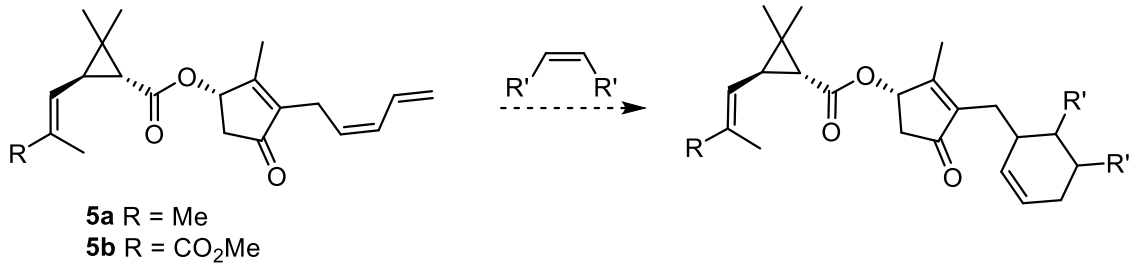

5a R = Me
5b R = CO_2Me

Scheme 1.7: Potential Diels-Alder cycloaddition of the natural pyrethrins **5**.

Further, the electron density of the pentadienyl unit may provide a means to explore the reactivity of the pyrethrins **5** under inverse electron demand Diels-Alder (IEDDA) conditions, with the pyrethrin double bond(s) serving as the dienophile with electron-deficient diene reagents. Exploring these different conditions can ultimately shed light into the reactivity of the natural Pyrethrins **5-7** whilst also allowing for the development of pyrethrin analogues with potential for increased stability.

Alternatively, the alkenes of the rethrolone side chain also have the capacity for versatile functionalisation with a range of aromatic structures through palladium-catalysed cross coupling. The introduction of these aromatic moieties into the pyrethrin scaffold can readily be achieved through Heck reaction (Scheme 1.8).

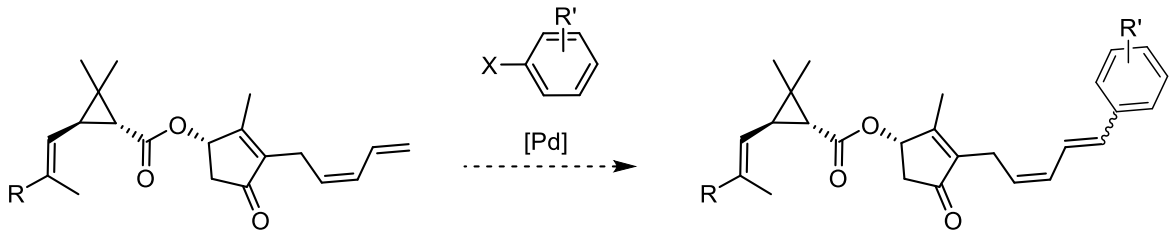

5a R = Me
5b R = CO_2Me

Scheme 1.8: Potential palladium-catalysed arylation of the natural pyrethrins **5**.

These aromatic motifs could potentially mimic some of the structural characteristics of the pyrethroids to ideally give stabilised pyrethrin-based equivalents.

1.6 Research outline

Described herein, is the exploration into the synthetic modification of particularly sensitive moieties in the natural pyrethrin scaffold in an effort to develop analogues with increased stability allowing for long-term storage and applicability. Notably this work has focussed on the selective modification of the pyrethrins **5** and testing of their viability in preliminary insecticidal activity assays. Specifically, Chapter 2 describes efforts into the selective reduction of the pyrethrins **5** to the jasmolin **7**. A number of reductive protocols are assessed for their viability in this transformation and a number of reduction products resulting from these pursuits are subjected to preliminary evaluation of their insecticidal activity yielding insight into pyrethrin structure-activity relationships. Chapter 3 explores the Diels-Alder reactivity of the pyrethrin **5** pentadienyl side chain under both normal electron demand and inverse electron demand. Chapter 4 further investigates the functionalisation of the pentadienyl unit in pyrethrins **5**, instead utilising palladium-catalysed methods. In particular, the use and optimisation of Heck conditions for the arylation of the pyrethrins **5** is studied leading to a series of arylated pyrethrin analogues. Lastly, Chapter 5 details attempts at the synthesis of the rethrolone of pyrethrins **5**, (*Z*)-pyrethrolone **21**, for its potential use as a future model for pyrethrin alteration.

1.7 References

1. Oberemok, V. V.; Laikova, K. V.; Gninenko, Y. I.; Zaitsev, A. S.; Nyadar, P. M.; Adeyemi, T. A., A short history of insecticides. *J. Plant Prot. Res.* **2015,** *55* (3), 221-226.
2. Peryea, F. J. In *Historical use of lead arsenate insecticides, resulting soil contamination and implications for remediation*, 16th World Congress of Soil Science, Montpellier, France, Montpellier, France, 1998.
3. Turusov, V.; Rakitsky, V.; Tomatis, L., Dichlorodiphenyltrichloroethane (DDT): ubiquity, persistence, and risks. *Environment Health Perspectives* **2002,** *110* (2), 125-128.
4. Gerber, R.; Smit, N. J.; Vuren, J. H. J. V.; Nakayama, S. M. M.; Yohannes, Y. B.; Ikenaka, Y.; Ishizuka, M.; Wepener, V., Bioaccumulation and human health risk assessment of DDT and other organochlorine pesticides in an apex aquatic predator from a premier conservation area. *Sci. Total Environ.* **2016,** *550*, 522-533.
5. Popovska-Gorevski, M.; Dubocovich, M. L.; Rajinarayanan, R. V., Carbamate Insecticides Target Human Melatonin Receptors. *Chem. Res. Toxicol.* **2017,** *30* (2), 574-582.
6. SafeWorkAustralia, Organophosphate pesticides health monitoring. https://www.safeworkaustralia.gov.au/doc/organophosphate-pesticides-health-monitoring, 2013.
7. Campos, E. V. R.; Oliveira, J. L. d.; Pascoli, M.; Lima, R. d.; Fraceto, L. F., Neem Oil and Crop Protection: From Now to the Future. *Front. Plant Sci.* **2016,** *7*, 1494.
8. Sparks, T. C.; Dripps, J. E.; Watson, G. B.; Paroonigian, D., Resistance and cross-resistance to the spinosyns- A review and analysis. *Pest. Biochem. Physiol.* **2012,** *102* (1), 1-10.
9. Bullivant, M. J.; Pattenden, G., Photodecomposition of Natural Pyrethrins and Related Compounds. *Pestic. Sci.* **1976,** *7*, 231-235.
10. Elliott, M., The Pyrethroids: Early Discovery, Recent Advances and the Future. *Pestic. Sci.* **1989,** *27*, 337-351.
11. Fujitani, J., Chemistry and pharmacology of insect powder. *Arch. Exp. Pathol. Pharmakol.* **1909,** *61*, 47-75.
12. Yamamoto, R., The insecticidal principle in *Chrysanthemum cinerariaefolium*. Part I. *J. Chem. Soc. Jap.* **1919,** *40*, 126.
13. Yamamoto, R., The insecticidal principle in *Chrysanthemum cinerariaefolium*. Parts II and III. On the constitution of pyrethronic acid. *J. Chem. Soc. Jap.* **1923,** *44*, 311.

14. Staudinger, H.; Ruzicka, L., Insketentötende Stoffe I. The Isolation and Constitution of the Active Part of Dalmatinisehen Insect Powder. *Helv. Chim. Acta* **1924,** *7*, 177-201.
15. Hutt, O. E.; Freemont, J. A.; Littler, S.; Duggan, P. J.; Tsanaktsidis, J.; Cole, H.; Kerr, M.; Ryan, J. H., Staudinger and Ruzicka's Altered Pyrethrolone: the Cyclopentadienone Dimers Derived from Pyrethrin I. *Acta Hortic.* **2015,** *1073*, 181-190.
16. Begley, M. J.; Crombie, L.; Simmonds, D. J.; Whiting, D. A., Absolute Configuration of the Pyrethrins. Configuration and Structure of (+)-Allethronyl (+)-*trans*-Chrysanthemate 6-Bromo-2,4-dinitrophenylhydrazone by X-Ray Methods. *J. Chem. Soc., Chem. Commun.* **1972**, 1276-1277.
17. Staudinger, H.; Ruzicka, L., Insketentötende Stoffe II. The Constitution of the Chrysanthemum Monocarboxylic acid and Dicarboxylic acid. *Helv. Chim. Acta* **1924,** *7*, 201-211.
18. Staudinger, H.; Ruzicka, L., Insketentötende Stoffe III. The Constituition of Pyrethrolone. *Helv. Chim. Acta* **1924,** *7*, 212-235.
19. LaForge, F. B.; Barthel, W. F., Constituents of Pyrethrum Flowers. XVI. Heterogeneous Nature of Pyrethrolone. *J. Org. Chem.* **1944,** *9*, 242-249.
20. LaForge, F. B.; Barthel, W. F., Constituents of Pyrethrum Flowers. XVII. The Isolation of Five Pyrethrolone Semicarbazones. *J. Org. Chem.* **1945,** *10*, 106-113.
21. LaForge, F. B.; Barthel, W. F., Constituents of Pyrethrum Flowers. XVIII. The Structure and Isomerism of Pyrethrolone and Cinerolone. *J. Org. Chem.* **1945,** *10*, 114-120.
22. Godin, P. J.; Sleeman, R. J.; Snarey, M.; Thain, E. M., The jasmolins, new insecticidally active constituents of *Chrysanthemum cinerariaefolium*. *J. Chem. Soc.* **1966,** *C*, 332-334.
23. Crombie, L.; Hemesley, P.; Pattenden, G., Synthesis of Ketols of the Natural Pyrethrins. *J. Chem. Soc.* **1969**, 1016-1024.
24. Freemont, J. A.; Littler, S. W.; Hutt, O. E.; Mauger, S.; Meyer, A. G.; Winkler, D. A.; Kerr, M. G.; Ryan, J. H.; Cole, H. F.; Duggan, P. J., Molecular Markers for Pyrethrin Autoxidation in Stored Pyrethrum Crop: Analysis and Structure Determination. *J. Agric. Food Chem.* **2016,** *64*, 7134-7141.
25. Xu, H.; Lybrand, D.; Bennewitz, S.; Tissier, A.; Last, R. L.; Pichersky, E., Production of *trans*-chrysanthemic acid, the monoterpene acid moiety of natural pyrethrin insecticides, in tomato fruit. *Metab. Eng.* **2018,** *47*, 271-278.

26. Xu, H.; Li, W.; Shilmiller, A. L.; Eekelen, H. v.; Vos, R. C. H. d.; Jongsma, M. A.; Pichersky, E., Pyrethric acid of natural pyrethrin insecticide: complete pathway elucidation and reconstruction in *Nicotiana benthamiana*. *New Phytol.* **2019,** *223* (2), 751-765.
27. Kikuta, Y.; Ueda, H.; Nakayama, K.; Katsuda, Y.; Ozawa, R.; Takabayashi, J.; Hatanka, A.; Matsuda, K., Specific Regulation of Pyrethrin Biosynthesis in *Chrysanthemum cinerariaefolium* by a Blend of Volatiles Emitted from Artificially Damaged Conspecific Plants. *Plant Cell Physiol.* **2011,** *52* (3), 588-596.
28. Ramirez, A. M.; Yang, T.; Bouwmeester, H. J.; Jongsma, M. A., A Trichome-Specific Linoleate Lipoxygenase Expressed During Pyrethrin Biosynthesis in Pyrethrum. *Lipids* **2013,** *48*, 1005-1015.
29. Li, W.; Zhou, F.; Pichersky, E., Jasmone Hydroxylase, a Key Enzyme in the Synthesis of the Alcohol Moiety of Pyrethrin Insecticides. *Plant Physiol.* **2018,** *177*, 1498-1509.
30. Kikuta, Y.; Ueda, H.; Takahashi, M.; Mitsumori, T.; Yamada, G.; Sakamori, K.; Takeda, K.; Furutani, S.; Nakayama, K.; Katsuda, Y.; Hatanaka, A.; Matsuda, K., Identification and characterization of a GDSL lipase-likeprotein that catalyzes the ester-forming reaction for pyrethrinbiosynthesis in *Tanacetum cinerariifolium* – a new target for plant protection. *Plant J.* **2012,** *71*, 183-193.
31. Hitmi, A.; Coudret, A.; Barthomeuf, C., The Production of Pyrethrins by Plant Cell and Tissue Cultures of *Chrysanthemum cinerariaefolium* and *Tagetes* Species. *Crit. Rev. Biochem. Mol. Biol.* **2000,** *35*, 317-337.
32. Yang, T.; Stoopen, G.; Wiegers, G.; Mao, J.; Wang, C.; Dicke, M.; Jongsma, M. A., Pyrethrins Protect Pyrethrum Leaves Against Attack by Western Flower Thrips, *Frankliniella occidentalis*. *J. Chem. Ecol.* **2012,** *38*, 370-377.
33. Brewer, J. G., Microhistological examination of the secretory tissue in pyrethrum florets. *Pyrethrum Post* **1973,** *12*, 17-22.
34. Chen, M.; Du, Y.; Zhu, G.; Takamatsu, G.; Ihara, M.; Matsuda, K.; Zhorov, B. S.; Dong, K., Action of six pyrethrins purified from the botanical insecticide pyrethrum on cockroach sodium channels expressed in *Xenopus* oocytes. *Pest. Biochem. Physiol.* **2018,** *151*, 82-89.
35. Davies, T. G. E.; Field, L. M.; Usherwood, P. N. R.; Williamson, M. S., DDT, Pyrethrins, Pyrethroids and Insect Sodium Channels. *IUBMB Life* **2007,** *59* (3), 151-162.

36. Atkinson, B. L.; Blackman, A. J.; Faber, H., The Degradation of the Natural Pyrethrins in Crop Storage. *J. Agric. Food Chem.* **2004,** *52*, 280-287.
37. Sudakin, D. L., Pyrethroid Insecticides: Advances and Challenges in Biomonitoring. *Clin. Toxicol.* **2008,** *44*, 31-37.
38. Gnaudinger, C. B.; Corl, C. S., Studies on Pyrethrum Flowers. V. The Presence of Pyrethrolone and Methyl Pyrethrolone in the Flowers. *J. Am. Chem. Soc.* **1933,** *55* (3), 1218-1223.
39. Chen, Y.-L.; Casida, J. E., Photodecomposition of Pyrethrin I, Allethrin, Phthalthrin, and Dimethrin. *J. Agric. Food Chem.* **1969,** *17* (2), 208-215.
40. Goldberg, A. A.; Head, S.; Johnston, P., Action of Heat on Pyrethrum Extract: The Isomerisation of Pyrethrins to Isopyrethrins. *J. Sci. Food Agric.* **1965,** *16*, 43-51.
41. Casida, J. E.; Kimmel, E. C.; Elliott, M.; Janes, N. F., Oxidative metabolism of pyrethrins in mammals. *Nature* **1971,** *230*, 326-327.
42. Picone, J. M. Microbial Degradation of the Natural Pyrethrins and its Implications for Pyrethrum Cropping. Honours Thesis, University of Tasmania, **1999**.
43. Ando, T.; Toia, R. F.; Casida, J. E., Epoxy and Hydroxy Derivatives of (*S*)-Bioallethrin and Pyrethrins I and II: Synthesis and Metabolism. *J. Agric. Food Chem.* **1991,** *39*, 606-611.
44. Suzuki, Y.; Ishizaka, S.; Kitamura, N., Spectroscopic studies on the photochemical decarboxylation mechanism of synthetic pyrethroids. *Photochem. Photobiol. Sci.* **2012,** *11*, 1897-1904.
45. Elroby, S. A. K.; Aziz, S. G., Understanding the decomposition reaction mechanism of chrysanthemic acid: a computational study. *Chem. Cent. J.* **2011,** *5* (66).
46. Caboni, P.; Minello, E. V.; Cabras, M.; Angioni, A.; Sarais, G.; Dedola, F.; Cabras, P., Degradation of Pyrethrin Residues on Stored Durum Wheat after Postharvest Treatment. *J. Agric. Food Chem.* **2007,** *55*, 832-835.
47. Sasaki, T.; Eguchi, S.; Ohno, M., Studies on Chrysanthemic Acid. IV. Photochemical Behavior of Chrysanthemic Acid and Its Derivatives. *J. Org.* **1970,** *35* (3), 790-793.
48. Matsui, M.; Yamashita, K.; Miyano, M.; Kitamuka, S.; Suzuki, Y.; Hamuro, M., Studies on Chrysanthemic Acid Part III. Oxidation and Reduction Products of Chrysanthemic Acid. *Bull. Agr. Chem. Soc.* **1956,** *20* (2), 89-94.
49. Elliott, M.; Janes, N. F., Chemistry of the Natural Pyrethrins. In *Pyrethrum: The Natural Insecticide*, Casida, J. E., Ed. **1973**; pp 55-100.

50. Kawano, Y.; Yanagihara, K.; Miyamoto, T.; Yamamoto, I., Examination of the Conversion Products of Pyrethrins and Allethrin Formulations Exposed to Sunlight by Gas Chromatography and Mass Spectrometry. *J. Chromatogr. A* **1980,** *198* (3), 317-328.
51. Campbell, A.; Mitchell, W. M., An Examination of Polymerised Pyrethrins. *J. Sci. Food Agric.* **1950,** *1* (5), 137-139.
52. Head, S. W., Composition of Pyrethrum Extract and Analysis of Pyrethrins. In *Pyrethrum: The Natural Insecticide*, Casida, J. E., Ed. Academic Press, Inc.: UK, **1973**.
53. Miskus, R. P.; Andrews, T. L., Stabilization of thin films of pyrethrins and allethrin. *J. Agric. Food Chem.* **1972,** *20*, 313-315.
54. Schechter, M. S.; Green, N.; LaForge, F. B., Constituents of Pyrethrum Flowers. XXIII. Cinerolone and the Synthesis of Related Cyclopentenolones. *J. Am. Chem. Soc.* **1949,** *71*, 3164-3173.
55. Perry, A. S.; Yamamoto, I.; Ishaaya, I.; Perry, R., Synthetic Pyrethroids. In *Insecticides in Agriculture and Environmnet*, Springer: Berlin, Heidelberg, **1998**.
56. Elliott, M.; Needham, P. H.; Potter, C., The Insecticidal Activity of Substances Related to the Pyrethrins. I. The Toxicities of Two Synthetic Pyrethrin-Like Esters Relative to That of the Natural Pyrethrins and the Significance of the Results in the Bioassay of Closely Related Compounds. *Ann. Appl. Bio.* **1950,** *37*, 490-507.
57. Elliott, M.; Farnham, A. W.; Janes, N. F.; Needham, P. H.; Pearson, B. C., 5-Benzyl-3-furylmethyl Chrysanthemate: a New Potent Insecticide. *Nature* **1967,** *213*, 493-494.
58. Katsuda, Y., Progress and Future of Pyrethroids. In *Pyrethroids: From Chrysanthemum to Modern Industrial Insecticide*, Matsuo, N.; Mori, T., Eds. Springer: Berlin Heidelberg, **2012**.
59. Elliott, M.; Farnham, A. W.; Janes, N. F.; Needham, P. H.; Pulman, D. A.; Stevenson, J. H., A Photostable Pyrethroid. *Nature* **1973,** *246*, 169-170.
60. Ujihara, K., The history of extensive structural modifications of pyrethroids. *J. Pestic. Sci.* **2019,** *44* (4), 215-224.
61. Elliott, M.; Farnham, A. W.; Janes, N. F.; Needham, P. H.; Pulman, D. A., Synthetic insecticide with a new order of activity. *Nature* **1974,** *248*, 710-711.
62. Cycon, M.; Piotrowska-Seget, Z., Pyrethroid-Degrading Microorganisms and Their Potential for the Bioremediation of Contaminated Soils: A Review. *Front. Microbiol.* **2016,** *7*, 1463-1489.

63. Antwi, F. B.; Reddy, G. V. P., Toxicological effects of pyrethroids on non-target aquatic insects. *Environ. Toxicol. Pharmacol.* **2015,** *40* (3), 915-923.

64. Weston, D. P.; Holmes, R. W.; You, J.; Lydy, M. J., Aquatic Toxicity Due to Residential Use of Pyrethroid Insecticides. *Environ. Sci. Technol.* **2005,** *39*, 9778-9784.

65. Ullah, S.; Li, Z.; Zuberi, A.; Arifeen, M. Z. U.; Baig, M. M. F. A., Biomarkers of pyrethroid toxicity in fish. *Environ. Chem. Lett.* **2019,** *17*, 945-973.

66. Katagi, T., Environmental Behaviour of Synthetic Pyrethroids. In *Pyrethroids: From Chrysanthemum to Modern Industrial Insecticide*, Matsuo, N.; Mori, T., Eds. Springer: Berlin Heidelberg, **2012**.

67. Fulton, M. H.; Key, P. B.; DeLorenzo, M. E., Inseciticide Toxicity in Fish. *Fish Physiology* **2013,** *33*, 309-368.

68. Gunning, R. V.; Easton, C. S.; Balfe, M. E.; Ferris, I. G., Pyrethroid resistance mechanisms in Australia *Helicoverpa armigera*. *Pestic. Sci.* **1991,** *33* (4), 473-490.

69. Müller, P.; Warr, E.; Stevenson, B. J.; Pignatelli, P. M.; Morgan, J. C.; Steven, A.; Yawson, A. E.; Mitchell, S. N.; Ranson, H.; Hemingway, J.; Paine, M. J. I.; Donnelly, M. J., Field-Caught Permethrin-Resistant Anopheles ganbiae Overexpress CYP6P3, a P450 That Metabolises Pyrethroids. *PLoS Genetics* **2008,** *4* (11), 1-10.

70. Souza, D.; Vieira, B. C.; Fritz, B. K.; Hoffmann, W. C.; Peterson, J. A.; Kruger, G. R.; Meinke, L. J., Western corn rootworm pyrethroid resistance confirmed by aerial application simulations of commercial insecticides. *Sci. Rep.* **2019,** *9*, 6713-6723.

71. Zhu, F.; Wigginton, J.; Romero, A.; Moore, A.; Ferguson, K.; Palli, R.; Potter, M. F.; Haynes, K. F.; Palli, S. R., Widespread distribution of knockdown resistance mutations in the bed bug, *Cimex lectularius (Hemiptera: Cimicidae)*, populations in the United States. *Arch. Insect Biochem. Physiol.* **2010,** *73* (4), 245-257.

72. Liu, N., Pyrethroid Resistance in Insects: Genes, Mechanisms and Regulation. In *Insecticides - Advances in Integrated Pest Management*, Perveen, F., Ed. InTech: 2012.

73. Zheng, Z.; Wang, J.; Zhang, D.; Guan, X.; Gao, S.; Chen, Z.; Zou, X., Design, Synthesis, and Insecticidal Activities of Novel Monohalovinylated Pyrethroids. *J. Agric. Food Chem.* **2011,** *59*, 1171-1177.

74. Ferroni, C.; Bassetti, L.; Borzatta, V.; Capparella, E.; Gobbi, C.; Guerrini, A.; Varchi, G., Polyenylcyclopropane carboxylic esters with high insecticidal activity. *Pest. Manag. Sci.* **2015,** *71*, 728-736.

75. Lindstrom, A. B.; Strynar, M. J.; Libelo, E. L., Polyfluorinated Compounds: Past, Present, and Future. *Environ. Sci. Technol.* **2011,** *45*, 7945-7961.

76. Buer, B. C.; Meagher, J. L.; Stuckey, J. A.; Marsh, E. N. G., Structural basis for the enhanced stability of highly fluorinated proteins. *Proc. Natl. Acad. Sci.* **2012,** *109*, 4810-4815.

77. Zhu, Q.; Yang, Y.; Lao, Z.; Zhong, Y.; Zhang, B.; Cui, X.; O'Neill, P.; Hong, D.; Zhang, K.; Zhao, S., Synthesis, insecticidal activities and resistance in *Aedes albopictus* and cytotoxicity of novel dihaloacetylated heterocyclic pyrethroids. *Pest Manag. Sci.* **2020,** *76*, 636-644.

78. Yang, Z.-B.; Li, P.; He, Y.-J.; Luo, J.; Zhou, J.; Wu, Y.; Chen, L., Novel pyrethrin derivatives containing an 1,3,4-oxadiazole thioether moiety: Design, synthesis and insecticidal activity. *J. Heterocyclic Chem.* **2020,** *57*, 81-88.

79. Casida, J. E., Pyrethrum Flowers and Pyrethroid Insecticides. *Environ. Health Perspect.* **1980,** *34*, 189-202.

Chapter 2 Selective Reduction of the Pyrethrins

2.1 Introduction

The pyrethrum concentrate has long been an insecticide of choice due to its highly beneficial properties in terms of crop and domestic pest control but also due to its lack of impact on the environment and low toxicity to mammals.[1, 2] As previously indicated (Chapter 1; Section 1.2.3) the environmentally favourable qualities of the pyrethrum stem from the long-term instability of the individual Pyrethrin esters **5-7** under typical environmental conditions.[3-5] Despite the higher prevalence of pyrethrin I **5a** and II **5b** in the concentrate, they are the more susceptible of the six esters to these degradative processes.[3, 6] Much of this reactivity can be attributed to the conjugated pentadienyl unit of the rethrolone moiety, which allows for stabilised radical formation (Chapter 1; Section 1.3.1) and possesses an increased number of reactive functional groups relative to the minor Pyrethrins; the cinerins **6** and jasmolins **7**.[3, 7]

Jasmolin I **7a** and II **7b** only differ from their pyrethrin counterparts **5** at the terminus of the penta-carbon system of the rethrolone moiety, where jasmolin **7** is saturated at this point. It was proposed that the pyrethrum concentrate could be simplified through a chemo- and regio-selective reduction of pyrethrin I **5a** and II **5b** to jasmolin I **7a** and II **7b** (Scheme 2.1). Ultimately, this transformation would afford a redistribution of the pre-existing natural esters from a mixture of six to a simplified mixture of four. Whilst the pyrethrins **5** are the more active of the esters,[8] this redistribution would allow for a modified concentrate that retains the beneficial environmental qualities of the original pyrethrum and improves upon its long-term storage.

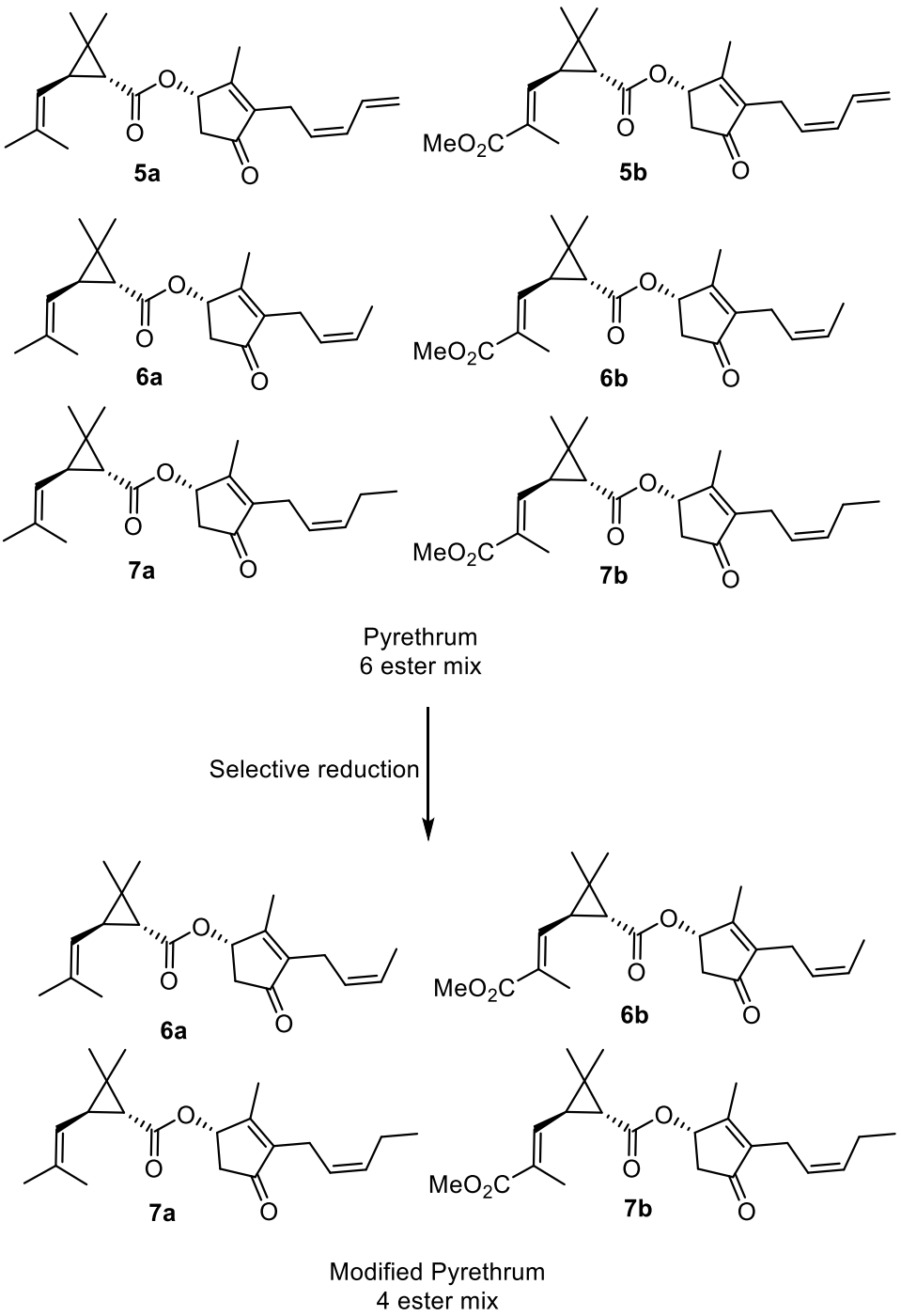

Scheme 2.1: Proposed modification of the pyrethrum concentrate, transforming pyrethrin I **5a** and II **5b** into jasmolin I **7a** and II **7b**.

Notably, the pyrethrin esters **5** have a high prevalence of unsaturated centres, with a number of carbon-carbon and carbon-oxygen multiple bonds spread throughout the skeleton (Figure 2.1) making chemo- and regio-selectivity paramount to target the terminal double bond.

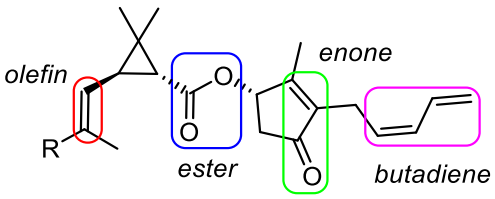

5a R = Me
5b R = CO_2Me

Figure 2.1: Functional groups within the pyrethrin scaffold susceptible to reductive modification.

In an attempt to afford this transformation of the two pyrethrins **5** into the jasmolins **7**, a number of reductive conditions were explored in this thesis. Firstly, the individual reactivity of the more sensitive pyrethrin esters **5** needed to be explored prior to implementation of the botanic extract. As such, an efficient method for the isolation of significant quantities of the individual pyrethrins **5** was necessary in order for them to be tested in the proposed selective synthetic protocols. With the purification of pyrethrins I **5a** and II **5b**, a range of reductive modifications could then be explored for the direct conversion of these into their more stable jasmolin analogues **7** prior to application on the pyrethrum concentrate. As a result, a number of reduced pyrethrin analogues were produced and subsequently subjected to preliminary insecticidal activity against a commercially relevant insect species.

2.2 Purification of the pyrethrum concentrate

The distribution of the various esters within the pyrethrum concentrate varies between growing regions however, the pyrethrins **5** are generally in the highest proportion typically comprising over half of the concentrate whilst the jasmolins **7** are in the lowest proportion.[3, 9, 10] Due to the similarity of the esters, separation of considerable quantities of the individual constituents has been difficult to achieve by cheap, conventional laboratory processes. Purification of the individual esters **5-7** has previously been accomplished, however generally for analytical scale applications or through the use of expensive equipment, like preparative HPLC.[11-15] As the reactivity of the pyrethrin esters **5** was to be explored, a method for the isolation of high purity pyrethrin I **5a** and II **5b** from the botanical concentrate was required for subsequent implementation into synthetic modifications.

2.2.1 Separating pyrethrins I from pyrethrins II

Pyrethrins II **5b-7b** are significantly more polar than their Pyrethrin I counterparts **5a-7a** due to the presence of a methyl ester functionality. This large polarity difference allows for the

well-resolved chromatographic separation of the subsets of Pyrethrins **5-7**. In particular, dry column vacuum chromatography (DCVC) is a convenient technique allowing for this purification to occur rapidly and with scalability, where gram quantities of pyrethrum concentrate can be subjected to the process at any given time. DCVC is a form of vacuum-assisted column chromatography, where controlled gradient elution can easily be accomplished.[16-18] Generally, the apparatus consists of a short silica gel column fitted to a solvent reservoir for fraction collection.[18] Small solvent fractions are then individually applied and collected through the separating funnel, where each fraction increases in percentage of the desired gradient.[16-18] DCVC is ideal for large scale separations, as is required for the pyrethrum concentrate, and allows for decreased silica and solvent consumption in comparison to typical chromatographic purifications.

Separation of 5-10 g quantities of the pyrethrum concentrate into the two Pyrethrin subsets was undertaken with DCVC. A modified version of the process described by Hutt *et. al,*[19] allowed for the Pyrethrins I **5a-7a** to be separated from Pyrethrins II **5b-7b** through gradient elution with solvent fractions of ethyl acetate in hexane. Individual fractions increased in ethyl acetate content by 1% increments from 1% to 25%. Typically, Pyrethrins I **5a-7a** were isolated over 7-14% ethyl acetate in hexane whilst Pyrethrins II **5b-7b** were eluted in 18-25% ethyl acetate in hexane. TLC analysis of the Pyrethrins II **5b-7b** fractions in 20% ethyl acetate in hexane showed that the later fractions contained purified pyrethrin II **5b** whilst earlier fractions were still mixtures. The pure fractions were combined and evaporated to dryness for subsequent use in synthetic transformations. Recycling the fractions containing Pyrethrins II **5b-7b** into the DCVC procedure allowed for increased amounts of enriched pyrethrin II **5b** to be isolated. The purified pyrethrin II **5b** was found to have a purity of 91% as determined by analytical HPLC[†] (Figure 2.2).

[†] Quoted purity is an estimate based on the area of the peaks in the HPLC chromatogram. As the impurities found in the pyrethrin I **5a** or II **5b** fractions are the closely related cinerins **6** and jasmolins **7**, the effect of the extinction co-efficients are comparable and should have little effect on the determination of purity.

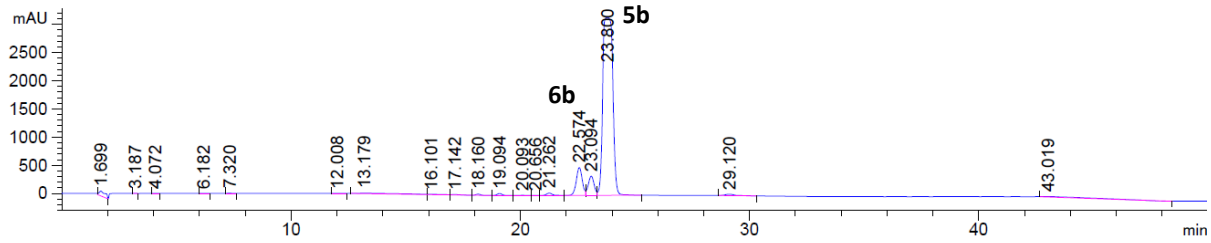

Figure 2.2: HPLC trace (C18, 235 nm) of enriched pyrethrin II **5b** purified by DCVC with pyrethrin II **5b** eluting at 23.8 min.

Conversely, TLC analysis of the Pyrethrins I **5a-7a** fractions showed that all fractions contained a mixture of the three Pyrethrin I esters **5a-7a**. The isolation of solely mixed Pyrethrins I **5a-7a** required further purification by a more controlled process. Therefore, these fractions were combined and evaporated to dryness for subsequent purification of pyrethrin I **5a** by silica gel column chromatography.

2.2.2 Column chromatography of Pyrethrins I mixtures

Following separation of the two pyrethrin subsets, the Pyrethrins I **5a-7a** mixture required further purification to give individual pyrethrin I **5a** for subsequent use in synthetic processes. Previously, the individual Pyrethrins **5-7** have been purified through preparative HPLC however, this process yields small amounts at high cost.[3] Alternatively, pyrethrin I **5a** can be separated from the two minor constituents through careful column chromatography on silica gel.[19] Early attempts at purification of pyrethrin I **5a** from the mixture made use of conventional silica gel column chromatography with elution achieved by a solvent gradient similar to Hutt *et. al.*[19] In these instances, it was difficult to obtain significant quantities of pure pyrethrin I **5a** due to the similarity in retention factors between the three components and the tendency for these esters to overlap however, small quantities of pure pyrethrin I **5a** could be obtained.

Alternatively, pyrethrin I **5a** can be isolated with high purity using a silica gel multibore, or tiered, column.[19] In this case a three-tiered glass column was employed, with each tier decreasing in diameter by 1 cm from the tier above, and an isocratic eluting solvent of 8% ethyl acetate in hexane. The multibore column significantly reduces the amount of solvent used and the time taken for the separation to occur whilst also increasing the resolution of the separation.[20, 21] The largest tier serves a capacity type purpose where it accommodates the amount of material loaded onto the column, with the following tiers acting to increase

resolution/separation.[20] The increased yield of purified pyrethrin I **5a** was thought to be a result of elongation of the individual component bands as they move through each tier of the column. This elongation stretches the individual bands, allowing for fractions of increased purity to be obtained after the point of fraction overlap. Using this method pyrethrin I **5a** was able to be isolated in synthetically useful quantities with a purity of 91%, as determined by HPLC analysis[‡](Figure 2.3).

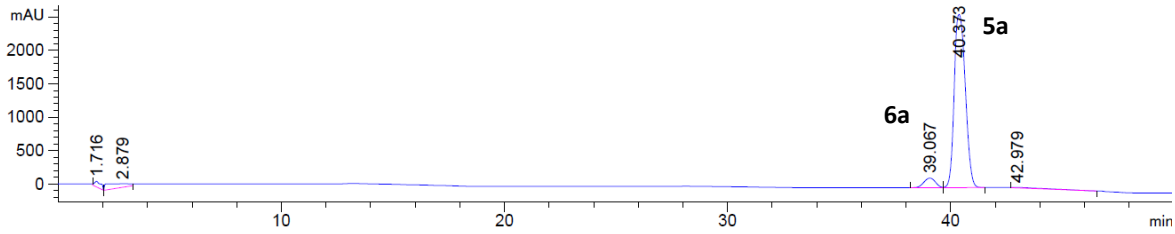

Figure 2.3: HPLC trace (C18, 235 nm) of enriched pyrethrin I **5a** purified by three-tiered column chromatography with pyrethrin I **5a** eluting at 40.37 min.

With the isolation of gram-scale quantities of pyrethrin I **5a** and II **5b**, the implementation of reductive protocols in the pursuit of a transformation to the more stable jasmolins **7** could be investigated.

2.3 Reduction with organoboranes and borohydrides

A range of different reduction reactions were investigated in an attempt to elicit the desired transformation of the less stable, more abundant pyrethrins **5** to their jasmolins equivalents **7**. Initial reactions implemented reductive protocols employing organoboranes, particularly those with bulky substituents in an attempt to mediate the selectivity.

2.3.1 Hydroboration-protonolysis

The electrophilic addition of boranes across carbon-carbon multiple bonds has long been a useful synthetic manipulation, particularly for monohydroxylation of alkenes.[22] Generally, the hydroboration of double bonds is successively followed by oxidation, however, the intermediate organoborane can be cleaved through protonolysis with an organic acid ultimately achieving a formal reduction of the unsaturated centre.[23, 24] This hydroboration-

[‡] Quoted purity is an estimate based on the area of the peaks in the HPLC chromatogram. As the impurities found in the pyrethrin I **5a** or II **5b** fractions are the closely related cinerins **6** and jasmolins **7**, the effect of the extinction co-efficients are comparable and should have little effect on the determination of purity.

protonolysis process was promising for the transformation of pyrethrin I **5a** and II **5b** into jasmolin I **7a** and II **7b** respectively. In order to achieve the desired reactivity, a number of constraints were implemented in the attempt to increase selectivity for the terminal double bond of the pentadienyl system.

A significant number of boranes are commercially available or can be prepared *in situ* for immediate reaction with the desired substrate. Due to the number of reducible functional groups within the pyrethrin structure (Figure 2.1), the regioselectivity and chemoselectivity of the borane needed to be tuned for the pursuit of jasmolin **7** production so as to address the selectivity criteria. In order for these conditions to be met, a borane with decreased reactivity and large steric hinderance was of particular interest. Both of these requirements could be met by implementing a disubstituted borane, where the substituents are significantly bulky to prevent reactivity at hindered sites of the pyrethrin scaffold. Substituted boranes have a decreased number of reactive sites allowing for increased control and selectivity in hydroboration reactions.[23] Provided the substituents on the chosen borane are of sufficient size, the regioselectivity of the hydroboration event can be manipulated to occur at the least hindered position of the pyrethrin **5**, more specifically the terminal alkene of the pentadienyl unit.

Disiamylborane **50** possesses the desired steric hindrance and singular site of reactivity due to its branched alkyl substituents and a documented history of chemoselective and regioselective hydroboration of alkenes.[25, 26] Due to its air and moisture sensitivity, disiamylborane **50** is generally prepared directly prior to use (Scheme 2.2), ensuring optimal reactivity with the alkene substrate. Prior to the hydroboration-protonolysis of the pyrethrins **5**, disiamylborane **50** was prepared from a 2 M 2-methylbut-2-ene **48** THF solution and a 1 M borane-THF **49** solution at 0 °C giving the hindered organoborane as a 0.5 M solution.

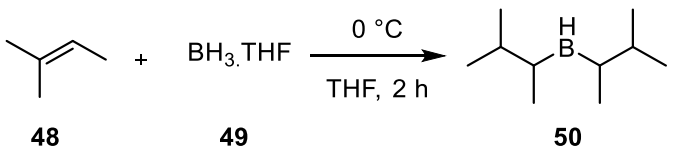

Scheme 2.2: Generation of the hydroborating reagent, disiamylborane 50.

The 0.5 M disiamylborane **50** solution could then be utilised in reactions with either pyrethrin I **5a** or II **5b** in an attempt to produce jasmolin I **7a** and II **7b** respectively. Typically, one

equivalent of disiamylborane **50** was added to the pyrethrin **5** in dry THF at room temperature under an inert atmosphere. The resulting solution was stirred for a further 5 h to allow for hydroboration and was subsequently treated with acetic acid to elicit protonolysis. The acidic solution was left for an additional 1 h before being quenched with sodium bicarbonate solution and was extracted with ethyl acetate. A crude oil was obtained with ^{1}H NMR analysis indicating a mixture of reduction products and evidence of some pyrethrin **5** starting material. The desired jasmolin **7** product was not indicated in the analysis of the isolated mixture, instead it was observed that the entirety of the pentadienyl moiety had been affected giving what appeared to be full saturation. Organoborane intermediate(s) of the pyrethrin starting material **5** were suggested to be a part of the isolated mixture due to the number of disiamyl resonances in the ^{1}H NMR spectrum however, their identity could not be fully elucidated. The presence of these organoborane intermediate(s) suggest the protonolysis procedure to be inefficient for complete conversion to the reduced material(s) however, attempts to remedy this by altered reaction times and temperatures were unsuccessful and the crude mixture of materials was also unable to be purified by column chromatography. An alternative borane reagent with increased steric hinderance and availability was proposed to prevent the aforementioned multiple reduction events from taking place.

The bicyclic, caged structure of 9-borabicyclo-[3.3.1]-nonane (9-BBN) was deemed to be of significant steric hinderance to impede access to alternate sites of reactivity within the pyrethrins **5** and possesses the pre-existing criteria necessary for selectivity. The commercial availability and decreased sensitivity to moisture of 9-BBN eliminated the need to prepare the reagent directly prior to use and minimised decomposition with handling. 9-BBN has previously been used specifically for the monohydroboration of conjugated dienes with the reaction showing preference for the least hindered site of the double bond.[27] This described regioselectivity of 9-BBN suggested its further potential in the selective reaction with pyrethrins **5** at the terminal position of the pentadienyl unit. A commercial 0.5 M solution of 9-BBN in THF was used in place of the disiamylborane solution described above with the isolated oil resulting from this hydroboration-protonolysis procedure identified as a mixture by NMR analysis. The presence of the alkene resonances of the pentadienyl unit suggested recovery of starting material whilst the large abundance of aliphatic hydrocarbon signals suggested the presence of organoborane intermediate as well as any residual 9-BBN that

remained unquenched. ^{11}B NMR spectroscopy was implemented as a qualitative analysis to determine if the isolated material contained residual hydroborating reagent or unreacted intermediate organoborane. The ^{11}B NMR spectrum exhibited three distinct resonances, all within the alkylborane region,[28] likely due to the presence of residual 9-BBN, quenched borane and potential organoborane intermediate(s). As such, it was suspected that the protonolysis procedure was not rigorous enough to elicit efficient cleavage of the intermediate and so, the hydroboration-protonolysis procedure was amended. Instead, the hydroboration was monitored by TLC until the pyrethrin material **5** appeared to be completely consumed (~5-7 h) and the subsequent protonolysis was run at elevated temperatures. The resulting oil was observed to be free from boron species suggesting complete protonolysis of the hydroborated species. Nevertheless, ^{1}H NMR analysis revealed that the alkene signals of the pentadienyl unit were still present in the resulting mixture, signifying the hydroboration event proceeded with alternate reactivity than desired.

The ^{13}C NMR spectrum exhibited a lack of a ketone resonance at 203 ppm, suggesting that reactivity was localised to the cyclopentenone of the rethrolone moiety. Ultimately, two products were able to be separated from the mixture of both pyrethrins **5** by column chromatography. One of the two products was readily identified as the allylic alcohol **51** through typical characterisation in yields of 15-19%. The ^{1}H NMR spectrum revealed the isolation of a single diastereomer from the reaction with 2D nOe correlation (Figure 2.4) used to determine the stereochemical configuration. The isolated stereoisomer of the allylic alcohol **51** showed a direct correlation between the 4′ proton and the 1′ proton suggesting they are on the same face of the cyclopentene which would give an (*R*)-configuration at the 4′ position.

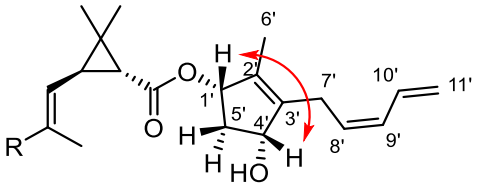

(4'*R*)-stereoisomer

(4'*R*)-51a R = Me
(4'*R*)-51b R = CO_2Me

Figure 2.4: nOe correlation, indicated by the red arrow, for the allyl alcohol **51** isolated from the hydroboration-protonolysis of pyrethrin **5**.

This stereoselectivity is likely to stem from the steric hindrance of the bulky bicyclic structure of 9-BBN and the bulk of the ester substituent at the pre-existing 1′ stereocentre. The second product was isolated as what appeared to be a mixture, potentially of stereoisomers. Infra-red spectroscopy indicated the presence of a second carbonyl-containing functionality within the structure and yet lacked the characteristic –OH stretch (>3000 cm^{-1}) of an alcohol. Mass spectrometry showed a protonated molecular ion corresponding to the molecular mass of the pyrethrin starting material **5** with an additional 43 *m/z*. This, in conjunction with the lack of ketone resonance in the ^{13}C NMR spectrum, implicates potential esterification/substitution of the newly formed pyrethrin alcohol **51** with the acetic acid used for protonolysis resulting in the corresponding allyl acetate **52** (Scheme 2.3).

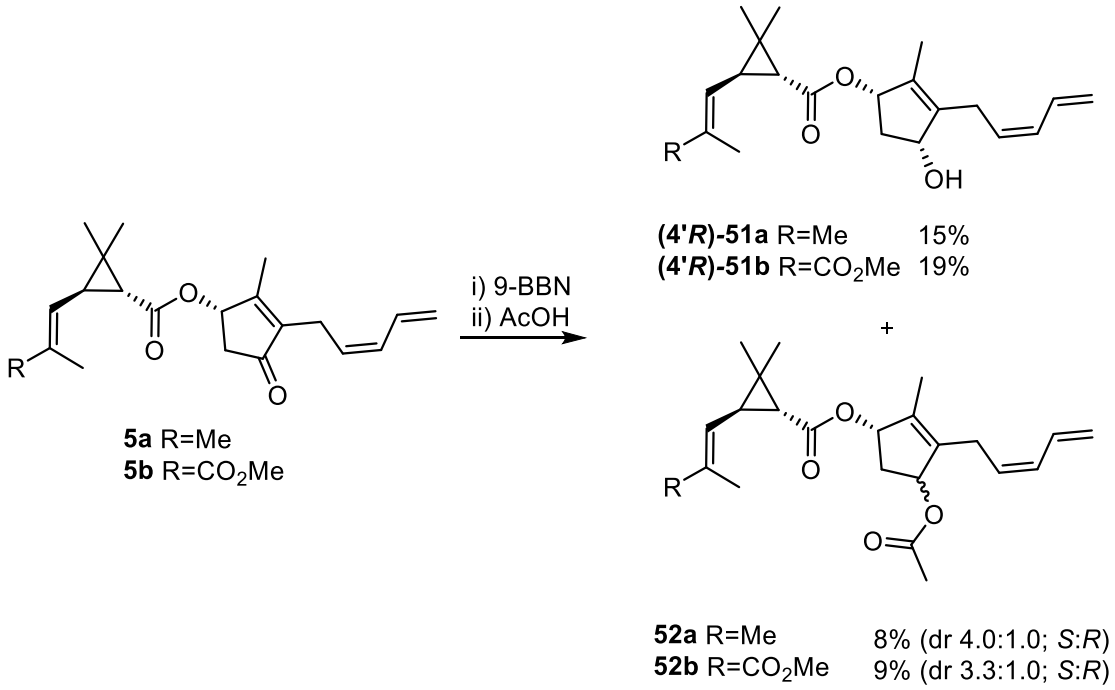

Scheme 2.3: Hydroboration-protonolysis of pyrethrins **5** giving allylic alcohols **51** and allylic acetates **52**.

In contrast, the allyl acetates **52** were isolated as a diastereomeric mixture in typical yields of 8-9%, which were later shown to have the *(S)*-isomer (Section 2.3.2) constituting the majority of the mixture (dr **52a** 4.0:1.0, dr **52b** 3.3:1.0) by comparison to purified allyl acetate **52** diastereomers. Attempts to resolve the two stereoisomers by column chromatography were unsuccessful and as such the allyl acetates **52** were characterised as the diastereomeric mixture.

This observed chemoselectivity for the enone, rather than the desired alkene, is proposed to be due to the electron deficiency of the boron in the 9-BBN hydroborating reagent and the large electron density of the carbonyl oxygen atom. In fact, it has been documented that 9-BBN exhibits chemoselective reactivity with aldehydes, ketones and their α,β-unsaturated variants in the presence of other reactive functional groups to give the corresponding alcohol.[29, 30] Some of the newly generated alcohol can subsequently esterify with the excess acetic acid under the harsh reflux conditions employed for the protonolysis of the intermediate organoborane, giving the observed acetate esters **52**. Despite the undesired reactivity, the enone reduction products were promising for the exploration into structure-activity relationships of pyrethrin-like materials. As such, efficient production of the allyl alcohol **51** and allyl ester **52** was pursued to acquire sufficient quantities for application in biological activity testing.

2.3.2 Production of pyrethrin allyl alcohols and allyl acetates with borohydrides

Borohydride reagents have been used for a range of reductive protocols including the chemoselective reduction of carbonyl functionality, particularly aldehydes and ketones.[31] Sodium borohydride ($NaBH_4$) was proposed as an appropriate reducing agent for the efficient conversion of pyrethrin **5** to the allylic alcohol **51** by direct carbonyl reduction without affecting the ester functionality present (Scheme 2.4). Typical reaction conditions with sodium borohydride and enone substrates can result in a mixture of both the 1,2- and 1,4-reduction producing the allyl alcohol or saturated ketone respectively.[32] However, using sodium borohydride in a 10% methanol in THF blend has previously been shown to favour the 1,2-reduction process to give higher quantities of the allylic alcohol product.[33] Stirring the desired pyrethrin starting material **5** in a solution of sodium borohydride in a 10% methanol-THF solvent blend at 0 °C under inert atmosphere resulted in nearly quantitative conversion to the allyl alcohol **51** as a mixture of diastereomers.

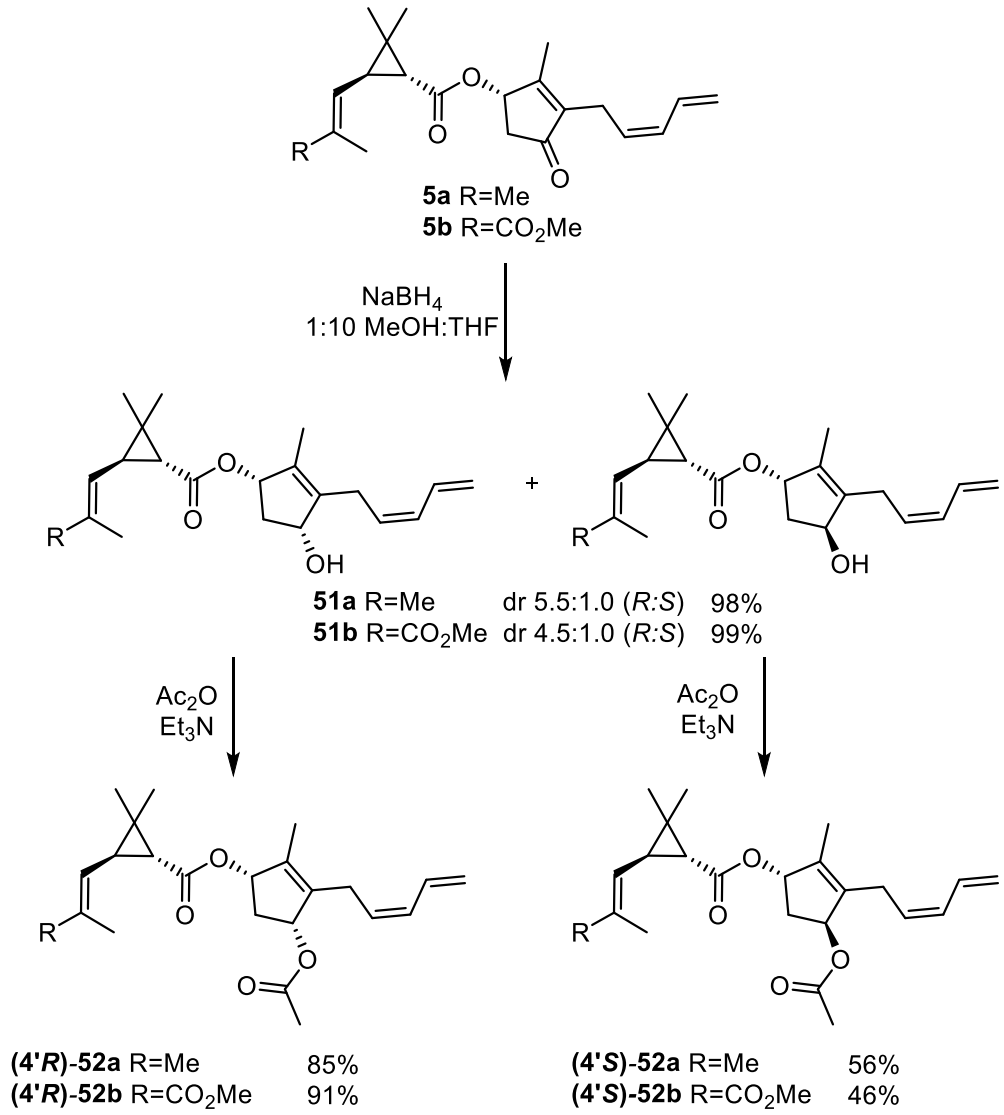

Scheme 2.4: Efficient production of allyl alcohols **51** and subsequent esterification giving the allyl esters **52**.

The individual stereoisomers could readily be resolved by column chromatography and subsequent analysis by nOe spectroscopy was undertaken to assign the configuration at the newly formed stereocentre. Much like the hydroboration process, the 4′ (*R*)-stereoisomer was found to be formed as the major constituent. The alternate 4′(*S*)-stereoisomer of the allylic alcohol **51** was determined to be the minor constituent with the 4′ proton correlating through the 5′ proton(s) to the 1′ proton on the opposite face of the ring (Figure 2.5).

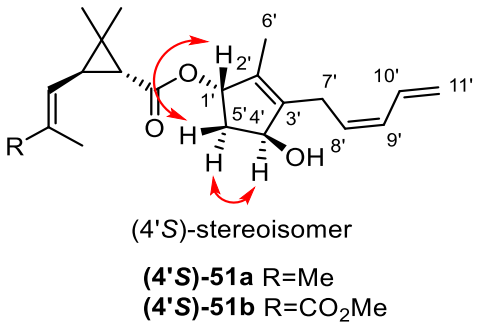

Figure 2.5: NOe correlations, as indicated by the red arrows, for the determination of (4′*S*)-configuration of the allyl alcohol **51**.

This 1,2-enone reduction showed reasonable stereoselectivity for the (4′*R*)-stereoisomer with diastereomeric ratios of 5.5:1.0 and 4.5:1.0 for pyrethrin I **5a** and II **5b** respectively. This moderate stereoselectivity observed can be attributed to the pre-existing (1′*S*)-stereocentre and the steric bulk associated with the ester substituent. The chrysanthemic ester moiety likely imparts significant bulk to hinder access by the borohydride reagent on the *re* face of the carbonyl.

This observed stereoselectivity with a relatively small reagent was believed to be potentially enhanced by employing a larger borohydride reagent. Employing L-selectride as the reducing agent was able to afford only the (4′*R*)-diastereomer of the allyl alcohol **51** in yields of 20-38% depending on the pyrethrin starting material **5** (Scheme 2.5).

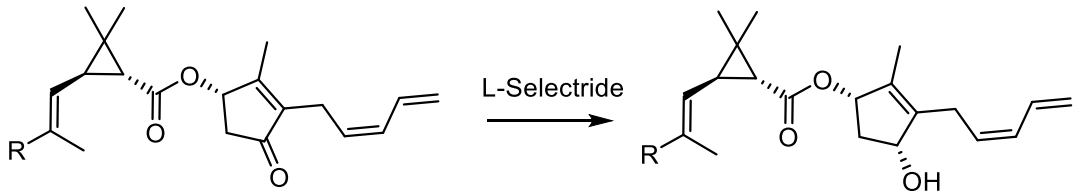

Scheme 2.5: Stereoselective reduction of the pyrethrins **5** with L-Selectride giving the (4′*R*)-stereoisomer of the allylic alcohol **51**.

The (4′*S*)-stereoisomer was not observed in crude reaction mixtures or isolated from the chromatographic process. Yields of the allyl alcohol **51** were significantly reduced in comparison to the sodium borohydride reaction which is likely due to the increased reactivity of L-selectride. Whilst the tri-*sec*-butyl substituents of L-selectride give significant steric

hinderance they also inductively activate the borohydride, ultimately making it more reactive, which can result in ester reduction.

These individual diastereomers of the allylic alcohol **51** could then be utilised to furnish the individual stereoisomers of the allylic esters **52** (Scheme 2.4) allowing for the exploration into the effect of stereochemical configuration at the 4' position on insecticidal activity. Each of the individual allylic alcohol **51** diastereomers were subjected to typical acetylation procedures using acetic anhydride in the presence of triethylamine to afford the allyl esters **52**. The (4'*R*)-allyl esters **52** were furnished in high yields of 85-91% whilst the (4'*S*)-allyl esters **52** were obtained in lower yields of 46-56%.

Despite these attempts at double bond selectivity with boron reducing agents, the desired transformation from pyrethrin **5** to jasmolins **7** was unable to be elicited. Alternatively, the chemoselective reduction of the enone moiety in a 1,2-fashion was able to produce both the allyl alcohol **51** and allyl acetate **52** of the pyrethrins **5** with the isolation of both of the possible diastereomers. In the pursuit of jasmolins **7** from pyrethrins **5**, hydrogenation protocols were explored as a means to elicit this change.

2.4 Hydrogenation of pyrethrins

The most conventional processes for the reduction of unsaturated moieties have been various forms of hydrogenation, whether through direct use of hydrogen gas or by hydrogen donor molecules.[34] Previous reduction of the pyrethrum extract (Scheme 2.6), before the identification of the jasmolins **7**, made use of catalytic hydrogenation protocols to give the tetrahydropyrethrins **53** and dihydrocinerins **54**.[35]

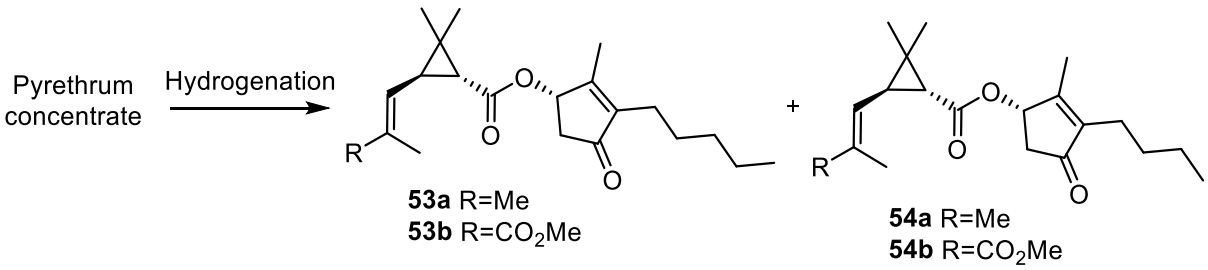

Scheme 2.6: Previous hydrogenation of pyrethrum concentrate giving the tetrahydropyrethrins **53** and dihydrocinerins **54**.[35]

Both the individual reduced esters and the hydrogenated mixtures were tested for their activity against the domestically relevant housefly (*Musca domestica*) where they showed a

significant lack of bioactivity in comparison to the original pyrethrum.[35, 36] Despite this, no attempt has been made to modulate this reductive protocol in the pursuit of selective reactivity on the terminal double bond of pyrethrins I **5a** and II **5b** to produce their jasmolin **7** equivalents.

2.4.1 Catalytic hydrogenation

Catalytic hydrogenation with hydrogen gas has served as a reliable method for the reduction of alkenes to their respective alkanes and can be achieved under relatively mild conditions.[37] Due to the undesired chemoselectivity observed with borane/borohydride reagents, hydrogenation became of interest for the specific reduction of the carbon-carbon double bond(s) in the pyrethrins **5** with potential for controlled, regioselective reduction of the terminal site. The sensitive nature of the pyrethrins **5** and the desire to achieve regioselective reduction required tailoring of the reaction conditions so as to minimise undesired reactivity. In this case, all hydrogenation protocols were performed at room temperature and atmospheric pressures of hydrogen gas to not only prevent the degradation of pyrethrin(s) **5** but also to attempt to regulate the reductive process. Direct hydrogenation can be carried out with a range of catalysts including both homogeneous and heterogeneous variants. In this case, palladium on carbon (Pd/C) was used due to its ready availability, relatively cheap cost in comparison to other metallic catalysts and its heterogeneous nature, allowing easy removal and reuse.[37] In an effort to further control this process, a range of catalyst loadings from 1-10 wt% Pd/C and the time of exposure to the hydrogen were explored.

Initially, the reaction mixtures were exposed to hydrogen for 4 h at room temperature in the presence of Pd/C with variation in the catalyst loading. Despite this attempt to control the regioselectivity by altering the amount of palladium available for catalysis, all reaction outcomes resulted in the isolation of the tetrahydropyrethrins **53** (Scheme 2.7). Tetrahydropyrethrin I **53a** and II **53b** were able to be isolated in high yields of 83% and 97% respectively with catalyst loading of 10 wt% and 1 wt% Pd/C respectively. Reducing the reaction time with the lowest catalyst loading (1 wt% Pd/C) was explored as a means of limiting the reaction process to attempt to isolate a semi-reduced product, however in most cases the tetrahydropyrethrins **53** were the only product isolated.

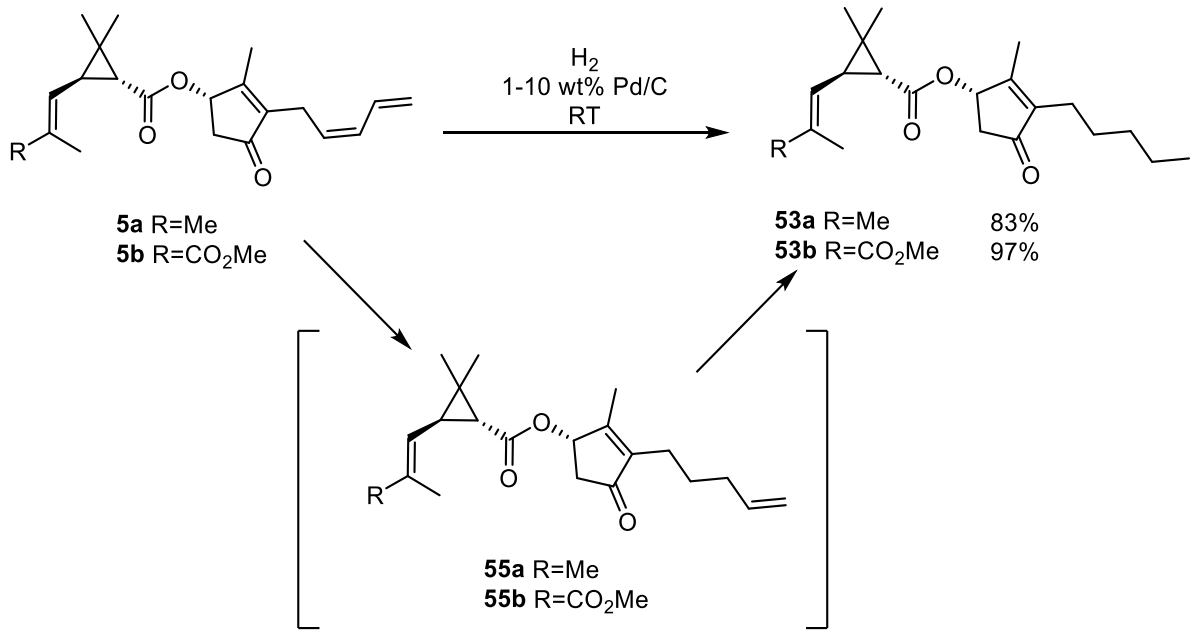

Scheme 2.7: Hydrogenation of pyrethrins **5** resulting in full saturation of the pentadienyl unit.

Despite these extensive attempts to further minimise the reactivity of the hydrogenation process, only small amounts of a semi-reduced analogue were implicated by ^{1}H NMR in a mixture with tetrahydropyrethrin **53** after 2 h with a 1 wt% Pd/C loading. This semi-reduced analogue was proposed to be a dihydropyrethrin **55** where the *cis*-alkene of the side chain was reduced whilst the terminal position remained intact (Scheme 2.7). Unfortunately, this dihydropyrethrin **55** was unable to be purified from the tetrahydropyrethrin **53** preventing further analysis and subsequent application into bioactivity testing.

This rapid over reduction of the pentadienyl moiety of pyrethrins **5** under typical hydrogenation conditions could potentially be overcome by more controlled reduction procedures. As such, transfer hydrogenation became a focus as a way of limiting the amount of hydrogen in the system through stoichiometric control of the hydrogen donor.

2.4.2 Transfer hydrogenation

The stoichiometric control of the amount of hydrogen within the system imposed by transfer hydrogenation processes was proposed to allow for a more regulated reduction process to potentially target the terminal double bond of pyrethrins **5**. This increased control is derived from the use of an organic molecule as hydrogen donor where the amount of hydrogen available is limited by the stoichiometric addition of said donor.[34] Ideally, addition of the hydrogen donor as one equivalent of hydrogen and the more step-wise addition of hydrogen

to the double bonds would allow for the desired regioselectivity without further reaction taking place.

Cyclohexene and cyclohexadiene are ideal hydrogen donors due to their well-documented use, availability and, the volatility of them and their common oxidation product benzene.[34, 38, 39] Initial attempts at transfer hydrogenation reactions made use of cyclohexene as the hydrogen donor in the presence of Pd/C at reflux in THF. Unfortunately, no reaction was observed with the recovery of only pyrethrin starting material **5** from the reaction mixtures. Cyclohexadiene was then used to replace cyclohexene as hydrogen donor due to its increased reactivity under transfer conditions.[38] Despite this change, the pyrethrins **5** were still recovered from the reaction unchanged. Typically, these hydrogen donors require higher temperatures to elicit the reduction at sufficient rates, which are not achievable with the thermally sensitive pyrethrins **5**.[39] As such, an alternative hydrogen donor was sought to elicit the desired change with the milder conditions employed.

Formic acid acts as hydrogen donor through thermal decomposition in the presence of a palladium catalyst to give the reducing species and CO_2. Direct incorporation of formic acid into the previous methodology was able to elicit a response from the pyrethrins **5** unlike the cyclohexene/cyclohexadiene protocols (Scheme 2.8). However, instead of the desired reduction it was observed that the alkeneswere affected by both *cis-trans* isomerism and migration events. Both the *trans*-pyrethrins **34** and double bond migration isomers **25** were readily separated by column chromatography giving yields of 9-14% and 15-19% respectively.

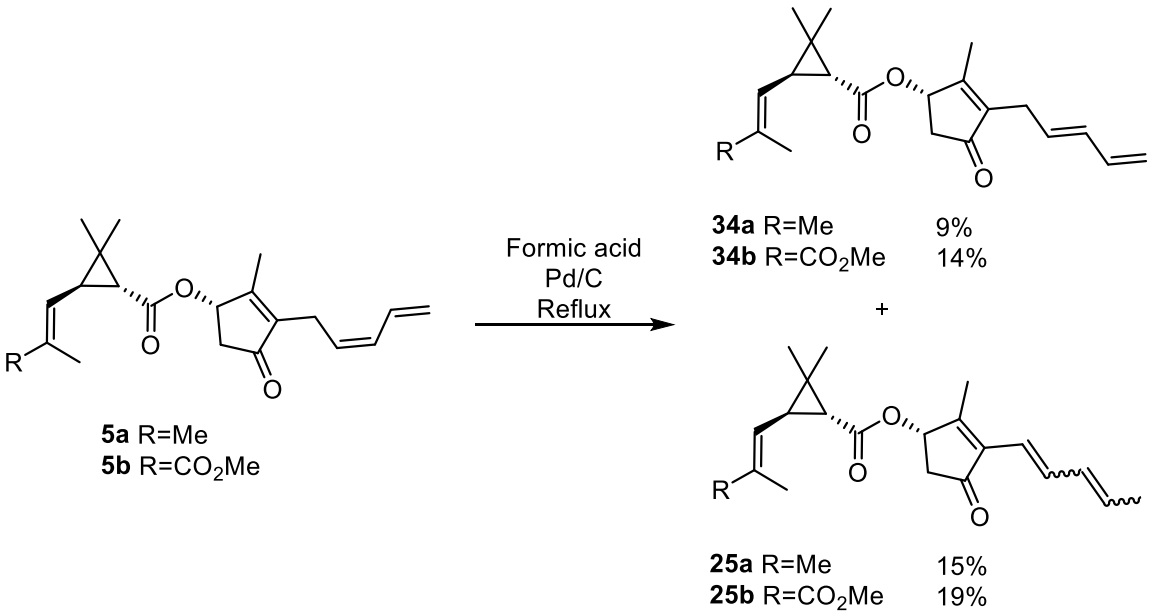

Scheme 2.8: Alkene isomerism and migration of pyrethrins **5** under transfer hydrogenation conditions with formic acid as hydrogen donor.

The observed reactivity is limited to the Pd/C-formic acid system with exploration into catalysts including platinum on carbon and palladium hydroxide yielding no reaction. Alternatively, controls without the catalyst and/or the formic acid resulted in recovery of the pyrethrin starting material **5**, eliminating solely thermal processes for the isomerism observed. Instead it is likely that the palladium hydride species formed as a result of the formic acid decomposition produces the observed changes (Scheme 2.9). The resultant active palladium hydride species, formed by the decomposition of the formic acid hydrogen donor,[40] can hydropalladate across the double bond(s) to give an intermediate organopalladium species **56**.[41, 42] This organopalladium species **56** then has the capacity to undergo free rotation about the previously unsaturated bond. Subsequent β-hydride elimination reinstalls the double bond ultimately giving the *trans*-isomer (Scheme 2.9, red arrows).[43] Alternatively, the β-hydride elimination can take place with the 7′ position resulting in migration of the double bond (Scheme 2.9, green arrows).[40]

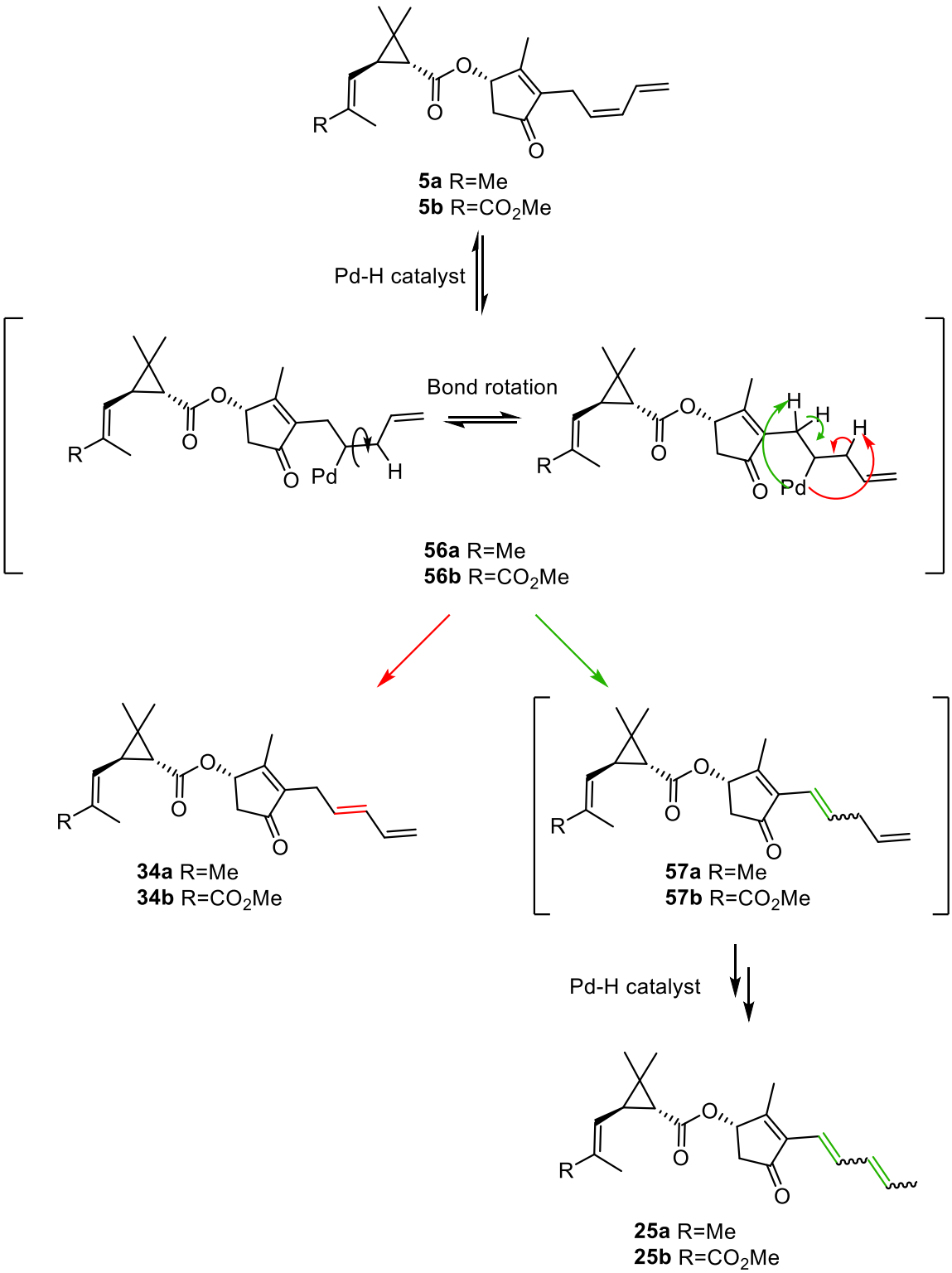

Scheme 2.9: Alkene isomerism by palladium hydride species formed under transfer hydrogenation conditions.

A second migration event shifts the terminal double bond giving isopyrethrins **25** placing the diene into complete conjugation with the enone. The intermediate migration isomer **57** was not observed, likely due to the increased resonance stability of the isopyrethrins **25**.

The isomerism process, whether *cis-trans* or migratory, was inefficient for the production of larger quantities of the isomers **34** and **25** with low yields after 8 h reaction times and significant recovery of pyrethrin starting material **5**. However, sufficient quantities were obtained to allow for biological activity testing. These transfer hydrogenation protocols were unable to elicit the desired transformation of pyrethrin **5** to jasmolin **7** leading to exploration of an alternate transfer procedure.

2.4.3 Diimide mediated transfer hydrogenation

Alternate means of transfer hydrogenation exist outside of these catalytic processes including reduction by short-lived species such as diimide. Diimide is a highly chemoselective reducing agent that specifically reduces unpolarised π-bonds such as alkenes, alkynes and diazenes.[44] Additionally, diimide reductions exhibit some regioselectivity due to the decrease in reaction rate with increasing substitution around the unsaturated site, making exposed terminal double bonds most susceptible.[45] The transient nature of diimide requires its generation *in situ* which can be achieved through a number of nitrogenous reagents. Some of the more common methods include the thermal decomposition of sulfonylhydrazides, decarboxylation of azodicarboxylates in acidic conditions or, the catalytic oxidation of hydrazine.[44] In this case, hydrazine oxidation was deemed ideal for the generation of diimide due to its ready accessibility, inexpensive reagent(s) and mild reaction conditions. These favourable reaction characteristics were deemed ideal for the site-specific reduction of pyrethrins **5** to their corresponding jasmolins **7**.

Initial attempts to produce diimide through the oxidation of hydrazine made use of potassium periodate as oxidant with catalytic quantities of copper(II) sulfate and acetic acid. The periodate was added in portions to a solution of the appropriate pyrethrin **5** with the corresponding catalytic material and hydrazine monohydrate in ethanol. Following complete addition of the oxidant, the reaction was left to stir at room temperature up to 2 h before removal of the insoluble inorganic material. The desired reaction product was identified in the ^{1}H NMR analysis of the crude material with the presence of jasmolins **7** as determined by comparison to the spectroscopic data of the naturally isolated ester. However, significant quantities of the pyrethrin starting material **5** remained in the mixture with conversions to jasmolin **7** up to 75%. The similar retention of pyrethrin **5** and jasmolins **7** in column chromatography made it difficult to give pure jasmolins **7** and as such higher conversions

would be preferred. The addition of up to 5 eq of periodate salt to the reaction in small portions can result in the ready over oxidation of the hydrazine to dinitrogen without the reactive diimide forming and as such a more steady means of diimide release was deemed likely to limit this process.

The oxidation of hydrazine can also be elicited through exposure to atmospheric oxygen allowing for the generation of the reductive species simply through stirring of the material open to air.[46, 47] Individual pyrethrins I **5a** and II **5b** could be subjected to conditions where the reaction mixture, with the same catalytic residues and presence of hydrazine, was simply stirred vigorously open to the atmosphere allowing for the steady production of diimide (Scheme 2.10). Monitoring the reaction by TLC, it was found that after approximately 8 h all of the pyrethrin starting material **5** was consumed and the equivalent jasmolins **7** were produced. The isolated material gave mass yields of 77% and 83% for pyrethrins I **5a** and II **5b** respectively with spectroscopic characterisation confirming their identity by comparison to the natural jasmolins **7**. However, HPLC analysis (Figure 2.6) revealed an unknown impurity, that did not correspond to any of the natural Pyrethrins **5-7**, eluting at 48.9 and 32.8 min for the reactions of pyrethrin I **5a** and II **5b** respectively. This unknown material was found to constitute approximately 25% of the isolated mixture in each of the individual diimide-mediated reductions.

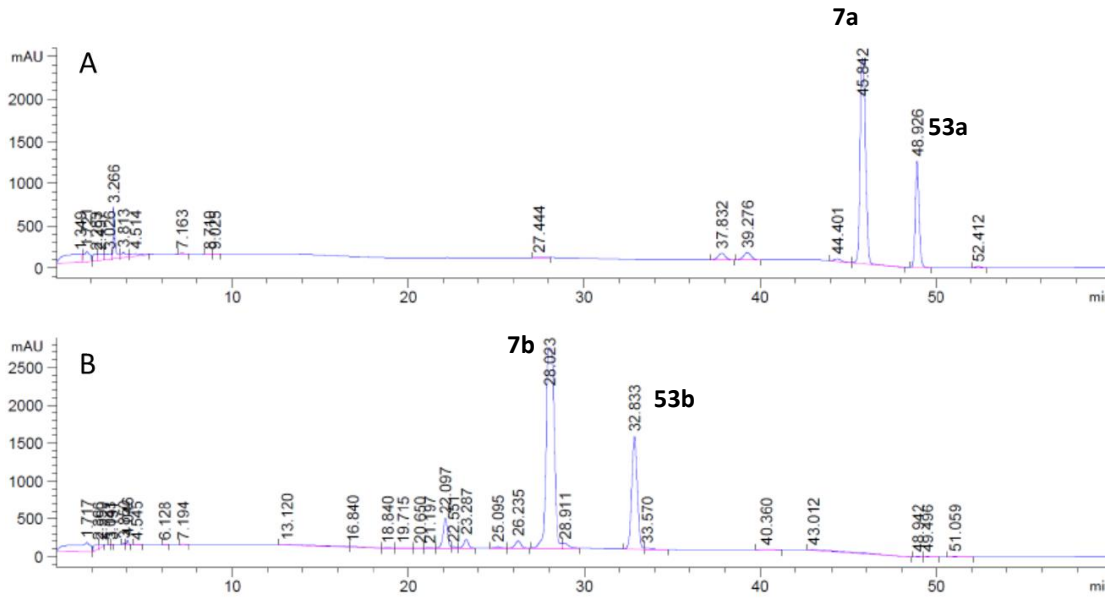

Figure 2.6: HPLC analysis (C18, 235 nm) of the diimide reduction of pyrethrins **5** resulting in jasmolin I **7a (A)** and jasmolin II **7b (B)** mixtures.

The unknown by-product was identified by LC-MS analysis as the corresponding tetrahydropyrethrin **53**, where further reduction had taken place at the *cis*-alkene of the resulting jasmolin **7**. Ultimately, the individual jasmolins **7** could be furnished in high proportions as a mixture with their tetrahydropyrethrin equivalents **53** from the purified pyrethrins **5** (Scheme 2.10).

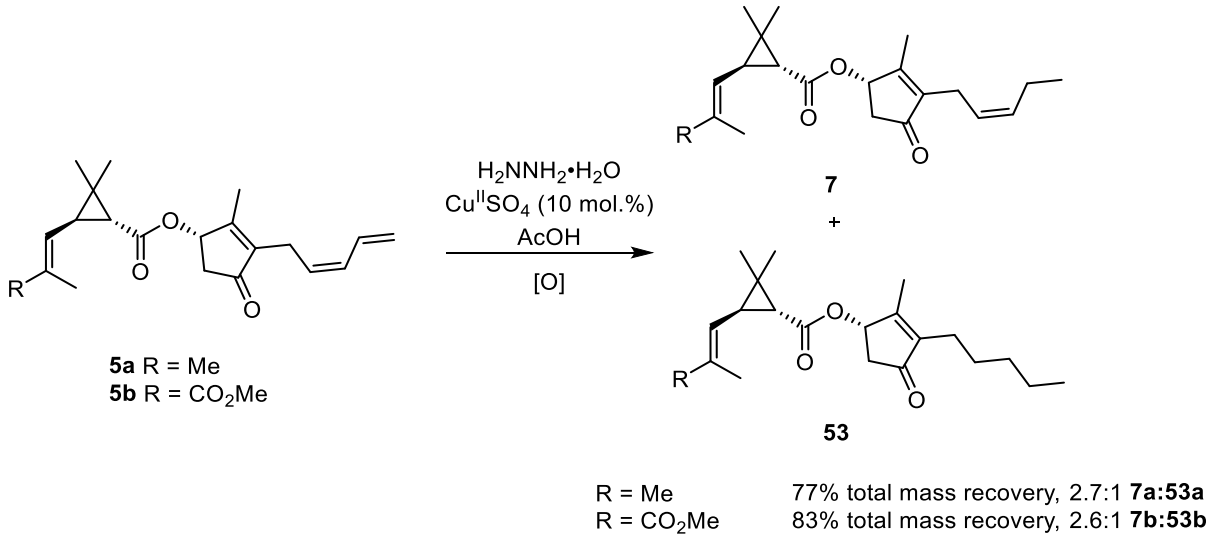

Scheme 2.10: Diimide mediated reduction of pyrethrins **5** to their jasmolins **7** and tetrahydropyrethrin **53** equivalents.

When subjected to UltraPerformance Convergence Chromatography (UPCC), undertaken by Marc McEwan at CSIRO, the semi-synthetic jasmolins in the mixture showed similar retention to the natural jasmolins **7** further confirming their identity. Additionally, when subjected to a range of chiral columns and solvent programs in the UPCC analysis the semi-synthetic jasmolin **7** signal showed no evidence of resolving into more than a single peak suggesting preservation of the natural stereochemical configuration of the pyrethrin starting materials **5**.

This diimide-mediated reduction was then directly applied to the pyrethrum concentrate, containing all six of the Pyrethrins **5-7**. Using the same methodology, it was found that pyrethrin I **5a** and II **5b** could be reduced to their respective jasmolins **7** in the presence of both the natural jasmolins **7** and cinerins **6** albeit with some over-reduction. It was found, by

HPLC analysis[§] (Figure 2.7), that the jasmolin **7** content of the extract increased from the original 7% up to approximately 65% following diimide treatment which coincides with the drop in pyrethrin **5** content from over 70% to 5%.

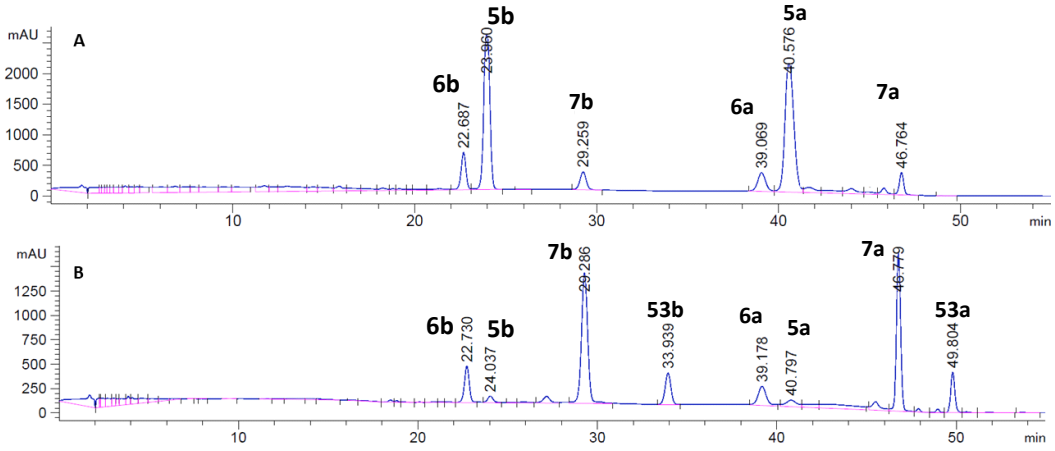

Figure 2.7: HPLC analysis (C18, 235 nm) of the pyrethrum concentrate before **(A)** and after **(B)** diimide reduction.

Much like the individual pyrethrin reactions, the diimide reduced pyrethrum extract showed the presence of both the tetrahydropyrethrins **53**, albeit in significantly lower amounts, constituting 15% of the altered extract. The cinerins **6** remained unaffected by the diimide treatment with no evidence of loss or production of a reduced variant.

The diimide-mediated reduction was able to be improved further with the reaction tolerating lower hydrazine quantities from 48 to as low as 10 eq before the reaction rate was adversely affected. Lower amounts of hydrazine resulted in longer reaction times and lower conversions due to the tendency for the diimide to undergo disproportionation to the original hydrazine and molecular nitrogen, as well as overoxidation events.[48] Further, the diimide reduction continues to progress with the omission of the catalytic copper(II) salt which may allow for more ready industrial application due to the mitigation of the need for heavy metal use and disposal. Generally, these copper-free reactions required increased reaction times and a higher proportion of hydrazine to elicit the same response as the original copper-catalysed variant due to the slower oxidation of the hydrazine. The copper-catalysed diimide-mediated protocol has shown promise in larger scale reactions, with up to gram amounts of pyrethrum

[§] Quoted purity is an estimate based on the area of the peaks in the HPLC chromatogram. As the impurities found in the reaction mixture are closely related pyrethrin derivatives, the effect of the extinction co-efficients are comparable and should have little effect on the determination of purity.

concentrate, demonstrating the conversion of the more sensitive pyrethrins **5** to the more stable jasmolins **7** albeit with small quantities of the tetrahydropyrethrins **53**.

2.5 Preliminary insecticidal activity of reduction analogues

Both the Pyrethrins **5-7** and pyrethroids act upon the target insect in the same manner, by affecting the voltage-gated sodium ion channels in the nervous system.[49] More specifically, the Pyrethrins **5-7**, or pyrethroids, bind to these ion channels causing them to remain open for longer periods of time than usual, ultimately allowing for a greater influx of ions. The result of this ion surge is the overstimulation of the nerve which can result in incapacitation of the insect, or 'knockdown', and eventual death with continued overexcitation of the nervous system.[49, 50] It has also been established by *in vitro* testing of cockroach sodium ion channels in *Xenopus* oocytes that the natural Pyrethrins **5-7** can act upon the closed form of the channel.[50]

The activities of the pyrethrum concentrate, individual natural Pyrethrins **5-7** and reduced pyrethrin analogues were determined by assay, undertaken by Dr. Andrew Kotze (CSIRO Agriculture and Food), against the commercially relevant pest *Lucilia cuprina* (Australian sheep blowfly).[51] The larvae of *L. cuprina* were exposed to the individual compounds and the inhibition of pupation used as an initial measure of their bioactivity. In conjunction with the aforementioned compounds two commercially utilised pyrethroids, α-cypermethrin **42** and deltamethrin **43**, were used as positive controls in the assays. Both dose-response curves (Figure 2.8) and IC_{50} data (Table 2.1) could then be generated to display the effectiveness of each pyrethrin analogue against the larvae.

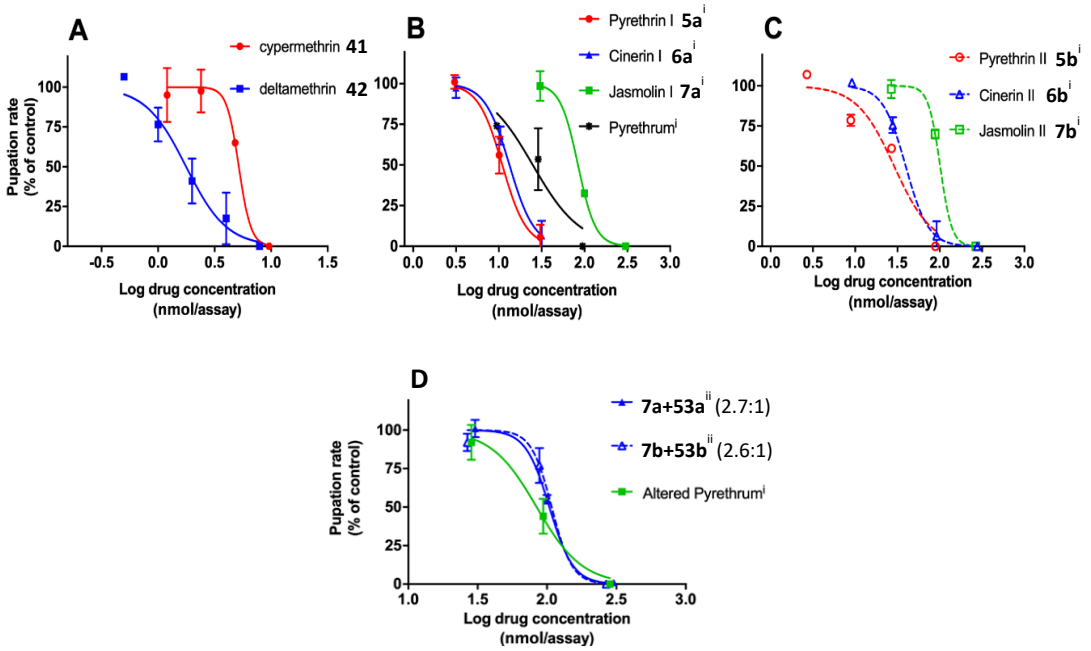

Figure 2.8: Dose-response curves of the pupation rate of *L. cuprina* larvae in response to commercial pyrethroid controls **(A)**, the natural Pyrethrins I **5a-7a** and pyrethrum concentrate **(B)**, the natural Pyrethrins II **5b-7b (C)**, and the diimide mediated reduction mixtures **(D)**. Each data point represents mean ±SE, n = 2 assays at each concentration.

Despite the minor differences between the natural Pyrethrins **5-7**, they exhibit a range of toxicities toward the *L. cuprina* larvae with all six showing significant activity (Figure 2.8B and C). Generally, the Pyrethrin II **5b-7b** variants were less active than their Pyrethrin I **5a-7a** counterparts on the live organism which is consistent with previous work on *Culex pipiens pallens* (common mosquito).[8] Of the individual esters, pyrethrin I **5a** and cinerin I **6a** were the most effective of the six esters with IC_{50} values of 11 and 13 nmol/assay respectively (Table 2.1). Jasmolin I **7a** was significantly less active than the other two esters in the series, with approximately 6.5 times the amount of cinerin I **6a** necessary to elicit the 50% inhibition of pupation. This trend was consistent in the Pyrethrins II **5b-7b** where pyrethrin **5b** was the most active and jasmolin **7b** was the least active against the larvae.

Early insecticidal testing of the Pyrethrins **5-7** explored the activity of the isolated pyrethrins **5** and cinerins **6** on both house fly (*Musca domestica*)[52] and mustard beetle (*Phaedon cochleariae*)[53] finding cinerin II **6b** the least potent of the four which is reflected with the aforementioned bioassays of *L. cuprina*. This general trend is also consistent with the *in vitro* testing on cockroach sodium ion channels where the order of activity was found to be pyrethrin **5**> cinerin **6**> jasmolin **7**.[50] The semi-synthetic jasmolin mixtures **7+53** showed

comparable activity to their natural jasmolins **7** counterparts likely due to the high content of jasmolins **7**. The pyrethrum extract was able to elicit responses similar to that of pyrethrin II **5b**, presumably due to the majority of the concentrate being made up of the pyrethrins **5**. Similarly, the diimide altered concentrate exhibited reduced activity correlating closely with its major jasmolin **7** constituents.

Table 2.1: IC_{50} bioactivity of the natural Pyrethrins **5-7** and the reduced analogues against *L. cuprina* larvae.

Compound	Structure	Activity (nmol/assay)		Compound	Structure	Activity (nmol/assay)	
α-cypermethrin **42**	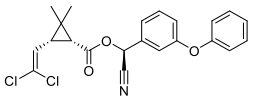	a	5.0	***4'R*-52a**	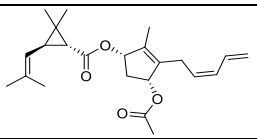	a	>200
		b	3.8-7.2				
Deltamethrin **43**	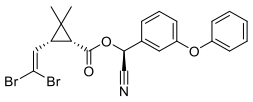	a	1.8	***4'S*-52a**	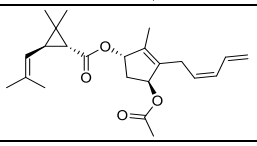	a	>200
		b	1.4-2.2				
Pyrethrum[i]	-	a	25	***4'R*-52b**	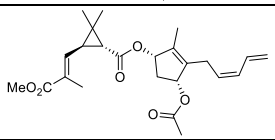	a	>200
		b	14-46				
Pyrethrin I **5a**[i]	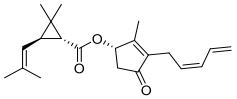	a	11	***4'S*-52b**	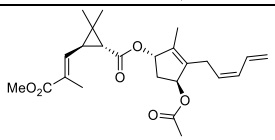	a	>200
		b	8-13				
Pyrethrin II **5b**[i]	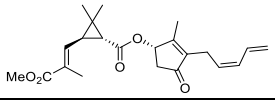	a	29	**52**	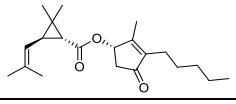	a	>200
		b	19-43				
Cinerin I **6a**[i]	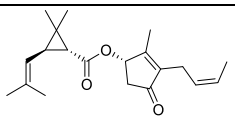	a	13	**52**	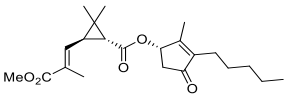	a	>200
		b	11-17				
Cinerin II **6b**[i]	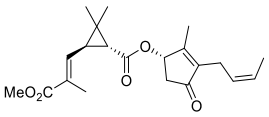	a	39	**34a**	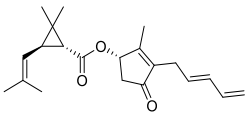	a	46
		b	33-47				35-60
Jasmolin I **7a**[i]	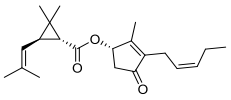	a	84	**34b**	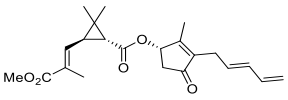	a	71
		b	66-110				37-140
Jasmolin II **7b**[i]	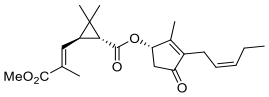	a	100	**25a**	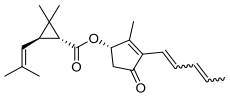	a	>200
		b	57-180				
***4'R*-51a**	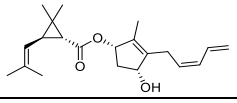	a	>200	**25a**	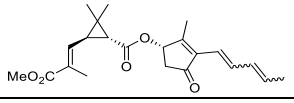	a	>200
***4'S*-51a**	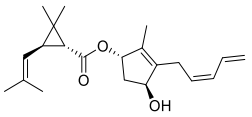	a	>200	**7a + 53a**[ii] (2.7:1)	-	a	100
						b	93-120
***4'R*-51b**	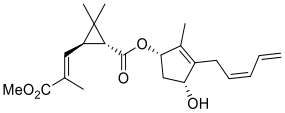	a	>200	**7b+ 53b**[ii] (2.6:1)	-	a	110
						b	36-330
***4'S*-51b**	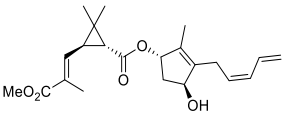	a	>200	Altered pyrethrum[ii]	-	a	84
						b	65-110

a) IC_{50}, b) 95% confidence interval, [i] Isolated from *T. cinerariifolium*, [ii] Obtained by reduction under diimide-mediated conditions.

Many of the other analogues produced from the reduction protocols described above showed no insecticidal activity towards the *L. cuprina* larvae. Both the allyl alcohol **51** and allyl acetate **52** failed to elicit any insecticidal activity indicating that alteration of the ketone in the rethrolone moiety is detrimental to the biological activity of the Pyrethrins **5-7**. This lack of activity may stem from a change in lipophilicity or conformation about the enone moiety. Additionally, complete saturation of the pentadienyl moiety in pyrethrins **5** adversely affects the activity towards the *L. cuprina* larvae. This lack of activity by the tetrahydropyrethrins **53** is consistent with the early literature which described a decreased effect on live insects.[35, 36, 54] The necessity for the unsaturation in the pentadienyl sidechain of the pyrethrins **5** is further highlighted in the docking studies by Dong, where it was implicated that these points of unsaturation in pyrethrin II **5b** were necessary for binding to the sodium channel.[50]

In conjunction, the importance of the regiochemistry of the double bonds in the pentadienyl side chain can be seen with the activities of the pyrethrin isomers **34** and **25** isolated from the transfer hydrogenation. The *trans*-pyrethrin isomers **34** both retained significant activity, greater or equivalent to the natural jasmolins **7**, however with diminished potency in comparison to the natural *cis* geometry of the pyrethrins **5**. Conversely, the migratory isomers **25** showed no inhibition of larval pupation in *L. cuprina* potentially due to the shift of the double bonds in the rethrolone moiety. More specifically, the shift of the double bonds into conjugation with the cyclopentenone ring reduces the flexibility of the side chain, which has been suggested to be necessary to allow for particular interactions in the sodium channel binding site.[50]

2.6 Conclusions

Significant quantities of individual pyrethrin I **5a** and II **5b** were able to be obtained by a dual chromatographic process. Firstly, dry column vacuum chromatography with stepwise elution was able to resolve the Pyrethrins I **5a-7a** from Pyrethrins II **5b-7b**. Subsequent column chromatography or repeated DCVC yielded gram quantities of pyrethrin I **5a** and II **5b** respectively, allowing for testing of prospective modifications.

Exploring the reduction chemistry of the natural Pyrethrins **5-7** in the pursuit of a site-selective reduction of the least stable pyrethrin I **5a** and II **5b** to the more stable jasmolins **7** resulted in the synthesis of a number of reduced analogues. Implementation of a

hydroboration-protonolysis procedure was unable to elicit the desired transformation instead acting upon the carbonyl unit of the enone moiety. This process gave rise to the allyl alcohols **51** and allyl esters **52** in relatively low yields of 15-19% and 8-9% respectively. The potential application of these materials for use in biological activity assays was deemed appropriate for the optimisation of such reaction. As a result, reduction by sodium borohydride was able to produce the allyl alcohol **51** in near quantitative yield with the individual diastereomers able to be readily resolved. Treatment of these individual alcohol stereoisomers with acetic anhydride gave good yields of the individual allyl acetate diastereomers **52**. Despite the success of the reductive transformation, these allyl alcohol derivatives **51** and **52** showed no observable activity in pupation inhibition assays.

Hydrogenation of the individual pyrethrins **5**, by standard catalytic means or through catalytic transfer processes, was unable to give the desired pyrethrin **5** to jasmolin **7** transformation. Attempts to limit catalytic hydrogenation through catalyst loading, hydrogen pressure and temperature were ineffectual in preventing over reduction of the pentadienyl unit, with the regular isolation of tetrahydropyrethrins **53**. A dihydropyrethrin variant **55**, where the interior *cis*-alkene of the pentadienyl unit was reduced, was implicated in the mildest reaction conditions however, was unable to be isolated and tested for biological activity. These tetrahydropyrethrins **53** were unable to inhibit the pupation of *L. cuprina* highlighting the necessity for unsaturation in the rethrolone side chain. Application of stoichiometrically controlled catalytic transfer hydrogenation resulted in isomers of pyrethrins where either *cis*-*trans* isomerism **34** or double bond migration **25** was observed due to the active palladium hydride species of such procedures. The resulting *trans*-pyrethrin isomers **34** retained insecticidal activity whilst their migratory counterparts **25** were ineffective in the assay against *L. cuprina* larvae.

Finally, reduction by diimide generated from hydrazine was able to reduce the terminal double bond of the pyrethrins **5** to give the jasmolins **7** as a mixture, effectively removing the more sensitive esters from the pyrethrum concentrate. The resulting mixtures retained insecticidal activity comparable to that of the natural jasmolin esters **7** despite the presence of the tetrahydropyrethrins **53**. The diimide-mediated process was found to be applicable under catalyst-free conditions up to gram scale and as such may be directly amenable to flow systems.

2.7 References

1. Bullivant, M. J.; Pattenden, G., Photodecomposition of Natural Pyrethrins and Related Compounds. *Pestic. Sci.* **1976,** *7*, 231-235.
2. Elliott, M., The Pyrethroids: Early Discovery, Recent Advances and the Future. *Pestic. Sci.* **1989,** *27*, 337-351.
3. Freemont, J. A.; Littler, S. W.; Hutt, O. E.; Mauger, S.; Meyer, A. G.; Winkler, D. A.; Kerr, M. G.; Ryan, J. H.; Cole, H. F.; Duggan, P. J., Molecular Markers for Pyrethrin Autoxidation in Stored Pyrethrum Crop: Analysis and Structure Determination. *J. Agric. Food Chem.* **2016,** *64*, 7134-7141.
4. Sudakin, D. L., Pyrethroid Insecticides: Advances and Challenges in Biomonitoring. *Clin. Toxicol.* **2008,** *44*, 31-37.
5. Atkinson, B. L.; Blackman, A. J.; Faber, H., The Degradation of the Natural Pyrethrins in Crop Storage. *J. Agric. Food Chem.* **2004,** *52*, 280-287.
6. Hayes, W., *Pesticides Studied in Man*. Williams and Wilkins: Baltimore/London, 1982.
7. Goldberg, A. A.; Head, S.; Johnston, P., Action of Heat on Pyrethrum Extract: The Isomerisation of Pyrethrins to Isopyrethrins. *J. Sci. Food Agric.* **1965,** *16*, 43-51.
8. Kawamoto, M.; Moriyama, M.; Ashida, Y.; Matsuo, N.; Tanabe, Y., Total Syntheses of All Six Chiral Natural Pyrethrins: Accurate Determination of the Physical Properties, Their Insecticidal Activities, and Evaluation of Synthetic Methods. *J. Org. Chem.* **2020,** *85*, 2984-2999.
9. Caboni, P.; Minello, E. V.; Cabras, M.; Angioni, A.; Sarais, G.; Dedola, F.; Cabras, P., Degradation of Pyrethrin Residues on Stored Durum Wheat after Postharvest Treatment. *J. Agric. Food Chem.* **2007,** *55*, 832-835.
10. Head, S. W., Composition of Pyrethrum Extract and Analysis of Pyrethrins. In *Pyrethrum: The Natural Insecticide*, Casida, J. E., Ed. Academic Press, Inc.: UK, 1973.
11. Wei, D.; Zhengguo, L.; Guomin, W.; Yingwu, Y.; Yinnguo, L.; Yuxian, X., Separation and Purification of Natural Pyrethrins by Reversed Phase High Performance Liquid Chromatography. *Chin. J. Anal. Chem.* **2006,** *34* (12), 1776-1778.
12. Dickinson, C. M., Stability of Individual Natural Pyrethrins in Solution after Separation by Preparative High Perfromance Liquid Chromatography. *Pyrethrum Post* **1987,** *16*, 105-110.

13. Henry, C. W.; McCarroll, M. E.; Warner, I. M., Separation of the insecticidal pyrethrin esters by capillary electrochromatography. *J. Chromatogr. A* **2001,** *905*, 319-327.
14. Henry, C. W.; Shamsi, S. A.; Warner, I. M., Separation of natural pyrethrum extracts using micellar electrokinetic chromatography. *J. Chromatogr. A* **1999,** *863*, 89-103.
15. Wang, I.-H.; Subramanian, V.; Moorman, R.; Burleson, J.; Ko, J., Direct determination of pyrethrins in pyrethrum extracts by reversed-phase high-performance liquid chromatography with diode-array detection. *J. Chromatogr. A* **1997,** *766*, 277-281.
16. Harwood, L. M., "Dry-Column" Flash Chromatography. *Aldrichimica Acta* **1985,** *18*, 25.
17. Harwood, L. M.; Moody, C. J.; Percy, J. M., 'Dry Flash' Column Chromatography. In *Experimental Organic Chemistry*, 2nd ed. ed.; Blackwell Science: Oxford, 1999.
18. Pederson, D. S.; Rosenbohm, C., Dry column vacuum chromatography. *Synthesis* **2001,** *2001* (16), 2431-2434.
19. Hutt, O. E.; Freemont, J. A.; Littler, S.; Duggan, P. J.; Tsanaktsidis, J.; Cole, H.; Kerr, M.; Ryan, J. H., Staudinger and Ruzicka's Altered Pyrethrolone: the Cyclopentadienone Dimers Derived from Pyrethrin I. *Acta Hortic.* **2015,** *1073*, 181-190.
20. Fischer, G. A.; Kabara, J. J., Simple, multibore columns for superior fractionation of lipids. *Anal. Biochem.* **1964,** *9* (3), 303-309.
21. Bazan, N. G.; Bazan, H. E. P., Analysis of Free and Esterified Fatty Acids in Neural Tissues Using Gradient-Thickness Thin-Layer Chromatrography (GT-TLC). In *Research Methods in Neurochemistry*, Marks, N., Ed. Springer Science & Business Media: 2012; Vol. 3.
22. Brown, H. C., Hydroboration-A Powerful Synthetic Tool. *Tetrahedron* **1961,** *12* (3), 117-138.
23. Bracher, F.; Litz, T., 9-Borabicyclo[3.3.1]nonane (9-BBN) in Organic Synthesis. *J. prakt. Chem.* **1996,** *338*, 386-389.
24. Brown, H. C.; Murray, K. J., Organoboranes for synthesis. 1 : Protonolysis of trialkylboranes. A convenient non-catalytic conversion of alkenes into saturated compounds via hydroboration-protonolysis. *Tetrahedron* **1986,** *42* (20), 5497-5504.
25. Brown, H. C.; Sweifel, G., Hydroboration. IX. The Hydroboration of Cyclic and Bicyclic Olefins - Stereochemistry of the Hydroboration Reaction. *J. Am. Chem. Soc.* **1961,** *83*, 2544-2551.

26. Negishi, E.; Yoshida, T.; Abramovitch, A.; Lew, G.; Williams, R. M., Highly stereoselective syntheses of conjugated E,E- and E,Z-dienes, E-enynes and E-1,2,3-butatriened via alkenylborane derivatives. *Tetrahedron* **1991,** *47*, 343-356.
27. Brown, H. C.; Liotta, R.; Kramer, G. W., Hydroboration. 49. Effect of Structure on the Selective Monohydroboration of Representative Conjugated Dienes by 9-Borabicyclo[3.3.1]nonane. *J. Org. Chem.* **1978,** *43* (6), 1058-1063.
28. Noth, H.; Wrackmeyer, B., ^{11}B Chemical Shifts of Three Coordinate Boron. In *Nuclear Magnetic Resonance Spectroscopy of Boron Compounds*, Diehl, P.; Fluck, E.; Kosfeld, R., Eds. Springer-Verlag: Berlin Heidelberg, 1978.
29. Brown, H. C.; Krishnamurthy, S.; Yoon, N. M., Selective Reductions. XXI. 9-Borabicyclo[3.3.1]nonane in Tetrahydrofuran as a New Selective Reducing Agent in Organic Synthesis. Reaction with Selected Organic Compounds Containing Representative Functional Groups. *J. Org. Chem.* **1976,** *41* (10), 1778-1791.
30. Krishnamurthy, S.; Brown, H. C., Selective Reductions. 22. Facile Reduction of α, β-Unsaturated Aldehydes and Ketones with 9-Borabicyclo[3.3.1]nonane. A Remarkably Convenient Procedure for the Selective Conversion of Conjugated Aldehydes and Ketones to the Corresponding Allylic Alcohols in the Presence of Other Functional Groups. *J. Org. Chem.* **1977,** *42* (7), 1197-1201.
31. Ward, D. E.; Rhee, C. K., Chemoselective reductions with sodium borohydride. *Can. J. Chem.* **1989,** *67*, 1206-1211.
32. Meyer, G. R., Conjugate and nonconjugate reduction with $LiAlH_4$ and $NaBH_4$. *J. Chem. Educ.* **1981,** *58* (8), 628-630.
33. Varma, R. S.; Kabalka, G. W., Allylic Alcohols Via the Chemoselective Reduction of Enone Systems with Sodium Borohydride in Methanolic Tetrahydrofuran. *Synth. Commun.* **1985,** *15* (11), 985-990.
34. Wang, D.; Astruc, D., The Golden Age of Transfer Hydrogenation. *Chem. Rev.* **2015,** *115*, 6621-6686.
35. Haller, H. L.; Sullivan, W. N., Toxicity of Hydrogenated Pyrethrins I and II to the Housefly. *J. Econ. Entomol.* **1938,** *31* (2), 276-277.
36. Gersdorff, W. A., Toxicity to House Flies of the Pyrethrins and Cinerins, and Derivatives, in Relation to Chemical Structure. *J. Econ. Entomol.* **1947,** *40* (6), 878-882.

37. Pandarus, V.; Gingras, G.; Beland, F.; Ciriminna, R.; Pagliaro, M., Selective Hydrogenation of Alkenes under Ultramild Conditions. *Org. Process. Res. Dev.* **2012,** *16*, 1230-1234.

38. Quinn, J. F.; Razzano, D. A.; Golden, K. C.; Gregg, B. T., 1,4-Cyclohexadiene with Pd/C as a rapid, safe transfer hydrogenation system with microwave heating. *Tetrahedron Lett.* **2008,** *49*, 6137-6140.

39. Brieger, G.; Nestrick, T. J., Catalytic Transfer Hydrogenation. *Chem. Rev.* **1974,** *74*, 567-580.

40. Gauthier, D.; Lindhardt, A. T.; Olsen, E. P. K.; Overgaard, J.; Skrydstrup, T., In Situ Generated Bulky Palladium Hydride Complexes as Catalysts for the Efficient Isomerization of Olefins. Selective Transformation of Terminal Alkenes to 2-Alkenes. *J. Am. Chem. Soc.* **2010,** *132*, 7998-8009.

41. Shen, R.; Chen, T.; Zhao, Y.; Qiu, R.; Zhou, Y.; Yin, S.; Wang, X.; Goto, M.; Han, L.-B., Facile Regio- and Stereoselective Hydrometalation of Alkynes with a Combination of Carboxylic Acids and Group 10 Transition Metal Complexes: Selective Hydrogenation of Alkynes with Formic Acid. *J. Am. Chem. Soc.* **2011,** *133*, 17037-17044.

42. Yu, J.; Spencer, J. B., Regioselective Hydrometalation of Alkenes Reveals the Amphipolar Nature of the Pd-H Bond in Hetereogeneous Hydrogenation. *J. Org. Chem.* **1997,** *62*, 8618-8619.

43. Tan, E. H. P.; Lloyd-Jones, G. C.; Harvey, J. N.; Lennox, A. J. J.; Mills, B. M., $[(RCN)_2PdCl_2]$-Catalyzed *E/Z* Isomerization of Alkenes: A Non-Hydride Binuclear Addition-Elimination Pathway. *Angew. Chem. Int. Ed.* **2011,** *50*, 9602-9606.

44. Miller, C. E., Hydrogenation with diimide. *J. Chem. Educ.* **1965,** *42* (5), 254-259.

45. Smit, C.; Fraaije, M. W.; Minnaard, A. J., Reduction of Carbon-Carbon Double Bonds Using Organocatalytically Generated Diimide. *J. Org. Chem.* **2008,** *73*, 9482-9485.

46. Hunig, S.; Muller, H. R.; Thier, W., The Chemistry of Diimine. *Angew. Chem. Int. Ed.* **1965,** *4* (4), 271-280.

47. Pieber, B.; Martinez, S. T.; Cantillo, D.; Kapper, C. O., In Situ Generation of Diimide from Hydrazine and Oxygen: Continuous-Flow Transfer Hydrogenation of Olefins. *Angew. Chem. Int. Ed.* **2013,** *52*, 10241-10244.

48. Imada, Y.; Iida, H.; Naota, T., Flavin-Catalyzed Generation of Diimide: An Environmentally Friendly Method for the Aerobic Hydrogenation of Olefins. *J. Am. Chem. Soc.* **2005,** *127* (42), 14544-14545.
49. Davies, T. G. E.; Field, L. M.; Usherwood, P. N. R.; Williamson, M. S., DDT, Pyrethrins, Pyrethroids and Insect Sodium Channels. *IUBMB Life* **2007,** *59* (3), 151-162.
50. Chen, M.; Du, Y.; Zhu, G.; Takamatsu, G.; Ihara, M.; Matsuda, K.; Zhorov, B. S.; Dong, K., Action of six pyrethrins purified from the botanical insecticide pyrethrum on cockroach sodium channels expressed in *Xenopus* oocytes. *Pest. Biochem. Physiol.* **2018,** *151*, 82-89.
51. Kotze, A. C.; Bagnall, N. H.; Ruffell, A. P.; Pearson, R., Cloning, recombinant expression and inhibitor profiles of dihydrofolate reductase from the Australian sheep blow fly, *Lucilia cuprina*. *Med. Vet. Entomol.* **2014,** *28* (3), 297-306.
52. Sawicki, R. M.; Elliott, M.; Gower, J. C.; Snarey, M.; Thain, E. M., Insecticidal activity of pyrethrum extract and its four insecticidal constituents against house flies. I.—Preparation and relative toxicity of the pure constituents; Statistical analysis of the action of mixtures of these components. *J. Sci. Food Agric.* **1962,** *13* (3), 172-185.
53. Ward, J., Separation of the Pyrethrin by Displacement Chromatography. *Chem. and Ind.* **1953**, 586-587.
54. Crombie, L.; Elliott, M.; Harper, S. H., Experiments on the Synthesis of the Pyrethrins. Part III. Synthesis of Dihydrocinerin-I and Tetrahydropyrethrin-I; a Study of the Action of N-Bromosuccinimide on 3-Methyl-2-n-alkyl (and alkenyl)-cyclopent-2-en-1-ones. *J. Chem. Soc.* **1950**, 971-978.

Chapter 3 Investigating the Diels-Alder Reactivity of the Pyrethrin Side Chain

3.1 Introduction

Cycloadditions have become an integral, well established way of introducing large, elaborate, and functionality rich cyclic scaffolds particularly in the total synthesis of natural products or biologically active small molecules.[1-5] A number of cycloadditions exist but the common feature between them is the movement of π-electrons forming new σ-bonds to give a cyclic adduct. Cycloaddition reactions can generate a number of ring sizes (Figure 3.1), depending on the number of participating atoms and π-electrons from each substrate. Generally these reactions can either be categorised by the atom participation from each substrate, (a+b), or more importantly the electron participation from each substrate, [c+d].[6] For example, the first reaction (Figure 3.1A) is a (2+1) where the two carbons from the alkene and the one carbon of the carbene participate in the reaction, or a [2+2] where both substrates contribute two electrons each, forming the cyclopropane ring.

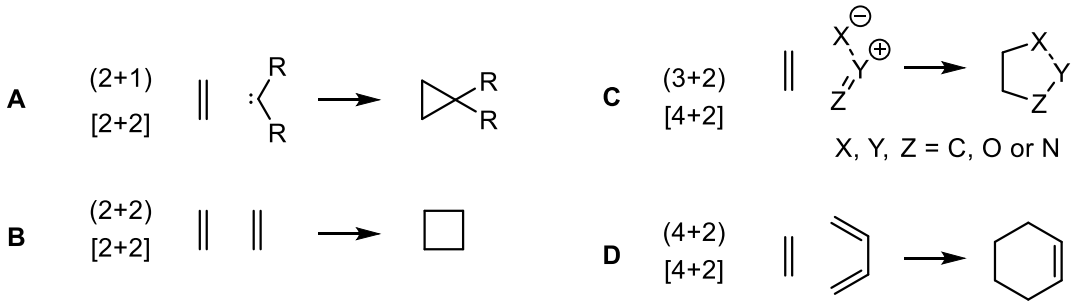

Figure 3.1: Cycloaddition reactions used to generate adducts of different ring sizes.

The most recognised of these cycloadditions is the Diels-Alder reaction named for the Nobel prize winning chemists who discovered it, Otto Diels and Kurt Alder.[4] At its simplest, this [4+2] cycloaddition reaction, initially discovered in 1928, utilises a conjugated diene containing 4π electrons and an alkene containing 2π electrons, more commonly referred to as a dienophile, to form a 6-membered cyclic adduct (Figure 3.1D).[7] This reactivity continues to see use in modern day synthesis with a number of variants now documented.

The electronic demands of the Diels-Alder cycloaddition have led to classification into three distinct classes; normal electron demand (Figure 3.2A), neutral electron demand (Figure 3.2B) and, inverse electron demand (IEDDA)(Figure 3.2C).[5, 8]

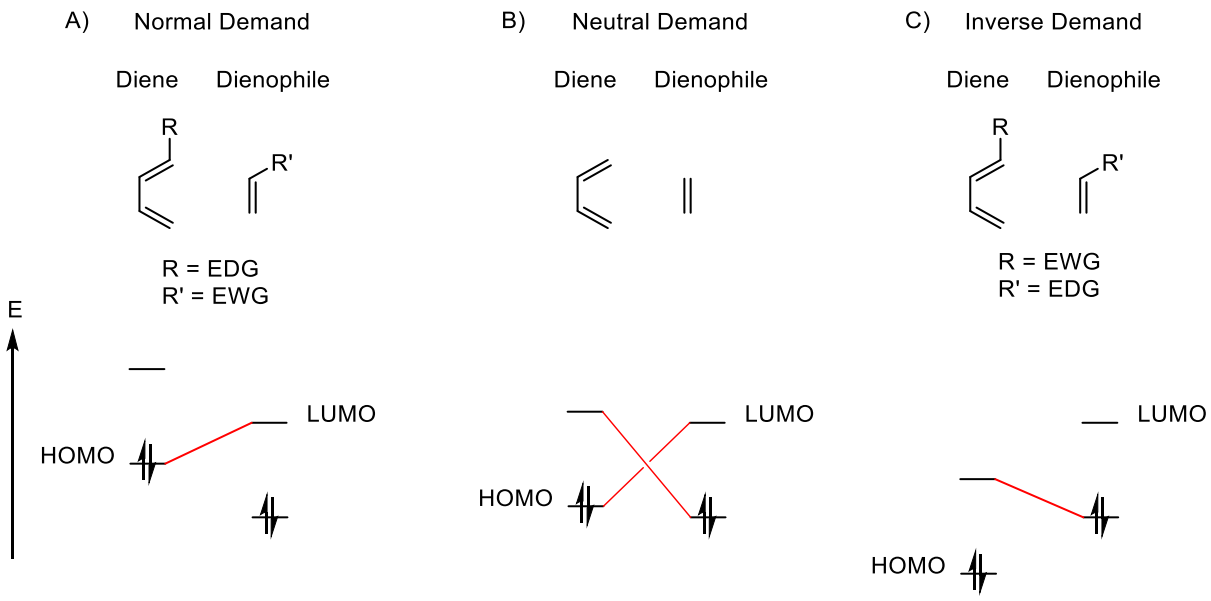

Figure 3.2: Frontier molecular orbital interactions of the normal electron demand **(A)**, neutral electron demand **(B)** and, inverse electron demand **(C)** Diels-Alder cycloadditions.

The most common of these is the normal electron demand Diels-Alder cycloaddition (Figure 3.2A), where the reaction is facilitated by the HOMO–LUMO energy gap of the diene's Highest Occupied Molecular Orbital (HOMO) and the dienophile's Lowest Unoccupied Molecular Orbital (LUMO). More specifically, this reactivity takes place when the $HOMO_{diene}$–$LUMO_{dienophile}$ gap is smaller than the reverse, i.e. $HOMO_{dienophile}$-$LUMO_{diene}$.[8] Generally, this reactivity is more pronounced when the diene possesses an electron donating substituent, increasing the energy of the $HOMO_{diene}$ and subsequently 'closing' the $HOMO_{diene}$–$LUMO_{dienophile}$ energy gap. In addition, dienophiles possessing an electron withdrawing substituent have a lower energy LUMO further reducing the energy difference between the $HOMO_{diene}$ and the $LUMO_{dienophile}$.[8]

The natural Pyrethrins **5-7** are rich with π-electron containing moieties, particularly pyrethrins I **5a** and II **5b**, which may lend themselves to application in cycloaddition reactions. Of particular interest is the conjugated pentadienyl side chain of the pyrethrins **5** which may be directly amenable to the Diels-Alder reaction. As previously discussed (Chapter 1; Section 1.3), this pentadienyl side chain is the source of significant degradation of the more prominent pyrethrin esters **5** and its alteration may help to stabilise the insecticidal compounds. Submission of the pyrethrins **5** to Diels-Alder conditions has potential to derivatise this oxidatively sensitive side chain to give stabilised analogues with rethrolone moieties

reminiscent of the synthetic pyrethroids. Notably, the application of Diels-Alder cycloadditions to the diene in the natural pyrethrins **5** has remained unexplored. As such, investigation into the Diels-Alder reactivity of the natural pyrethrins **5** was undertaken to develop stabilised insecticidal analogues.

3.2 Conventional Diels-Alder cycloadditions with pyrethrins

Initial investigation into the Diels-Alder reactivity of the pentadienyl moiety in pyrethrins **5** focussed on model reactions utilising well-known, highly reactive dienophiles like maleic anhydride **59**. It has been well established that modelling of the frontier molecular orbitals of the diene/dienophile can give qualitative insight into the Diels-Alder reactivity and regioselectivity of said substrates.[9] As such, the feasibility of the Diels-Alder reactions were explored through computational modelling of the frontier molecular orbitals of the pyrethrins **5** and the dienophiles of interest.

3.2.1 Evaluation of the Diels-Alder with the natural pyrethrins

Molecular modelling (Spartan '16, Wavefunction, Inc.)[10] of the involved molecular orbitals (DFT B3LYP/6-31G*) of pyrethrins I **5a** and II **5b** (Figure 3.3) as well as some conventionally Diels-Alder active dienophiles was undertaken to determine the energies of the HOMO and LUMO of each substrate.

The molecular modelling of both pyrethrin I **5a** and II **5b** revealed that the HOMO and LUMO were not directly associated with the pentadienyl unit but rather with the acid and enone moieties respectively. However, the Next-to-Highest Molecular Orbital (NHOMO or HOMO−1) and Second Lowest Molecular Orbital (SLUMO or LUMO+1) were observed over the pentadienyl side chain (Figure 3.3). Ultimately, both pyrethrin I **5a** and II **5b** shared similar energies for both the HOMO and LUMO of approximately −6.2 and −0.5 eV respectively.

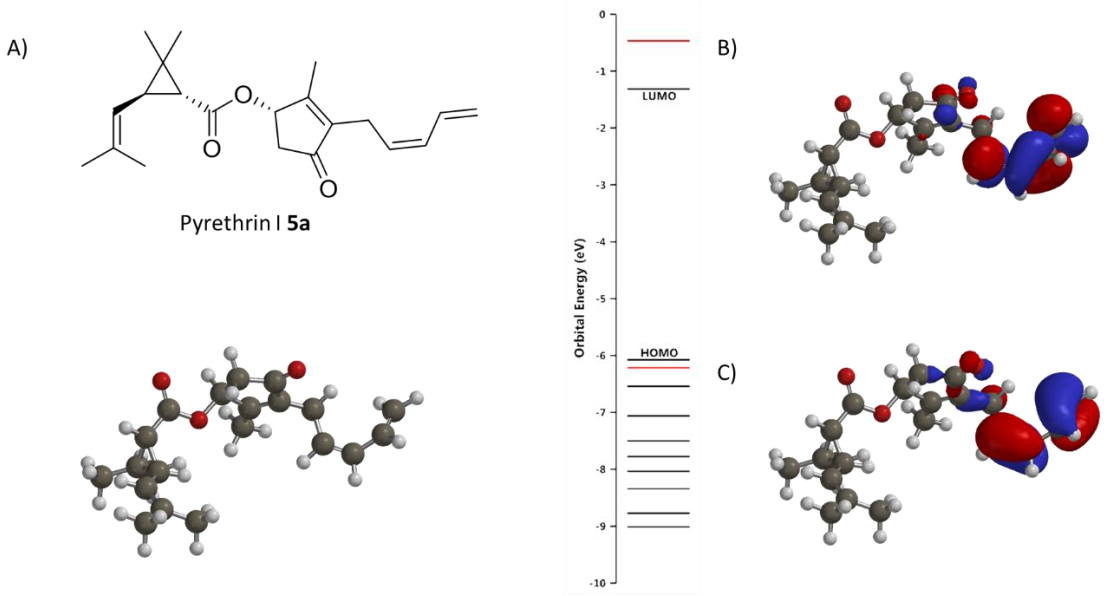

Figure 3.3: Molecular modelling (DFT B3LYP/6-31G*) showing pyrethrin I **5a (A)**, the lowest unoccupied molecular orbital (LUMO+1) **(B)** and, the highest occupied molecular orbital (HOMO−1) of the pentadienyl moiety of pyrethrin I **5a (C)**.

Evaluation of the $HOMO_{diene}$–$LUMO_{dienophile}$ gap between the pyrethrin substrates **5** and the conventional dienophiles **58-60** (Figure 3.4) revealed energy differences consistent with normal demand Diels-Alder reactivity.[11]

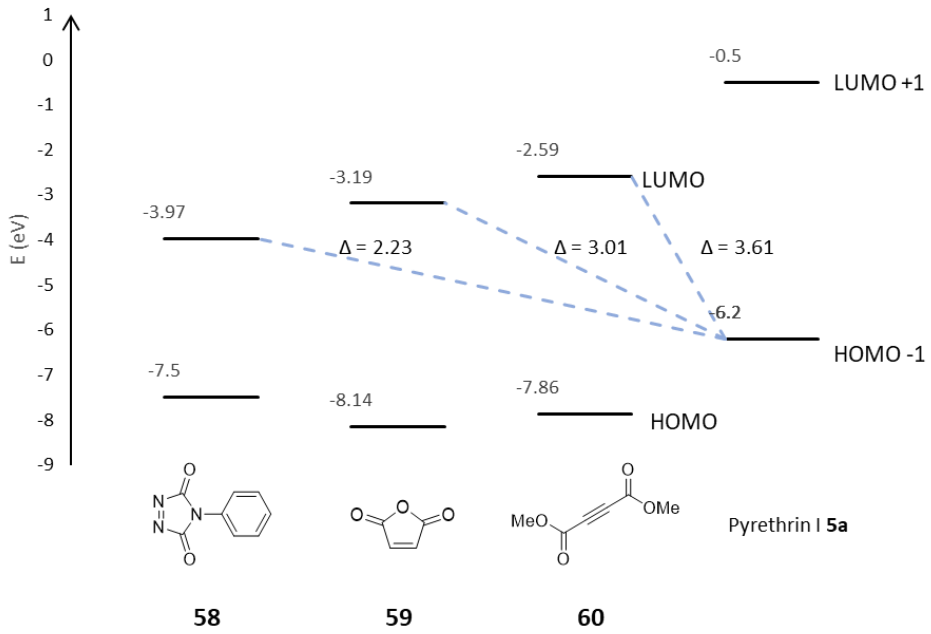

Figure 3.4: HOMO-LUMO energy profiles of some electron-withdrawn dienophiles **58-60** and pyrethrin I **5a** determined by molecular modelling (DFT B3LYP/6-31G*).[10]

This theoretical viability as well as the atom economy, selectivity and general efficiency of the Diels-Alder cycloaddition made it potentially applicable to derivatisation of the sensitive pentadienyl unit in the natural pyrethrins **5a**.[7] Initial attempts focussed on the conventional, electron-deficient dienophiles theoretically modelled to elicit Diels-Alder reactivity.

3.2.2 Attempts at normal Diels-Alder reactions on pyrethrins

The theoretical evaluation of application of the normal electron demand Diels-Alder to the most abundant pyrethrins **5** showed promise with a selection of typical, electron-deficient dienophiles. More specifically, the calculated $HOMO_{diene}$–$LUMO_{dienophile}$ gaps (Figure 3.4) showed all three of the dienophiles to be viable for reaction with the pyrethrins **5** by Diels-Alder cycloaddition. As such, exploration into the practical reactivity of these dienophiles with the pentadienyl moiety of pyrethrin I **5a** and II **5b** as diene commenced.

The electron-withdrawing methyl esters of dimethyl acetylenedicarboxylate (DMAD) **60** have made the alkynyl unit the ideal dienophile, so much so that it has been used as a measure for the efficiency/activity of the Diels-Alder reaction.[12] Similarly, the alkene of maleic anhydride **59** is sufficiently electron-deficient, due to the carbonyl units either side, to elicit efficient Diels-Alder cycloaddition. These favourable dienophile qualities allowed DMAD **60** and maleic anhydride **59** to be used as model dienophiles to probe the Diels-Alder reactivity of the natural pyrethrins **5**.

Initial attempts of the normal Diels-Alder with pyrethrins **5** were undertaken by purely thermal means where the pyrethrin **5** and dienophile were heated under reflux (Scheme 3.1). Reaction with DMAD **60** as the dienophile with pyrethrins **5** in THF was monitored by TLC for reaction progression but no change was observed over reaction times reaching 24 h. Subsequent isolation of the crude reaction mixture and analysis by ^{1}H NMR showed no change in the pyrethrin starting material **5** and some degradation of the DMAD **60** to the equivalent acid(s). Notably, the $HOMO_{diene}$–$LUMO_{dienophile}$ energy gap between the pyrethrin **5** and DMAD **60** is significantly larger than that of the other two dienophiles investigated (Figure 3.4) which may be indicative of reduced reactivity in comparison to these alternative dienophiles. As such, a substrate with a smaller $HOMO_{diene}$–$LUMO_{dienophile}$, namely maleic anhydride **59**, was then used as dienophile in the pursuit of invoking normal demand Diels-Alder reactivity. However, much like the reactions with DMAD **60**, no reaction was observed to take place by TLC analysis and the NMR spectra of crude isolates showed only small amounts of hydrolysis

of the maleic anhydride **59** amongst the starting materials. Finally, substitution of the dienophile for one with an even smaller $HOMO_{diene}$–$LUMO_{dienophile}$ gap was attempted with a well-known, highly reactive substrate.

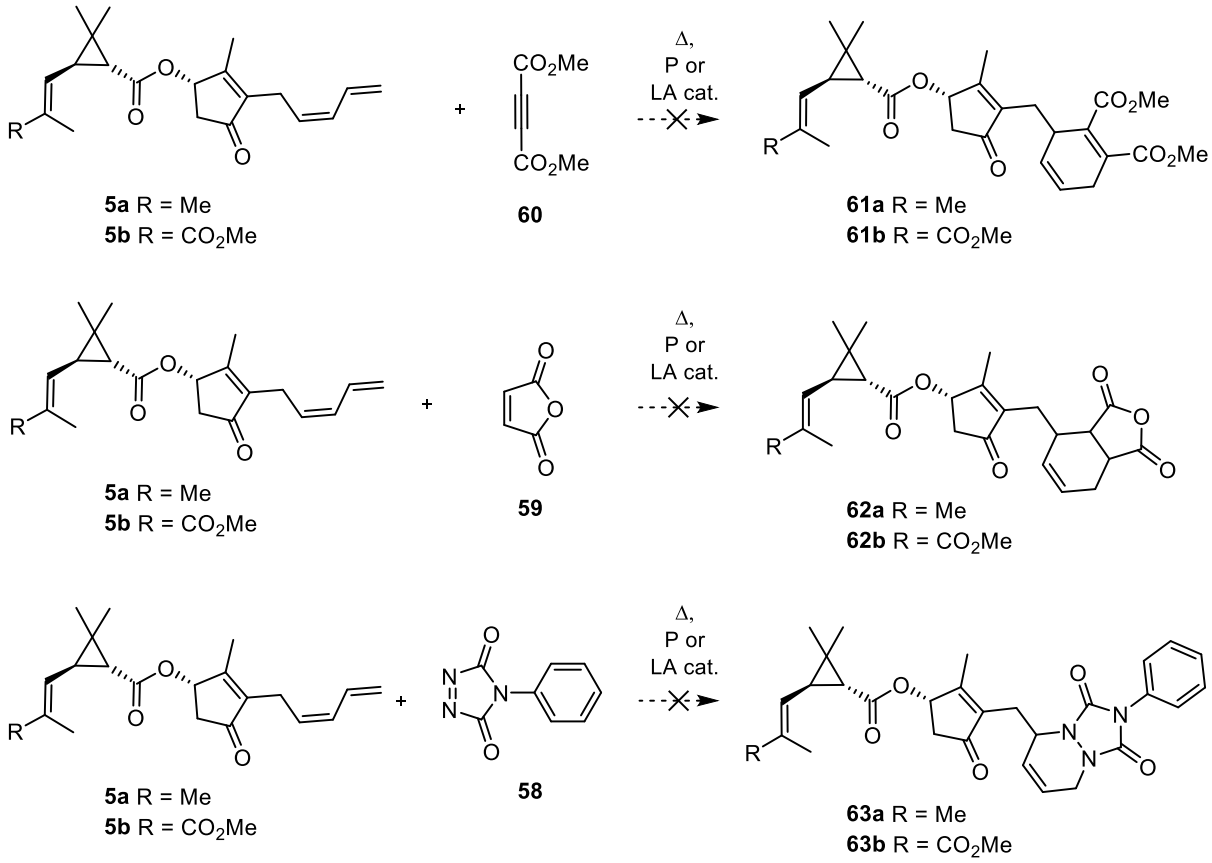

Scheme 3.1: Unsuccessful normal electron demand Diels-Alder reactions of pyrethrins **5** with electron-deficient dienophiles **58-60** under reflux (Δ), high pressure (P) or Lewis acid (LA) catalysis.

4-Phenyl-1,2,4-triazoline-3,5-dione (PTAD) **58** has been used as a dienophile not only for the introduction of heteroatoms into the resulting cycloadduct but also for its incredibly high reactivity under normal demand Diels-Alder conditions, which correlates with the smaller $HOMO_{diene}$–$LUMO_{dienophile}$ energy gap calculated above with the natural pyrethrins **5** (Figure 3.4).[13, 14] Nevertheless, its direct application into the thermal Diels-Alder reaction with pyrethrins **5** was unable to elicit any change in the pentadienyl moiety as only starting material was recovered. Unfortunately, the various cycloadducts **61-63** resulting from reaction with these electron-deficient dienophiles **58-60** were unable to be formed (Scheme 3.1) by purely thermal means and as such alternate, more forcing reaction conditions were explored to elicit the Diels-Alder reaction.

The Diels-Alder reaction can be enhanced by a range of different physical and chemical processes including catalysis, sonication and, high pressure.[15-18] High pressure activation of Diels-Alder substrates has been extensively studied as a means of enhancing reactions with thermally sensitive substrates, like the natural Pyrethrins **5-7**.[19-21] A number of factors involved in the chemical reactivity can be affected by high pressures, including the solvent properties and the intermolecular distances between reactants, that result in the observed increased reaction rates.[21, 22] The potential for increased reactivity at thermally mild conditions from high pressure reactions was attractive for the Diels-Alder cycloaddition of pyrethrins **5**. Applying pressure to the Diels-Alder reaction of pyrethrin **5** with the aforementioned dienophiles **58-60** (Scheme 3.1) up to 35 MPa in DCM for 24 h was unable to afford any cycloadduct, no matter the dienophile, instead the pyrethrin starting material **5** was isolated in its entirety. Finally, catalysis was explored as a means of increasing the reactivity between the diene and dienophile.

Lewis acid catalysis has been a well-established approach to accelerate the Diels-Alder reaction through further activation of the dienophile.[16, 17, 23] Complexation of the Lewis acid to the electron withdrawing groups, i.e. carbonyls, further removes electron density away from the dienophilic π-system ultimately lowering the $LUMO_{dienophile}$ energy and as such the $HOMO_{diene}$–$LUMO_{dienophile}$ energy gap.[16, 24, 25] This is directly reflected in modelling of the HOMO-LUMO energies of the conventional, electron-withdrawn dienophiles complexed with aluminium chloride (Figure 3.5).

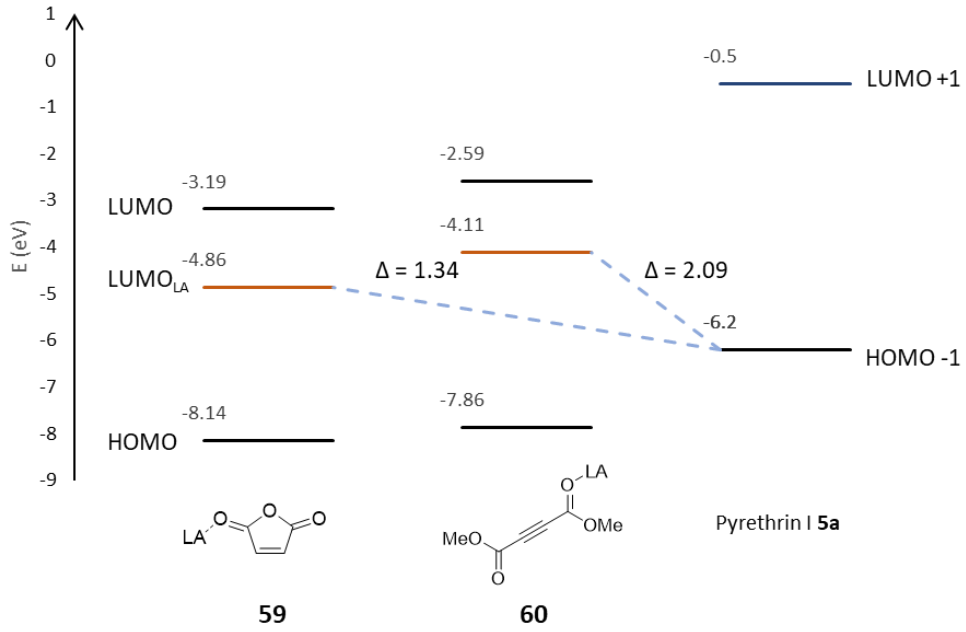

Figure 3.5: $HOMO_{diene}$–$LUMO_{dienophile}$ energy gaps with the Lewis acid (LA) $AlCl_3$ complexed to the dienophile determined by molecular modelling (DFT B3LYP/6-31G*).[10]

This significant drop in the energy of the $LUMO_{dienophile}$, and consequent decrease in $HOMO_{diene}$–$LUMO_{dienophile}$ energy gap, should allow for increased reactivity with the dienophile and as such increase the Diels-Alder reaction rate. Experimental application of Lewis acid catalysis was pursued with the introduction of aluminium chloride into the reaction mixture and substitution of the original THF solvent due to its Lewis basic properties (Scheme 3.1).[26] Addition of the Lewis acid to the reaction mixture was accompanied by a rapid colour change to light pink suggesting complexation of the aluminium chloride. Nevertheless, after 24 h of reflux no reaction was observed by TLC and only recovery of the individual starting materials was observed in the ^{1}H NMR spectrum. The carbonyl containing functional groups in the pyrethrins **5** may interfere and preferentially complex with the Lewis acid catalyst preventing the desired lowering of the $LUMO_{dienophile}$ energy. Alternatively, the *cis* geometry of the pentadienyl unit of the pyrethrins **5** may hinder their reactivity in the normal Diels-Alder cycloaddition. More specifically, the conformational restrictions of the *cis*-alkene may prevent adoption of the necessary *s-cis* geometry due to steric interaction with the 7' methylene and enone moieties (Figure 3.6).

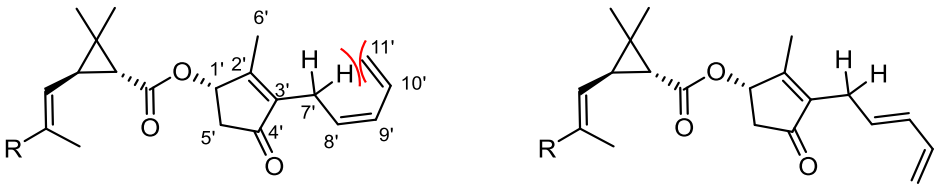

Figure 3.6: Steric hinderance of the *s-cis* geometry needed for Diels-Alder reactivity.

3.2.3 Pyrethrin isomerism and subsequent Diels-Alder reactivity

The *trans*-isomer of pyrethrins **34** is likely less conformationally restricted, due to the *s-cis* geometry no longer encumbered by the 7′ methylene unit of the side chain (Figure 3.6). There is precedent in literature for the Diels-Alder reactivity of this isomer where *(E)*-pyrethrolone **64** has been removed from diastereomeric mixtures by Diels-Alder reaction with tetracyanoethylene (Scheme 3.2) and subsequent column chromatography of the cycloadduct **65**.[27]

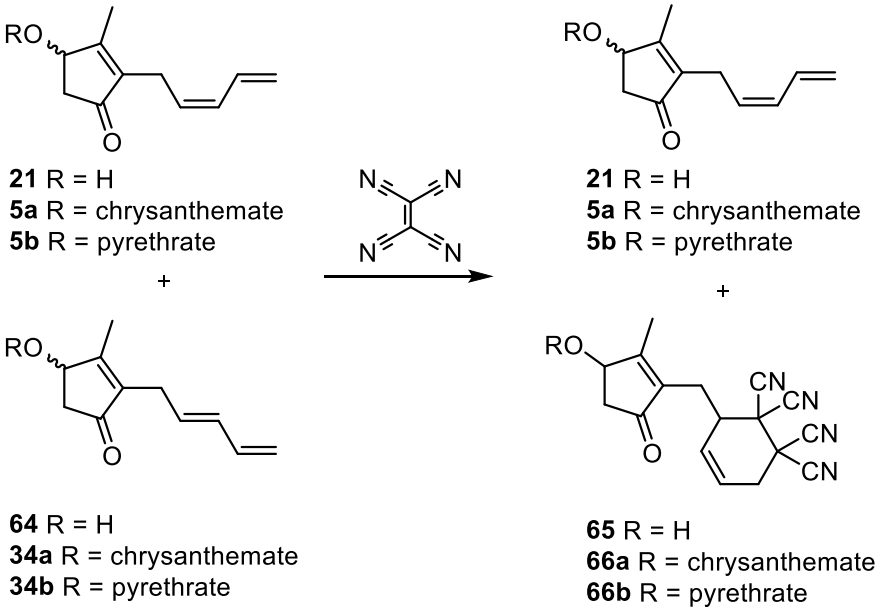

Scheme 3.2: Removal of the *trans*-rethrolone isomer from diastereomeric mixtures by Diels-Alder reaction with tetracyanoethylene.[27, 28]

Further to this, synthetic diastereomeric mixtures of pyrethrin **5** have been treated in a similar manner where the (*E*)-isomer **34** undergoes cycloaddition with the tetracyanoethylene and the cycloadduct **66** is readily removed by column chromatography to give purified pyrethrin **5** with the natural *cis* geometry.[28] As such, isomerism of the *cis*-alkene to the *trans*-geometry

followed by reaction with appropriate dienophiles should allow for the normal Diels-Alder process to take place with the natural pyrethrins **5**.

It has been well established that the natural Pyrethrins **5-7** are susceptible to *cis-trans* isomerism, particularly under photochemical conditions (Chapter 1; Section 1.3.2).[29-31] In this work, preliminary experiments were undertaken utilising a short term exposure of solutions, with intermittent analysis to monitor the process, of the pyrethrins **5** to UV light (254 nm) to isomerise the *cis*-alkene. Generally after a total of 16 h of UV exposure, the pyrethrins **5** were obtained as diastereomeric mixtures with ratios of 1:1.3 and 1:2.2 (*E:Z*; **34**:**5**), determined by ^{1}H NMR, for pyrethrin I **5a** and II **5b** respectively. These mixtures were then added to a solution with maleic anhydride **59** and heated under reflux (Scheme 3.3). Reaction monitoring with TLC showed the development of a new spot, indicating the potential formation of a Diels-Alder cycloadduct. Following work-up, the crude material was shown to possess new alkene ^{1}H resonances (5.96 and 5.76 ppm) consistent with the expected cycloadduct **62** and no residual *trans*-pyrethrin **34** was observed suggesting complete consumption of the Diels-Alder active isomer in the starting mixture.

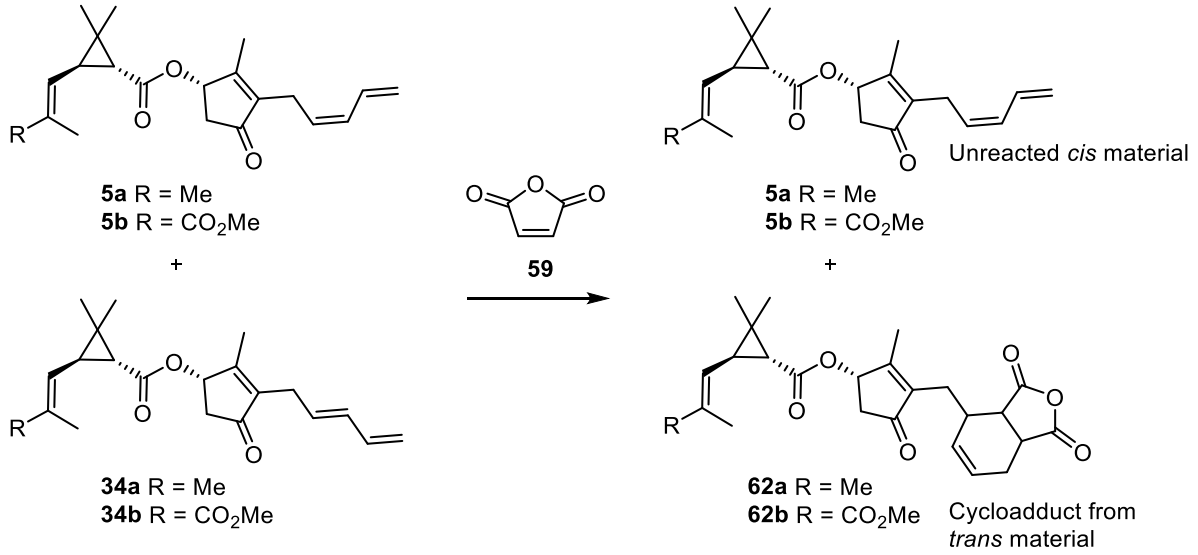

Scheme 3.3: Diels-Alder reaction of isomerised pyrethrin mixtures with maleic anhydride 59 as dienophile.

Unfortunately, attempts to purify the cycloadduct **62** from the residual *cis*-pyrethrin **5** were unsuccessful with the desired material decomposing on the silica during column chromatography likely through hydrolysis of the anhydride. As a result of this decomposition and the inefficiency of the isomerism under the preliminary conditions, the normal Diels-

Alder procedure was not pursued further however, this remains a potential for derivatisation of the natural pyrethrins **5**. Instead, alternative Diels-Alder reactivity was pursued where the pyrethrin **5** was utilised as a dienophile.

3.3 Inverse electron demand Diels-Alder reactions of the pyrethrins

3.3.1 The inverse electron demand Diels-Alder reaction

In contrast to the normal electron demand Diels-Alder reaction, the IEDDA reaction takes place with an electron-rich dienophile and an electron-deficient diene. In this variant of the Diels-Alder cycloaddition, the reactivity is driven by the $HOMO_{dienophile}$–$LUMO_{diene}$ interaction instead of the $HOMO_{diene}$–$LUMO_{dienophile}$ interaction of normal Diels-Alder cycloadditions (Figure 3.2).[5, 32] Under these conditions, the pyrethrins **5** are more likely to act as a dienophile with electron-deficient dienes due to the large electron density of the terminal double bond in the pentadienyl chain.

A range of different electron-deficient dienes have been the focus of IEDDA studies including 2-pyrones **67**,[33, 34] 1-oxa-1,3-butadienes **68**,[35] and nitrogen-rich heterocycles **69-70** (Figure 3.7).[5, 36]

67 **68** **69** **70**

Figure 3.7: Common electron-deficient dienes that participate in IEDDA cycloadditions.

The most extensively used dienes in the IEDDA reaction are the 1,2,4,5-tetrazines, e.g. **70**, due to their rapid reactivities without the need for catalysis.[37] The 1,2,4,5-tetrazines were first found to participate in the IEDDA reaction in 1959,[38] and have since been implemented in a range of applications, including chemical biology and materials chemistry, due to their rapid reactivity, bioorthogonal properties and ability to introduce heterocyclic scaffolds *via* these cycloadditions.[5, 32, 39] Not only are the tetrazines well-documented and highly reactive but they can be readily afforded by synthetic means, particularly the symmetrical, 3,6-bis-substituted variants.

3.3.2 Preparation of 3,6-bis-substituted tetrazines

A range of syntheses exist for the production of 1,2,4,5-tetrazines but by far the most common is the reaction of nitriles with hydrazine via the Pinner synthesis to give a dihydrotetrazine which is subsequently oxidised to give the final aromatic tetrazine (Scheme 3.4).[40, 41]

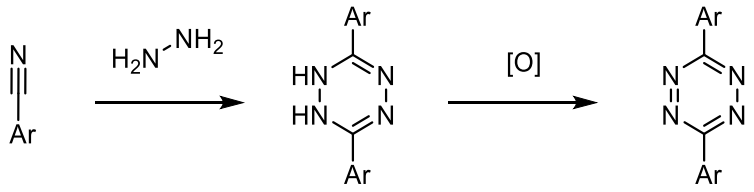

Scheme 3.4: Pinner synthesis for the production of aromatic bis-substituted 1,2,4,5-tetrazines.

Generally, the Pinner synthesis is used for the production of 3,6-bisaryl-1,2,4,5-tetrazines whilst other methods are more efficient for synthesis of 3,6-bisalkyl-1,2,4,5-tetrazines. The Pinner synthesis can be modified by additions of catalytic or stoichiometric additives like transition metal ions and elemental sulfur, respectively, to increase the yields of these aromatic tetrazines.[40, 42-44] The modified Pinner synthesis employing elemental sulfur is most common and readily accessible due to the use of inexpensive reagents and adaptability to gram scale quantities.

A series of 3,6-bisaryl-1,2,4,5-tetrazines **71-74** (Scheme 3.5) were furnished through a modified Pinner synthesis amended from literature.[45] Specifically, hydrazine monohydrate was added slowly to a suspension of an aromatic nitrile and sulfur in ethanol followed by 4 h under reflux. Following reaction, the mixture was cooled over an ice-bath allowing the dihydrotetrazine to precipitate and be readily obtained by filtration. The dihydrotetrazine was observed to begin to oxidise with exposure to air, with a colour change from bright yellow to pink/purple. As such, the dihydrotetrazine was immediately subjected to oxidation without purification. Oxidation was undertaken by the dropwise addition of an aqueous solution of sodium nitrite to a suspension of the dihydrotetrazine in acetic acid. Following reaction quench and collection of the resulting solid, the tetrazine could be readily purified by recrystallisation with ethanol.

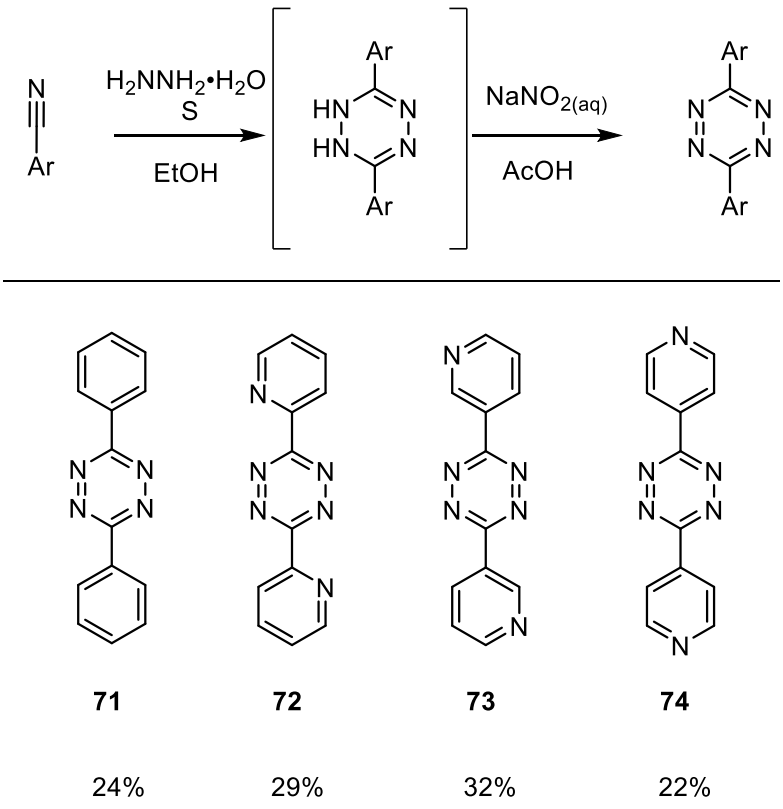

Scheme 3.5: The modified Pinner synthesis used to furnish a series of 3,6-bisaryl-1,2,4,5-tetrazines; yield from nitrile.

As well as these 3,6-bisaryl-1,2,4,5-tetrazines **71-74**, 3,6-bis(3',5'-dimethylpyrazol-1'-yl)-1,2,4,5-tetrazine **78** and 3,6-dichlorotetrazine **80** were of interest as dienes due to their potential to allow access to alternatively substituted materials by nucleophilic displacement of the substituents.[42] These tetrazines could be readily afforded through modified literature procedures (Scheme 3.6).[41, 46, 47]

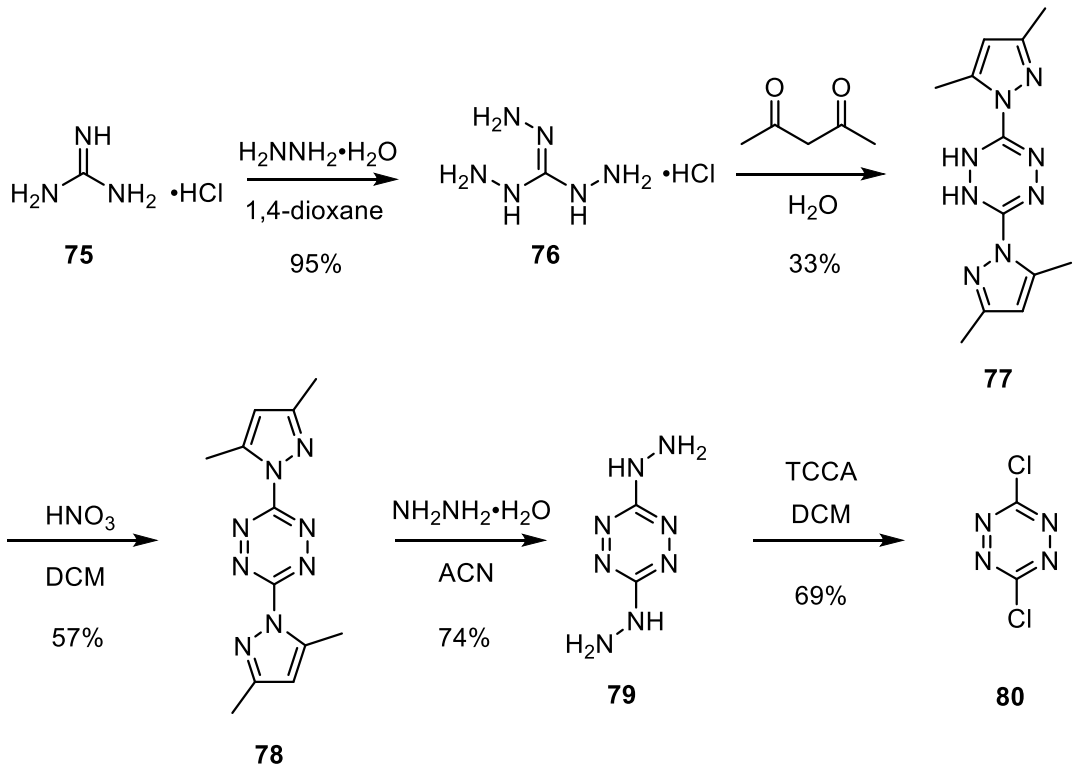

Scheme 3.6: Synthesis of 3,6-bis(3′,5′-dimethylpyrazol-1′-yl)-1,2,4,5-tetrazine **78** and 3,6-dichlorotetrazine **80** by modified literature procedures.[41, 46, 47]

Triaminoguanidine hydrochloride **76** was generated in near-quantitative yields by treatment of guanidine hydrochloride **75** with hydrazine monohydrate in 1,4-dioxane.[46] Condensation of the triaminoguanidine salt **76** with 2,4-pentandione in aqueous conditions with subsequent recrystallisation gave 3,6-bis(3′,5′-dimethylpyrazol-1′-yl)-1,2-dihydro-1,2,4,5-tetrazine **77** in a modest yield of 33%.[46] Successive oxidation with nitric acid and recrystallisation gave pure 3,6-bis(3′,5′-dimethylpyrazol-1′-yl)-1,2,4,5-tetrazine **78** in a good yield of 57%. The dichlorotetrazine **80** could then be afforded through the 3,6-bis(3′,5′-dimethylpyrazol-1′-yl)-1,2,4,5-tetrazine **78**. Due to the pyrazole group's leaving group ability,[42] the dihydrazinyltetrazine **79** was generated by nucleophilic substitution with hydrazine.[41, 47] Subsequent reaction with chlorine gas generated from trichloroisocyanuric acid (TCCA) afforded the desired dichlorotetrazine **80**. With a range of 3,6-bis-substituted-1,2,4,5-tetrazine readily prepared, their application in the IEDDA reaction with the natural pyrethrins **5** was explored.

3.3.3 Pyridazine pyrethrin analogues

The IEDDA reaction with 1,2,4,5-tetrazines can be utilised in the production of 1,2-diazines (pyridazines) **87** (Scheme 3.7). The [4+2] cycloaddition proceeds with the tetrazine **82** as diene forming a nitrogen-bridged bicyclic adduct **83** which rapidly undergoes a retro-Diels-Alder process expelling molecular nitrogen forming a dihydropyridazine **84**.[48] The resulting 4,5-dihydropyridazine **84**, which can quickly undergo a 1,3-shift to the 1,4-dihydropyridazine **85**,[37, 49] can subsequently be oxidised to restore aromaticity to the ring giving the pyridazine product **86**.[50]

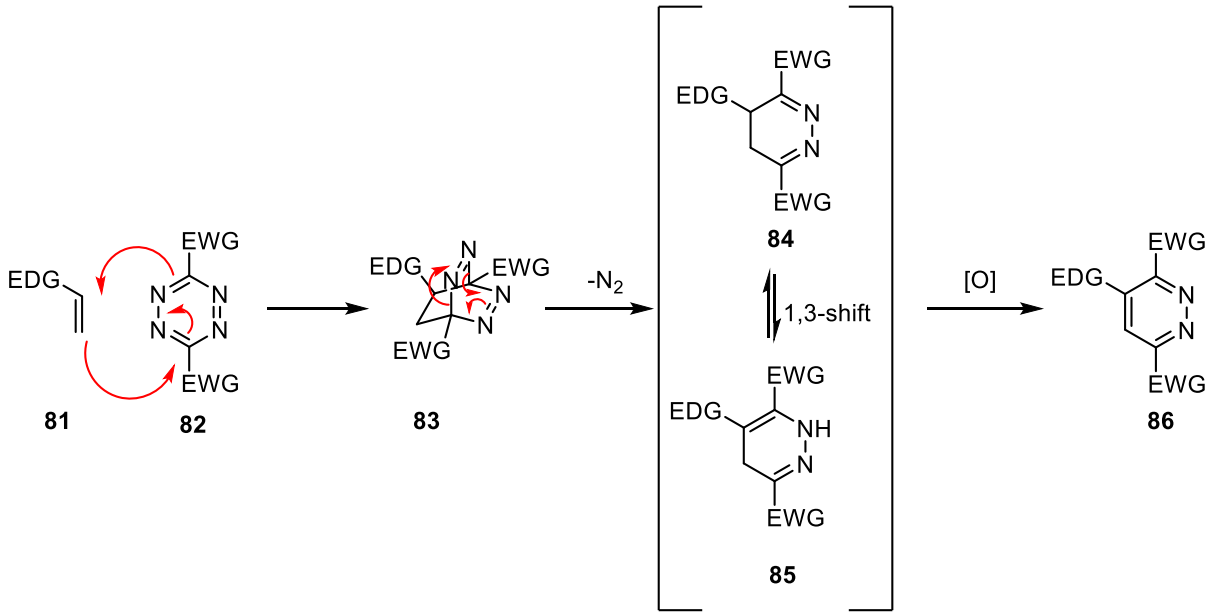

Scheme 3.7: Production of pyridazines by a IEDDA cycloaddition-oxidation process.

Initial attempts at this IEDDA process made use of individual pyrethrin I **5a** or II **5b** and 3,6-bis(2'-pyridyl)-1,2,4,5-tetrazine **72**. These two reagents were heated under reflux in anhydrous THF in an attempt to facilitate the cycloaddition cascade (Scheme 3.8). Due to the bright colour of the tetrazine starting material the reaction could be visually monitored with this bright purple material serving as a colourimetric indicator of reaction progression where the consumption of the tetrazine starting material was accompanied by a colour change to yellow. This reaction with the 2'-pyridyl variant **72** proceeded over an 8 h period and was subsequently cooled for the following oxidation. Once at room temperature, 2,3-dichloro-5,6-dicyano-1,4-benzoquinone (DDQ) was added as oxidant and the reaction mixture was stirred overnight. After work-up, a dark brown, viscous oil was obtained and subsequent analysis by NMR indicated reactivity at the terminal double bond of the pentadienyl moiety of the

pyrethrin **5** (Scheme 3.8). This reactivity was postulated due to the observation of shifted *cis*-alkene ^{1}H resonances downfield and the presence of an aromatic singlet (8.60 ppm) which is likely the result of the only aromatic proton in the pyridazine ring of the expected cycloadduct **87**. Aside from the desired cycloadduct **87**, the crude material was isolated as a complex mixture containing residual pyrethrin **5** and tetrazine **72**.

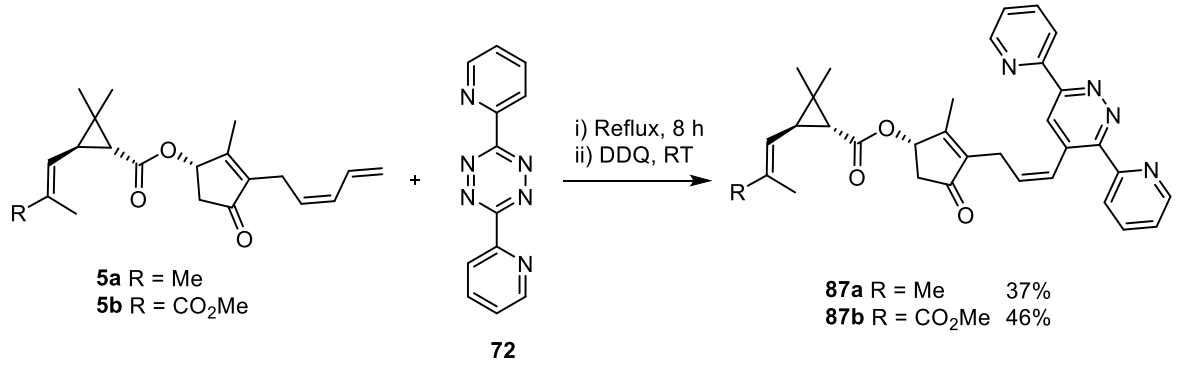

Scheme 3.8: IEDDA reactivity of pyrethrins **5** with 3,6-bis(2′-pyridyl)-1,2,4,5-tetrazine **72**.

Purification of the resulting pyridazine **87** was initially attempted through chromatographic means. Use of silica gel column chromatography was unable to sufficiently purify the cycloadduct **87** as it had a tendency to streak along the silica despite exhaustive investigation into eluting solvents. This affinity for the silica stationary phase may be the result of the basic properties of the pyridyl substituents and their interaction with the acidic silica. Despite this, the pyrethrin starting material **5** was readily removed due to its relatively non-polar character in comparison to the cycloadduct **87**, giving an enriched mixture of the cycloadduct **87**. Further exploration into purification focussed on the solubility of the cycloadduct **87** in comparison to the residual materials either by recrystallisation or trituration. Ultimately, trituration with warm hexane and subsequent cooling allowed a precipitate to form that was readily identified as the purified pyridazine **87**. Ultimately this trituration could be implemented directly on the crude reaction mixture still containing pyrethrin **5** giving the pyridazine adduct **87** in moderate yields of 37 and 46% for pyrethrin I **5a** and II **5b** respectively.

The IEDDA reaction sequence was then applied to the other synthesised tetrazines albeit with slightly altered reaction times. Reactions with the 4′-pyridyl- **74**, pyrazolyl- **78** and dichloro-1,2,4,5-tetrazine **80** proceeded within the 8 h reflux time period but the 3′-pyridyl- **73** and diphenyl-1,2,4,5-tetrazine **71** reactions required extended reflux times up to 24 h. The necessity for extended reaction times with these two tetrazines is likely due to the reduced

electron withdrawing capability of the phenyl groups in 3,6-bisphenyl-1,2,4,5-tetrazine **71** and reduced resonance effect of the 3'-pyridyl groups of 3,6-bis(3'-pyridyl)-1,2,4,5-tetrazine **73** in comparison to its 2'- **72** and 4'-counterparts **74**; deactivating the diene in the Diels-Alder process.[51]

Unlike the 2'-pyridylpyridazine **87**, the other cycloaddition adducts were able to be purified by silica gel column chromatography. The bisphenylpyridazine **88** and bispyrazolylpyridazine **91** adducts were able to be readily separated with solvent mixtures of ethyl acetate and hexane whilst the pyridyl containing cycloadducts (3'-pyridyl **89** and 4'-pyridyl **90**) required elution by higher polarity solvents. These pyridyl adducts **89** and **90** required blends of DCM and methanol or DCM, methanol and TEA to allow for purification of the desired materials respectively. Additionally, the 3'-pyridyl variants **89** were optimised to forego the oxidation step with DDQ due to the complexity of the resulting crude mixture. The resulting product mixture was found to aerobically oxidise to give the desired aromatic ring and was more readily purified by column chromatography.

Ultimately, a range of IEDDA cycloadducts were prepared from the pyrethrins **5** and 3,6-bissubstituted-1,2,4,5-tetrazines in varying yields depending on the tetrazine substituents (Table 3.1).

Table 3.1: IEDDA reaction of the pyrethrins **5** with various 3,6-bissubstituted tetrazines.

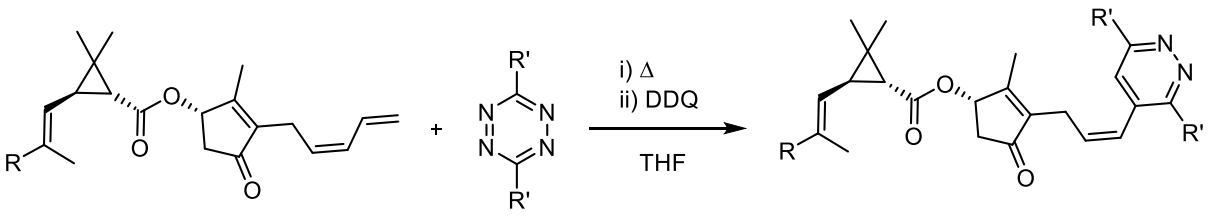

5a R = Me
5b R = CO_2Me

Compound	R	R′	Reaction time (h)[a]	Yield (%)
88a	Me	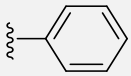	24	24
88b	CO_2Me	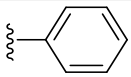	24	18
87a	Me	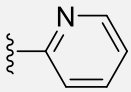	8	37
87b	CO_2Me	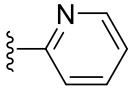	8	46
89a[b]	Me	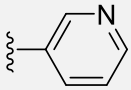	24	43 (dr 1:2 *E:Z*)
89b[b]	CO_2Me	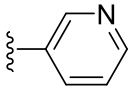	24	46 (dr 1:2.3 *E:Z*)
90a	Me	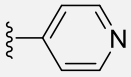	8	47
90b	CO_2Me	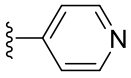	8	60
91a	Me	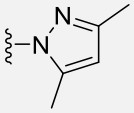	8	42
91b	CO_2Me	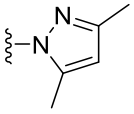	8	45
92a+93a	Me		8	31[c]
92b+93b	CO_2Me		8	30[c]

[a] Time reaction heated under reflux. [b] Oxidation with DDQ omitted from process. [c] Mass yield of isolated mixture.

In the case of IEDDA, particularly with tetrazines, the $HOMO_{dienophile}$–$LUMO_{diene}$ interaction involves the highly delocalised LUMO+1 (Figure 3.8B) rather than the heteroaromatic central LUMO (Figure 3.8A).[52, 53] Following modelling of these frontier orbitals, the experimental reactivities of the various substituted tetrazines were found to be in relatively good agreement with theoretically calculated $HOMO_{dienophile}$–$LUMO_{diene}$ energy gaps (Figure 3.8). Specifically, the 1,2,4,5-tetrazines with lower LUMO energies result in increased reaction rate in the IEDDA reaction ultimately giving higher yields in the same timeframe as those with larger $HOMO_{dienophile}$–$LUMO_{diene}$ energy gaps. The considerably lower yields of the bisphenylpyridazine adducts **88**, even after 24 h reaction times, are likely due to the diminished electron withdrawing effects the phenyl substituents have on the tetrazine in comparison to the other substituents, as is reflected in the $LUMO_{diene}$ energy (Figure 3.8C), ultimately decreasing reaction rate.[52, 54]

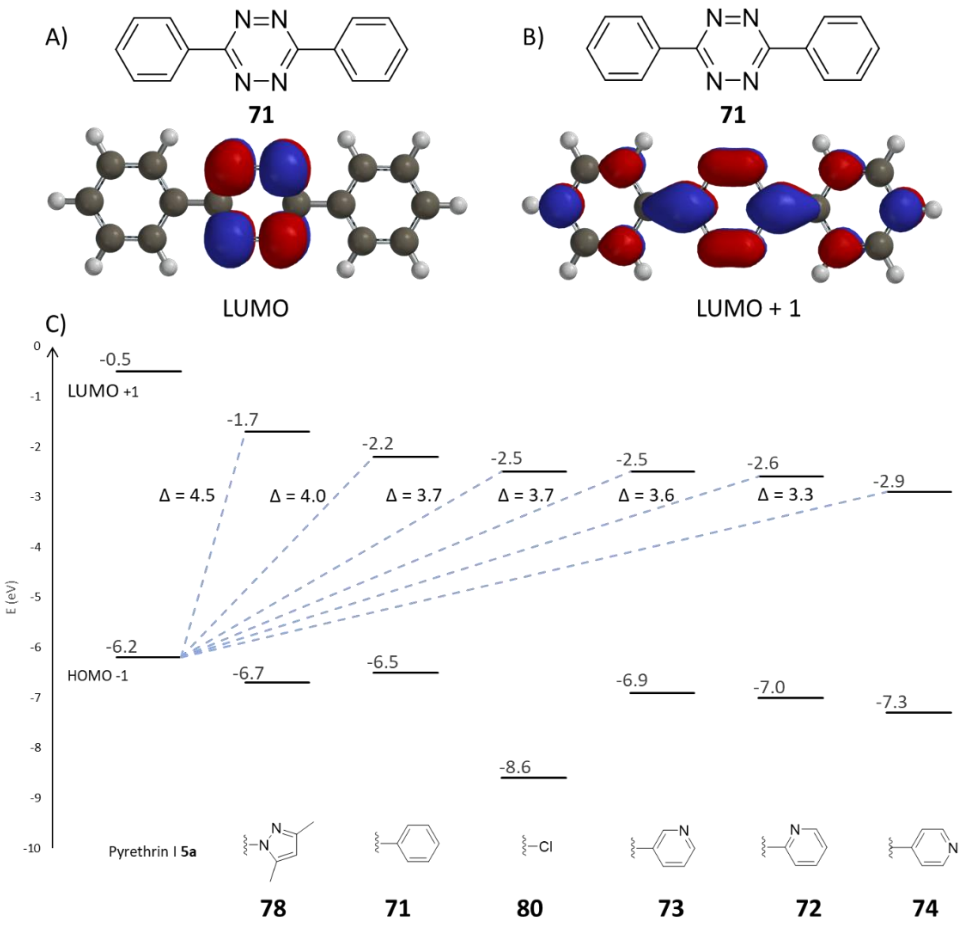

Figure 3.8: Representative LUMO **(A)** and LUMO+1 **(B)** of 3,6-diphenyl-1,2,4,5-tetrazine **71**, and the $HOMO_{dienophile}$–$LUMO_{dienophile}$ relationships of various substituted tetrazines and pyrethrin I **5a** determined by molecular modelling (DFT B3LYP/6-31G*) **(C)**.[10]

The 3′-pyridyl adducts **89** were able to be isolated in yields comparable to that of the rest in the series albeit with significantly longer reaction times despite the $LUMO_{diene}$ energy of the tetrazine **73** being comparable to that of the 3,6-bis(2′-pyridyl)-1,2,4,5-tetrazine **72**. Similarly, the 3,6-bis(3′5′-dimethylpyrazol-1′-yl)-1,2,4,5-tetrazine **78** exhibited faster reactivity than the diphenyltetrazine **71** despite a higher LUMO energy. Previous studies on the IEDDA reaction have highlighted that other factors, such as the interaction energy, strain and distortion of the employed substrates play a major role in the reactivity of the diene and dienophile which may result in the deviation from the theoretical trend of the aforementioned tetrazines.[25, 52, 55]

Alternate products were also isolated from reactions involving 3,6-bis(3′-pyridyl)-1,2,4,5-tetrazine **73** and 3,6-dichlorotetrazine **80**. More specifically, the 3′-pyridyl products **89** were isolated as mixtures of (*E*)- and (*Z*)-isomers, where the remaining double bond in the side chain of the cycloadduct **89** undergoes *cis-trans* isomerism under the reaction conditions. This is likely the result of extended exposure to the thermal conditions necessary for the Diels-Alder reaction and the increased conjugation of the new side chain. Evidence for this isomerism taking place by thermal means was shown with variable temperature NMR experiments (Figure 3.9) of the purified *cis*-isomer of the 2′-pyridyl pyrethrin II adduct **87b**. ^{1}H NMR spectra were taken at defined time intervals at 85 °C to observe the change from the *cis*-isomer of the cycloadduct to the *trans*-isomer.

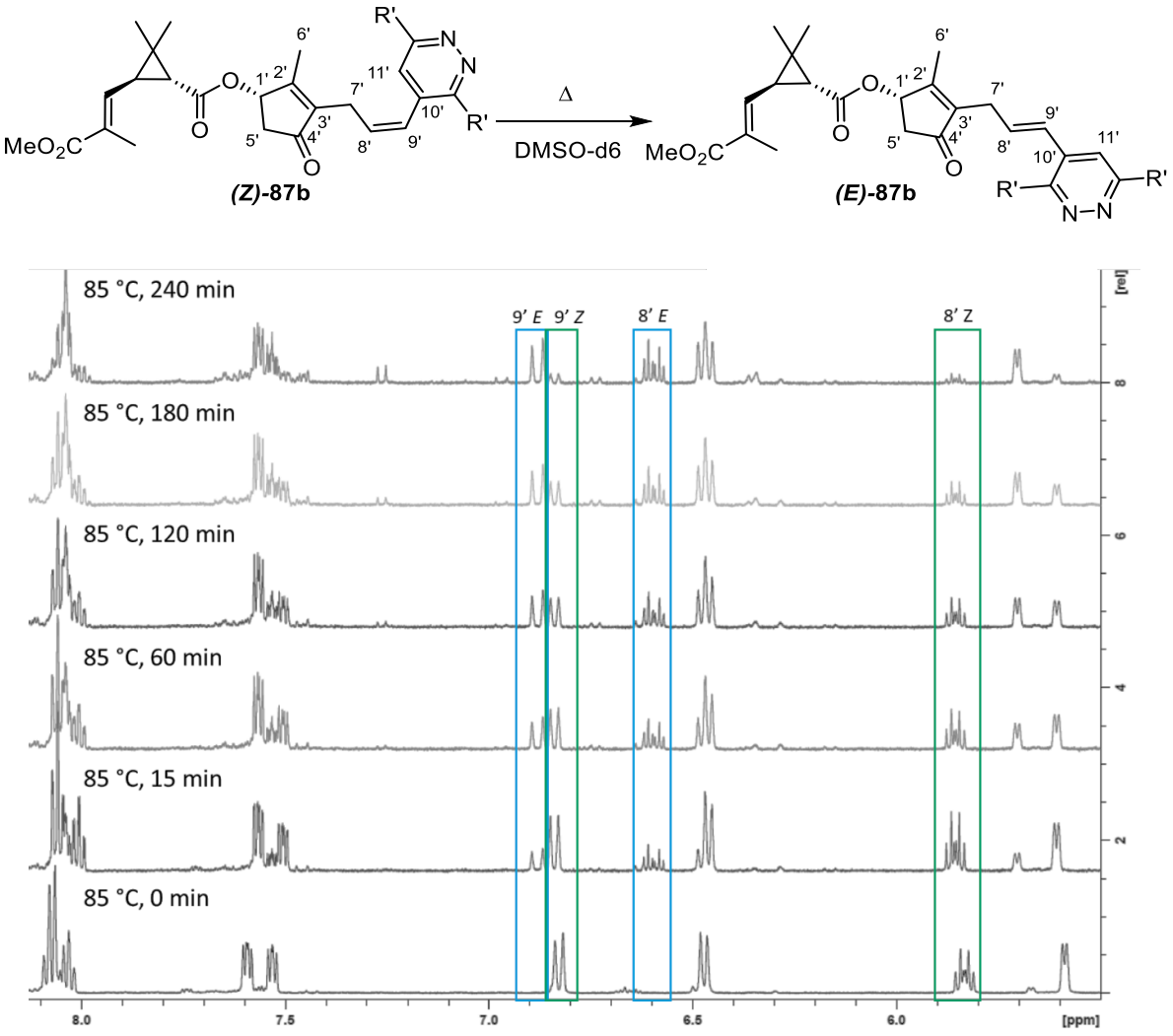

Figure 3.9: Partial ^{1}H NMR spectra at 85 °C monitoring the *cis-trans* isomerism of the 2′-pyridyl pyrethrin II cycloadduct **87b** over a 4 h period. Diagnostic resonances from the (*Z*)-isomer are highlighted in green and resonances from the (*E*)-isomer are highlighted in blue.

Within the first 15 min of heating in the NMR, the rapid isomerism of the purified pyridazine **87b** was observed with the appearance of the *trans*-alkene ^{1}H resonances at 6.59 ppm (H8′) and 6.88 ppm (H9′), as characterised by the larger coupling constant (*J* = 11.6 Hz *cis*, *J* = 15.8 Hz *trans*). After 4 h, the *cis*-isomer of the pyridazine adduct **87b** was almost completely converted to the more energetically stable *trans*-isomer. The ready thermal isomerism of these pyridazine adducts is likely due to the increased conjugation with the terminal aromatic system lowering the energy barrier necessary for the isomerism process.[56] Despite this, the pyridazine adduct **87b** remains stable for extended periods of time at 65 °C with variable temperature NMR experiments showing no change over 4 h of heating.

In addition, the reaction of pyrethrins **5** with 3,6-dichloro-1,2,4,5-tetrazine **80** (Scheme 3.9) results in an inseparable mixture of two compounds following purification by a silica gel plug. The mixture was identified as containing two Diels-Alder adducts with the presence of two separate aromatic singlets in a ratio of 1:2.3 and 1:2.3 for pyrethrins I **5a** and II **5b** respectively. Changing NMR solvent from $CDCl_3$ to DMSO-d_6 in the NMR analysis was able to resolve the ^1H resonance at 6.57 ppm into two alkene resonances, at 6.89 and 6.53 ppm, consistent with the minor product retaining the *cis*-alkene of the pentadienyl unit. As such, it was proposed that the IEDDA cycloaddition between the dichlorotetrazine **80** and natural pyrethrins **5** resulted in the production of a saturated cycloadduct **93** as a mixture with the expected cycloadduct **92** (Scheme 3.9) where the saturated material comprised the majority of the product distribution.

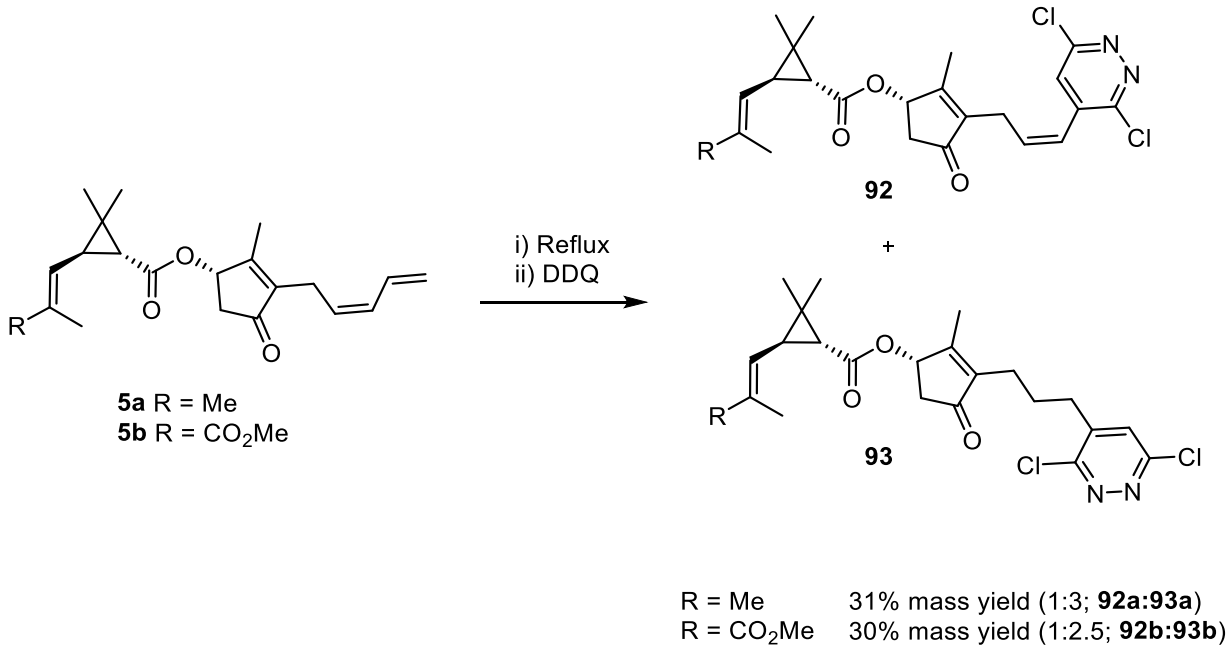

Scheme 3.9: IEDDA cycloaddition of the natural pyrethrins **5** and 3,6-dichloro-1,2,4,5-tetrazine **80** with oxidation.

Attempts to further separate and characterise the mixture by LCMS were unsuccessful in resolving the two compounds from one another however, the mass spectrum of the co-eluted mixture was able to allow for some differentiation. The natural isotope abundance of chlorine, being 75% ^{35}Cl and 25% ^{37}Cl, allows for the differentiation of the number of chlorine substituents present in a given material through the resulting isotope pattern observed in the mass spectrum.[57] The acquired mass spectrum (Figure 3.10) shows masses that were found

to correlate with the protonated cycloadduct **92** ($M+H^+$), a sodium adduct ($M+Na^+$) and, in the case of the pyrethrin II variant **92b** a fragment with loss of the methyl ester (461 *m/z*).

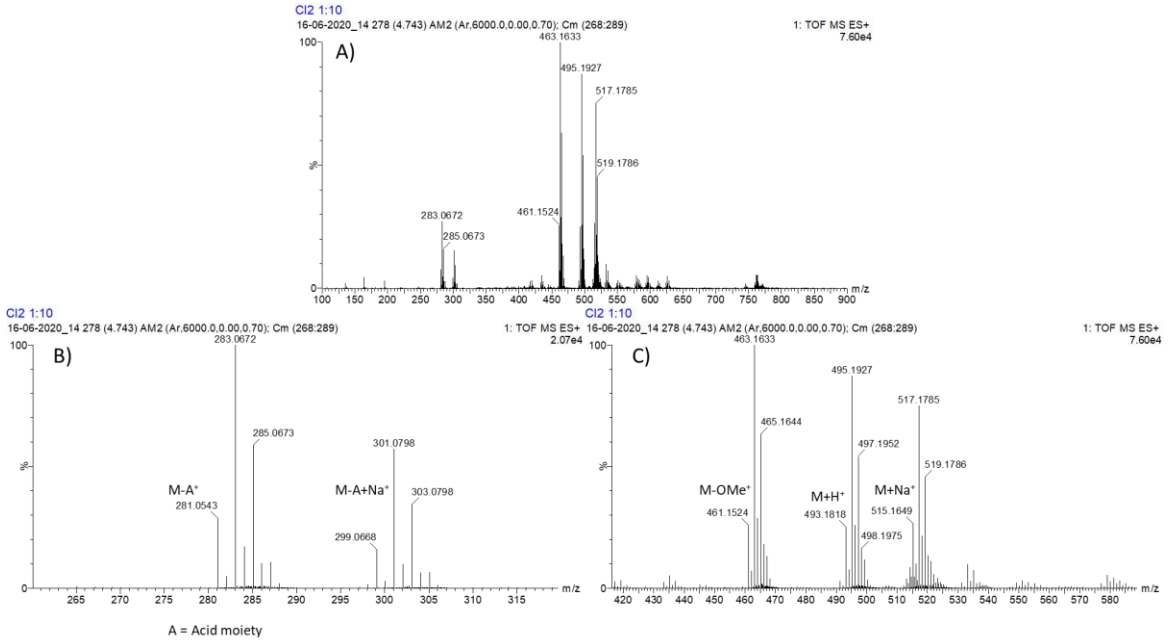

Figure 3.10: Representative mass spectrum, acquired by LCMS, of the cycloadduct mixture isolated from the reaction of dichlorotetrazine **80** and pyrethrin II **5b** from 100-900 *m/z* **(A)**, 260-320 *m/z* **(B)** and, 420-590 *m/z* **(C)**.

Despite the presence of these masses, the isotopic pattern did not appear to be consistent with the 9:6:1 ratio expected for a cycloadduct containing two chlorine atoms, namely the anticipated pyridazine **92**. The fragment and its corresponding sodium adduct, at 281 and 299 *m/z* respectively (Figure 3.10B), retained the unexpected isotopic pattern and were consistent with the loss of the acid moiety of the individual pyrethrins **5**. This highlighted that the mass discrepancy is limited to the rethrolone moiety, where the IEDDA reactivity has shown precedent for. It was then proposed that the co-eluting mixture contained the desired cycloadduct **92** and a similar product with a saturated site ($M+H_2$) resulting in overlapping isotopic patterns consistent with two chlorine atoms being present. This saturated cycloadduct constituted the majority of the crude mixture and was proposed to be either the unoxidised dihydropyridazine or the remaining double bond of the sidechain was reduced **93**. In an attempt to identify the unknown dihydro compound, selective 1D correlation NMR spectroscopy was pursued.

Selective 1D correlation experiments, much like their 2D counterparts, allow for the investigation into the connectivity of chemical environments within a given compound. In

contrast to the 2D equivalent, 1D correlation spectroscopy allows for the investigation into the connectivity associated with a given resonance and more rapid, resolved data acquisition.[58, 59] More specifically, selective 1D TOCSY experiments allow for the investigation into the spin system associated with a given chemical environment i.e. any proton signal within a continuous chain of spin-spin coupled proton environments.[60] Selective 1D TOCSY experiments (Figure 3.11) were undertaken on the product mixture isolated from the dichlorotetrazine **80** reactions with irradiation of the unknown aromatic signal at 7.44 ppm (Figure 3.11B) and the 7′ methylene proton of the unknown at 2.37 ppm (Figure 3.11C).

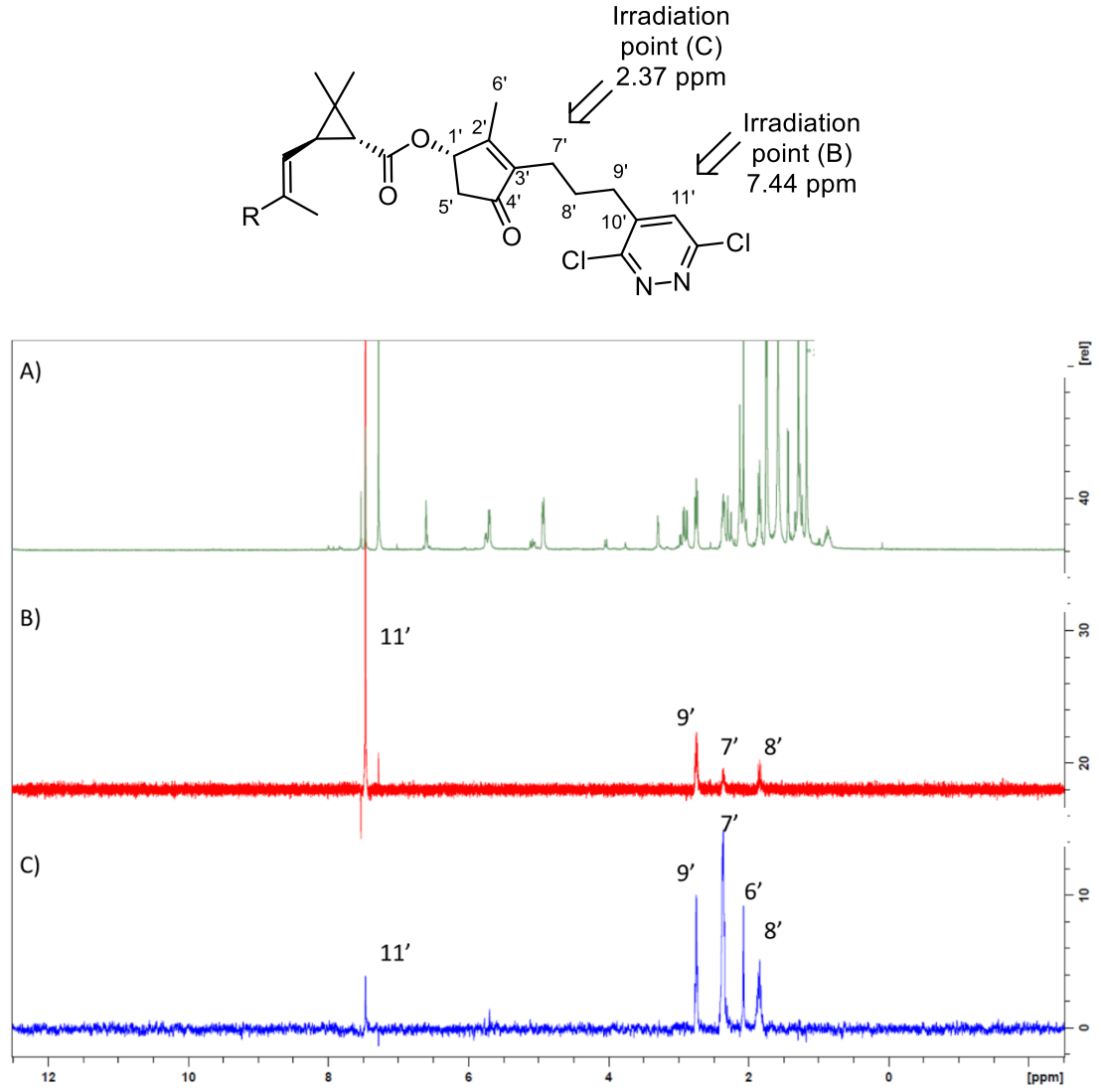

Figure 3.11: Representative analysis of the dichlorotetrazine adduct mixture of pyrethrin I **5a** showing the full ^{1}H NMR spectrum **(A)**, 1D TOCSY of the unknown aromatic signal irradiated at 7.44 ppm **(B)** and, 1D TOCSY of the unknown 7′ methylene signal irradiated at 2.37 ppm **(C)**.

From these selective 1D TOCSY correlations, it was found that the unidentified cycloadduct was likely the saturated variant **93** of the desired product **92**. This was determined by the selective irradiation of the aromatic signal of the unknown (7.44 ppm) which showed a spin system containing the irradiated aromatic and three individual aliphatic proton environments. Of the three aliphatic signals, the proton resonance at 2.37 ppm was determined to be the 7′ methylene of the rethrolone side chain as when it was selectively irradiated it not only correlated to the same spin system as the aromatic proton but also showed correlation to the 6′ (2.05 ppm) protons of the methyl substituent of the enone. As such, it is likely that the proton resonances at 2.72 and 1.83 ppm are the 9′ and 8′ protons of the side chain of the reduced cycloadduct **93**. As such, the 11′ proton likely couples directly to the 9′ proton and each successive proton environment couples down the side chain spin system to the 7′ methylene. Ultimately, this TOCSY analysis provided further evidence for the proposed saturated cycloadduct **93**. Attention turned to identifying the potential route this saturated cycloadduct **93** may have been formed through.

Control experiments where the oxidation with DDQ was omitted were undertaken to determine whether the intramolecular hydrogen transfer to the alkene was taking place during the Diels-Alder or the oxidative component of the reaction cascade. After reflux of the pyrethrin **5** with the dichlorotetrazine **80** the solvent was removed, and the crude mixture analysed by NMR. The analysis of the crude material showed the same saturated cycloadduct **93** contained in the mixture as was observed under the original reaction conditions. The presence of the aromatic material suggests the oxidation is either aerobic, with introduction of the atmosphere during work-up, or occurs *in situ*. It was proposed that the reduced cycloadduct **93** is potentially formed by an intramolecular transfer of hydrogen from the dihydropyridazine **94** resulting from the Diels-Alder cascade ultimately providing aromaticity to the pyridazine and the saturation of the sidechain in the reduced cycloadduct **93**. This transfer of hydrogen to the alkene was proposed to take place through a series of tautomerism events of the dihydropyridazine **94** (Scheme 3.10). The resulting 4,5-dihydropyridazine **94** formed as a result of the cycloaddition readily undergoes a 1,3-shift to give the 1,4-tautomer **95** due to its increased stability.[37, 49] Tautomerism of this 1,4-tautomer **95** could shift the double bond into the exocyclic position **96** which is likely to readily shift into the ring, providing aromaticity to give the saturated pyridazine product **93**.

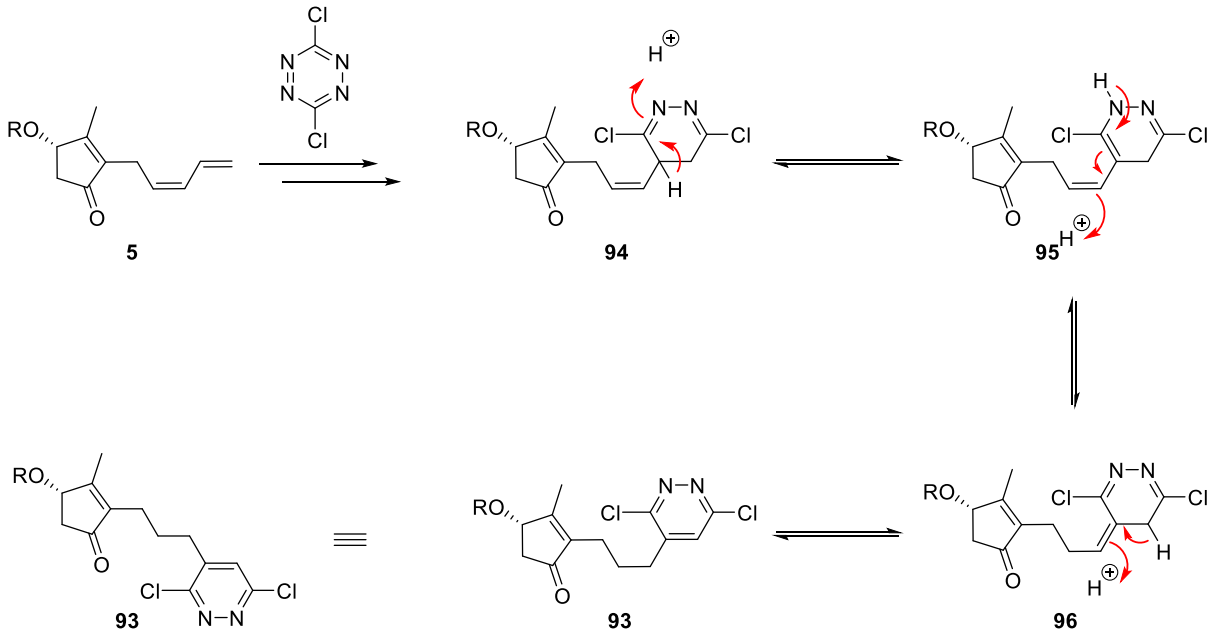

Scheme 3.10: Proposed tautomerism of the dihydropyridazine intermediate **94** to the saturated pyridazine product **93**.

Some precedent for this tautomerism process exists in literature, where a payload (RXH) is released by bioorthogonal click reactions with tetrazines *via* the dihydropyridazine adduct **99** (Scheme 3.11).[61-63] In this instance, the exocyclic pyridazine **101** is formed by an electron-cascade elimination of the 1,4-dihydropyridazine tautomer **100** releasing the appropriate payload (RXH) and CO_2. The exocyclic pyridazine **101** then readily rearranges to give the more stable, aromatic pyridazine product **102**.

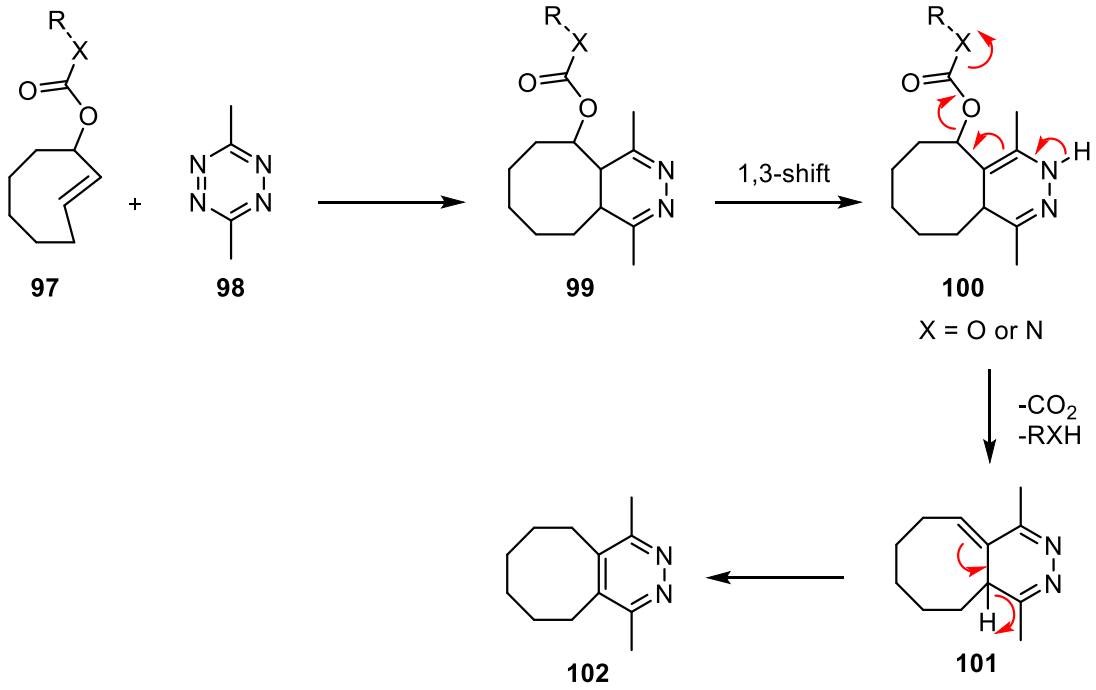

Scheme 3.11: Click and release of a payload (RXH) from the IEDDA reaction of 3,6-dimethyl-1,2,4,5-tetrazine **98** and *trans*-cyclooctenes **97**.[61-63]

Whilst 3,6-dimethyl-1,2,4,5-tetrazine **98** was found to rapidly undergo this elimination process, 3,6-bis(2'-pyridyl)-1,2,4,5-tetrazine **72** and other bisaryl-1,2,4,5-tetrazines were found to retain the payload and remain as the dihydopyridazine.[61, 64] Similarly, the various IEDDA cycloadditions employing diaromatic tetrazines with pyrethrins **5** showed no detectable quantities of a saturated cycloadduct likely due to the stabilisation of the dihydropyridazine through conjugation to the aromatic substituents.

3.4 Preliminary insecticidal activity of IEDDA pyrethrin cycloadducts

Preliminary investigation into the insecticidal activity of these pyridazine products was undertaken, by Andrew Kotze (CSIRO Agriculture and Food), through assay of pupation inhibition against *L. cuprina* larvae. All of the pyridazine adducts **87-91** were subjected to this assay, except for the dichloropyridazine **92** mixtures due to the presence of the saturated variant **93**. Unfortunately, these preliminary assays revealed a lack of insecticidal activity of these pyridazine pyrethrin analogues **87-91**. This is likely the result of the large steric bulk now incorporated at the end of the pyrethrin chain, particularly with the bis-substitution of the pyridazine ring.

3.5 Conclusions

The pentadienyl unit of the natural pyrethrins **5** was initially proposed to be primed for functionalisation by normal electron demand Diels-Alder cycloaddition. The viability of this reactivity was investigated by molecular modelling of the frontier molecular orbitals of pyrethrins **5** and several conventional, reactive dienophiles **58-60**. This theoretical investigation showed $HOMO_{diene}$–$LUMO_{dienophile}$ energy profiles consistent with normal electron demand Diels-Alder reactions and as such experimental implementation of this reaction was pursued. Unfortunately, under typical reaction conditions no cycloadduct was obtained and the starting materials were readily isolated. Application of more forcing conditions, including higher temperatures, Lewis acid catalysis and high pressure were unable to elicit any response with the starting materials recovered unreacted. As a result of this lack of reactivity, it was proposed that the pyrethrins **5** are conformationally restricted and are unable to access the necessary *s-cis* geometry required for the [4+2] cycloaddition. Preliminary investigations revealed that eliciting *cis-trans* isomerism of the pyrethrins **5** by exposure to UV light and subsequent reaction with maleic anhydride **59** was able to afford Diels-Alder reactivity. Despite this, attempts to purify the cycloadduct **62** resulted in decomposition and the efficiency of isomerism was low making it difficult to obtain appreciable quantities of the Diels-Alder active pyrethrin isomer **34**.

Alternative Diels-Alder conditions were then explored where the pyrethrin **5** acted as dienophile in IEDDA reactions. A range of electron-deficient 3,6-bis-substituted-1,2,4,5-tetrazines were prepared and implemented as diene with the pyrethrin dienophiles **5**. From this, a range of pyridazine cycloadducts were produced in moderate to good yields with the Diels-Alder reactivity remaining relatively consistent with calculated $HOMO_{dienophile}$–$LUMO_{diene}$ energy differences. Two notable exceptions were the 3,6-bis(3′,5′-dimethylpyrazol-1′-yl)-1,2,4,5-tetrazine **78** and 3,6-bis(3′-pyridyl)-1,2,4,5-tetrazine **73** where the difference in reactivity likely results from other factors like the interaction energy and distortion of the substrates. In conjunction, two alternate reaction product profiles were obtained from the reactions utilising 3,6-bis(3′-pyridyl)-1,2,4,5-tetrazine **73** and 3,6-dichloro-1,2,4,5-tetrazine **80**. It was found that the longer reaction times necessary for the cycloadditions with the 3′-pyridyl variant **89** resulted in *cis-trans* isomerism of the remaining double bond in the side chain giving *E/Z* mixtures of the cycloadduct. This isomerism process

was found to be relatively general for the bisarylpyridazine adducts as shown by variable temperature NMR monitoring of the 2′-pyridylpyridazine adduct **87b** at 85 °C. Use of the 3,6-dichloro-1,2,4,5-tetrazine **80** in the IEDDA procedure resulted in the isolation of a mixture that was found to contain the saturated pyridazine cycloadduct **93** and the expected pyridazine cycloadduct **92**. Omitting the oxidation procedure resulted in the isolation of the same reaction profile containing the saturated cycloadduct **93**. As such it was proposed to have formed as a result of a cascade of tautomerism events of the intermediate dihydropyridazine **94**.

3.6 References

1. Sarkar, D.; Bera, N.; Ghosh, S., [2+2] Photochemical Cycloaddition in Organic Synthesis. *Eur. J. Org. Chem* **2020,** *2020*, 1310-1326.
2. Yin, Z.; He, Y.; Chiu, P., Application of (4+3) cycloaddition strategies in the synthesis of natural products. *Chem. Soc. Rev.* **2018,** *47*, 8881-8924.
3. Pellissier, H., Recent Developments in the [5+2] Cycloaddition. *Adv. Synth. Catal.* **2018,** *360*, 1551-1583.
4. Nicolaou, K. C.; Snyder, S. A.; Montagnon, T.; Vassilikogiannakis, G., The Diels-Alder Reaction in Total Synthesis. *Angew. Chem. Int. Ed.* **2002,** *41* (10), 1668-1698.
5. Zhang, J.; Shukla, V.; Boger, D. L., Inverse Electron Demand Diels-Alder Reactions of Heterocyclic Azadienes, 1-Aza-1,3-Butadienes, Cyclopropenone Ketals, and Related Systems. A Retrospective. *J. Org. Chem.* **2019,** *84* (15), 9397-9445.
6. Mandal, D. K., Chapter 3 - Pericyclic Reactions: Introduction, Classification and the Woodward-Hoffmann Rules. In *Pericyclic Chemistry: Orbital Mechanisms and Stereochemistry*, Elsevier Inc.: Amsterdam, Netherlands, 2018; pp 63-106.
7. Gregoritza, M.; Brandl, F. P., The Diels-Alder reaction: A powerful tool for the design of drug delivery systems and biomaterials. *Eur. J. Pharm. Biopharm.* **2015,** *97*, 438-453.
8. Sauer, J.; Sustmann, R., Mechanistic Aspects of Diels-Alder Reactions: A Critical Survey. *Angew. Chem. Int. Ed.* **1980,** *19*, 779-807.
9. Singh, R. K.; Tsuneda, T., Reaction Energetics on Long-Range Corrected Density Functional Theory: Diels-Alder Reactions. *J. Comput. Chem.* **2013,** *34*, 379-386.
10. *Spartan '16 for Windows*, Wavefunction Inc.: 18401 Von In Karman Avenue, Suite 370, Irvine, CA 92612 U.S.A.
11. Fleming, I., Thermal Pericyclic Reactions. In *Molecular Orbitals and Organic Chemical Reactions*, John Wiley and Sons: Chichester, West Sussex, 2010.
12. Sahoo, M. K., Dimethyl Acetylene Dicarboxylate. *Synlett* **2007,** (13), 2142-2143.
13. Korobitsyna, I. K.; Khalikova, A. V.; Rodina, L. L.; Shisherina, N. P., 4-phenyl-1,2,4-triazoline-3,5-dione in organic synthesis (review). *Chem. Heterocycl. Compd.* **1983,** *19* (147-169).
14. Jensen, F.; Foote, C. S., Reaction of 4-Phenyl-1,2,4-triazoline-3,5-dione with Substituted Butadienes. A Nonconcerted Diels-Alder Reaction. *J. Am. Chem. Soc.* **1987,** *109*, 6376-6385.

15. Pindur, U.; Lutz, G.; Otto, C., Acceleration and Selectivity Enhancement of Diels-Alder Reactions by Special and Catalytic Methods. *Chem. Rev.* **1993,** *93*, 741-761.
16. Vermeeren, P.; Hamlin, T. A.; Fernandez, I.; Bickelhaupt, M., How Lewis Acids Catalyze Diels-Alder Reactions. *Angew. Chem. Int. Ed.* **2020,** *59* (15), 6201-6206.
17. Fringuelli, F.; Piermatti, O.; Pizzo, F.; Vaccaro, L., Recent Advances in Lewis Acid Catalyzed Diels-Alder Reactions in Aqueous Media. *Eur. J. Org. Chem* **2001,** *2001*, 439-455.
18. Wei, K.; Gao, H.-T.; Li, W.-D. Z., Facile Synthesis of Oxabicyclic Alkenes by Ultrasonication-Promoted Diels-Alder Cycloaddition of Furano Dienes. *J. Org. Chem.* **2004,** *69*, 5763-5765.
19. Vidis, A.; Laurenczy, G.; Kusters, E.; Sedelmeier, G.; Dyson, P. J., High-pressure effects on the Diels-Alder reaction in room temperature ionic liquids. *J. Phys. Org. Chem.* **2007,** *20*, 109-114.
20. Dauben, W. G.; Baker, W. R., Organic reactions at high pressure. The Diels-Alder reaction of *p*-benzoquinone with dienic esters. *Tetrahedron Lett.* **1982,** *23* (26), 2611-2614.
21. Klarner, F.-G.; Wurche, F., The Effect of Pressure on Organic Reactions. *J. Prakt. Chem.* **2000,** *342* (7), 609-636.
22. Kiselev, V. D.; Konovalov, A. I.; Asano, T.; Kashaeva, E. A.; Iskhakova, G. G.; Shihab, M. S.; Medvedeva, M. D., Solvent effect on the volume of activation and volume of the Diels-Alder reaction. *J. Phys. Org. Chem.* **2001,** *14*, 636-643.
23. McCulloch, A. W.; Smith, D. G.; McInnes, A. G., Influence of Lewis Acids on the Diels-Alder Reaction. V. The Reaction of Furan with Dimethyl Acetylenedicarboxylate. *Can. J. Chem.* **1973,** *51* (24), 4125-4136.
24. Yepes, D.; Perez, P.; Jaque, P.; Fernandez, I., Effect of Lewis acid bulkiness on the stereoselectivity of Diels-Alder reactions between acyclic dienes and α,β-enals. *Org. Chem. Front.* **2017,** *4*, 1390-1399.
25. Yu, P.; Li, W.; Houk, K. N., Mechanisms and Origins of Selectivities of the Lewis Acid-Catalyzed Diels-Alder Reactions between Arylallenes and Acrylates. *J. Org. Chem.* **2017,** *82*, 6398-6402.
26. Grau, E.; Lesage, A.; Norsic, S.; Coperet, C.; Monteil, V.; Sautet, P., Tetrahydrofuran in $TiCl_4$/THF/$MgCl_2$: a Non-Innocent Ligand for Supported Ziegler-Natta Polymerization Catalysts. *ACS Catal.* **2013,** *3*, 52-56.
27. Tsuji, J.; Yamakawa, T.; Mandai, T., Application of Palladium Catalyses to a Simple Synthesis of (±)-Pyrethrolone. *Tetrahedron Lett.* **1979,** *39*, 3741-3744.

28. Sasaki, M.; Okada, K.; Matsui, M., A Convenient Conversion of Allethrolone to Pyrethrolone. *Agric. Biol. Chem.* **1979,** *43* (2), 379-381.
29. Bullivant, M. J.; Pattenden, G., Photodecomposition of Natural Pyrethrins and Related Compounds. *Pestic. Sci.* **1976,** *7*, 231-235.
30. Elliott, M.; Janes, N. F., Chemistry of the Natural Pyrethrins. In *Pyrethrum: The Natural Insecticide*, Casida, J. E., Ed. 1973; pp 55-100.
31. Kawano, Y.; Yanagihara, K.; Miyamoto, T.; Yamamoto, I., Examination of the Conversion Products of Pyrethrins and Allethrin Formulations Exposed to Sunlight by Gas Chromatography and Mass Spectrometry. *J. Chromatogr. A* **1980,** *198* (3), 317-328.
32. Png, Z. M.; Zeng, H.; Ye, Q.; Xu, J., Inverse-Electron-Demand Diels-Alder Reactions: Principles and Applications. *Chem. Asian J.* **2017,** *12*, 2142-2159.
33. Boger, D. L.; Mullican, M. D., Inverse electron demand Diels-Alder reaction of 3-carbomethoxy-2-pyrones with 1,1-dimethyoxyethylene: a simple and mild method of aryl annulation. *Tetrahedron Lett.* **1982,** *23* (44), 4551-4554.
34. Hashimoto, Y.; Abe, R.; Morita, N.; Tamura, O., Inverse-electron-demand Diels-Alder reaction of α,β-unsaturated hydrazones with 3-methoxycarbonyl α-pyrones. *Org. Biomol. Chem.* **2018,** *16*, 8913-8916.
35. Palasz, A., Recent Advances in Inverse-Electron-Demand Hetero-Diels-Alder Reactions of 1-Oxa-1,3-Butadienes. *Top. Curr. Chem.* **2016,** *374* (24).
36. Anderson, E. D.; Boger, D. L., Inverse Electron Demand Diels-Alder Reactions of 1,2,3-Triazines: Pronounced Substituent Effects on Reactivity and Cycloaddition Scope. *J. Am. Chem. Soc.* **2011,** *133*, 12285-12292.
37. Oliveira, B. L.; Guo, Z.; Bernardes, G. J. L., Inverse electron demand Diels-Alder reactions in chemical biology. *Chem. Soc. Rev.* **2017,** *46*, 4895-4950.
38. Carboni, R. A.; Lindsey, R. V., Reactions of Tetrazine with Unsaturated Compounds. A New Synthesis of Pyridazines. *J. Am. Chem. Soc.* **1959,** *81* (16), 4342-4346.
39. Bagge, R. E.; Mauldin, T. C.; Boday, D. J.; Kobilka, B. M.; Loy, D. A., Transforming Polybutadiene with Tetrazine Click Chemistry into Antioxidant Foams That Fluoresce with Oxidation. *Chem. Mater.* **2017,** *29* (18), 7953-7960.
40. Mayer, S.; Lang, K., Tetrazines in Inverse-Electron-Demand Diels-Alder Cycloadditions and Their Use in Biology. *Synthesis* **2017,** *49*, 830-848.

41. Gong, Y.-H.; Miomandre, F.; Meallet-Renault, R.; Badre, S.; Galmiche, L.; Tang, J.; Audebert, P.; Clavier, G., Synthesis and Physical Chemistry of *s*-Tetrazines: Which Ones are Fluorescent and Why? *Eur. J. Org. Chem* **2009,** *2009* (35), 6121-6128.
42. Clavier, G.; Audebert, P., *s*-Tetrazines as Building Blocks for New Functional Molecules and Molecular Materials. *Chem. Rev.* **2010,** *110* (6).
43. Audebert, P.; Sadki, S.; Miomandre, F.; Clavier, G.; Vernieres, M. C.; Saoud, M.; Hapiot, P., Synthesis of new substituted tetrazines: electrochemical and spectroscopic properties. *New. J. Chem.* **2004,** *28*, 387-392.
44. Yang, J.; Karver, M. R.; Li, W.; Sahu, S.; Devaraj, N. K., Metal-Catalyzed One-Pot Synthesis of Tetrazines Directly from Aliphatic Nitriles and Hydrazine. *Angew. Chem. Int. Ed.* **2012,** *51* (21), 5222-5225.
45. Li, C.; Ge, H.; Yin, B.; She, M.; Liu, P.; Li, X.; Li, J., Novel 3,6-unsymmetrically disubstituted-1,2,4,5-tetrazines S-induced one-pot synthesis, properties and theoretical study. *RSC Adv.* **2015,** *5*, 12277-12286.
46. Coburn, M. D.; Buntain, G. A.; Harris, B. W.; Hiskey, M. A.; Lee, K. Y.; Ott, D. G., An Improved Synthesis of 3,6-Diamino-1,2,4,5-tetrazine. II. From Triaminoguanidine and 2,4-Pentanedione. *J. Heterocyclic Chem.* **1991,** *28*, 2049-2050.
47. Chavez, D. E.; Hiskey, M. A., 1,2,4,5-tetrazine based energetic materials. *J. Energ. Mater.* **1999,** *17*, 357-377.
48. Devaraj, N. K.; Weissleder, R., Biomedical Applications of Tetrazine Cycloadditions. *Acc. Chem. Res.* **2011,** *44* (9), 816-827.
49. Warrener, R. N.; Harrison, P. A., π-Bond Screening in Benzonorbornadienes: The Role of 7-Substituents in Governing the Facial Selectivity for the DielsAlder Reaction of Benzonorbornadienes with 3,6-Di(2-pyridyl)-s-Tetrazine. *Molecules* **2001,** *6*, 353-369.
50. Pagel, M., Inverse electron demand Diels-Alder (IEDDA) reactions in peptide chemistry. *J. Pep. Sci.* **2018,** *25*, e3141.
51. Cativiela, C.; Garcia, J. I., Electronic effects of heterocyclic substituents. Spectroscopical and theoretical (AM1) study in a series of heterocyclic carboxaldehydes. *Can. J. Chem.* **1990,** *68*, 1477-1481.
52. Liu, F.; Liang, Y.; Houk, K. N., Theoretical Elucidation of the Origins of Substituent and Strain Effects on the Rates of Diels-Alder Reactions of 1,2,4,5-Tetrazines. *J. Am. Chem. Soc.* **2014,** *136*, 11483-11493.

53. Li, Y.; Miomandre, F.; Clavier, G.; Galmiche, L.; Alain-Rizzo, V.; Audebert, P., Inverse Electron Demand Diels-Alder Reactivity and Electrochemistry of New Tetrazine Derivatives. *ChemElectroChem* **2017,** *4*, 430-435.
54. Hoge, B.; Bader, J., A qualitative scale for the electron withdrawing effect of substituted phenyl groups and heterocycles. *J. Fluor. Chem.* **2007,** *128*, 857-861.
55. Liu, F.; Paton, R. S.; Kim, S.; Liang, Y.; Houk, K. N., Diels-Alder Reactivities of Strained and Unstrained Cycloalkenes with Normal and Inverse-Electron-Demand Dienes: Activation Barriers and Distortion/Interaction Analysis. *J. Am. Chem. Soc.* **2013,** *135*, 15642-15649.
56. Wyman, G. M., The Cis-Trans Isomerization of Conjugated Compounds. *Chem. Rev.* **1955,** *55* (4), 625-657.
57. Gross, R. A., A Mass Spectral Chlorine Rule for Use in Structure Determinations in Sophomore Organic Chemistry. *J. Chem. Educ.* **2004,** *81* (8), 1161-1168.
58. Parella, T., High-Quality Specta by Implemention Pulsed-Field Gradients as the Coherence Pathway Selection Procedure. *Magn. Reson. Chem.* **1996,** *34* (5), 329-347.
59. Kessler, H.; Mronga, S.; Gemmecker, G., Multi-dimensional NMR experiments using selective pulses. *Magn. Reson. Chem.* **1991,** *29* (6), 527-557.
60. Kontogianni, V. G.; Tsiafoulis, C. G.; Roussis, I. G.; Gerothanassis, I. P., Selective 1D TOCSY NMR method for the determination of glutathione in white wine. *Anal. Methods* **2017,** *9*, 4464-4470.
61. Versteegen, R. M.; Rossin, R.; Hoeve, W. t.; Janssen, H. M.; Robillard, M. S., Click to Release: Instantaneous Doxorubicin Elimination upon Tetrazine Ligation. *Angew. Chem. Int. Ed.* **2013,** *52*, 14112-14116.
62. Versteegen, R. M.; Hoeve, W. t.; Rossin, R.; Geus, M. A. R. d.; Janssen, H. M.; Robillard, M. S., Click-to-Release from *trans*-Cyclooctenes: Mechanistic Insights and Expansion of Scope from Established Carbamate to Remarkable Ether Cleavage. *Angew. Chem. Int. Ed.* **2018,** *57*, 10494-10499.
63. Onzen, A. H. A. M. v.; Versteegen, R. M.; Hoeben, F. J. M.; Filot, I. A. W.; Rossin, R.; Zhu, T.; Wu, J.; Hudson, P. J.; Janssen, H. M.; Hoeve, W. t.; Robillard, M. S., Bioorthogonal Tetrazine Carbamate Cleavage by Highly Reactive *tran*-Cyclooctene. *J. Am. Chem. Soc.* **2020,** *142*, 10955-10963.

64. Blackman, M. L.; Royzen, M.; Fox, J. M., Tetrazine Ligation: Fast Bioconjugation Based on Inverse-Electron-Demand Diels-Alder Reactivity. *J. Am. Chem. Soc.* **2008,** *130*, 13518-13519.

Chapter 4 Heck Arylation of the Pyrethrins

4.1 Introduction

Palladium-catalysed cross coupling reactions have become a staple in organic chemistry for the construction of carbon-carbon and carbon-heteroatom bonds leading to extended organic frameworks.[1] The use of these reactions is widespread throughout the research sector and has been implemented in the industrial syntheses of several pharmaceuticals and agrochemicals.[2, 3] By far the most recognised forms of these palladium-catalysed couplings are the Suzuki, Negishi and Heck reactions (Scheme 4.1) with the award of the Nobel prize in 2010 to their namesakes. The earliest of these reactions was developed by Richard F. Heck in 1968, initially making use of aromatic organomercury compounds **103** and electron-deficient olefins **104** as coupling partners with palladium (II) salts as catalyst giving arylated alkenes similar to **105** (Scheme 4.1A).[4] This early version of the Heck reaction was later refined and evolved into the modern iteration with the use of aryl or vinyl halides **106**, any alkene with a free C(sp^2)-H **107** and palladium (0) complexes giving rise to a larger scope of substituted alkenes **108** (Scheme 4.1B).[1, 5, 6]

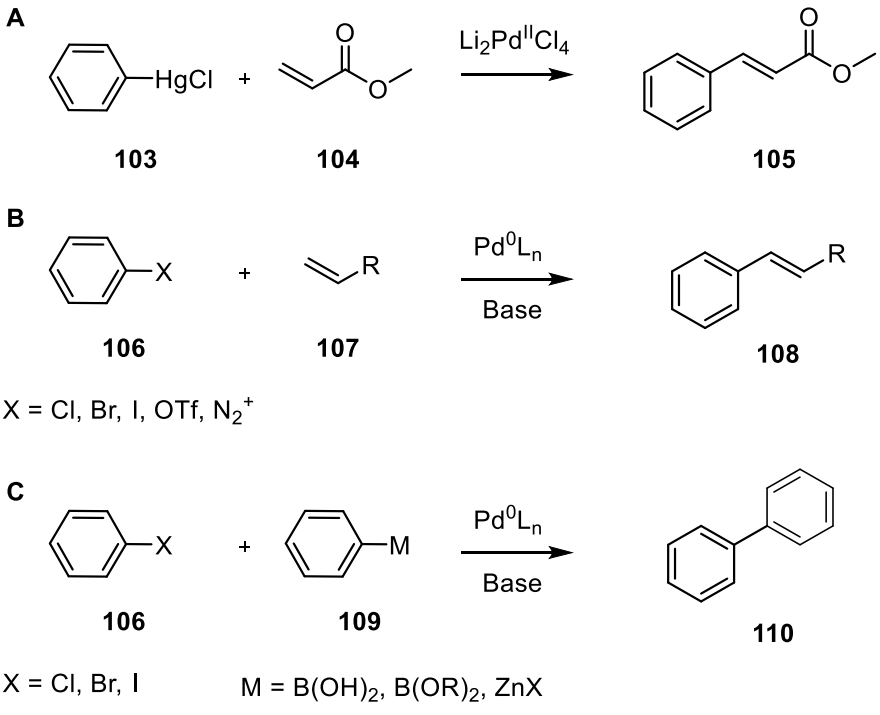

Scheme 4.1: Early development of the Heck reaction **(A),** the modern day iteration **(B)** and, general Suzuki and Negishi coupling **(C)**.

Soon after the development of the Heck reaction, Negishi explored the coupling of organozinc reagents **109** with aryl halides **106** that could be catalysed by either nickel or palladium catalysts (Scheme 4.1C).[7, 8] In conjunction, Suzuki established the palladium-catalysed coupling of boronic acids **109** with aryl and vinyl halides **106** (Scheme 4.1C).[9, 10] Both the Negishi and Suzuki coupling reactions can generate substituted alkenes **108**, much like the Heck reaction, as well as biaryl systems **110**. Whilst all three of these coupling reactions make use of palladium(0) catalysis, the catalytic cycles (Scheme 4.2) of the Suzuki/Negishi coupling and the Heck reaction differ following the oxidative addition (Scheme 4.2A) of the aryl halide reagent **106** to the palladium(0) catalyst. Both the Suzuki and Negishi couplings rely on a transmetallation (Scheme 4.2B) from the boronic acid/ester or organozinc **109** respectively to the palladium catalyst whilst the Heck reaction has direct interaction with the unfunctionalised olefin coupling partner.

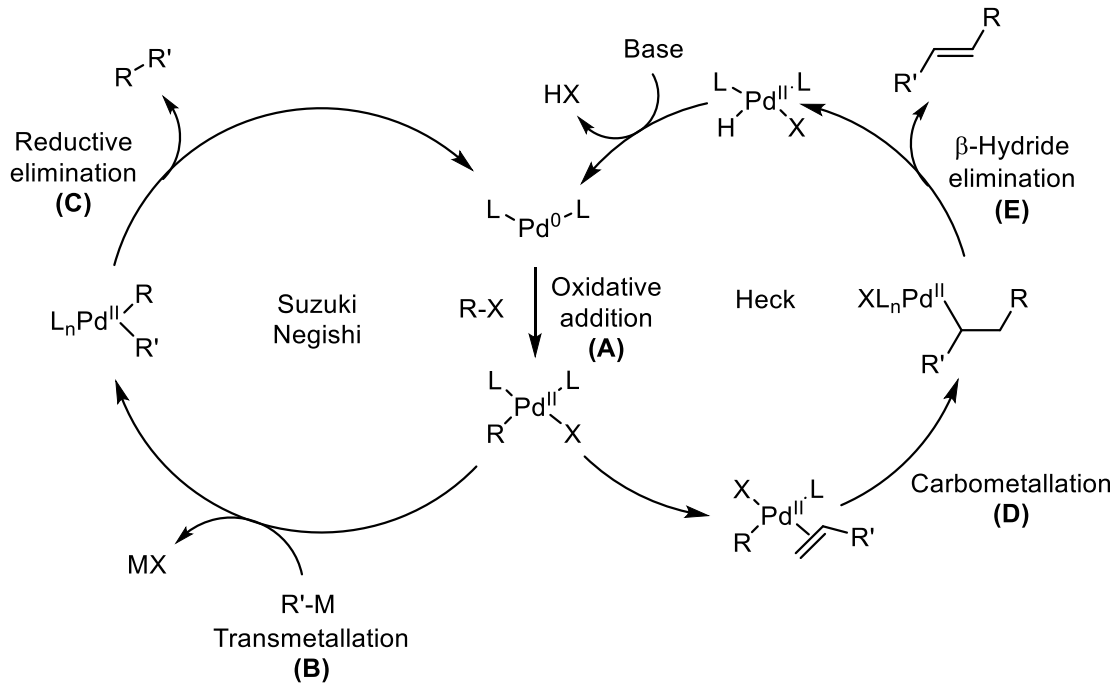

Scheme 4.2: General catalytic cycles of the Suzuki, Negishi and Heck reactions.[1]

This direct interaction and its extensive history make the Heck reaction attractive due to the accessibility to substrates, foregoing the need for functionalisation prior to coupling.

The natural Pyrethrins **5-7** are rich with alkene C-H sites that may lend themselves to functionalisation by the palladium-catalysed Heck reaction. The various alkene double bonds are mostly contained to the rethrolone moiety of the pyrethrin scaffold, the more sensitive

component of the Pyrethrins **5-7**. Many of the rethrolone moieties of the pyrethroids are based on aromatic scaffolds, with the phenoxybenzyl group a common feature (Chapter 1; Figure 1.7). Introduction of an aromatic system to the rethrolone component of the natural Pyrethrins **5-7** may serve to produce analogues with similar characteristics to the synthetic pyrethroids. The presence of several alkenes and palladium interactive functional groups within the Pyrethrins **5-7**, in particular the more abundant pyrethrins **5**, makes both chemo- and regio-selectivity a high priority in developing reaction protocols for the introduction of aryl substituents *via* the Heck reaction. As such, initial investigations in this thesis turned to developing reaction conditions to facilitate the Heck coupling of the pyrethrins **5** with aryl coupling partners in a site-selective manner.

4.2 Screening reaction conditions

Whilst the Heck reaction shows particular efficiency in the coupling of electron-deficient olefins, specifically acrylates and styrenes, with aryl halides, including triflates and diazoniums,[11, 12] there has been significant progress towards generality with the implementation of electron-rich olefins (Scheme 4.1B).[13] A range of conditions exist throughout literature for this coupling process that can be modified to facilitate regioselectivity and enhance reactivity of inefficient coupling partners, i.e. aryl chlorides.[14-16] As such, it was necessary to develop Heck conditions that not only allowed for the coupling to take place with the pyrethrins **5** but also resulted in regioselectivity and prevented any alternate reactivity from taking place with other palladium interactive functional groups.

Initially, relatively general conditions were implemented as a means of screening the reactivity of the natural pyrethrins **5** in Heck reactions (Scheme 4.3). The relatively electron-rich alkenes of the pyrethrin scaffold make them somewhat deactivated to the Heck process so aryl iodides were explored as coupling partners due to their increased reactivity in the palladium catalytic cycle (Scheme 4.2), particularly in the oxidative addition to the palladium centre.[14, 17] In conjunction, early attempts to elicit the coupling made use of tetrakis(triphenylphosphine)palladium(0) ($Pd(PPh_3)_4$) as catalyst due to its general use across palladium-catalysed cross-coupling chemistry. With this catalyst, iodobenzene as the aryl halide coupling partner and triethylamine as base initial attempts at the Heck reaction of pyrethrins **5** were undertaken. The various reaction components were added to a solution of the pyrethrin **5** in dry THF under inert atmosphere and was followed by heating the mixture

under reflux for up to 24 h. The reaction mixture was sampled and analysed by ^{1}H NMR to monitor the progress of the reaction, however, little change was observed over the reaction period. Ultimately no coupled product was detected in the crude mixture isolated from the reaction (Scheme 4.3) prompting alteration and extensive screening into the reaction conditions.

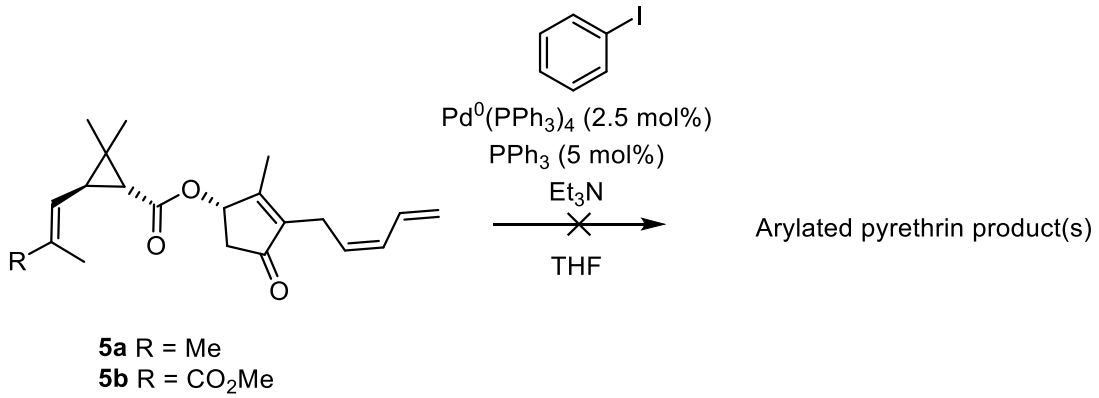

Scheme 4.3: Initial attempt at Heck reaction of the pyrethrins **5** with iodobenzene.

Screening of alternate reaction conditions began by exploring sources of palladium(0) as a means of eliciting the Heck reaction of the pyrethrins **5**. Generally, the catalytically active palladium species is of the form $Pd(0)L_2$ which in the case of $Pd(PPh_3)_4$ requires two of the phosphine ligands to dissociate from the palladium complex.[18, 19] However, the stability of the $Pd(PPh_3)_4$ 18-electron complex makes this dissociation slow, preventing efficient formation of the catalytically active complex and as such inhibiting turnover of the catalytic cycle.[18] Tris(dibenzylideneacetone)dipalladium(0) (Pd_2dba_3) is another common source of palladium(0) for use in palladium-catalysed organic reactions. Unlike $Pd(PPh_3)_4$, the dibenzylideneacetone ligands in Pd_2dba_3 are easily displaced and substituted for other ligands, making it ideal for the *in situ* production of catalytically active palladium complexes.[20] As such, Pd_2dba_3 was used as catalyst in the aforementioned Heck reactions (Scheme 4.4) along with triphenylphosphine as a ligand for formation of the catalytically active $Pd(0)L_2$. Following overnight reaction, the crude isolate was analysed by ^{1}H NMR and was found to have small quantities of an unknown coupled product. The formation of this coupled material was surmised based on the presence of new alkene resonances showing coupling consistent with arylation on the terminal site of the sidechain **111** (Scheme 4.4). Despite this, conversion

remained less than 10% after 24 h showing low efficiency of the catalytic process and the necessity for further screening of reaction conditions.

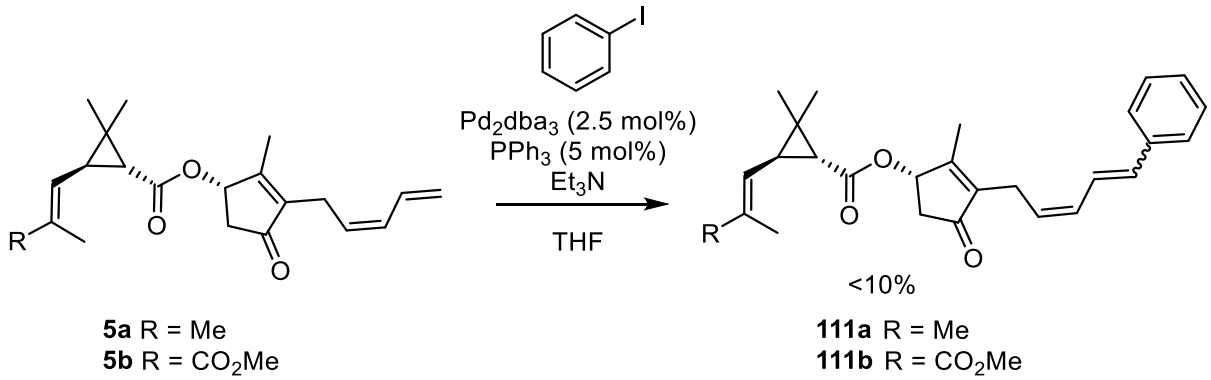

Scheme 4.4: Inefficient terminal arylation of pyrethrins **5** with iodobenzene under Heck conditions.

Choice of solvent is another parameter of importance to explore for reaction development and eventual optimisation. *N,N*-Dimethylformamide (DMF) is a common solvent used in the Heck reaction for its capacity to solvate both organic and inorganic reagents, ability to participate as a ligand in some metal catalysed processes, and has a high boiling point allowing for higher reflux temperatures.[21] Utilising DMF also allows for screening of different bases, more specifically the use of organic or inorganic bases. Therefore, the model Heck reaction with pyrethrins **5** and iodobenzene was undertaken in DMF, retaining the Pd_2dba_3/PPh_3 catalytic system, with either triethylamine or potassium carbonate as base (Scheme 4.5).

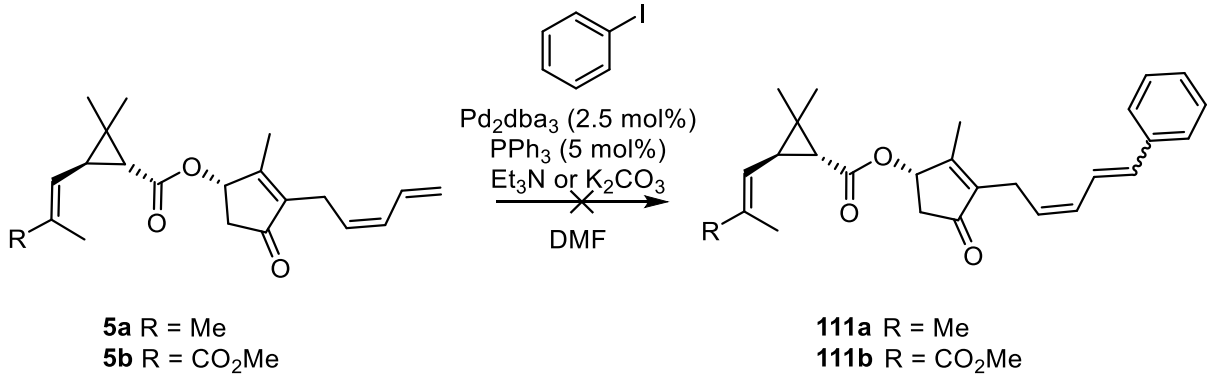

Scheme 4.5: Desired Heck reaction of pyrethrins **5** in DMF.

Introduction of potassium carbonate resulted in a rapid colour change of the reaction mixture from colourless to brown. Upon reaction completion and work-up it was found the reaction mixture no longer contained the pyrethrin starting material **5** and showed no evidence of the

previously observed coupled product **111**. Whilst DMF has the capacity to solvate ionic species, its ability to solvate anions is low resulting in the enhanced reactivity of anionic or basic reagents.[22-24] As a result of this marked increase in base reactivity, a mixture of Diels-Alder cycloadducts, **36** and **37,** of the rethrolone moiety of the pyrethrins **5** was isolated (Scheme 4.6).

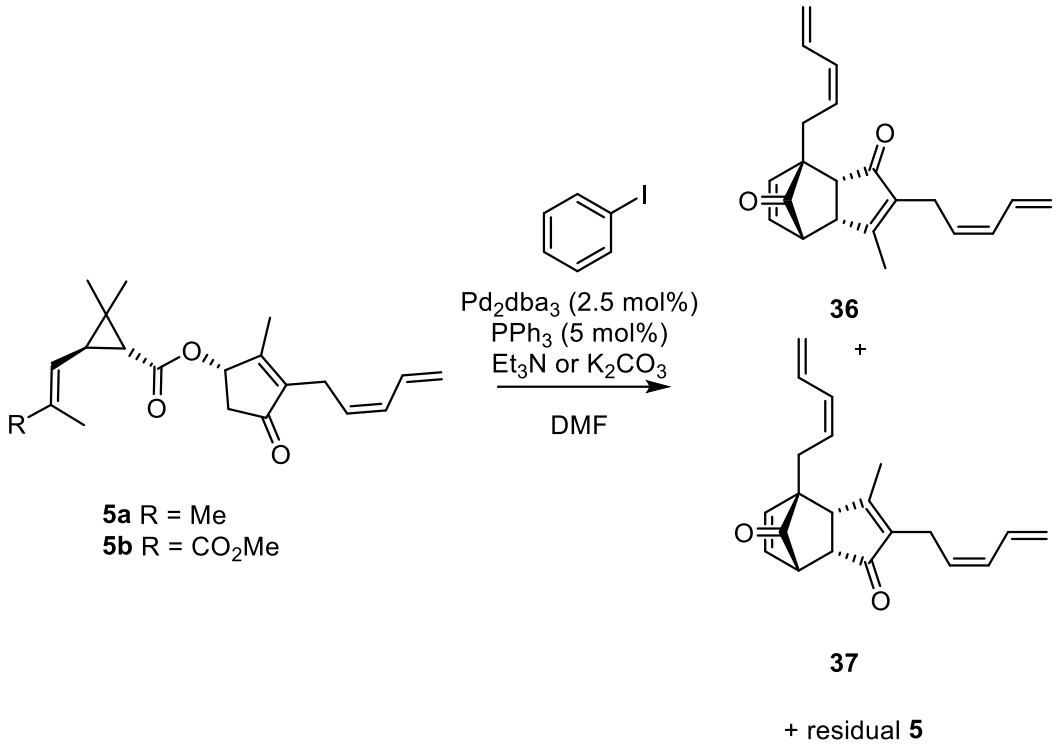

Scheme 4.6: Observed reactivity of the pyrethrins 5 under Heck conditions in DMF.

This reactivity of the pyrethrins **5** (Scheme 4.7) has been well-established where elimination of the ester on the enone moiety under basic conditions results in the cyclopentadienone analogue **35** which rapidly undergoes Diels-Alder cycloaddition with a second equivalent of this analogue giving two rethrolone dimers **36** and **37**.[25]

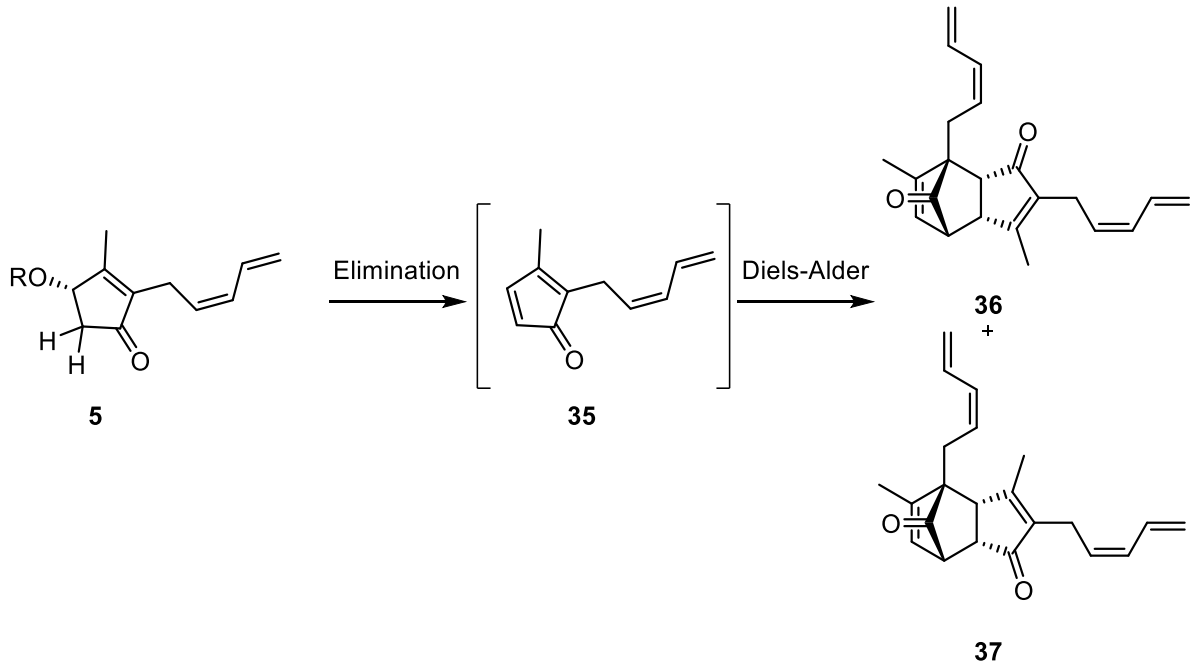

Scheme 4.7: Elimination and Diels-Alder cycloaddition pathway of the natural pyrethrins **5** under basic conditions.

The use of triethylamine in DMF resulted in a similar colour change and product distribution (Scheme 4.6), namely the rethrolone dimers **36** and **37**, however at a decreased rate with the presence of some remaining pyrethrin starting material **5** in the resulting crude product mixture. This similar reactivity likely stems from the stabilisation of the resulting cationic conjugate acid of the triethylamine through strong interaction with the DMF solvent. As such, an alternate solvent was necessary to prevent this reactivity which led to the use of acetonitrile to retain polar aprotic properties but to a much smaller extent.[26]

The model Heck reaction with pyrethrins **5** and iodobenzene was revisited retaining the previous catalytic materials, Pd_2dba_3 and triphenylphosphine, and triethylamine in acetonitrile (Scheme 4.8). Much like the previous attempt in THF, the reaction failed to result in significant conversion to a coupled product prompting further investigation into alternative catalytic conditions.

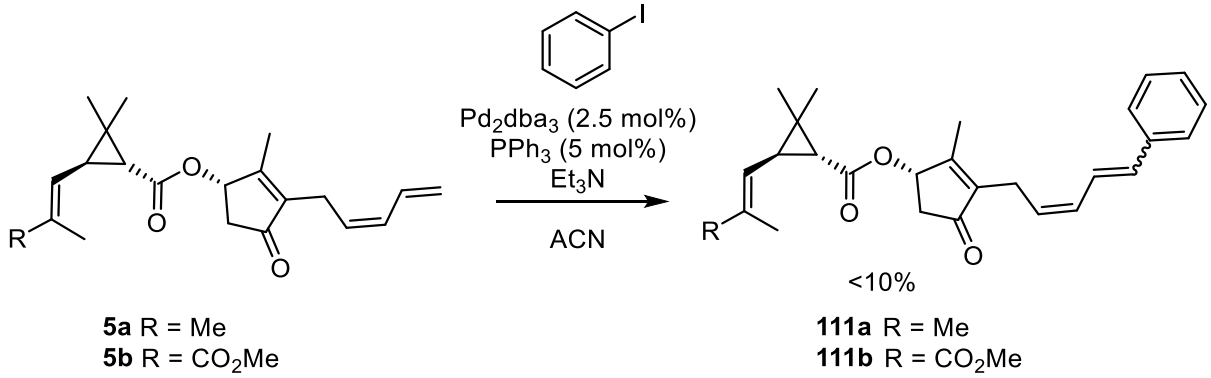

Scheme 4.8: Revisited Heck conditions employing a palladium(0) catalyst and polar aprotic solvent.

Commonly, Heck reactions make use of a palladium (II) precatalyst that is reduced and undergoes ligand exchange *in situ* to give the catalytically active palladium (0) complex.[17, 27] Palladium (II) acetate ($Pd(OAc)_2$) is by far the most common of these palladium (II) salts used as a precatalyst which readily undergoes the pre-activation pathway to a catalytically active palladium (0) complex in the presence of triphenylphosphine (Scheme 4.9).[28-30] The generally accepted mechanism for the production of the active palladium (0) catalyst **112** with triphenylphosphine starts with a rapid association of two phosphine ligands to the $Pd(OAc)_2$ followed by a slower elimination of acetoxytriphenylphosphonium acetate to give monotriphenylphosphine palladium (0) **113**. Rapid association of two more phosphine ligands to the palladium centre give the tristriphenylphosphine palladium (0) complex **114** that, upon dissociation of a phosphine ligand, can then enter the Heck catalytic cycle. The residual acetoxytriphenylphosphonium acetate decomposes rapidly to acetate and triphenylphosphonium oxide.

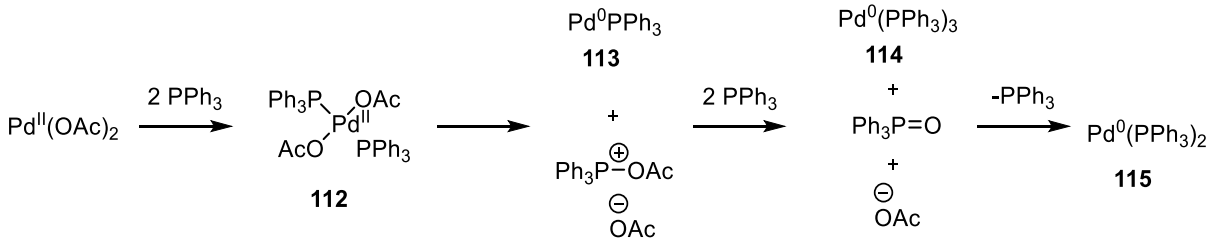

Scheme 4.9: *In situ* activation of the palladium(II) precatalyst with triphenylphosphine for use in the Heck reaction catalytic process.

Unfortunately, implementation of this palladium(II) pre-activation pathway still resulted in minor conversion of the pyrethrin starting material **5** to any coupled product (Scheme 4.10).

Ultimately, it was found that the lack of conversion was due to the lack of turnover in the catalytic cycle of the Heck reaction.

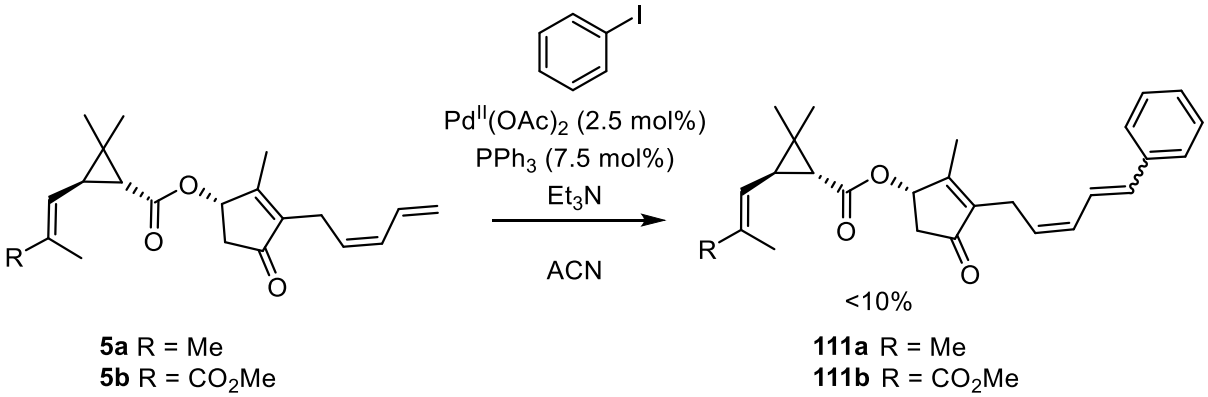

Scheme 4.10: Attempted Heck reaction utilising a palladium (II) precatalyst.

The catalytic cycle of the Heck reaction can proceed either through a neutral pathway or by a cationic pathway however they both take place *via* the same three main steps (Scheme 4.11): oxidative addition of the aryl halide to the palladium catalyst (Scheme 4.11A), carbometallation to the olefin substrate (Scheme 4.11B) and β-hydride elimination to give the arylated olefin (Scheme 4.11C).[14]

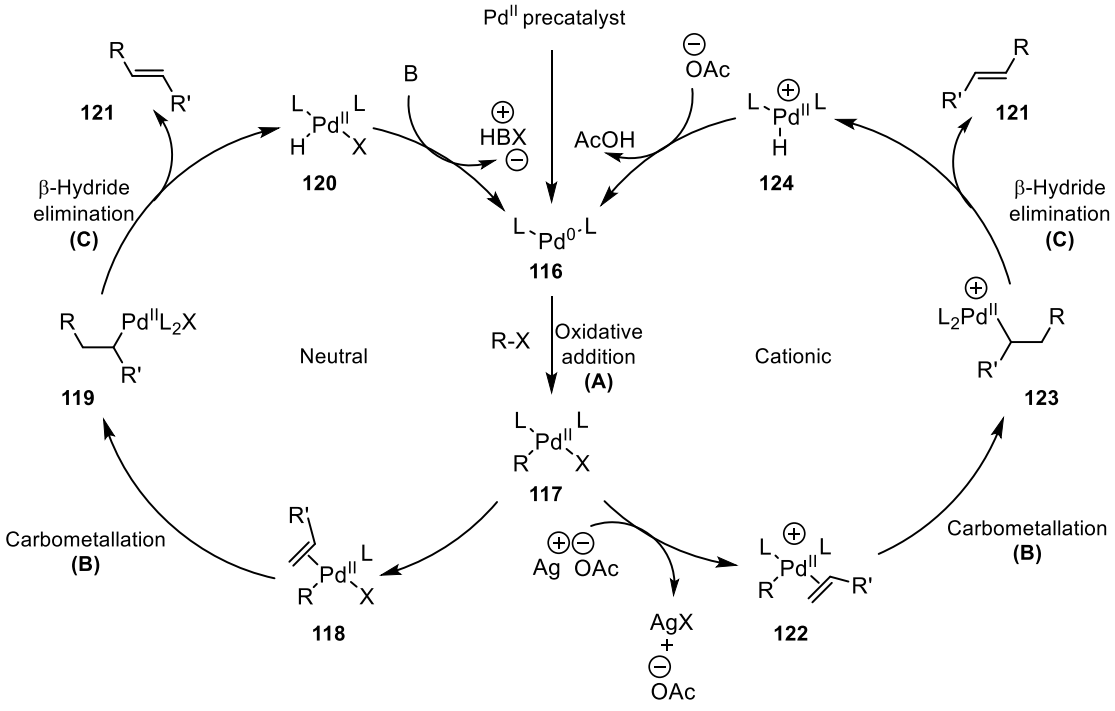

Scheme 4.11: The two potential catalytic cycles of the Heck reaction.

As outlined above (Scheme 4.11), oxidative addition (Scheme 4.11A) of the aryl halide gives the palladium(II) complex **117** which then coordinates to the π-system of the alkene substrate to give either the neutral **118** or cationic **122** palladium intermediate depending on the conditions employed. In the neutral pathway the π-coordinated palladium complex **118** is formed through dissociation of a ligand whilst in the cationic pathway the halide/pseudohalide is lost resulting in the cationic palladium complex **122**. Typically, the cationic process is favoured when aryl triflates are used due to the ready dissociation of the triflate from the palladium(II) centre or,[12, 31] when a silver(I) or thallium(I) salt is added to abstract the halide from the palladium(II) complex **117**.[32-35] Following carbometallation (Scheme 4.11B), the coupled product **121** is afforded by β-hydride elimination (Scheme 4.11C) along with a palladium(II) hydride complex **120** or **124** which is then reduced with a base to regenerate the palladium(0) catalyst **116**. The Heck reaction *via* the cationic catalytic cycle works particularly well for electron-rich olefins and has been demonstrated to have high regio- and chemo-selectivity for the terminal position in conjugated dienes.[33, 36]

With the electron-rich nature of the alkenes in the rethrolone side chain of the pyrethrins **5** and the potential for regioselective coupling, the cationic pathway of the Heck reaction was explored for arylation of the terminal position. In a bid to promote the cationic catalytic cycle, silver(I) acetate was employed in stoichiometric quantities to abstract the halide from the post oxidative addition palladium(II) complex **117** (Scheme 4.11). The use of silver(I) acetate also allows for the omission of the previously employed base as it can act in this capacity, allowing for regeneration of the catalytic palladium(0) after cross-coupling. The new conditions were directly applied to the model Heck reaction of the pyrethrins **5** with iodobenzene using the palladium(II) acetate precatalyst and silver(I) acetate in anhydrous acetonitrile (Scheme 4.12). Ultimately, work-up and analysis of the resulting crude material showed a substantial increase in consumption of the pyrethrin starting material **5**. Purification by column chromatography resulted in the isolation of two isomeric arylated pyrethrin analogues where the expected terminal regioselectivity was achieved (Scheme 4.12). Characterisation of the two materials confirmed their identities as the arylated analogue with either *cis*-*trans* isomerism of the *cis*-alkene **111** or migration of both double bonds into conjugation with the enone **125** respectively. Notably both arylated pyrethrin isomers, **111** and **125,** were isolated as the (*E,E*)-diastereomer.

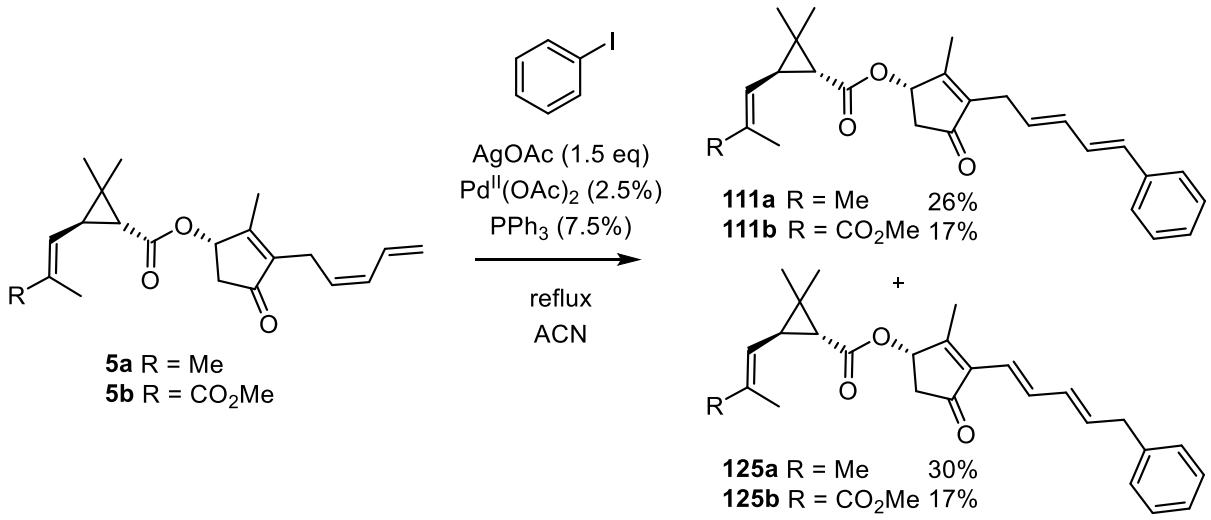

Scheme 4.12: Heck arylation of the natural pyrethrins **5** with iodobenzene *via* a cationic catalytic cycle.

The *trans*-geometry of the coupled alkene is unsurprising given the high stereoselectivity exhibited by the Heck reaction. The carbometallation takes place in a *syn* fashion followed by the carbopalladated material **123** rapidly reorganising to minimise the steric encumbrance between the palladium complex and newly arylated position, shifting the palladium onto the same face as the hydride (Scheme 4.13).[31] The subsequent β-hydride elimination also proceeds in a *syn* manner, delivering the *trans*-alkene **121**.[14, 31]

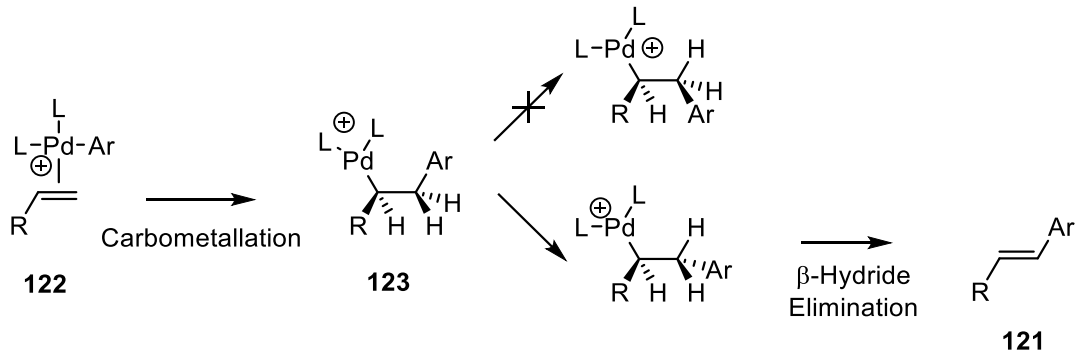

Scheme 4.13: Rearrangement of the carbopalladate **122** resulting in the favourable *trans*-arylation product.

In conjunction, the isolation of both the (*E*)-isomer **111** and migration isomer **125** of the arylated pyrethrins can be rationalised through the Heck reaction catalytic cycle and the reactivity of the intermediates.

The β-hydride elimination (Scheme 4.11C) that ultimately furnishes the arylated alkene **121** also results in the production of a palladium hydride **120** or **124**, which can then be reduced to regenerate the catalyst. Alternatively, the palladium hydride **120/124** can hydropalladate

the alkenes of the rethrolone side chain (Scheme 4.14), similar to the proposed reactivity of the palladium-catalysed transfer hydrogenation shown in Chapter 2 (Section 2.4.2; Scheme 2.9). More specifically, hydropalladation can occur on the *cis*-alkene of the rethrolone side chain giving the palladated intermediate **126**. Much like the aforementioned transfer hydrogenation, the palladated intermediate **126** likely reorganises to the lower energy *trans* geometry which, following a β-hydride elimination to regenerate the alkene, gives the *E,E*-arylated product **111** (Scheme 4.14A, red arrows). The alternate product is likely furnished through the β-hydride elimination proceeding on the 7' methylene unit resulting in the *E*-migration isomer **127** which is followed by a second hydropalladation-β-hydride elimination process on the benzylic alkene to give the doubly migrated product **125** (Scheme 4.14A, green arrows).[14, 37]

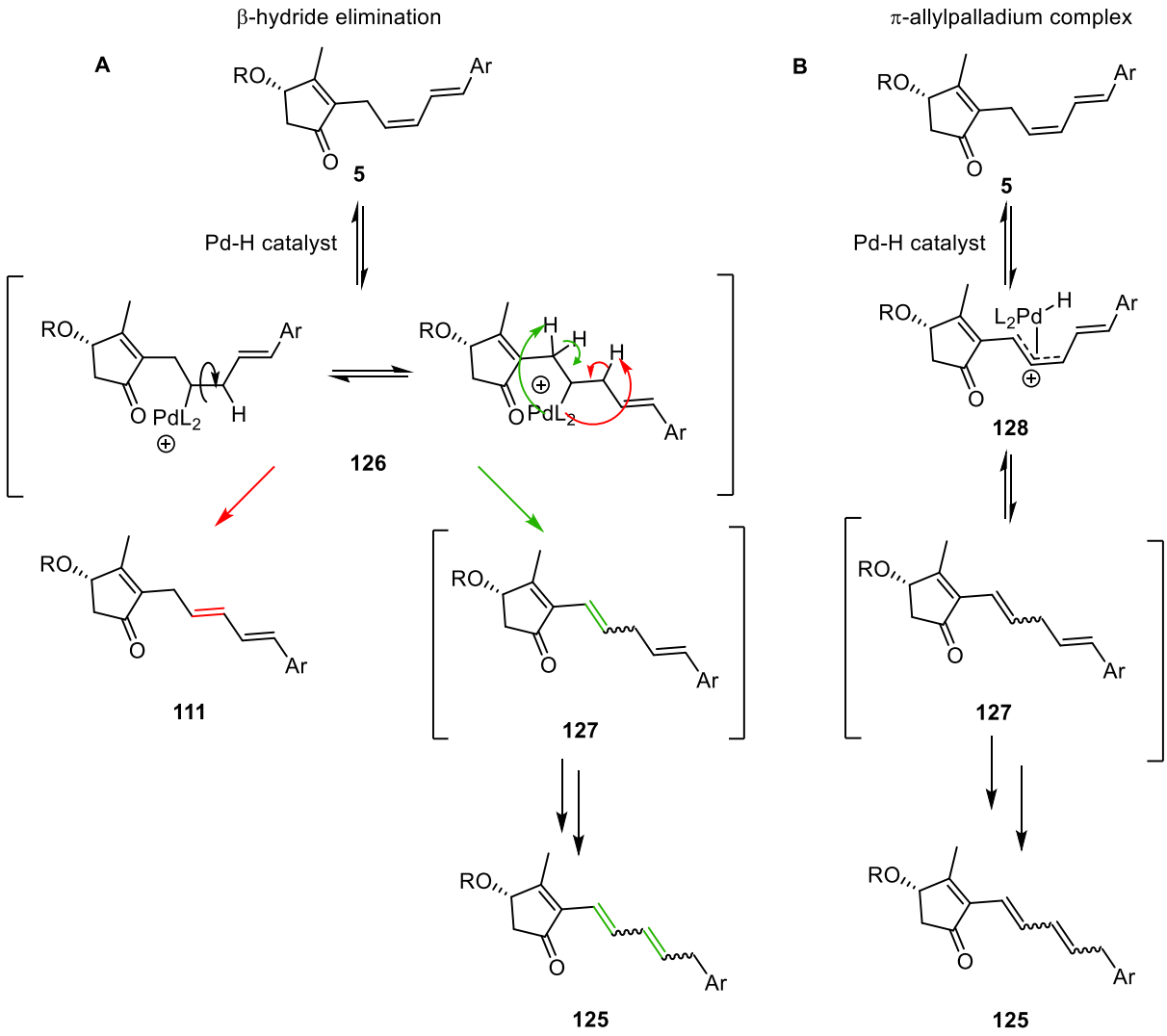

Scheme 4.14: Isomerism and double bond migration of the arylated pyrethrins by hydropalladation β-hydride elimination **(A)** or π-allyl palladium complexes **(B)**.

Alternatively, the isomerism can also take place through the generation of π-allyl palladium complexes of the alkene system (Scheme 4.14B).[38, 39] In this case, a palladium complex co-ordinates to the π-system and abstracts a hydrogen to give a cationic π-allyl palladium complex **128**. Subsequent reductive elimination regenerates the palladium complex and results in the 1,3-shift of the hydrogen to give the migrated isomer **127**.[39] Following two consecutive migrations with this π-allyl palladium pathway, the migration isomer **125** is generated.

With the development of reaction conditions that facilitate regioselective Heck arylation of the pyrethrins **5**, the application of the aforementioned reaction conditions with a range of substituted aryl iodides was undertaken.

4.3 Arylated analogues of pyrethrins

Implementation of a selection of substituted aryl iodides into the Heck reaction with the pyrethrins **5** resulted in a variety of arylated analogues with varying yields and product distribution (Table 4.1), depending on the electronic character of the aryl substrate. Generally, the electron-deficient aryl iodides resulted in increased yields of the arylated product and were more prone to retaining the alkene regiochemistry of the pyrethrin starting material **5**.

Table 4.1: Palladium-catalysed Heck reaction of the pyrethrins **5** with a range of aryl iodides.

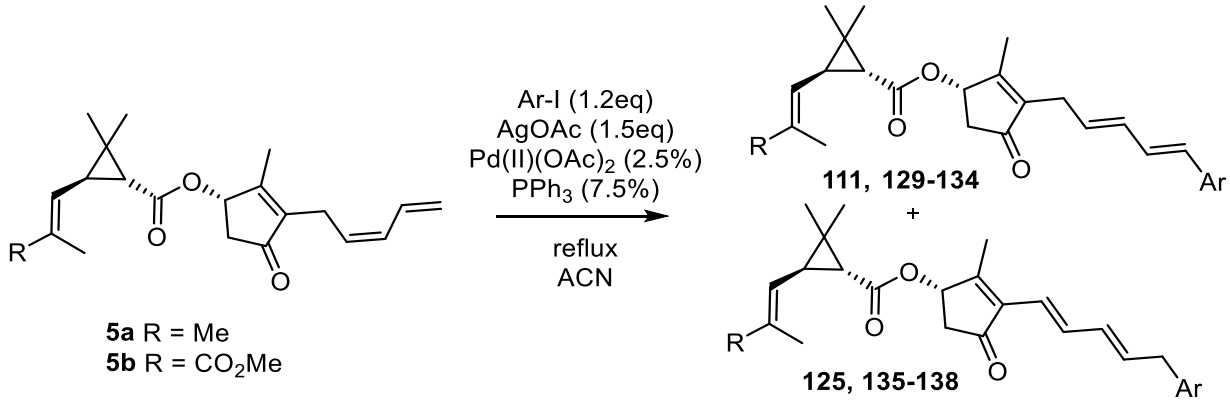

	R	Ar	Yield (%)[a]		R	Ar	Yield (%)[a]
1	Me	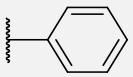	**111a**: 26 **125a**: 30	**10**	CO_2Me	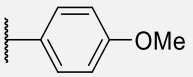	**132b**: 13 **137b**: 15
2	CO_2Me	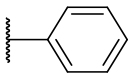	**111b**: 17 **125b**: 17	**11**	Me	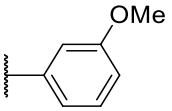	**133a**: 8 **138a**: 18
3	Me	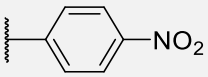	**129a**: 44	**12**	CO_2Me	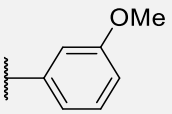	**133b**: 7 **138b**: 13
4	CO_2Me	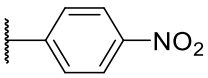	**129b**: 31	**13**	Me	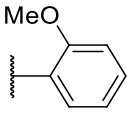	- [b]
5	Me	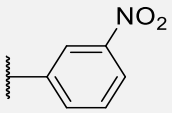	**130a**: 30 **135a**: 19	**14**	CO_2Me	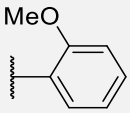	- [b]
6	CO_2Me	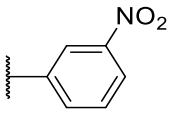	**130b**: 15 **135b**: 11	**15**	Me	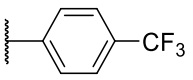	**134a**: 13
7	Me	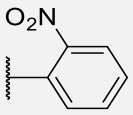	**131a**: 30 **136a**: 7	**16**	CO_2Me	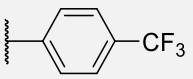	**134b**: 14
8	CO_2Me	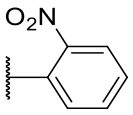	**131b**: 20 **136b**: 12	**17**	Me	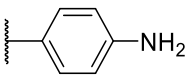	- [b]
9	Me	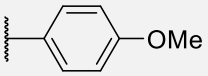	**132a**: 8 **137a**: 13	**18**	CO_2Me	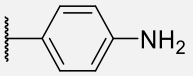	- [b]

[a] Isolated yields. [b] No product isolated.

Prior to final purification, crude mixtures of the reactions utilising nitro-substituted aryl iodides showed observable quantities of the unsubstituted arylation products **111** and **125** in ^{1}H NMR analyses. The formation of the phenyl adducts **111** and **125** is not entirely unprecedented with recent literature describing the reactivity of nitroarenes under palladium catalysis.[40, 41] Reductive denitration of nitroarenes is one of these reported palladium-catalysed reactions that is likely furnishing the phenyl arylation products **111** and **125** observed in the reaction with nitro-substituted aryl iodides. The proposed reactivity (Scheme 4.15) details that the nitroarene **141** is able to undergo oxidative addition (Scheme 4.15A) to a palladium(0) catalyst **116** followed by the introduction of a hydride source. The resulting palladium hydride species **140** can then undergo reductive elimination (Scheme 4.15B) to furnish the reduced aromatic **142** (Scheme 4.15).[40] Generally, these palladium-catalysed reactions of nitroarenes require much higher temperatures to be significantly effective in the generation of the reduced aromatic hence, the milder conditions employed for the Heck reaction of pyrethrins **5** only allows for minor quantities of the denitrated product(s) to form.[40-42]

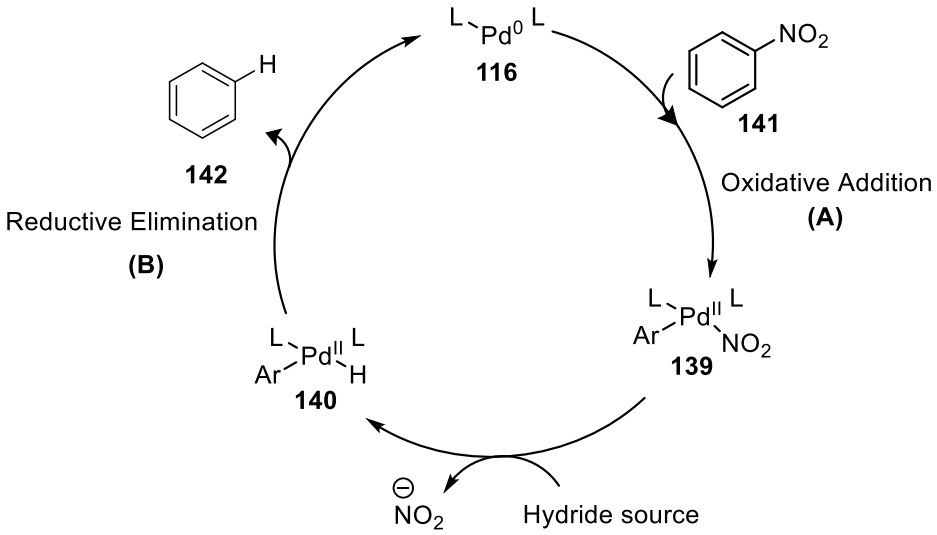

Scheme 4.15: Proposed catalytic cycle for the reductive denitration of nitroarenes **141**.[40]

Ultimately, 24 arylated pyrethrin analogues were produced from the application of substituted aryl iodides in the Heck reaction with pyrethrins **5** (Table 4.1). Generally, the electron-deficient nitro-substituted aryl iodides, particularly the 2- and 4-substituted variants, resulted in higher yields of the arylated analogues likely due to the greater polarisation and as such weaker C-I bond allowing for ready oxidative addition (Scheme 4.11A).[43-45] The 4-trifluoromethyl variant exhibited a significantly lower yield likely due to the decreased

electron-withdrawing capability of the trifluoromethyl group in comparison to the nitro group.[46] In conjunction, aryl iodides bearing a 2-substituent gave significantly lower yields than their 4-substituted counterparts due to the steric encumbrance imposed by the proximity of the substituent to the reactive iodide (Table 4.1).[47] In the case of 2-iodoanisole, the combination of the steric hinderance imposed by the *ortho*-substitution and the electron-donating effect of the methoxy group rendered reactivity such that neither of the expected arylated adducts could be isolated. In addition, the electronic nature of the substituent on the aryl iodide had a significant effect on the product distribution of the arylated pyrethrins.

As described earlier, the Heck reaction with the pyrethrins **5** and substituted aryl iodides resulted in the production of two arylated pyrethrin regioisomers with the distribution of the two dependent on the aromatic coupling partner. Interestingly, the distribution of these regioisomers was dependent on the differing substitution on the aromatic coupling partner particularly in terms of their electronic character. Generally, the electron-deficient substrates resulted in higher proportions of the unmigrated regioisomer, i.e. retaining the regiochemistry of the natural pyrethrins **5**, whilst the electron-rich substrates were more prone to the migration (Table 4.1). This difference in product distribution is likely due to the formation of positive charge on the newly benzylic position, potentially through the formation of π-allyl palladium complexes (Scheme 4.14B). Specifically, the electron-rich aryl groups stabilise this positive charge allowing for the migration to take place more readily, whilst the electron-deficient groups destabilise the cationic character resulting in the retention of the double bond regiochemistry.

4.3 Preliminary insecticidal activity of arylated pyrethrins

The various arylated pyrethrin analogues were subjected to preliminary insecticidal activity testing, undertaken by Dr. Andrew Kotze (CSIRO Agriculture and Food), against *L. cuprina* larvae. Unfortunately, none of these arylated pyrethrin analogues showed activity against the *L. cuprina* larvae. Based on previous docking studies of pyrethrin II **5b** to a model cockroach sodium ion channel, the lack of activity of these arylated analogues is likely due to the extension of the pentadienyl sidechain and the subsequent disruption to pre-established interactions by the terminal double bond.[48] Further, the migration isomers likely reduce the flexibility of the rethrolone sidechain, much like the migration isomer **25** formed from the

transfer hydrogenation protocols in Chapter 2, which has been suggested to be necessary to allow for specific interactions with the sodium channel.[48]

4.4 Conclusions

Derivatisation of the natural pyrethrins **5** was explored under palladium-catalysed conditions, specifically the well-established Heck reaction, coupling aryl halides with olefins. Initially, the reactivity and conditions necessary for the natural pyrethrins **5** to undergo Heck reaction with aryl halide substrates were screened. From this screening process it was found that palladium(0) catalysts resulted in little or no turnover of the catalytic cycle and as such no coupled product was able to be isolated from the reaction employing these palladium species. Substitution of the solvent for DMF resulted in the decomposition of the pyrethrin starting material **5** due to the effect of the highly polar aprotic solvent on the bases employed. Shift to a slightly less polar solvent in the form of acetonitrile and use of a palladium(II) precatalyst resulted in similar conversions as the reactions performed with the palladium(0) catalysts, indicating issue with catalytic turnover. Finally, it was found a silver salt additive could be used to fulfil both the role of base and drive the Heck reaction through a cationic catalytic cycle to give much higher conversions to the arylated pyrethrins that were able to be purified and characterised. Ultimately, these Heck arylations resulted in the isolation of two isomers of an arylated pyrethrin analogue where coupling had taken place with high regioselectivity at the terminal double bond of the rethrolone side chain. The isomers were determined to both have (*E,E*)-diene geometry where one retained the alkene regiochemistry of the natural pyrethrins **5** whilst the other showed migration of the double bonds into conjugation with the enone moiety.

With a protocol developed, the Heck reaction of the pyrethrins **5** was applied to a range of substituted aryl iodides which resulted in the production of 24 arylated pyrethrin analogues with the yields and product distribution dependent on the electronic nature of the aromatic system. Generally, use of the electron poor aryl iodides resulted in higher yields overall with the product distribution favouring the unmigrated isomer. Conversely, electron-rich systems gave lower overall yields with higher proportions of the migrated isomer. Ultimately, the yield of arylated product appeared to be dependent on the oxidative addition of the aryl iodide to the palladium centre. In conjunction, the product distribution relied upon the stabilisation of any positive charge on the benzylic position of the arylated analogues.

4.5 References

1. Seechurn, C. C. C. J.; Kitching, M. O.; Colacot, T. J.; Snieckus, V., Palladium-Catalyzed Cross-Coupling: A Historical Contextual Perspective to the 2010 Nobel Prize. *Angew. Chem. Int. Ed.* **2012,** *51*, 5062-5085.
2. Torborg, C.; Beller, M., Recent Applications of Palladium-Catalyzed Coupling Reactions in the Pharmaceutical, Agrochemical, and Fine Chemical Industries. *Adv. Synth. Catal.* **2009,** *351*, 3027-3043.
3. Devender, P.; Qu, R.-Y.; Kang, W.-M.; Yang, G.-F., Palladium-Catalyzed Cross-Coupling Reactions: A Powerful Tool for the Synthesis of Agrochemicals. *J. Agric. Food Chem.* **2018,** *66* (34), 8914-8934.
4. Heck, R. F., Arylation, Methylation, and Carboxyalkylation of Olefins by Group VIII Metal Derivatives. *J. Am. Chem. Soc.* **1968,** *90* (20), 5518-5526.
5. Heck, R. F.; Nolley, J. P., Palladium-catalyzed vinylic hydrogen substitution reactions with aryl, benzyl, and styryl halides. *J. Am. Chem. Soc.* **1972,** *37* (14), 2320-2322.
6. Mizoroki, T.; Mori, K.; Ozaki, A., Arylation of Olefin with Aryl Iodide Catalyzed by Palladium. *Bull. Chem. Soc. Jpn.* **1971,** *44* (2), 581.
7. King, A. O.; Okukado, N.; Negishi, E.-I., Highly General Stereo-, Regio- and Chemo-selective Synthesis of Terminal and Internal Conjugated Enynes by the Pd-catalysed Reaction of Alkynylzinc Reagents with Alkenyl Halides. *J. Chem. Soc., Chem. Commun.* **1977**, 683-684.
8. Negishi, E.-I.; King, A. O.; Okukado, N., Selective Carbon-Carbon Bond Formation via Transition Metal Catalysis. 3. A Highly Selective Synthesis of Unsymmetrical Biaryls and Diarylmethanes by the Nickel- or Palladium-Catalyzed Reaction of Aryl- and Benzylzinc Derivatives with Aryl Halides. *J. Org. Chem.* **1977,** *42*, 1821-1823.
9. Miyaura, N.; Suzuki, A., Stereoselective Synthesis of Arylated (*E*)-Alkenes by the Reaction of Alk-1-enylboranes with Aryl Halides in the Presence of Palladium Catalyst. *J. Chem. Soc., Chem. Commun.* **1979**, 866-867.
10. Miyaura, N.; Yamada, K.; Suzuki, A., A New Stereospecific Cross-Coupling by the Palladium-Catalyzed Reaction of 1-Alkenylboranes with 1-Alkenyl or 1-Alkynyl Halides. *Tetrahedron Lett.* **1979,** *20*, 3437-3440.
11. Zhu, C.; Chu, H.; Li, G.; Ma, S.; Zhang, J., Pd-Catalyzed Enantioselective Heck Reaction of Aryl Triflates and Alkynes. *J. Am. Chem. Soc.* **2019,** *141*, 19246-19251.

12. Sabino, A. A.; Machado, A. H. L.; Correia, C. R. D.; Eberlin, M. N., Probing the Mechanism of the Heck Reaction with Arene Diazonium Salts by Electrospray Mass and Tandem Mass Spectrometry. *Angew. Chem. Int. Ed.* **2004,** *43*, 2514-2518.
13. Crisp, G. T., Variations on a theme - recent developments on the mechanism of the Heck reaction and their implications for synthesis. *Chem. Soc. Rev.* **1998,** *27*, 427-436.
14. McCartney, D.; Guiry, P. J., The asymmetric Heck and related reactions. *Chem. Soc. Rev.* **2011,** *40*, 5122-5150.
15. Xu, H.-J.; Zhao, Y.-Q.; Zhou, X.-F., Palladium-Catalyzed Heck Reaction of Aryl Chlorides under Mild Conditions Promoted by Organic Ionic Bases. *J. Org. Chem.* **2011,** *76* (19), 8036-8041.
16. McConville, M.; Saidi, O.; Blacker, J.; Xiao, J., Regioselective Heck Vinylation of Electron-Rich Olefins with Vinyl Halides: Is the Neutral Pathway in Operation? *J. Org. Chem.* **2009,** *74* (7), 2692-2698.
17. Knowles, J. P.; Whiting, A., The Heck-Mizoroki cross-coupling reaction: a mechanistic perspective. *Org. Biomol. Chem.* **2006,** *5*, 31-44.
18. Jutand, A., Mechanisms of the Mizoroki-Heck Reaction. In *The Mizoroki-Heck Reaction*, Oestreich, M., Ed. Wiley: United Kingdom, 2009; pp 1-50.
19. Felpin, F.-X.; Nassar-Hardy, L.; Collonnec, F. L.; Fouquet, E., Recent advances in the Heck-Matsuda reaction in heterocyclic chemistry. *Tetrahedron* **2011,** *67*, 2815-2831.
20. Zalesskiy, S. S.; Ananikov, V. P., Pd_2dba_3 as a Precursor of Soluble Metal Complexes and Nanoparticles: Determination of Palladium Active Species for Catalysis and Synthesis. *Organometallics* **2012,** *31*, 2302-2309.
21. Sherwood, J.; Clark, J. H.; Fairlamb, I. J. S.; Slattery, J. M., Solvent effects in palladium catalysed cross-coupling reactions. *Green Chem.* **2019,** *21*, 2164-2213.
22. Buncel, E.; Symons, E. A.; Dolman, D.; Stewart, R., The H-acidity function for dimethylformamide-water. *Can. J. Chem.* **1970,** *48*, 3354-3357.
23. Clare, B. W.; Cook, D.; Ko, E. C. F.; Mac, Y. C.; Parker, A. J., Solvation of Ions. IX. The Effect of Anion Solvation on Acid Dissociation Constants in Methanol, Water, Dimethylformamide, and Dimethyl Sulfoxide. *J. Am. Chem. Soc.* **1966,** *88*, 1911-1916.
24. Boes, E. S.; Livotto, P. R.; Stassen, H., Solvation of monovalent anions in acetonitrile and *N,N*-dimethylformamide: Parametization of the IEF-PCM model. *Chem. Phys.* **2006,** *331*, 142-158.

25. Hutt, O. E.; Freemont, J. A.; Littler, S.; Duggan, P. J.; Tsanaktsidis, J.; Cole, H.; Kerr, M.; Ryan, J. H., Staudinger and Ruzicka's Altered Pyrethrolone: the Cyclopentadienone Dimers Derived from Pyrethrin I. *Acta Hortic.* **2015,** *1073*, 181-190.
26. Parker, A. J., Protic-Dipolar Aprotic Solvent Effects on Rates of Bimolecular Reactions. *Chem. Rev.* **1969,** *69*, 1-32.
27. Beletskaya, I. P.; Cheprakov, A. V., The Heck Reaction as a Sharpening Stone of Palladium Catalysis. *Chem. Rev.* **2000,** *100*, 3009-3066.
28. Carole, W. A.; Colacot, T. J., Understanding Palladium Acetate from a User Perspective. *Chem. Eur. J.* **2016,** *22*, 7686-7695.
29. Amatore, C.; Jutand, A.; M'Barki, M. A., Evidence of the formation of zerovalent palladium from $Pd(OAc)_2$ and triphenylphosphine. *Organometallics* **1992,** *11*, 3009-3013.
30. Fumiyuki, O.; Akihiko, K.; Tamio, H., Generation of Tertiary Phosphine-Coordinated Pd(0) Species from $Pd(OAc)_2$ in the Catalytic Heck Reaction. *Chem. Lett.* **1992,** *21*, 2177-2180.
31. Cabri, W.; Candiani, I., Recent Developments and New Perspectives in the Heck Reaction. *Acc. Chem. Res.* **1995,** *28*, 2-7.
32. Karabelas, K.; Westerlund, C.; Hallberg, A., The Effect of Added Silver Nitrate on the Palladium-Catalyzed Arylation of Allyltrimethylsilanes. *J. Org. Chem.* **1985,** *50*, 3896-3900.
33. Jeffery, T., Palladium-catalysed Arylation of 1,3-Dienes: A Highly Chemo, Regio and Stereoselective Synthesis of (*E,E*) Conjugated Dienic Aromatics. *Tetrahedron Lett.* **1992,** *33*, 1989-1992.
34. Cabri, W.; Candiani, I.; Bedeschi, A.; Santi, R., Palladium-Catalyzed α-Arylation of Vinyl Butyl Ether with Aryl Halides. *Tetrahedron Lett.* **1991,** *32*, 1753-1756.
35. Grigg, R.; Loganathan, V.; Santhakumar, V.; Sridharan, V.; Teasdale, A., Suppression of Alkene Isomerisation in Products from Intramolecular Heck Reactions by Addition of Tl(I) Salts. *Tetrahedron Lett.* **1991,** *32*, 687-690.
36. Cabri, W.; Candiani, I.; Bedeschi, A., 1,10-Phenanthroline Derivatives: A New Ligand Class in the Heck Reaction. Mechanistic Aspects. *J. Org. Chem.* **1993,** *58*, 7421-7426.

37. Wheatley, B. M. M.; Keay, B. A., Use of Deuterium Labeling Studies to Determine the Stereochemical Outcome of Palladium Migrations during an Asymmetric Intermolecular Heck Reaction. *J. Org. Chem.* **2007,** *72*, 7253-7259.
38. Biswas, S., Mechanistic Understanding of Transition-Metal-Catalyzed Olefin Isomerization: Metal-Hydride Insertion-Elimination vs. π-Allyl Pathways. *Comment. Inorg. Chem.* **2015,** *35*, 300-330.
39. Sen, A.; Lai, T.-W., Mechanism of Palladium(II)-Catalyzed C=C Bond Isomerization in Olefins. *Inorg. Chem.* **1984,** *23*, 3257-3258.
40. Kashihara, M.; Yadav, M. R.; Nakao, Y., Reductive Denitration of Nitroarenes. *Org. Lett.* **2018,** *20*, 1655-1658.
41. Okita, T.; Asahara, K. K.; Muto, K.; Yamaguchi, J., Palladium-Catalyzed Mizoroki-Heck Reaction of Nitroarenes and Styrene Derivatives. *Org. Lett.* **2020,** *22*, 3205-3208.
42. Yadav, M. R.; Nagaoka, M.; Kashihara, M.; Zhong, R.-L.; Miyazaki, T.; Sakaki, S.; Nakao, Y., The Suzuki-Miyaura Coupling of Nitroarenes. *J. Am. Chem. Soc.* **2017,** *139*, 9423-9426.
43. Whitcombe, N. J.; Hii, K. K. M.; Gibson, S. E., Advances in the Heck chemistry of aryl bromides and chlorides. *Tetrahedron* **2001,** *57*, 7449-7476.
44. Chinchilla, R.; Najera, C., Recent advances in Sonogashira reactions. *Chem. Soc. Rev.* **2011,** *2011* (40), 5084-5121.
45. Espino, G.; Kurbangalieva, A.; Brown, J. M., Aryl bromide/triflate selectivities reveal mechanistic divergence in palladium-catalysed couplings; the Suzuki-Miyaura anomaly. *Chem. Commun.* **2007**, 1742-1744.
46. Remya, G. S.; Suresh, C. H., Quantification and classification of substituent effects in organic chemistry: a theoretical molecular electrostatic potential study. *Phys. Chem. Chem. Phys.* **2016,** *18*, 20615-20626.
47. Feuerstein, M.; Doucet, H.; Santelli, M., Palladium/Tetraphosphine Catalysed Heck Reaction with *ortho*-Substituted Aryl Bromides. *Synlett* **2001,** *12*, 1980-1982.
48. Chen, M.; Du, Y.; Zhu, G.; Takamatsu, G.; Ihara, M.; Matsuda, K.; Zhorov, B. S.; Dong, K., Action of six pyrethrins purified from the botanical insecticide pyrethrum on cockroach sodium channels expressed in *Xenopus* oocytes. *Pest. Biochem. Physiol.* **2018,** *151*, 82-89.

Chapter 5 Towards a More Efficient Synthesis of (*Z*)-Pyrethrolone

5.1 Introduction

The rethrolone moiety of the Pyrethrins **5-7** is the most functionality-rich portion of the pyrethrin scaffold with many of them bearing some instability to oxygen, light and heat. Notably, these functional groups contribute to the environmentally friendly qualities of the Pyrethrins **5-7**, with their high reactivity leading to rapid degradation and preventing persistence in the environment. However, these moieties have proved detrimental to the long-term storage and widespread application of pyrethrum insecticides, particularly in the agricultural sector. (*Z*)-pyrethrolone **21** (Figure 5.1), the rethrolone of pyrethrins I **5a** and II **5b**, is especially sensitive to degradation with its pentadienyl side chain being implicated in many of the degradative pathways.[1, 2]

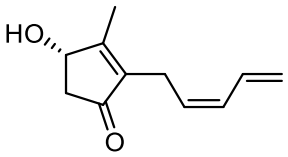

21

Figure 5.1: (*Z*)-pyrethrolone **21**, the rethrolone moiety of the pyrethrins **5**.

Due to the high content of these reactive functional groups found in (*Z*)-pyrethrolone **21** its efficient synthesis may serve as a means to explore the degradative properties of this rethrolone moiety in more depth and has potential as a model for future synthetic manipulation of the pyrethrins **5**. A number of pre-existing syntheses have been published in the literature since the elucidation of the rethrolone structure however, many are lengthy or make use of undesirable, toxic reagents. Some of these efforts will now be examined in more detail.

Crombie and co-workers explored a number of synthetic pathways for the production of (*Z*)-pyrethrolone **21** with early attempts detailed in 1956.[3, 4] The first attempt was based on their assignment of the *cis*-geometry of natural pyrethrolone **21**[5] and earlier work detailing the synthesis of alkyl- and alkenyl-substituted rethrolone structures.[6] This effort to prepare the desired (*Z*)-pyrethrolone **21** focussed on the generation of the *cis*-pentadienyl sidechain required for (*Z*)-pyrethrolone **21** with initial attempts concentrating on a vinyl acetylenic intermediate **147** (Scheme 5.1A). Unfortunately, the proposed elimination-substitution

chemistry of bis-tosylated diols **144** did not yield the desired α-propargyl tosylate intermediate **146**. This procedure relied on the selective elimination of one tosylate to give the terminal alkene of the side chain whilst the α-propargylic tosylate, with proposed pseudohalogen character, would allow for nucleophilic substitution with the sodium enolate of ethyl acetoacetate (Scheme 5.1A). Focus then turned to producing the vinyl acetylene intermediate **147** *via* a stepwise tosylation (Scheme 5.1B), where the first tosyl **150** served as a means for substitution and the second **152** allowed for the desired elimination. Ultimately, the vinyl acetylene **147** could be generated by this stepwise approach, where the first tosylate **150** underwent substitution with the sodium enolate of ethyl acetoacetate followed by ester hydrolysis and decarboxylation to give **151**. Following the second tosylation, elimination with sodium ethoxide afforded the vinyl acetylene **147** which was subsequently implemented in a previously described rethrolone synthesis.[6] Specifically, a β-dicarbonyl **153** was generated from the condensation of the vinyl acetylene **147** with diethyl carbonate in the presence of sodium hydride. Subsequently, the β-dicarbonyl **153** could then be used to furnish the linear carbon structure **154** through aldol addition to pyruvaldehyde. Cyclisation of this linear structure **154** could then be achieved under basic conditions to give the rethrolone scaffold **155**. Finally, attempts to selectively semi-hydrogenate the alkyne to give the *cis*-alkene was explored in a bid to give the *(Z)*-pyrethrolone product **21** (Scheme 5.1B). Unfortunately, the selective hydrogenation procedure to give (*Z*)-pyrethrolone **21** resulted in <1% reported yield in the final step with significant contamination from isomerised and over-reduced product.[4]

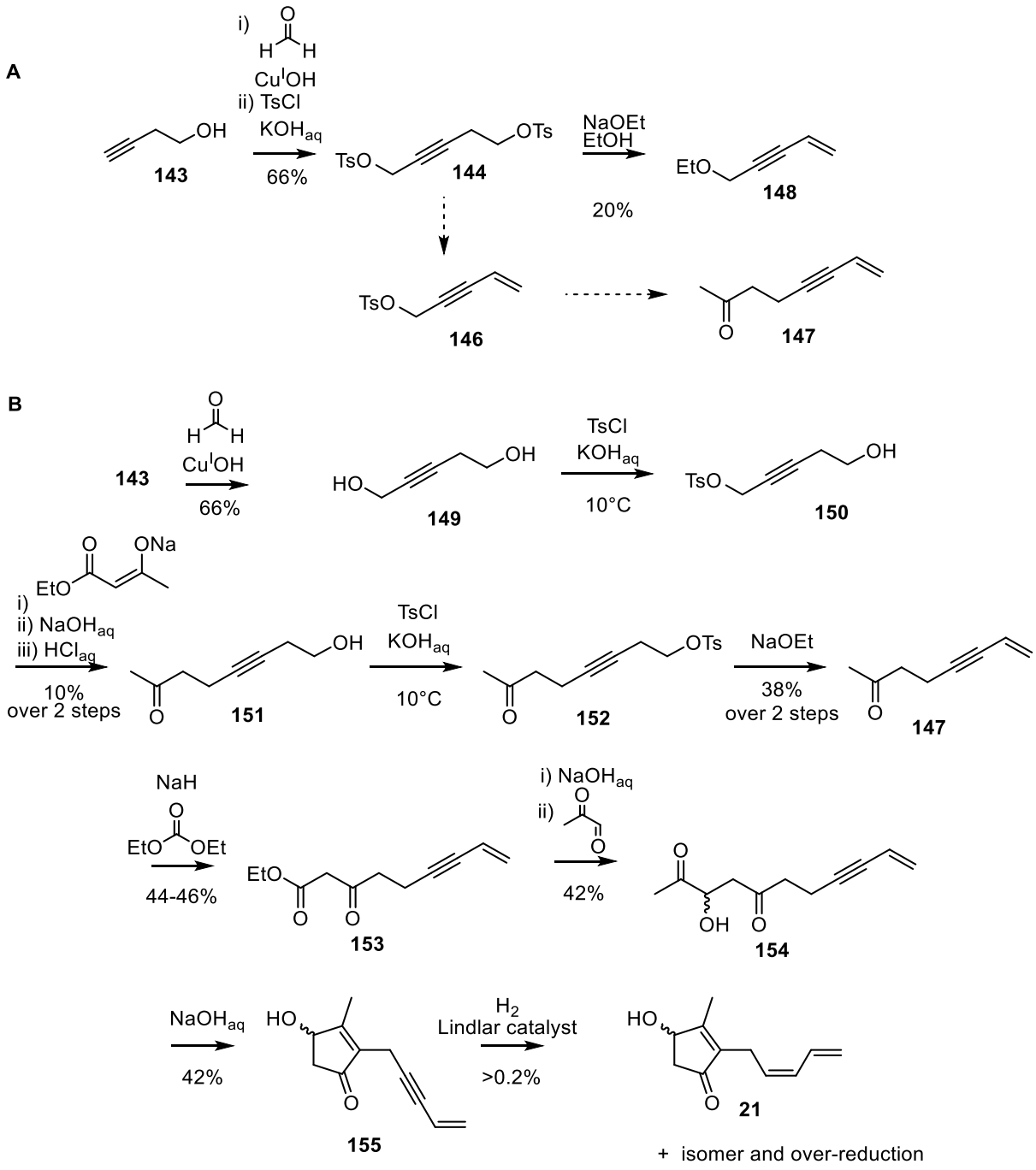

Scheme 5.1: Crombie's attempted synthesis of (*Z*)-pyrethrolone **21** by bistosylates **(A)**[3] and subsequent inefficient synthesis of (*Z*)-pyrethrolone **21** through selective hydrogenation **(B)**.[4]

Crombie later devised a more general procedure (Scheme 5.2) allowing for the production of not only (*Z*)-pyrethrolone **21** but also the rethrolone moieties of the minor pyrethrin esters, (*Z*)-jasmolone **20** and (*Z*)-cinerolone **22**.[7]

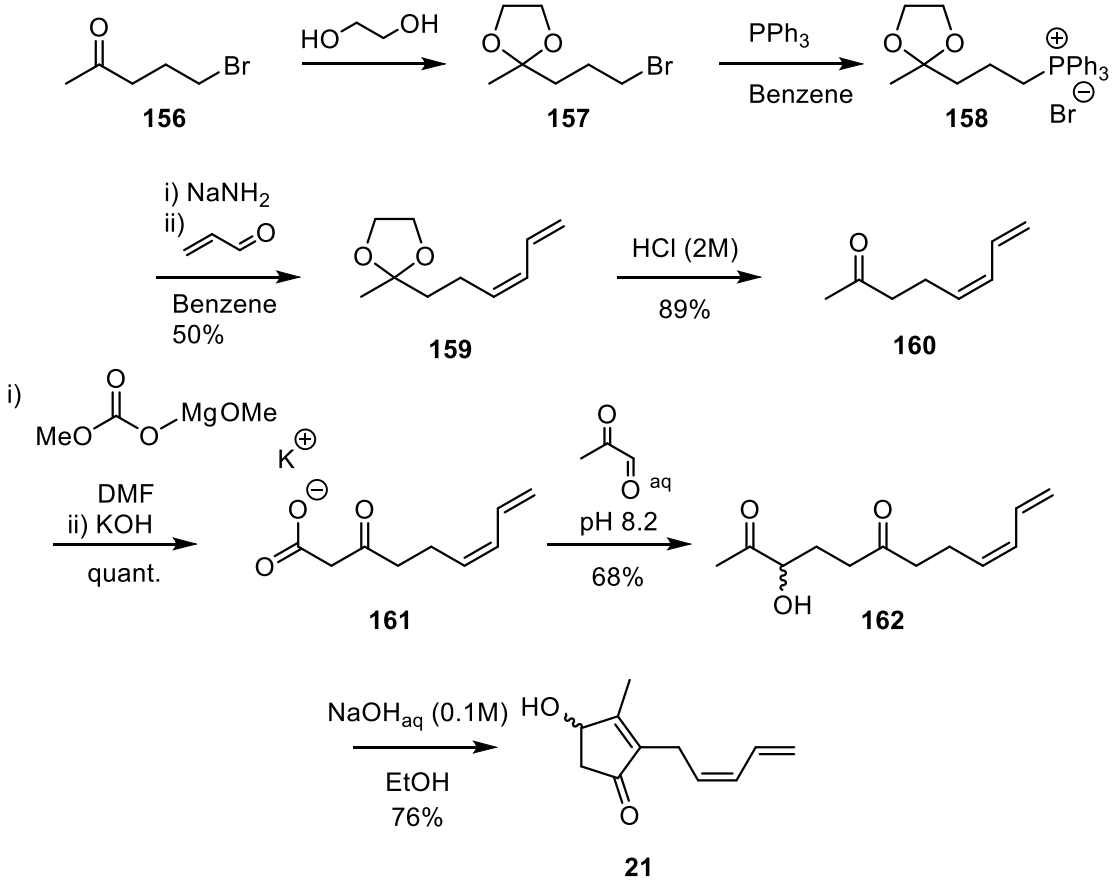

Scheme 5.2: Crombie's revised synthesis of (*Z*)-pyrethrolone **21** without alkynyl intermediates.[7]

This procedure allowed for installation of the pentadienyl side chain without the use of an acetylenic intermediate, foregoing the need for semi-hydrogenation of the alkyne. The installation of this dienyl moiety, or respective side chain of cinerolone **22** or jasmolone **20**, was achieved through Wittig olefination of triphenylphosphonium bromide **158** giving **159**. Subsequent deprotection of the ketone and carboxylation with methyl magnesium carbonate yielded the carboxylate salt **161** which was subjected to a decarboxylative aldol reaction to yield the linear carbon scaffold **162**. Similar to the aforementioned synthesis (Scheme 5.1), this linear scaffold **162** could then be cyclised under basic conditions to yield the desired (*Z*)-pyrethrolone **21**. Whilst this synthesis was fruitful, with the production of racemic (*Z*)-pyrethrolone **21** (Scheme 5.2) in 21% overall yield, it made use of the highly toxic acrolein and required carbonyl protection-deprotection resulting in an extended synthetic route.

In 1979, Tsuji and co-workers were able to produce (*Z*)-pyrethrolone **21** by generating the pentadienyl intermediate **160** from 1,3-butadiene **163** via a series of palladium-catalysed reactions which were then subjected to Crombie's earlier synthetic pathway (Scheme 5.3).[3, 4, 8] More specifically, the carbon skeleton **164/165** of the side chain was established by

palladium-catalysed telomerisation of 1,3-butadiene **163** with phenoxide as nucleophile. The necessary carbonyl group **166/167**, for subsequent implementation into Crombie's synthesis,[7] was installed by Wacker-Tsuji oxidation followed by a palladium-catalysed elimination of phenol to give the appropriate diene **160**.

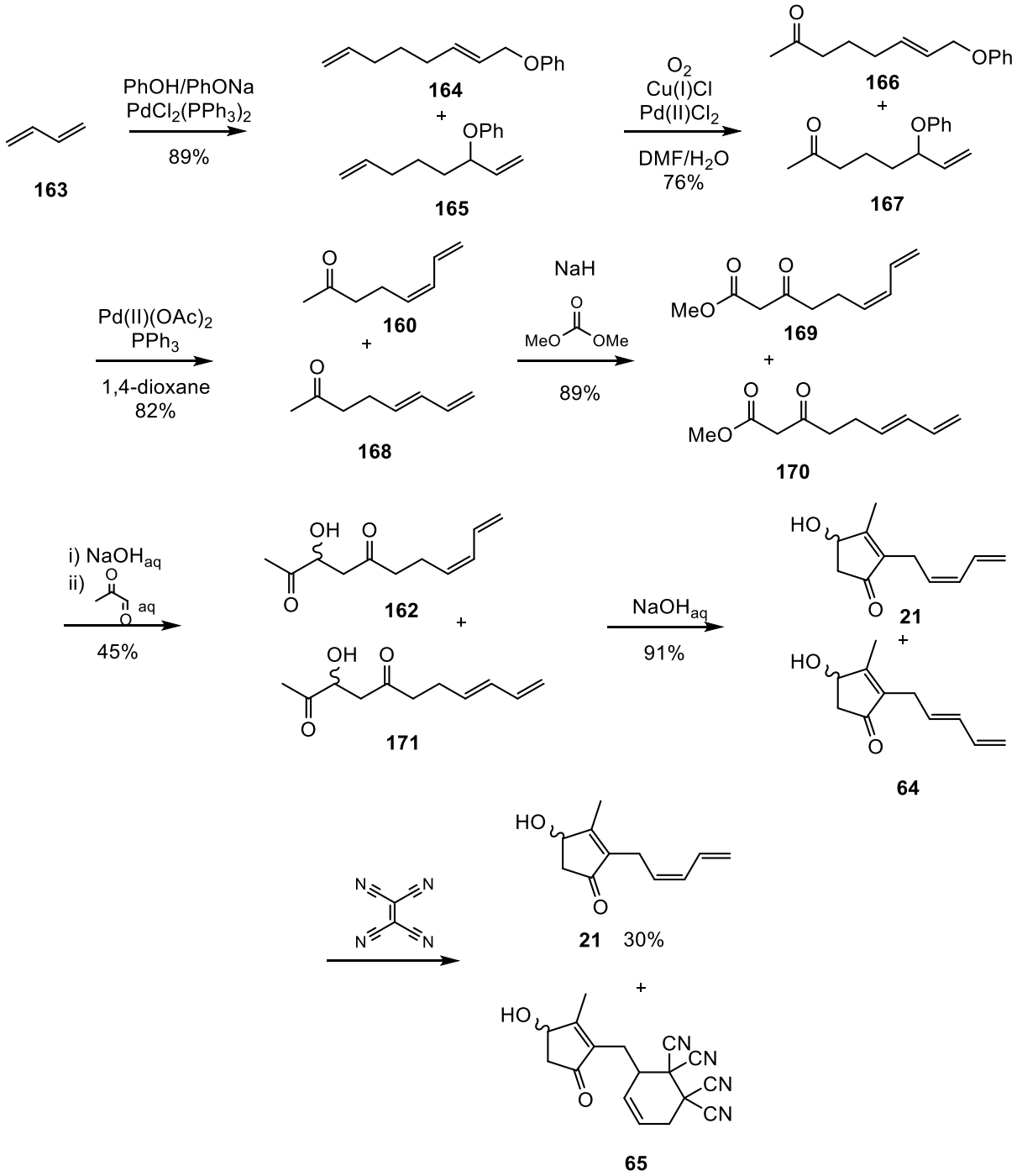

Scheme 5.3: Tsuji's synthesis of (*Z*)-pyrethrolone **21** by palladium-catalysed production of the pentadienyl moiety.[8]

Unfortunately, reliance on palladium catalysis resulted in a mixture of the *cis*- **160** and *trans*-pentadiene **168** intermediates which was subsequently used in the following synthesis. This then required the resulting (*E*)-pyrethrolone **64** in the mixture to be derivatised through Diels-Alder cycloaddition with tetracyanoethylene and subjected to subsequent column chromatography to remove the resulting adduct **65**.

The most recent synthesis of (*Z*)-pyrethrolone **21** was by Matsuo and co-workers over five synthetic steps (Scheme 5.4).[9-11] Notably, an enzymatic chiral resolution, described previously by Danda,[12] was employed to afford the natural (*S*)-stereoisomer. Dimethyl 3-oxoglutarate **172** was used as an easily accessible starting material. The enolate of the oxoglutarate **172** was generated with magnesium methoxide and was subsequently alkylated using propargyl chloride in a yield of 71%. The purified monoalkylated oxoglutarate **173** was subjected to a one-pot ester hydrolysis, decarboxylation and aldol addition giving the linear 1,4-diketones **174** in 80%. This mixture of diketones **174** was subsequently used in an intramolecular aldol condensation to give the desired cyclopentenones **175** with 62% yield. This enantiomeric mixture was resolved via chemical and enzymatic processes to give the (*S*)-isomer in 74% yield with 90% ee. The (*S*)-cyclopentenone **175** was subjected to chain extension via Sonogashira cross coupling conditions with vinyl bromide giving the desired carbon skeleton **155** in 64%. Finally, the alkynyl unit was reduced to the *cis*-alkene using activated zinc in a water/n-propanol mixture giving (*S*)-(*Z*)-pyrethrolone **21** in 85% yield with a 14% overall yield.

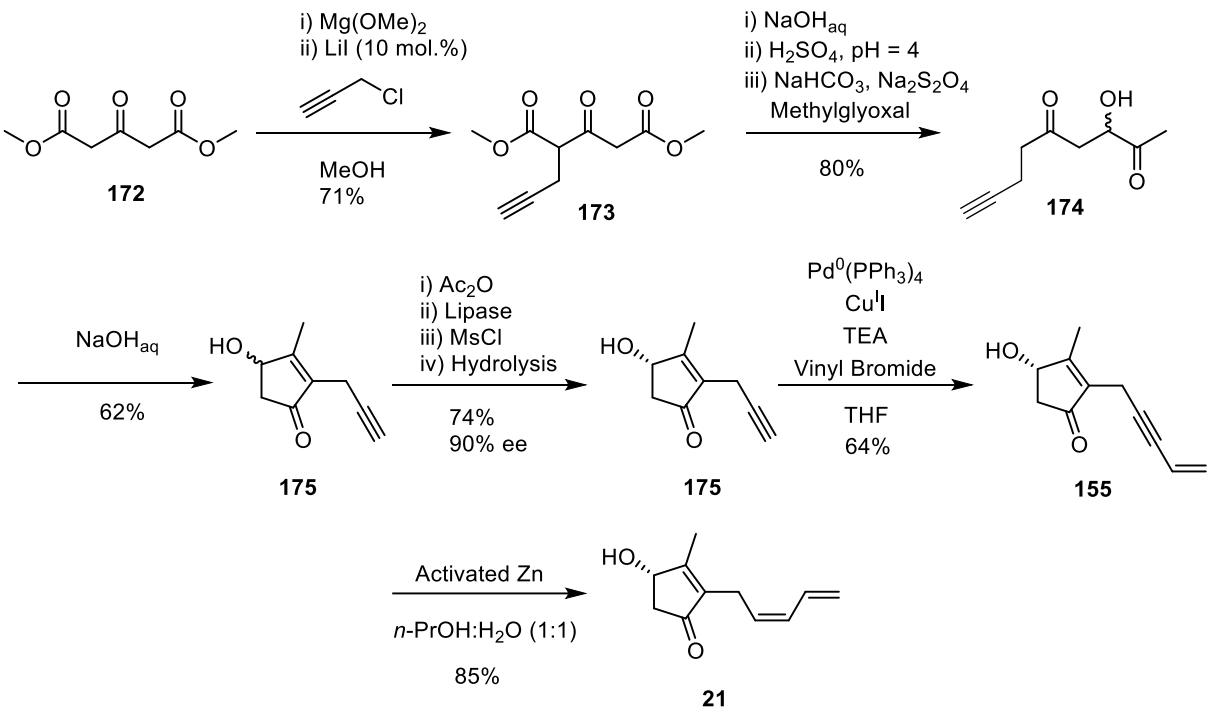

Scheme 5.4: Matsuo's synthesis of (*Z*)-pyrethrolone **21** with enzymatic chiral resolution to afford the natural (*S*)-stereochemistry. [9-11]

The availability of the starting materials, concise synthesis and relatively good yields, made the pathway developed by Matsuo and co-workers,[9-11] omitting the chiral resolution, of interest to produce racemic (*Z*)-pyrethrolone **21** as a potential model compound for future investigations into pyrethrin reactivity and potential modifications.

5.2 Attempted synthesis by published procedures

The pathway devised by Matsuo was attractive and relevant to the work in this thesis for the production of (*Z*)-pyrethrolone **21** for a number of key reasons. The synthetic pathway undertaken was a suitable, five-step synthetic protocol reportedly applicable up to multi-gram scale with relatively high yields, allowing for sufficient quantities of the (*Z*)-pyrethrolone **21** to be produced for future use. Additionally, the starting materials utilised were easy to access, cheap and relatively safe to use in significant amounts. As such attempts to replicate the synthesis were attempted. The first step of this synthetic pathway uses well-established enolate alkylation to produce a mono-alkylated oxoglutarate **173**.

5.2.1 Alkylation of dimethyl 3-oxoglutarate

The protocol described by Matsuo for the first step of the synthetic pathway utilises propargyl chloride to alkylate the magnesium enolate of dimethyl 3-oxoglutarate **173** in the presence

of catalytic amounts of lithium iodide. Addition of the lithium iodide to the reaction was depicted as increasing not only the reaction rate, likely through the formation of an intermediate propargyl iodide *via* the Finkelstein reaction, but also the yield of monoalkylated product **173**.[9]

Implementing this described protocol, albeit with substitution of the propargyl chloride with its bromide equivalent due to its availability, was undertaken for the attempted production of the monopropargyl oxoglutarate **173** (Scheme 5.5). Magnesium methoxide was generated for enolate formation through reaction of powdered magnesium metal with methanol under anhydrous conditions. The enolate could then be furnished through slow addition of the oxoglutarate **172** to the basic solution and subsequent stirring at 60 °C for 1.5 h. The propargyl bromide was then added along with 10 mol% lithium iodide followed by a 4 h reaction time with heating under reflux.

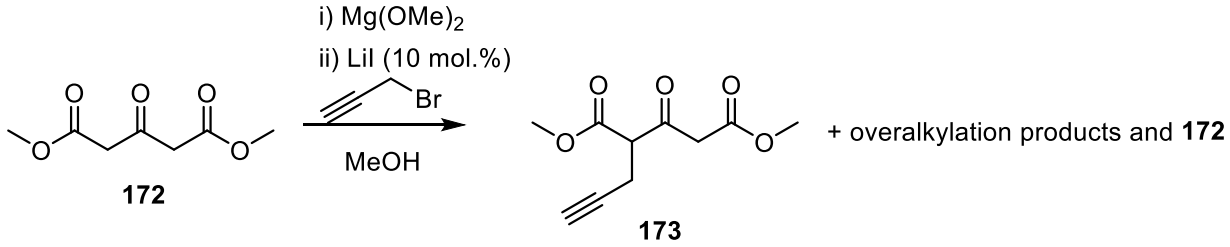

Scheme 5.5: Alkylation of dimethyl 3-oxoglutarate **172** with propargyl bromide under Matsuo's described conditions.[9]

Following reaction quench and work-up, the isolated crude material was found to be a complex mixture denoted by the abundance of propargylic alkyne proton resonances around 2 ppm in the ^{1}H NMR spectrum, characterised by their small coupling of J = 2-3 Hz. The desired monoalkylated product **173** was observed, indicated by comparison to literature spectroscopic data, with a number of multialkylated variants **176-178** and residual starting material **172**. In an effort to increase the selectivity and conversion to the monopropargyl oxoglutarate **173**, altered synthetic conditions were explored.

Matsuo's original conditions made use of considerable excess of the magnesium methoxide in enolate generation, with four equivalents of base to the oxoglutarate starting material **173**. This large excess of base could lead to a variety of side reactions resulting in the observed multiple alkylation events. One such pathway could result following the first alkylation event,

where a new enolate may be generated with the excess base present (Scheme 5.6). Further alkylation *via* this pathway is likely to occur on the already alkylated position, due to the increased stability of the now thermodynamic enolate, giving the asymmetric dialkylated oxoglutarate **176**. This dialkylated derivative **176** still retains another acidic β-dicarbonyl site that can undergo further enolisation events to furnish the tri- **177** and tetra-propargyl oxoglutarates **178**.

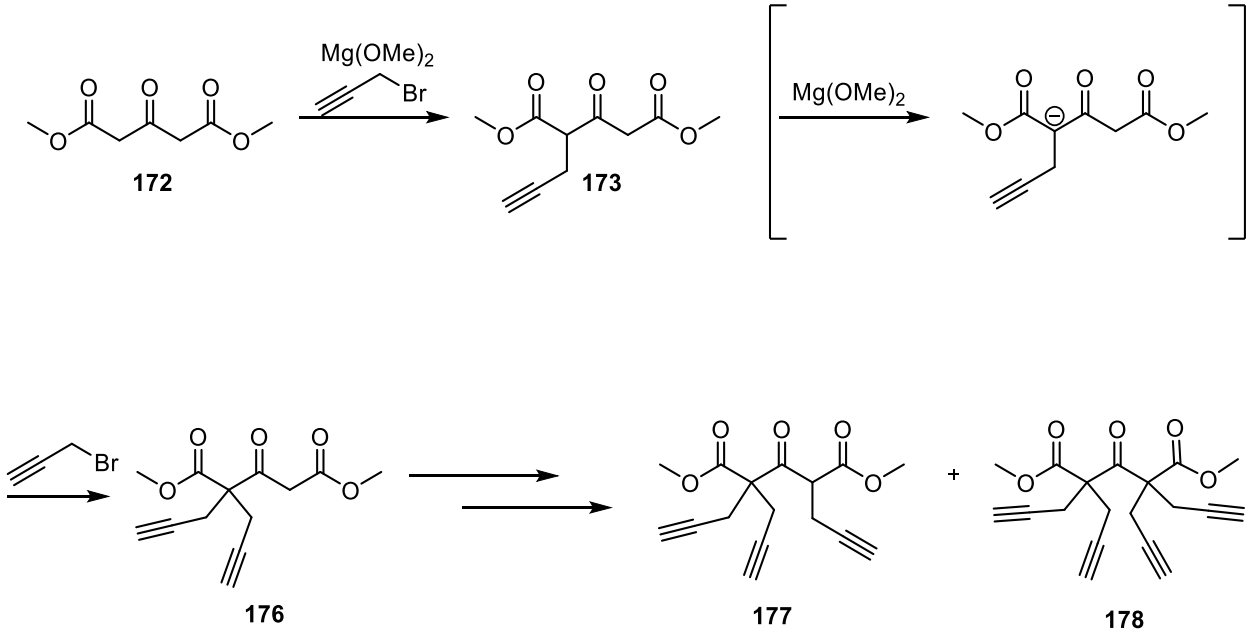

Scheme 5.6: Potential pathway to multialkylation products 176-178 *via* multi-step enolate formation.

Initial attempts to alleviate this multi-alkylation issue focussed on tuning of the stoichiometry, so as to prevent the generation of successive enolates as described above. Sequential reduction of the base stoichiometry from 4 to 2, 1.5 and 1 was explored. However regardless of the amount of base used, significant dialkylation **176** was observed in the crude isolates by both NMR and GCMS analyses. This is potentially the result of stabilised enolate production through chelation to the magnesium cation[13] and as such utility of alternate bases was proposed to potentially ameliorate the increased reactivity. Nevertheless, attempts to substitute the base for sodium methoxide, sodium hydride or even potassium carbonate resulted in isolation of similar crude reaction profiles containing multi-alkylated **176-178** and unreacted dimethyl 3-oxoglutarate **172**. As a result, efforts shifted to purification of the desired monopropargyl oxoglutarate **173**.

Purification of the crude alkylation mixture was attempted, first through the described distillation.[9] Unfortunately, attempting to purify the alkylation mixture through conventional distillation at reduced pressure still required the use of temperatures of approximately 150 °C which ultimately led to decomposition of the alkylated material giving a viscous resin. Alternate means of purification were sought so as to obtain sufficient quantities of the alkylated intermediate **173** for continuation of the synthetic pathway (Scheme 5.4). Separation of the alkylated adducts **173** and **176-178** was pursued through column chromatography to avoid application of harsh thermal conditions and subsequent decomposition of the material. However, whilst the alkylated components remained chemically intact, exhaustive attempts to separate the mixture by column chromatography with a range of solvent systems resulted in co-elution of the alkylated constituents **173** and **176-178**. Short-path distillation, by Kugelrohr, was employed to minimise the exposure of the alkylation mixture to the high temperatures needed to distil the desired monopropargyl oxoglutarate **173**. Endeavours to distil the alkylated oxoglutarate mixture by such means prevented the significant decomposition seen in the conventional distillation however, the desired monoalkyl oxoglutarate **173** co-distilled with the dimethyl 3-oxoglutarate **172** starting material. Despite the isolation of a mixture, the removal of higher alkylated products **176-178** gave an enriched mixture of the desired product **173**. This simplified mixture was then subjected to the next step, a decarboxylative aldol procedure, without further purification.

5.2.2 Production of 3-hydroxy-8-nonyne-2,5-dione by decarboxylative aldol addition

The second step of Matsuo's synthetic methodology towards (*Z*)-pyrethrolone **21** was a one-pot reaction allowing for ester hydrolysis, decarboxylation, and aldol addition to extend the carbon framework.[9] The presence of the propargyl unit was proposed to allow for rapid decarboxylation of the neighbouring carboxylate ultimately giving the desired regioselectivity for the subsequent aldol addition on the unsubstituted β-dicarbonyl region of the carbon skeleton (Scheme 5.7).[9] Notably, this regioselectivity was contributed to the greater withdrawing capabilities of the propargyl unit in comparison to a previously implemented allyl derivative that exhibited no regioselectivity.[9]

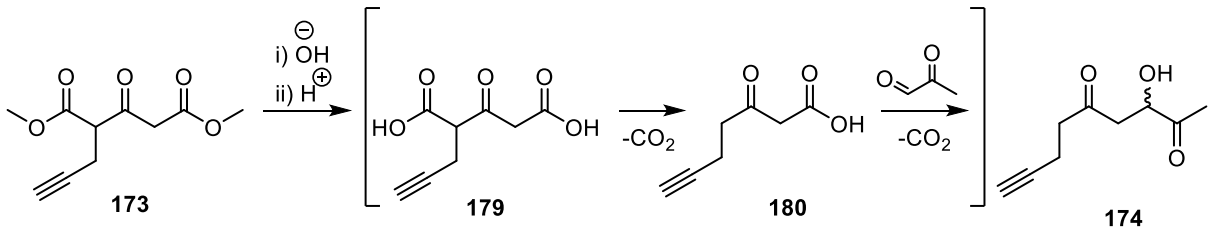

Scheme 5.7: Proposed reactivity for the one-pot Aldol process giving the acyloin intermediate **174**.

The semi-purified oxoglutarate mixture isolated from the previous step was subjected to the above literature procedure for the one-pot decarboxylative aldol[9] to generate the linear 1,4-diketone intermediates **174**. The oxoglutarate mixture of **172** and **173** was slowly added to a cooled aqueous sodium hydroxide solution. The biphasic reaction mixture was warmed to 30 °C for 5 h during which the mixture became a homogeneous, yellow solution. The resulting solution was then cooled over an ice-bath and the pH adjusted with concentrated sulfuric acid which resulted in the observable evolution of gas from the decarboxylation. The reaction was allowed to progress overnight after which sodium bicarbonate, sodium dithionite and toluene were added. The mixture was warmed to 36 °C and a 40% aqueous methylglyoxal solution was added slowly. The reaction was left to stir with continued heating overnight throughout which time the organic layer became a dark orange colour. Following extraction from the aqueous layer, the crude material was found to be a mixture of reaction products including minor amounts of the desired acyloin **174**. Notably, the addition of sodium dithionite has been implicated in preventing the formation of a previously identified by-product, a catechol formed from consecutive aldol events.[14] However, the mechanism in which this inhibition proceeds by remains unknown.

Despite clear reaction progression, a number of undesired by-products were formed from both the reactivity of the residual oxoglutarate starting material **172** and alternate reactions of the propargylated oxoglutarate **173** (Scheme 5.8). The most prevalent of these side reactions was the decarboxylation of the starting material without aldol addition taking place. Instead, the unalkylated material **172** could undergo mono- or di-decarboxylation yielding either the monocarboxylate **181** or acetone **182** respectively (Scheme 5.8A). Similarly, the monopropargyl oxoglutarate **173** could undergo similar decarboxylation giving carboxylates **180** and **183** or 5-hexyne-2-one **184** (Scheme 5.8B).

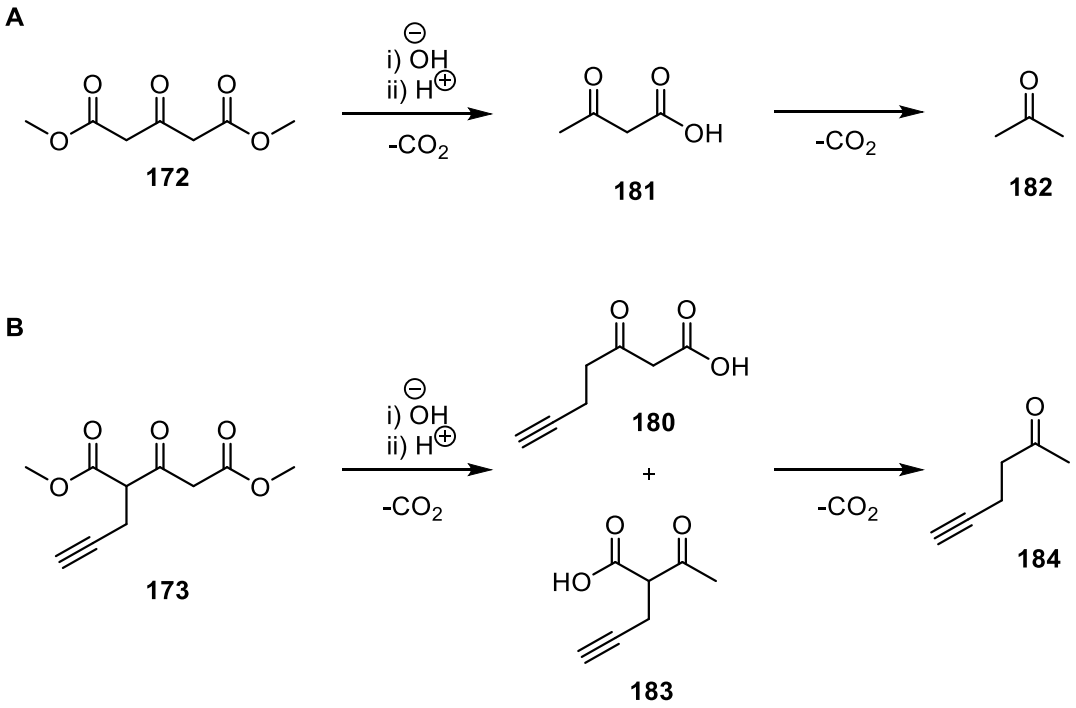

Scheme 5.8: Alternate reactivity of the oxoglutarate starting mixture where the unalkylated (A) and monoalkylated (B) materials undergo decarboxylation.

GCMS analysis of the crude mixture indicated 5-hexyn-2-one **184** was the most abundant by-product originating from complete decarboxylation of the alkylated starting material. By extension, acetone **182** is a probable by-product from similar reactivity of the dimethyl 3-oxoglutarate **172** in the reaction however, it is likely to have been removed during evaporation of the extraction solvent on work-up. Intermediate decarboxylation by-products **180**, **181** and, **183** were also implicated in the GCMS analysis of the reaction mixture in much lower quantities. The increased presence of these decarboxylated impurities **180-184** is likely due to the strength of the employed acid and the time of exposure to this acid prior to the aldol addition resulting in premature loss of carbon dioxide. In conjunction to these decarboxylated by-products **180-184**, alternate aldol reactivities were also observed (Scheme 5.9) with the presence of minor aldol addition adducts in the reaction mixture. The most prevalent of these adducts was the unalkylated equivalent **185** of the desired product stemming from residual dimethyl 3-oxoglutarate **172** (Scheme 5.9A) or the alternate regioisomer **186** from the alkylated oxoglutarate **173** (Scheme 5.9B).

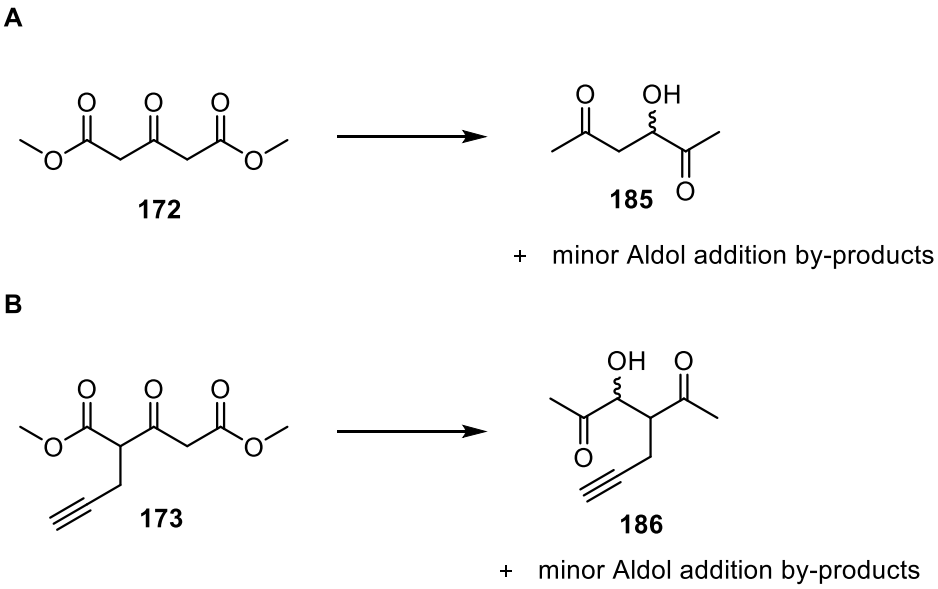

Scheme 5.9: Aldol addition products observed in the one-pot decarboxylative Aldol protocol from the residual dimethyl 3-oxoglutarate **172 (A)** and the monoalkylated oxoglutarate **173 (B)**.

Unfortunately, attempts to purify the mixture isolated from this decarboxylative aldol protocol were unsuccessful due to the abundance and structural similarity of by-products formed from both the propargyl **173** and unsubstituted **172** oxoglutarates in the alkylation mixture. Whilst milder conditions may act to counteract the formation of the undesired decarboxylation by-products **180-184**, the alternate aldol adducts **185** and **186** may still be formed complicating the purification process. In addition, continuation of the pathway became unfeasible with the build-up of impurities that were unable to be removed at each successive step. As such, alternate protocols were investigated for the production of pivotal intermediates in the pathway.

5.2.3 The pursuit of an alternate synthesis

In spite of the exhaustive attempts to mimic and optimise the early stages of the synthesis described by Matsuo,[9] the desired intermediates could not be isolated in high purity with compounding impurities occurring with each successive step in the pathway (Scheme 5.10).

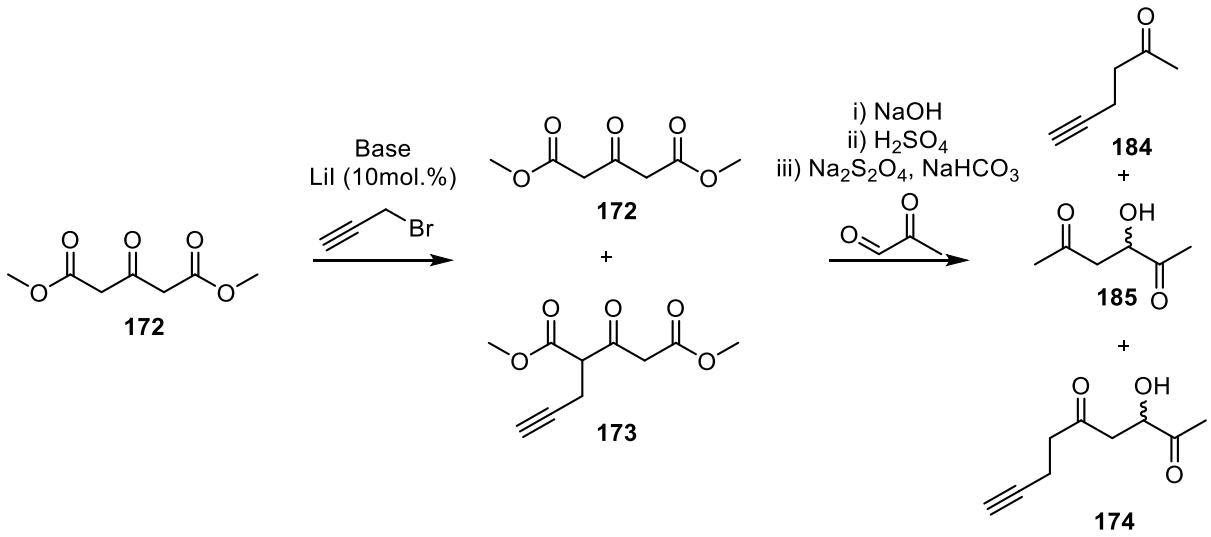

Scheme 5.10: Attempted steps of Matsuo's described synthesis for (*Z*)-pyrethrolone **21** showing the major products isolated.

The complication encountered when attempting to purify the important products early in the synthesis suggests alternate means of producing them or an alternate pathway is necessary in an attempt to combat the development of unwanted by-products.

5.3 A modified synthesis for (*Z*)-pyrethrolone

An altered synthesis for the production of (*Z*)-pyrethrolone **21** was necessary to avoid the issues described above however, it was desirable to maintain the attractive qualities of Matsuo's published pathway.[9, 10] This meant that the new or modified protocols needed to remain scalable and accessible for high throughput production of (*Z*)-pyrethrolone **21** whilst being reliable for the production of pure materials. The reliable manufacture of the acyloin **174** was of particular interest for the direct application to the rest of the published procedures, i.e. chain extension and alkyne reduction.[9, 10] Retrosynthetic analysis (Scheme 5.11) highlighted ethyl acetoacetate **187** as a potential replacement of dimethyl 3-oxoglutarate **172** as starting material because, once selectively alkylated, it is amenable to the decarboxylate aldol addition.

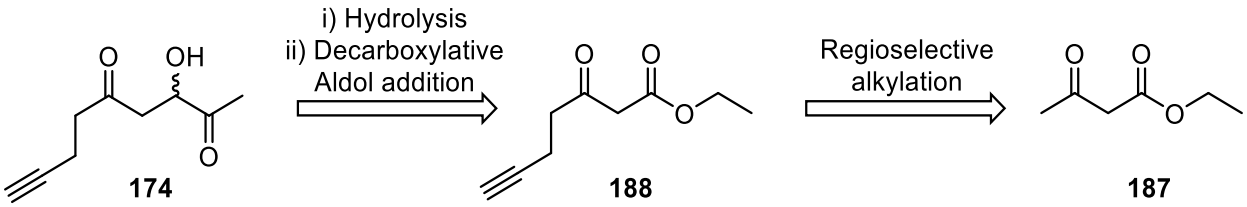

Scheme 5.11: Retrosynthetic analysis for a more efficient synthesis of 3-hydroxy-8-nonyne-2,5-dione **174**.

5.3.1 Dianion alkylation of ethyl acetoacetate

Ethyl acetoacetate **187** much like dimethyl 3-oxoglutarate **172** is cheap, readily available and has little mammalian toxicity. In contrast to the oxoglutarate **172**, ethyl acetoacetate **187** only has a single ester available to react under the decarboxylative aldol protocol, allowing for site specific addition, and can be regioselectively alkylated. The regioselective alkylation of a β-keto ester can be achieved through the generation of its dianion where the more reactive terminal anion is alkylated preferentially.[15] This well-documented dianion reactivity was proposed as a replacement alkylation procedure for alleviating the multi-alkylation reactivity observed with the oxoglutarate **172** and as such purification complications encountered in the prior alkylation reaction.

Treatment of ethyl acetoacetate **187** with sodium hydride at decreased temperature generated the monoanion enolate **189** at the β-carbon (Scheme 5.12), indicated by the change from a colourless suspension to a light-yellow solution. Subsequent addition of *n*-butyllithium at −78 °C readily afforded the dianion **190**, monitored by the further change to a deep orange solution. The alkylating agent, propargyl bromide, was then added and the mixture warmed to room temperature. During this time a precipitate formed, likely lithium bromide, from reaction of the lithiated enolate, and a rapid colour change to light brown was observed. Quench and work-up of the reaction gave a mixture containing the desired alkylation product **188** as the major constituent.

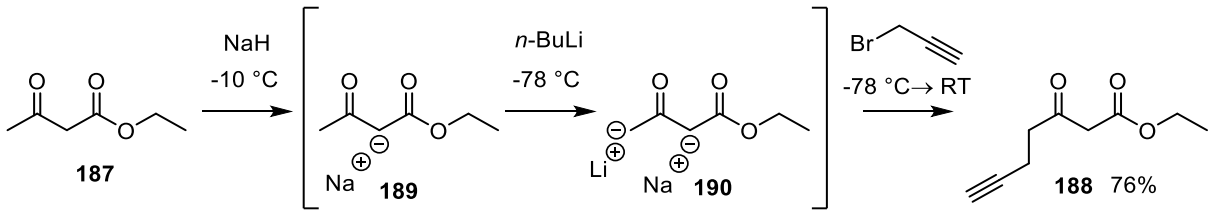

Scheme 5.12: Dianion alkylation of ethyl acetoacetate **187** with propargyl bromide.

Due to the prior issues with large scale conventional distillation, Kugelrohr short-path distillation was used to purify the mixture giving ethyl 3-oxohept-6-ynoate **188** in a 76% yield with characterisation in agreement with literature.[16] Replacing this first step in the synthetic sequence allowed for the clean production of an alternate alkylation product that was proposed to be directly amenable to a modified version of the ester hydrolysis-decarboxylative aldol addition described by Matsuo.[9]

5.3.2 Decarboxylative aldol addition revisited

A modified method of Matsuo's one-pot ester hydrolysis-decarboxylative aldol protocol remained a viable route to afford the 1,4-diketones **174** utilising the propargylated ethyl acetoacetate **188**. Unlike the dimethyl 3-oxoglutarate equivalent **173**, ethyl 3-oxohept-6-ynoate **188** only has a single site for reaction to take place allowing for regioselectivity in the aldol component of the procedure hence, minimising the formation of unwanted by-products.

Hydrolysis of the ethyl ester was undertaken as before with the addition of the alkylated material **188** to a cooled solution of aqueous sodium hydroxide which was subsequently warmed to room temperature and left to stir. With progression of the hydrolysis, the reaction mixture became homogeneous indicating formation of the carboxylate anion. Deviating from Matsuo's protocol (Scheme 5.13),[9] dilute hydrochloric acid was added to the cooled reaction mixture until approximately pH 5 was achieved. Sodium dithionite and toluene were added immediately after pH adjustment followed by the dropwise addition of an aqueous solution of methylglyoxal. The resulting biphasic mixture was left to slowly stir overnight at room temperature, during which the organic layer slowly became a dark yellow colour. Following work-up, the alkyne by-product **184** was removed by Kugelrohr short-path distillation giving the desired aldol addition adducts **174** in a combined yield of 66%.

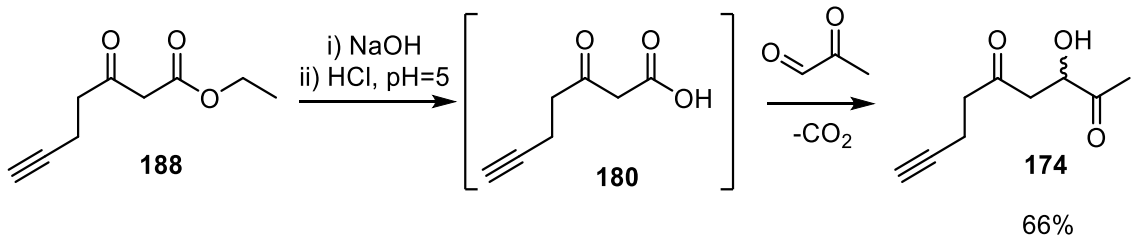

Scheme 5.13: Decarboxylative aldol procedure giving acyloin intermediate **174**.

Substitution of the concentrated sulfuric acid used in the initial procedure for 1 M hydrochloric acid minimised premature decarboxylation, which would normally give increased quantities of the alkyne by-product **184**. Unlike the protocol described by Matsuo[9] which relies on regioselective decarboxylation followed by aldol addition at the remaining β-dicarbonyl, this revised methodology immediately adds the dithionite and methylglyoxal as the reactive enol species is likely furnished as a result of the decarboxylation process (Scheme 5.13).

The successful application of an altered hydrolysis-decarboxylative aldol addition to ethyl 3-oxohept-6-ynoate **188** allowed the 1,4-diketones **174** to be subjected to an intramolecular aldol condensation to furnish the cyclic enone scaffold **175** of (*Z*)-pyrethrolone **21**.

5.3.3 Intramolecular aldol condensation for cyclisation

The third reaction of Matsuo's production of (*Z*)-pyrethrolone **21**[9] remained a feasible step to generate the cyclic enone framework **175**. This intramolecular aldol condensation of an intermediate 1,4-diketone is a common feature amongst many of the previous rethrolone syntheses[4, 7-9] demonstrating its reliability in cyclopentenone production.

As per the published procedure,[9] the 1,4-diketones **174** was added dropwise to a cooled, biphasic mixture of aqueous sodium hydroxide and toluene. Following a total 5 h reaction time, the reaction mixture was quenched with concentrated hydrochloric acid and the subsequent work-up yielded a crude mixture containing the desired rethrolone **175**. However, the mixture also contained significant quantities of what appeared to be rethrolone dimers **192** and **193**. It has been well established that hydrolysis of pyrethrins **5** under alkali conditions results in ready yielding a cyclopentadienone **35**. This cyclopentadienone **35**, like many others, readily undergoes [4+2] Diels-Alder cycloaddition giving the two dimers **36** and **37** known more commonly as 'altered pyrethrolone' (Chapter 1; Scheme 1.5).[17-19] By

extension of this phenomenon, it is likely that the rethrolone formed **175** can react in an analogous way (Scheme 5.14) to produce the observed dimer impurities **192** and **193** with extended exposure to the basic conditions.

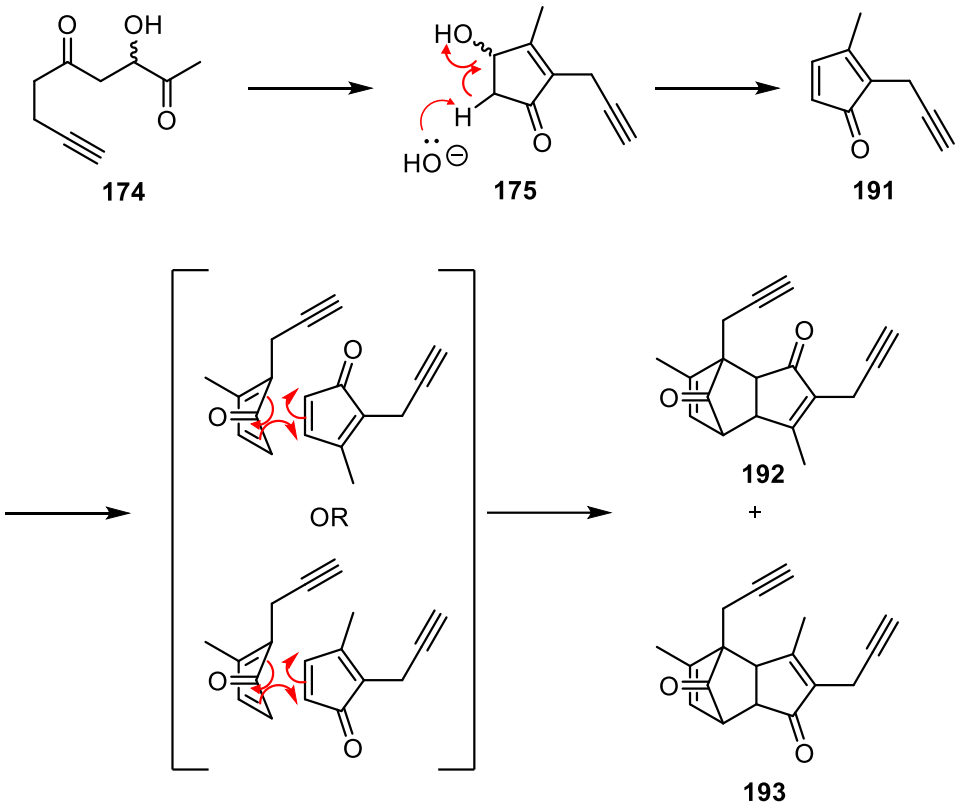

Scheme 5.14: Elimination and subsequent Diels-Alder dimerisation of the rethrolone 175 intermediate under basic conditions.

Optimisation of the conditions (Scheme 5.15) allowed for a shorter reaction time of 1.5 h, minimising exposure of the rethrolone **175** to the alkaline environment and therefore limiting the formation of the undesired cyclopentadienone dimers **192** and **193**. After Kugelrohr short-path distillation, cyclopentenone **175** was isolated in a good yield of 72% allowing for successive carbon chain extension by Sonogashira cross-coupling.

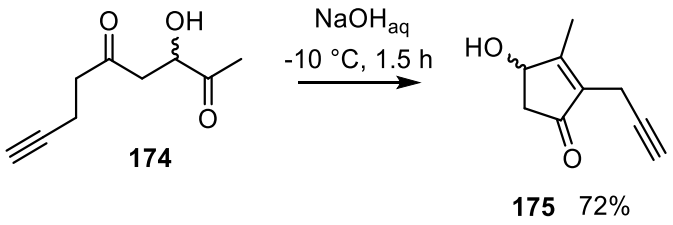

Scheme 5.15: Optimised cyclisation of acyloin 174 to give cyclopentenone 175.

5.3.4 Sonogashira side chain extension

Extension of the hydrocarbon side chain of the alkynyl rethrolone **175** was necessary to install the required carbon skeleton for (*Z*)-pyrethrolone **21**. The methodology described by Matsuo,[10] albeit substituting the carcinogenic benzene reaction solvent for dry THF, was applied to the isolated rethrolone **175** (Scheme 5.16). Under an atmosphere of nitrogen, the catalytic palladium(0) and copper(I) were added to a solution of rethrolone **175** in dry THF. Successive addition of the vinyl bromide was followed by a 20 h reaction period at room temperature. Following work-up, analysis of the crude product revealed a lack of the desired material. Instead, the protocol had resulted in the production of a homodimer **194** of the alkynyl rethrolone **175** rather than reactivity with the vinyl halide.

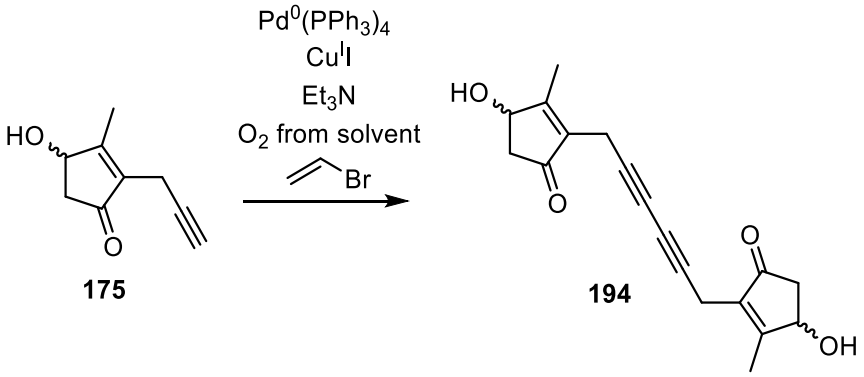

Scheme 5.16: Copper(I)-catalysed Glaser coupling affording the rethrolone homodimer 194 from the attempted Sonogashira cross coupling.

Sonogashira cross-coupling reactions make use of a co-catalytic system with palladium(0) and copper(I) (Scheme 5.17). Whilst not fully understood, the copper catalyst is proposed to form a reactive copper acetylide **198** with the alkynyl reagent **201** which is then transmetallated to the palladium centre.[20] However when oxygen is present, this copper acetylide intermediate **198** can readily dimerise with another alkynyl equivalent **201** via Glaser coupling to give the homodimer **199** (Scheme 5.17).[21]

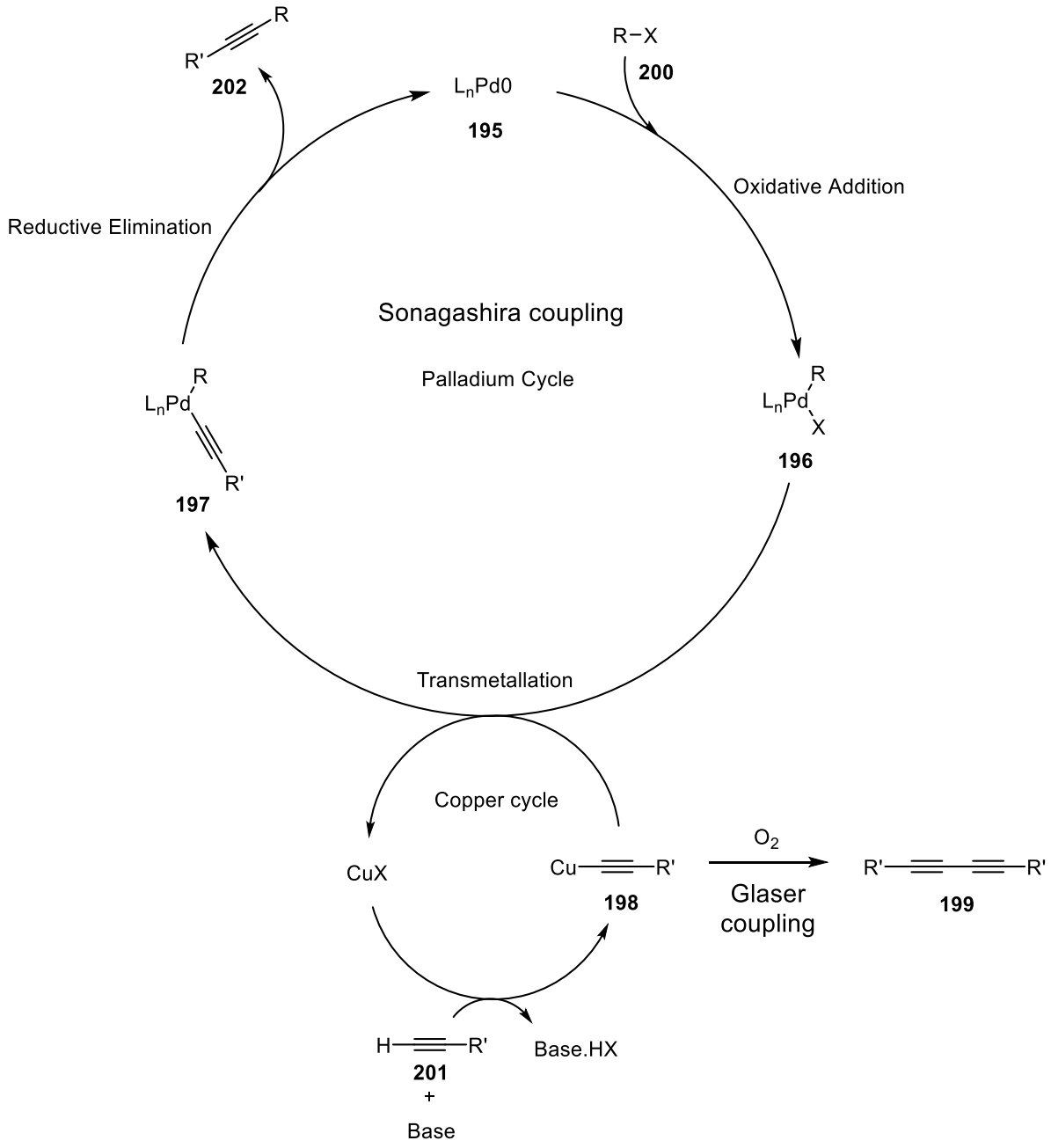

Scheme 5.17: Sonogashira cross-coupling co-catalytic cycle showing Glaser coupling side reactivity.

The presence of the homodimer **194** in the crude product from the Sonogashira protocol employed suggests that oxygen in the system caused preferential Glaser coupling rather than the desired two carbon chain extension. Strictly oxygen-free conditions, achieved through thorough de-oxygenation of the solvent with argon, were employed to remedy this homocoupling with successful Sonogashira coupling giving the desired enyne **155** in 62% yield following purification by short silica gel plug (Scheme 5.18).

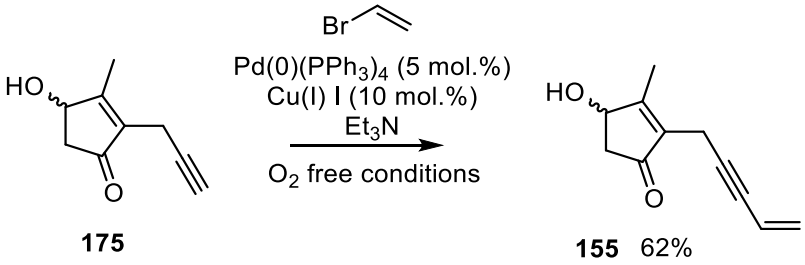

Scheme 5.18: Sonogashira coupling of rethrolone 175 and vinyl bromide.

The isolation of this final intermediate **155** in sufficient yields allowed exploration into the semi-reduction of the alkynyl-unit to give the desired (*Z*)-pyrethrolone **21**.

5.3.5 Reduction to (Z)-pyrethrolone

The final step to afford (*Z*)-pyrethrolone **21** was the partial hydrogenation of the enyne **155** to the *cis*-alkene. Traditionally this transformation is achieved through hydrogenation in the presence of a poisoned catalyst to prevent over-reduction to the alkane. Such a protocol is widely accessible and generally operationally simple and therefore, served as a starting point for the reduction of the enyne rethrolone **155** to (*Z*)-pyrethrolone **21**.

Initial attempts at this controlled reduction utilised Lindlar catalyst under atmospheric pressure of hydrogen in an effort to limit reactivity. Unfortunately, under these conditions transformation of the enyne **155** to the desired (*Z*)-pyrethrolone **21** was not observed, potentially indicating a need for harsher conditions. Consequently, the reaction (Scheme 5.19A) was conducted under Parr conditions with up to 200 kPa of hydrogen applied. The resulting material was unaffected by the increased hydrogen pressure, with the sole isolation of the starting enyne **155**.

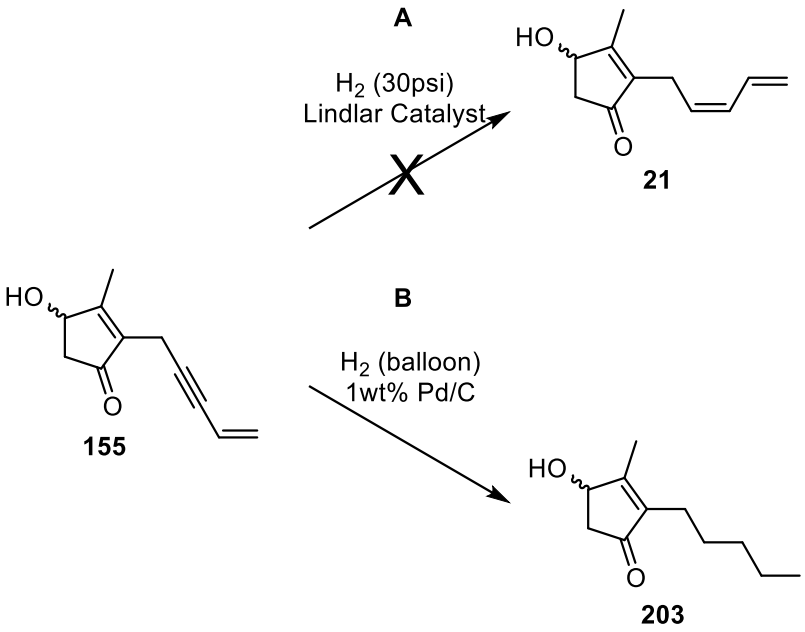

Scheme 5.19: Attempted hydrogenation of the enyne rethrolone 155 under high pressure poisoned conditions (A) and atmospheric pressures with Pd/C catalyst (B).

In an attempt to induce a transformation, the atmospheric pressure hydrogenation protocol was undertaken in the presence of typical Pd/C catalysts (Scheme 5.19B). In this case, the penta-carbon side chain was readily reduced to the completely saturated analogue **203** no matter how short the exposure time. A more controlled means of hydrogenation then became of interest to limit reactivity.

Transfer hydrogenation protocols allow for the stoichiometric control of hydrogen in a given reaction system and as such are a more controllable reductive methodology. In this instance, the enyne **155** was heated under reflux in the presence of the formic acid hydrogen donor and a Pd/C catalyst in THF (Scheme 5.20). This protocol was successful in producing minor quantities of the desired (*Z*)-pyrethrolone **21** however, regularly resulted in production of both the *E*-isomer **64** and the migration isomer **204** as well as significant over reduction to the fully saturated analogue **203**.

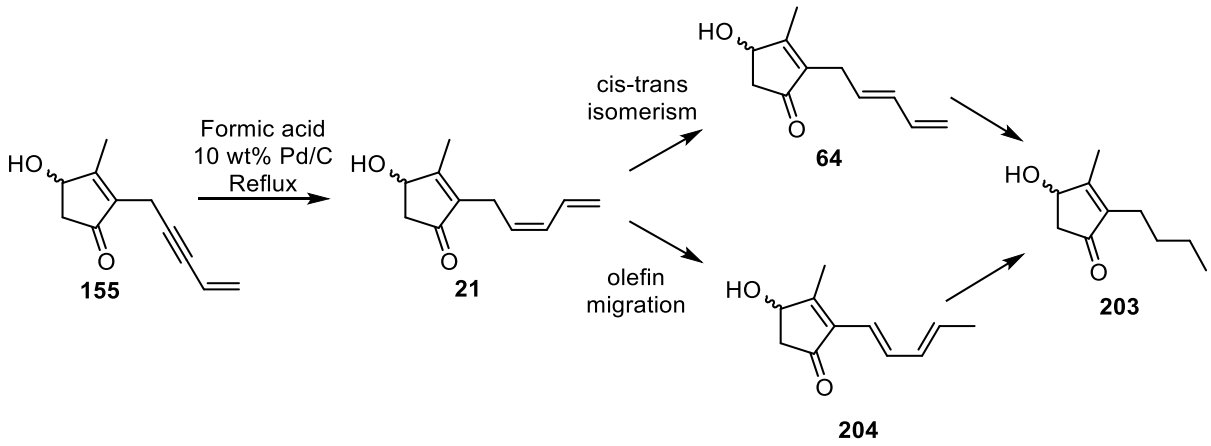

Scheme 5.20: Catalytic transfer hydrogenation of enyne **155** and the continued reaction of (*Z*)-pyrethrolone **21** under such conditions.

Much like attempts with the pyrethrins **5** (Chapter 2; Section 2.4.2), these alternate pyrethrolone isomers **64** and **204** are the result of the competing β-hydride eliminations where either: i) rotation about the intermediate single bond and subsequent elimination will generate the *trans*-isomer **64** or ii) elimination on the alternate β-hydrogen results in the migration of the double bond(s) **204**.[22, 23] Unfortunately, purification by distillation was undesirable due to the thermal instability of the (*Z*)-pyrethrolone **21** and attempts to purify by column chromatography resulted in co-elution of the structurally similar isomers. After exhausting these typical hydrogenation methods, the activated zinc protocol described by Matsuo was investigated.[10]

The literature alkyne controlled reduction made use of metallic zinc in an aqueous *n*-propanol solvent mix to produce the (*Z*)-pyrethrolone product **21**.[10] Enyne **155** in *n*-propanol was added to a suspension of zinc, activated by hydrochloric acid, in water and the resulting mixture heated under reflux for 30 h (Scheme 5.21). Following isolation of the crude material, ^{1}H NMR analysis indicated complete consumption of the enyne starting material **155** however, no (*Z*)-pyrethrolone **21** was observed. The (*Z*)-pyrethrolone **21** continued to react under the reductive conditions ultimately giving over saturated products. Repetition of the protocol with close monitoring revealed that reaction times extending beyond 2 hr resulted in further reduction of the (*Z*)-pyrethrolone **21** with no observable quantities after 5 hr. Optimised protocols utilised a 1.5 hr reaction time giving small quantities of the (*Z*)-pyrethrolone **21** as a mixture with the enyne starting material **155**. Attempts to purify by chromatographic means did not yield pure (*Z*)-pyrethrolone **21** due to the high structural similarity with the starting

material **155**. As prior, the sensitivity of the (*Z*)-pyrethrolone **21** to thermal conditions and its high boiling point, even under reduced pressure, prevented purification by distillation. As a result, the model (*Z*)-pyrethrolone **21** was isolated as a mixture in a yield of 11% as determined by NMR (Scheme 5.21).

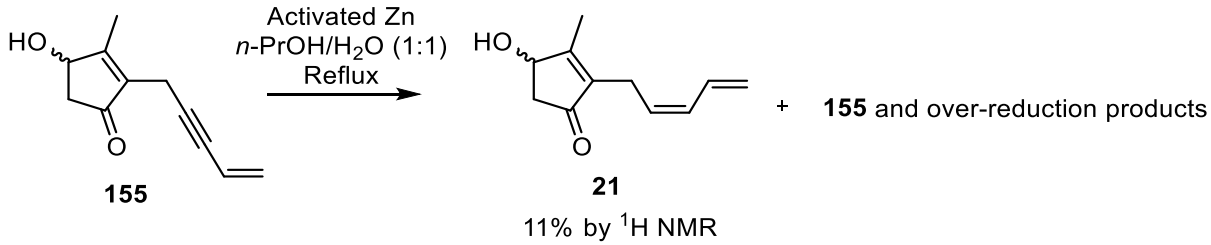

Scheme 5.21: Reduction of enyne **155** by the activated zinc protocol described by Matsuo.[10]

5.4 Conclusions

In the pursuit of a model compound to test future synthetic modifications of pyrethrins **5** on, the alcohol moiety (*Z*)-pyrethrolone **21** was most suited. This rethrolone possessed the desired functionality for the prospective modifications and had previously been prepared by a number of synthetic pathways.[4, 7-11]

In an attempt to acquire the (*Z*)-pyrethrolone **21** in appreciable quantities, the most recent synthesis by Matsuo (Scheme 5.4) was attempted.[9, 10] Unfortunately, replicating the initial alkylation of dimethyl 3-oxoglutarate **172** resulted in a mixture of multi-propargylated oxoglutarates **176-178** amongst the desired material. Attempts to purify this mixture were unsuccessful but an enriched mixture with the starting material was obtained by short-path distillation. Application of this mixture in the following ester hydrolysis-decarboxylative aldol addition protocol was unable to yield the desired intermediate **174** in significant purity due to the build-up of by-products and the reactivity of residual starting material **172**. Due to these complications an alternate pathway was explored for the production of (*Z*)-pyrethrolone **21**.

A modified synthetic pathway (Scheme 5.22) was developed for the production of (*Z*)-pyrethrolone **21** with an alternate starting material and alkylation procedure implemented. Dianion alkylation of ethyl acetoacetate **187** was able to remedy the multi-alkylation complications from Matsuo's original propargylation of dimethyl 3-oxoglutarate **172**[9] giving an intermediate **188** directly amenable to the ester hydrolysis-decarboxylative aldol addition

process. This aldol process was then able to be optimised to minimise premature decarboxylation giving the 1,4-diketones **174** in fair yield. Cyclisation of the 1,4-diketones **174** by intramolecular aldol condensation gave the rethrolone moiety, with decreased reaction times reducing the exposure of the rethrolone **175** to detrimental alkali conditions. Modified Sonogashira conditions gave the carbon framework of (*Z*)-pyrethrolone **21** in the form of enyne **155** which could be subjected to semi-reduction protocols. Unfortunately, despite exhaustive attempts, racemic (*Z*)-pyrethrolone **21** was only able to be isolated as a mixture in low yields due to complications with over-reduction of the penta-carbon unit.

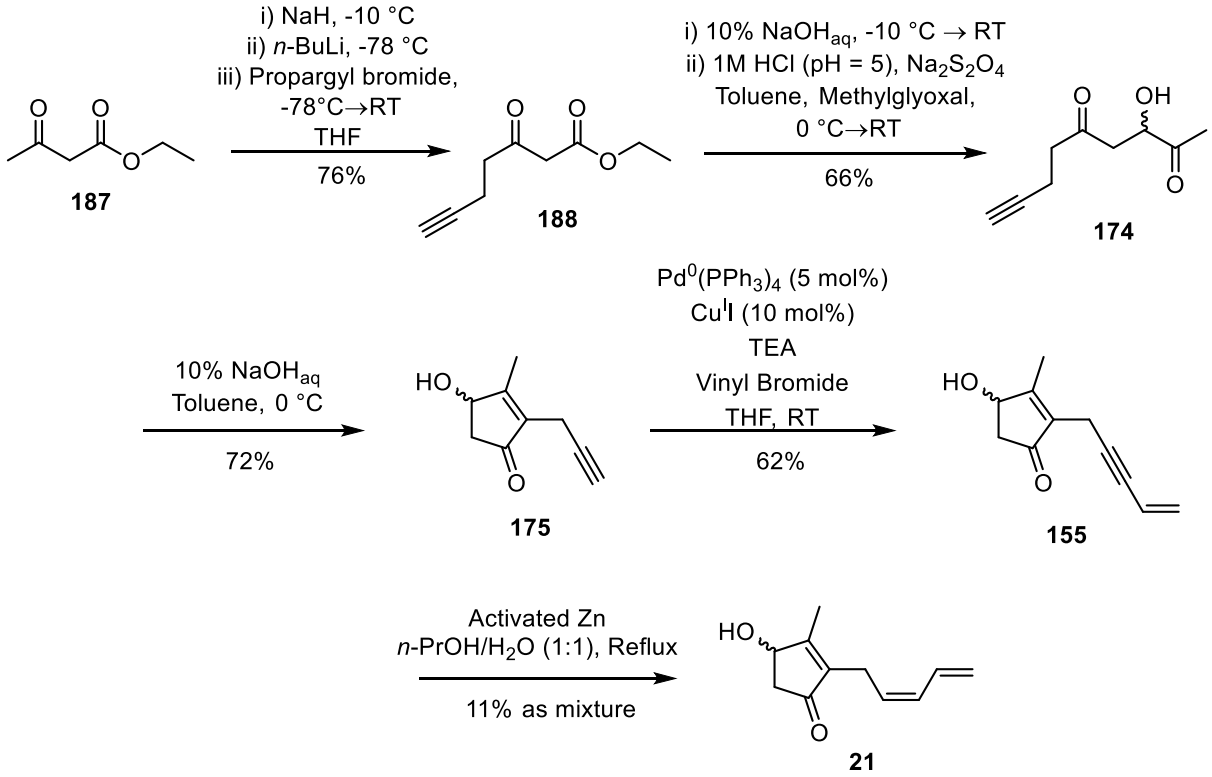

Scheme 5.22: Modified synthesis of (*Z*)-pyrethrolone **21**.

Whilst not completely successful, the modified synthesis of racemic (*Z*)-pyrethrolone **21** was achieved over 5 steps in 2.5% overall yield albeit as a mixture with over-reduction products. Despite the improvement on Crombie's early synthesis of less than 1% as a mixture[4] and Tsuji's production of the undesired geometric isomer,[8] the modified synthesis described here was unable to improve upon Crombie's revised synthesis.[7] Ultimately, the desired model for pyrethrin modification, (*Z*)-pyrethrolone **21**, was unable to be manufactured in large, pure quantities despite extensive reaction optimisation and purification attempts.

5.5 References

1. Freemont, J. A.; Littler, S. W.; Hutt, O. E.; Mauger, S.; Meyer, A. G.; Winkler, D. A.; Kerr, M. G.; Ryan, J. H.; Cole, H. F.; Duggan, P. J., Molecular Markers for Pyrethrin Autoxidation in Stored Pyrethrum Crop: Analysis and Structure Determination. *J. Agric. Food Chem.* **2016,** *64*, 7134-7141.
2. Goldberg, A. A.; Head, S.; Johnston, P., Action of Heat on Pyrethrum Extract: The Isomerisation of Pyrethrins to Isopyrethrins. *J. Sci. Food Agric.* **1965,** *16,* 43-51.
3. Crombie, L.; Harper, S. H.; Newman, F. C.; Thompson, D.; Smith, R. J. D., Experiments on the synthesis of the pyrethrins. Part X. Intermediates for the synthesis of *cis*-pyrethrolone. *J. Chem. Soc.* **1956,** *1956*, 126-135.
4. Crombie, L.; Harper, S. H.; Newman, F. C., Experiments on the synthesis of the pyrethrins. Part XI. Synthesis of *cis*-pyrethrolone and pyrethrin I: Introduction of the *cis*-penta-2:4-dienyl system by selective hydrogenation. *J. Chem. Soc.* **1956,** *1956*, 3963-3971.
5. Crombie, L.; Harper, S. H.; Thompson, D., Experiments on the synthesis of the pyrethrins. Part VII. Synthesis of *trans*-pyrethrone, *trans*-pyrethrolone, and a pyrethrin-I. *J. Chem. Soc.* **1951,** *1951*, 2906-2915.
6. Crombie, L.; Edgar, A. J. B.; Harper, S. H.; Lowe, M. W.; Thompson, D., Experiments on the synthesis of the pyrethrins. Part V. Synthesis of side-chain isomers and analogues of cinerone, cinerolone, and cinerin-I. *J. Chem. Soc.* **1950,** *1950*, 3552-3563.
7. Crombie, L.; Hemesley, P.; Pattenden, G., Synthesis of Ketols of the Natural Pyrethrins. *J. Chem. Soc.* **1969**, 1016-1024.
8. Tsuji, J.; Yamakawa, T.; Mandai, T., Application of Palladium Catalyses to a Simple Synthesis of (±)-Pyrethrolone. *Tetrahedron Lett.* **1979,** *39*, 3741-3744.
9. Matsuo, N.; Fujita, F.; Magara, O.; Yamazaki, H.; Aketa, K.; Nishioka, T.; Itaya, N., A Convenient Synthesis of 4-Hydroxy-3-methyl-2-(2-propynyl)-cyclopent-2-enone, an Alcohol Moiety of a Synthetic Pyrethroid Having Strong Killing and Knockdown Activity. *Agr. Biol. Chem.* **1982,** *46* (7), 1911-1912.
10. Matsuo, N.; Takagaki, T.; Watanabe, K.; Ohno, N., The First Practical Synthesis of (S)-Pyrethrolone, an Alcohol Moiety of Natural Pyrethrins I and II. *Biosci. Biotech. Biochem.* **1993,** *57* (4), 693-694.
11. Kawamoto, M.; Moriyama, M.; Ashida, Y.; Matsuo, N.; Tanabe, Y., Total Syntheses of All Six Chiral Natural Pyrethrins: Accurate Determination of the Physical Properties, Their

Insecticidal Activities, and Evaluation of Synthetic Methods. *J. Org. Chem.* **2020,** *85*, 2984-2999.

12. Danda, H.; Maehara, A.; Umemura, T., Preparation of (4S)-4-hydroxy-3-methyl-2-(2'-propynyl)-2-cyclopentenone by combination of enzymatic hydrolysis and chemical transformation. *Tetrahedron Lett.* **1991,** *32* (38), 5119-5122.
13. Caine, D., Magnesium Methoxide. In *Encyclopedia of Reagents for Organic Synthesis*, 2001.
14. Kato, T.; Mochizuki, M.; Okano, S.; Matsuo, N., A Novel Catechol Compound, an Unusual Side Reaction Product of a β-Ketoester with Pyruvic Aldehyde and Its Inhibition by Sodium Dithionite. *Synth. Commun.* **2003,** *33*, 3977-3982.
15. Huckin, S. N.; Weiler, L., Alkylation of dianions of β-ketoesters. *J. Am. Chem. Soc.* **1974,** *96* (4), 1082-1087.
16. Kaewsri, W.; Norseeda, K.; Ruengsangtongkul, S.; Chaisan, N.; Thongsornkleeb, C.; Tummatorn, J.; Ruchirawat, S., Synthesis of 2-Cyclohexenone-2-carboxylate and 4-Chloro-2-cyclohexenone-2-carboxylate Derivatives by Cyclisation of Alkyne-Tethered 1,3-Ketoesters. *Asian J. Org. Chem.* **2017,** *7* (1), 203-211.
17. Allen, C. F. H.; VanAllan, J. A., Dimerisation of Cyclopentadienones. *J. Am. Chem. Soc.* **1950,** *72* (11), 5165-5167.
18. Harmata, M.; Gomes, M. G., Intermolecular [4+2] Cycloadditions of a Reactive Cyclopentadienone. *Eur. J. Org. Chem* **2006,** *2006* (10), 2273-2277.
19. Hutt, O. E.; Freemont, J. A.; Littler, S.; Duggan, P. J.; Tsanaktsidis, J.; Cole, H.; Kerr, M.; Ryan, J. H., Staudinger and Ruzicka's Altered Pyrethrolone: the Cyclopentadienone Dimers Derived from Pyrethrin I. *Acta Hortic.* **2015,** *1073*, 181-190.
20. Chinchilla, R.; Najera, C., Recent advances in Sonogashira reactions. *Chem. Soc. Rev.* **2011,** *2011* (40), 5084-5121.
21. Siemsen, P.; Livingston, R. C.; Diederich, F., Acetylenic Coupling: A Powerful Tool in Molecular Construction. *Angew. Chem. Int. Ed.* **2000,** *39*, 2632-2657.
22. Gauthier, D.; Lindhardt, A. T.; Olsen, E. P. K.; Overgaard, J.; Skrydstrup, T., In Situ Generated Bulky Palladium Hydride Complexes as Catalysts for the Efficient Isomerization of Olefins. Selective Transformation of Terminal Alkenes to 2-Alkenes. *J. Am. Chem. Soc.* **2010,** *132*, 7998-8009.

23. Tan, E. H. P.; Lloyd-Jones, G. C.; Harvey, J. N.; Lennox, A. J. J.; Mills, B. M., $[(RCN)_2PdCl_2]$-Catalyzed *E/Z* Isomerization of Alkenes: A Non-Hydride Binuclear Addition-Elimination Pathway. *Angew. Chem. Int. Ed.* **2011,** *50*, 9602-9606.

Chapter 6 Conclusions and Future Work

6.1 General conclusions

The work outlined in this thesis has focussed on attempts to selectively synthetically modify the natural pyrethrin scaffold towards analogues with increased stability to the environmental factors that would normally result in the degradation and loss of the Pyrethrins **5-7**. As a result, a library of pyrethrin analogues has been developed with varying degrees of alteration on the rethrolone side chain of the pyrethrin scaffold. Whilst many proved to be inactive in preliminary insecticidal activity studies, they provided new insight into the reactivity and structure-activity relationships of this sensitive moiety.

The increased susceptibility of the pyrethrins **5** to the degradative processes that affect the pyrethrum concentrate prompted exploration into their chemo- and regio-selective reduction to the more stable jasmolins **7**. As a result of this exploration into several reductive protocols (Chapter 2), a number of reduced pyrethrin analogues were prepared allowing for application into preliminary insecticidal activity. In addition, a diimide-mediated reduction of the pyrethrins **5** was developed allowing for the production of their jasmolins counterparts **7** albeit as a mixture with the overreduction product, tetrahydropyrethrins **53** (Scheme 6.1A). Of particular note was the applicability of this diimide reduction to the pyrethrum extract, effectively removing the least stable of the pyrethrin esters **5** giving a modified version of the extract with insecticidal activity comparable to the jasmolins **7**.

Further elaboration of the pyrethrin scaffold was achieved through both Diels-Alder cycloaddition (Chapter 3) and palladium-catalysed arylation (Chapter 4). A range of pyridazine adducts of the natural pyrethrins **5** were prepared under IEDDA conditions with the terminal double bond of the pentadienyl moiety serving as dienophile and 3,6-bissubstitued-1,2,4,5-tetrazines as diene (Scheme 6.1B). Of these, cycloaddition with 3,6-dichloro-1,2,4,5-tetrazine **80** resulted in some unprecedented reactivity resulting in a dihydro-analogue **93** likely formed through a series of tautomerism events of the intermediate dihydropyridazine **94**. In addition, Heck reaction of the natural pyrethrins **5** with a series of aryl iodides was achieved through a cationic catalytic cycle. Of particular interest was the production of the arylated analogue and its corresponding migration isomer, both isolated as the *E,E*-diastereomer (Scheme 6.1C). The

electronic properties of the aryl iodide coupling partner significantly affected the yield as well as the ratio in which the two regioisomers were produced.

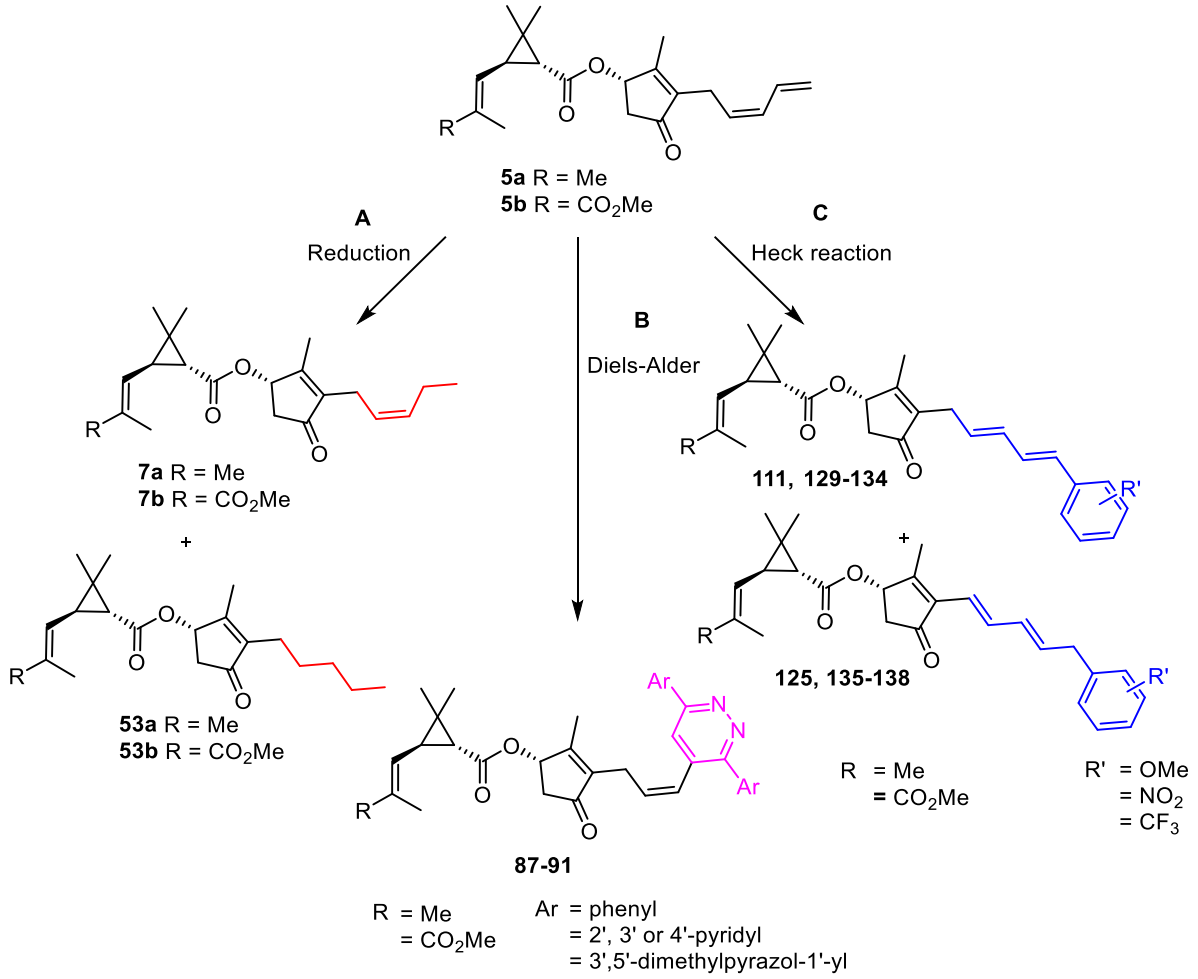

Scheme 6.1: Production of a range of pyrethrin analogues through reduction **(A)**, Diels-Alder cycloaddition **(B)** and, palladium-catalysed Heck reaction **(C)**.

Preliminary insecticidal activity testing of the various pyrethrin analogues was undertaken, by Andrew Kotze (CSIRO Agriculture and Food), against a commercially relevant pest, *L. cuprina*. Whilst a majority of the prepared pyrethrin analogues showed no notable affect against *L. cuprina* larvae, they revealed new insight into the structure-activity relationships of the natural Pyrethrins **5-7**. Most notably, significant alteration to the terminal double bond of the pyrethrin side chain, like those afforded by the Diels-Alder and Heck reactions, results in complete loss of activity towards the *L. cuprina* larvae, likely due to the increased steric encumbrance imposed by the newly introduced aromatic motifs. In conjunction, the positioning and number of alkenes in the rethrolone side chain contribute significantly to the activity of the pyrethrins **5**. More specifically, shift of these bonds towards the enone moiety

likely imposes some structural constraints that prevent the necessary movement of the side chain for specific interactions with the sodium channel.

Whilst the various synthetic modifications explored throughout this thesis are likely to be beneficial towards the long-term storage of these pyrethrin analogues, they result in a significant loss of biological activity. As such, further exploration into the synthetic manipulation of the natural Pyrethrins **5-7** remains viable for the development of analogues with increased storage capabilities and retention of their insecticidal characteristics. In addition, further alteration of the pyrethrin scaffold could illuminate structure-activity relationships allowing for more tailored insecticidal materials.

6.2 Future directions

The success in the conversion of the pyrethrins **5** to the jasmolins **7** utilising diimide mediated reduction (Chapter 2) facilitates further investigation into optimisation of the reaction conditions so as to minimise the overreduction process to the tetrahydropyrethrins **52** and allow potential scale up for industrial viability. Specifically, the development of flow-based protocols would be of particular interest as they would allow for higher throughput conversion of the pyrethrins **5** to the jasmolins **7**, can minimise hazard associated with the reaction and facilitate faster reactivity.[1, 2] Previous work by Kappe, *et. al* has shown that *in situ* diimide generation can be achieved within flow systems, without the presence of typical catalysts like the copper(II) salt employed here, resulting in the near quantitative reduction of terminal alkenes.[3] Application of similar conditions to the natural pyrethrins **5** could allow for the desired high-throughput, on-flow conversion to their jasmolin counterparts **7**.

Given the precedent and observed reactivity of the *trans*-isomer of the pyrethrins **34** (Chapter 3), further investigation of their ability to participate in normal electron demand Diels-Alder reactions could allow for access to the described cycloadducts **61-63** and others. Obtaining significant quantities of the *trans*-isomer of the pyrethrins **34** was the biggest challenge due to the long UV exposure times, low isomerism efficiency or, formation of regioisomers under palladium catalysis. This may be overcome by employing higher intensity UV light to increase the rate of isomerism. Alternatively, using a photocatalyst to more efficiently transfer the photochemical energy to the substrate as well as allowing the use of visible light instead of harmful UV light would be highly desirable.[4, 5] In conjunction, preliminary attempts should

make use of maleimide instead of maleic anhydride **59** as it is likely to minimise degradation during purification due to its increased hydrolytic stability. Ultimately, the implementation of various dienophiles followed by oxidation should facilitate aromatisation of the cycloadduct giving rethrolone moieties reminiscent of the phenoxybenzyl moiety of pyrethroids (Scheme 6.2).

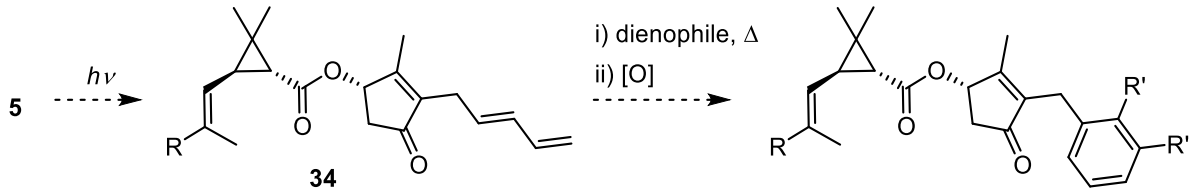

Scheme 6.2: Potential isomerism and subsequent normal electron demand Diels-Alder of pyrethrins **5** to generate pyrethroid-like analogues.

The synthetic success of the IEDDA reaction with a range of aromatic substituted tetrazines allowed for a range of adducts to be synthesised (Chapter 4) however, they possess relatively large substituents that proved detrimental to insecticidal activity in the preliminary assays against *L. cuprina* larvae. The modified Pinner synthesis is generally considerably less effective for the synthesis of alkyl substituted 1,2,4,5-tetrazines making it far more difficult to access similarly substituted pyrethrin cycloadducts. However, both the 3,6-dichloro- **80** and 3,6-bis(3',5'-dimethylpyrazol-1-yl)-1,2,4,5-tetrazines **78** are well-known to readily undergo nucleophilic substitution at the electron-deficient carbons of the tetrazine core.[6] Such reactivity would allow for replacement of the more sterically demanding aromatic substituents with smaller nucleophilic species including thiols, amines and alcohols. Preliminary experiments using 3,6-bis(3',5'-dimethylpyrazol-1yl)-1,2,4,5-tetrazine **78** and short alkyl chain amines were able to produce 3,6-bisamino-1,2,4,5-tetrazines **205** and **206** which exhibited some activity in the IEDDA reaction with pyrethrins **5** (Scheme 6.3). These preliminary findings suggest there is potential to optimise and extend this work to other nucleophilic species.

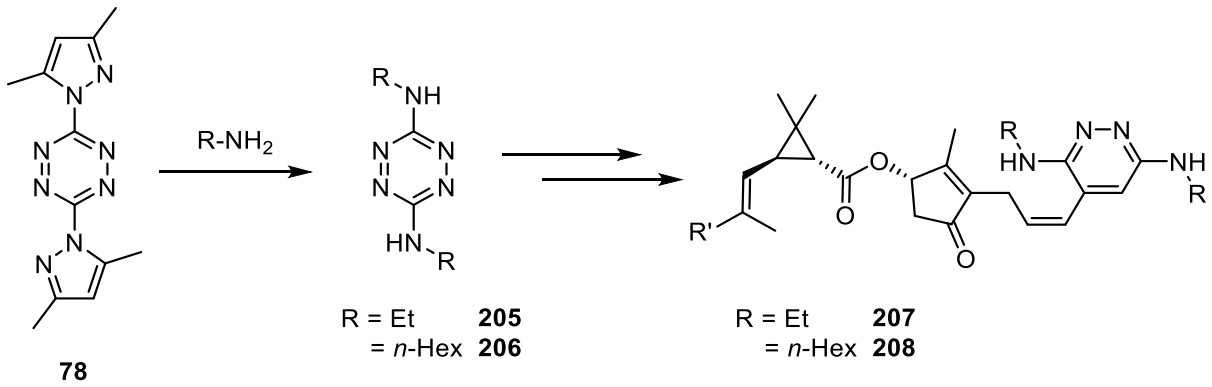

Scheme 6.3: Nucleophilic substitution of 3,6-bis(3′,5′-dimethylpyrazol-1yl)-1,2,4,5-tetrazine **78** with alkyl amines and subsequent implementation into the IEDDA process with pyrethrins **5**.

Alternatively, the 3,6-dichloro-1,2,4,5-tetrazine **81** and its mono-substituted 3-chloro-1,2,4,5-tetrazine analogues have potential for direct carbon substitution through the implementation of palladium-catalysed cross couplings (Scheme 6.4). There is precedent for this reactivity with Sonogashira, Stille and Suzuki couplings of these tetrazines present in literature.[7-9]

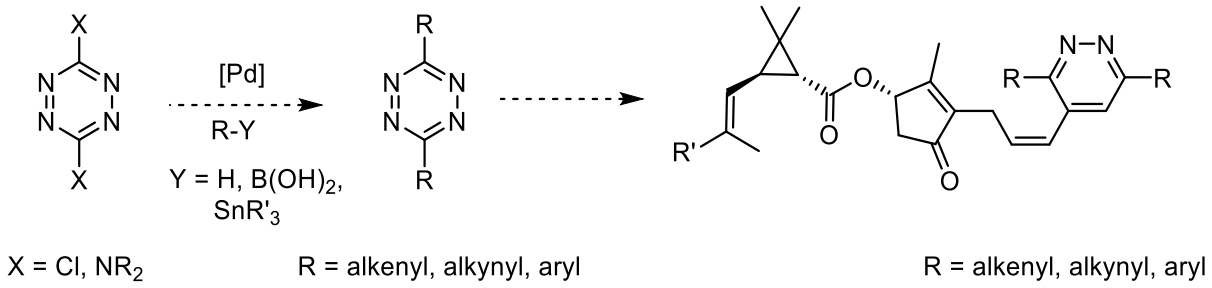

Scheme 6.4: Production of alternatively substituted 3,6-disubstituted-1,2,4,5-tetrazines by palladium-catalysed reactions and their subsequent use in IEDDA reactions with the natural pyrethrins **5**.

This variety in 1,2,4,5-tetrazine substitution may ultimately allow for the production of a range of pyrethrin analogues allowing for thorough structure-activity determination in insecticidal assays.

In addition, further exploration into the reactivity occurring between 3,6-dichloro-1,2,4,5-tetrazine **80** and pyrethrins **5** may allow for the production of the expected cycloadduct **92** (Scheme 6.5) and give mechanistic insight into this reactivity. Introduction of triethylamine as base has been shown to suppress the 1,3-shift of 4,5-dihydropyridazines to the 1,4-dihydropyridazines allowing for further Diels-Alder reactivity at high pressure.[10] As such, tautomerism of the 4,5-dihydropyridazine **94** to the 1,4-dihydropyridazine **95** may be prevented with pH control by the addition of a sterically hindered, non-nucleophilic base

ultimately impeding the proposed tautomerism cascade that is proposed to result in the saturated cycloadduct **93**. The success of this suppression would not only result in isolation of the expected cycloadduct **92** but would provide further evidence for the proposed tautomerism cascade as a means for the formation of the saturated pyridazine **93**.

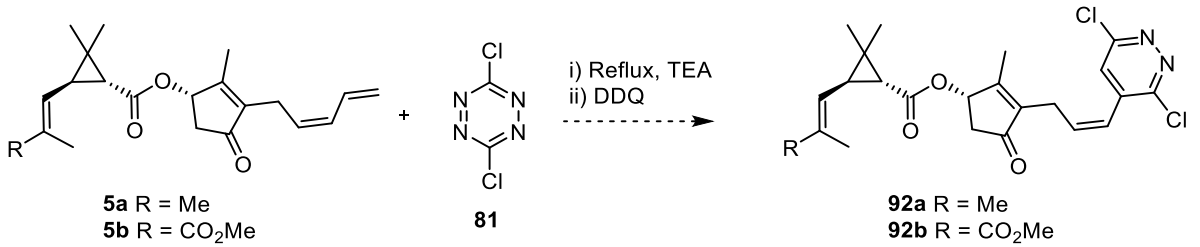

Scheme 6.5: Synthesis of the dichloropyridazine cycloadduct 92 of the pyrethrins 5 by suppression of the dihydropyridazine tautomerism cascade with a non-nucleophilic base.

Despite the lack of activity exhibited by the arylated pyrethrins produced by the palladium-catalysed Heck reaction (Chapter 4), the exploration of other transition-metal mediated functionalisation remains a potential route for pyrethrin modification. Activation of seemingly inert C-H bonds has become a major area of focus for the direct incorporation of functionality with emerging strategies allowing for site selectivity.[11] C-H activation/functionalisation could be a means of introducing key functionality at sites prone to high reactivity under the degradative processes that affect pyrethrins **5**. Specifically, the doubly allylic position of the rethrolone side chain in the pyrethrins has been implicated as a site for hydrogen atom abstraction, producing a delocalised radical that ultimately takes part in oxidative degradation.[12] Allylic C-H activation has been extensively explored, with the development of the highly effective White catalyst for amination, alkylation and oxidation of allylic substrates.[13-15] Notably, both branched and linear products can be generated from these allylic C-H functionalisation procedures with product distribution controlled with employed conditions.[15] In this instance, the branched product is preferable due to the observed lack of activity exhibited by the migration products produced by palladium-catalysed processes (Chapter 2 and 4). Application of the allylic C-H functionalisation procedures could allow for the formation of a range of pyrethrin analogues with oxygen, nitrogen and carbon linked substituents at the 7'-methylene (Scheme 6.6). In conjunction, fluorination of the doubly allylic 7'-methylene unit of this side chain (Scheme 6.6) would be of interest due to the

bioisosteric relationship fluorine has with hydrogen and the increased stability of the carbon-fluorine bond.[16-18]

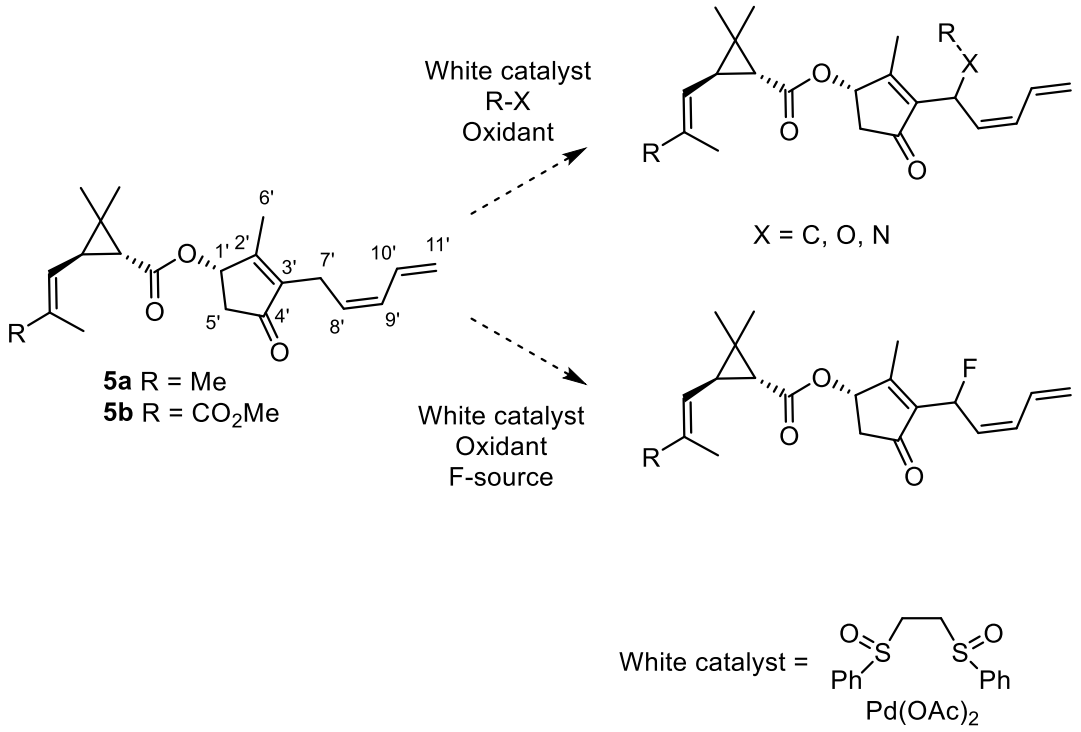

Scheme 6.6: Allylic C-H functionalisation of the natural pyrethrins **5**.

Fluorine's bioisosteric relationship with hydrogen means its incorporation in place of the 7' methylene protons should retain the biological activity of the pyrethrins **5** albeit with increased stability.[18, 19] In particular, the increased strength of the carbon-fluorine bond and its effect on the remaining C-H bond on the 7' methylene should limit the hydrogen atom abstraction that leads to the oxidation of the rethrolone side chain and as such slow the loss of pyrethrin content in the pyrethrum concentrate.[18] Notably, this allylic C-H functionalisation may have applicability to all six of the Pyrethrin esters **5-7** ultimately increasing the stability, without detriment to the insecticidal activity, of all of the constituents contributing to the pyrethrum concentrate's biological activity.

As previously highlighted (Chapter 2), the pyrethrins **5** are the most abundant of the esters in the pyrethrum concentrate but are also the most sensitive to the degradative processes leading to pyrethrin loss.[12, 20] Alteration of the saturation and bulk of this side chain has proven to be detrimental to insecticidal activity, as exhibited through the reduction (Chapter 2) and further functionalisation (Chapter 3 and 4) explored in this thesis, limiting the potential derivatisation of this moiety. Notably the cinerins **6** and jasmolins **7** show increased stability

in comparison to their pyrethrin counterparts **5** albeit with decreased insecticidal activity. Whilst production of the jasmolins **7** from the pyrethrins **5** was explored (Chapter 2), the insecticidal activity of the jasmolins **7** is significantly less than even the cinerins **6** and significant amounts of the over-reduced tetrahydropyrethrins **53** were observed. Olefin metathesis may serve as a means of altering the rethrolone side chain of the pyrethrins **5** by replacing the alkene rich carbon chain. As the cinerins **6** exhibit greater stability than the pyrethrins **5** and retain higher levels of insecticidal activity than the jasmolins **7** it would be an ideal candidate for production through cross metathesis with propylene (Scheme 6.7). Alternatively, the pyrethroid allethrin **38** could be furnished through similar means utilising ethylene (Scheme 6.7).

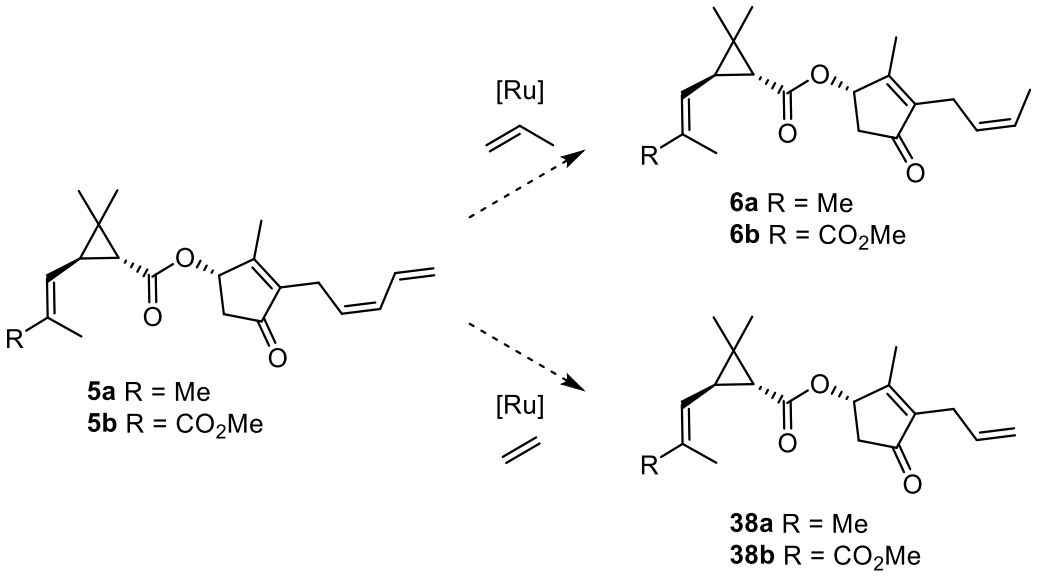

Scheme 6.7: Olefin metathesis of the pyrethrins to give the more stable cinerins **6** or the pyrethroid allethrin **38**.

Ethenolysis and propenolysis are well established cross metathesis routes particularly for the conversion of fatty acids, and their methyl ester derivatives, into more economically useful substrates.[21] The biggest challenge associated with these cross metathesis processes, in particular those utilising polyenes, is the regioselectivity. However, there remains potential to tailor selectivity based on the catalytic system employed with a range of different catalysts now readily available, each with different reactivities.[22] Provided reaction conditions can be customised to afford the desired metathesis regioselectivity, the cross metathesis process has potential to be applied to the pyrethrum concentrate effectively transforming all six esters **5-7** into two esters solely differing in the chrysanthemic acid moiety.

Whilst the focus of this thesis has been directed toward modification of the sensitive pentadienyl chain of the rethrolone moiety of pyrethrins **5**, alteration of the chrysanthemic acid moiety remains of interest. As previously noted (Chapter 1), the cyclopropyl unit can be the subject of degradation particularly through photochemical processes. Interestingly, the influence of altering this three-carbon unit, either through degradation or synthetically, has not been explored in terms of insecticidal activity. Notably, many of the modern pyrethroids have introduced acid moieties far different than the original chrysanthemic acid analogues of the Pyrethrins **5-7** and classic pyrethroids. The substitution of the cyclopropyl in the natural Pyrethrins **5-7** resembles that of donor-acceptor cyclopropanes, where the substituted C-C bond(s) are polarised by the electronic properties of the substituents i.e. one is an electron donor whilst the other is an acceptor. This polarisation, which can be enhanced by the introduction of a Lewis acid to complex with the acceptor substituent, weakens the C-C bond leading to heterolytic cleavage affording a zwitterionic, reactive intermediate. This type of reactivity allows several routes of alteration in the chrysanthemate moiety including ring opening by nucleophiles (Scheme 6.8A), [3+2] dipolar cycloadditions (Scheme 6.8B) and rearrangements (Scheme 6.8C) similar to those observed in chrysanthemic acid photolysis.[23] The rearrangement process is analogous to one of the photolytic degradation pathways of chrysanthemic acids allowing for direct determination of the effect this pathway may have on the insecticidal activity.

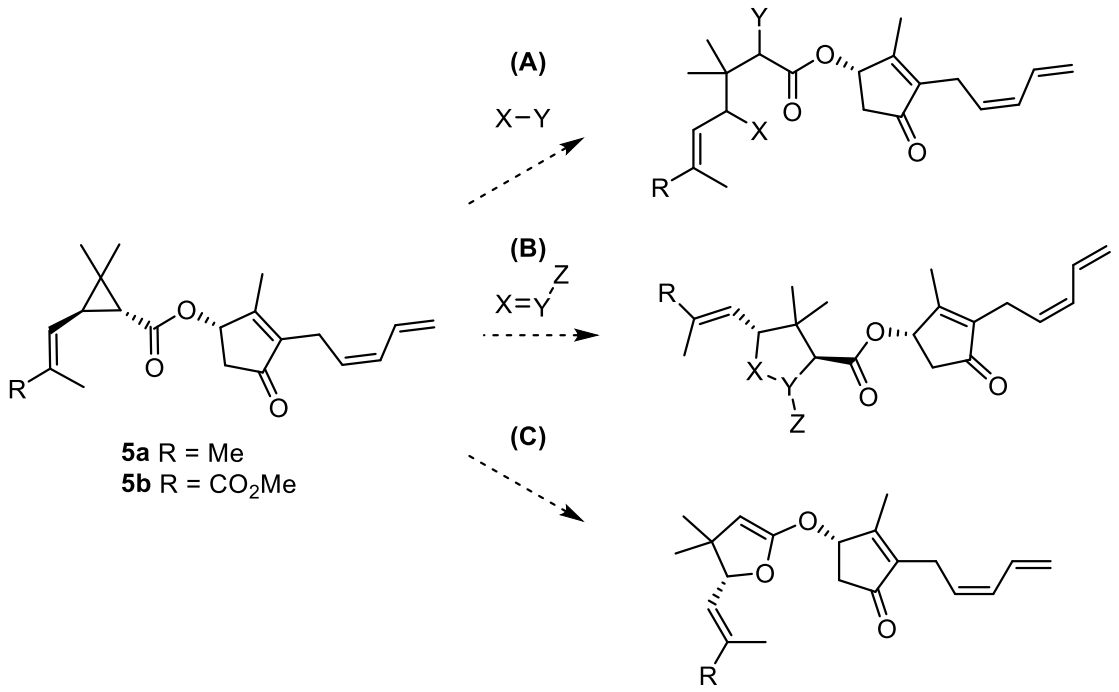

Scheme 6.8: Potential routes of reaction utilising pyrethrins **5** as donor-acceptor cyclopropanes.

The effect these modifications have on insecticidal activity will be of particular interest considering the large variation of this moiety now seen in modern synthetic pyrethroids.

6.3 References

1. Yoshida, J.-i.; Kim, H.; Nagaki, A., Green and Sustainable Chemical Synthesis Using Flow Microreactors. *ChemSusChem* **2011,** *4*, 331-340.
2. Hughes, D. L., Applications of Flow Chemistry in the Pharmaceutical Industry-Highlights of the Recent Patent Literature. *Org. Process. Res. Dev.* **2020,** *24*, 1850-1860.
3. Pieber, B.; Martinez, S. T.; Cantillo, D.; Kapper, C. O., In Situ Generation of Diimide from Hydrazine and Oxygen: Continuous-Flow Transfer Hydrogenation of Olefins. *Angew. Chem. Int. Ed.* **2013,** *52*, 10241-10244.
4. Zhu, S.; Wang, D., Photocatalysis: Basic Principles, Diverse Forms of Implementations and Emerging Scientific Opportunities. *Adv. Energy Mater.* **2017,** *7* (23), 1700841.
5. Zhan, K.; Li, Y., Visible-Light Photocatalytic *E* to *Z* Isomerization of Activated Olefins and Its Application for the Syntheses of Coumarins. *Catalysts* **2017,** *7*, 337-346.
6. Tolshchina, S. G.; Rusinov, G. L.; Charushin, V. N., 1,2,4,5-Tetrazines and Azolo[1,2,4,5]tetrazines: Synthesis and Reactions with Nucleophiles. *Chem. Heterocycl. Compd.* **2013,** *49*, 66-91.
7. Novak, Z.; Kotschy, A., First Cross-Coupling Reactions on Tetrazines *Org. Lett.* **2003,** *5*, 3495-3497.
8. Bender, A. M.; Chopko, T. C.; Bridges, T. M.; Lindsley, C. W., Preparation of Unsymmetrical 1,2,4,5-Tetrazines via a Mild Suzuki Cross-Coupling Reaction. *Org. Lett.* **2017,** *19*, 5693-5696.
9. Leconte, N.; Keromnes-Wuillaume, A.; Suzenet, F.; Guillamet, G., Efficient Palladium-Catalyzed Synthesis of Unsymmetrical (Het)aryl-tetrazines. *Synlett* **2007,** *2007*, 0204-0210.
10. Warrener, R. N.; Margetic, D.; Russell, R. A., The Preparation of Rigid Alicyclic Molecules Bearing Effector Groups from Alkene BLOCKs using *s*-Tetrazines and 1,3,4-Triazines as Stereoselective Coupling Agents. *Synlett* **1998,** *6*, 585-587.
11. Davies, H. M. L.; Morton, D., Recent Advances in C-H Functionalisation. *J. Org. Chem.* **2016,** *81*, 343-350.
12. Freemont, J. A.; Littler, S. W.; Hutt, O. E.; Mauger, S.; Meyer, A. G.; Winkler, D. A.; Kerr, M. G.; Ryan, J. H.; Cole, H. F.; Duggan, P. J., Molecular Markers for Pyrethrin Autoxidation in Stored Pyrethrum Crop: Analysis and Structure Determination. *J. Agric. Food Chem.* **2016,** *64*, 7134-7141.

13. Young, A. J.; White, M. C., Catalytic Intermolecular Allylic C-H Alkylation. *J. Am. Chem. Soc.* **2008,** *130*, 14090-14091.
14. Delcamp, J. H.; White, M. C., Sequential Hydrocarbon Functionalization: Allylic C-H Oxidation/Vinylic C-H Arylation. *J. Am. Chem. Soc.* **2006,** *128*, 15076-15077.
15. Chen, M. S.; Prabagaran, N.; Labenz, N. A.; White, M. C., Serial Ligand Catalysis: A Highly Selective Allylic C-H Oxidation. *J. Am. Chem. Soc.* **2005,** *127*, 6970-6971.
16. Meanwell, N. A., Fluorine and Fluorinated Motifs in the Design and Application of Bioisosteres for Drug Design. *J. Med. Chem.* **2018,** *61*, 5822-5880.
17. Patani, G. A.; LaVoie, E. J., Bioisosterism: A Rational Approach in Drug Design. *Chem. Rev.* **1996,** *96*, 3147-3176.
18. Lemal, D. M., Perspective on Fluorocarbon Chemistry. *J. Org. Chem.* **2004,** *69*, 1-11.
19. Braun, M.-G.; Doyle, A. G., Palladium-Catalyzed Allylic C-H Fluorination. *J. Am. Chem. Soc.* **2013,** *135*, 12990-12993.
20. Casida, J. E., Pyrethrum Flowers and Pyrethroid Insecticides. *Environ. Health Perspect.* **1980,** *34*, 189-202.
21. Byun, S.; Park, S.; Choi, Y.; Ryu, J. Y.; Lee, J.; Choi, J.-H.; Hong, S., Highly Efficient Ethenolysis and Propenolysis of Methyl Oleate Catalyzed by Abnormal N-Heterocyclic Carbene Ruthenium Complexes in Combination with a Phosphine-Copper Cocatalyst. *ACS Catal.* **2020,** *10*, 10592-10601.
22. Chatterjee, A. K.; Choi, T.-L.; Sanders, D. P.; Grubbs, R. H., A General Model for Selectivity in Olefin Cross Metathesis. *J. Am. Chem. Soc.* **2003,** *125*, 11360-11370.
23. Schneider, T. F.; Kaschel, J.; Werz, D. B., A New Golden Age for Donor-Acceptor Cyclopropanes. *Angew. Chem. Int. Ed.* **2014,** *53*, 5504-5523.

Chapter 7 Experimental

7.1 General methods

Pyrethrum concentrate (80% Pyrethrins stabilised with 5 wt% BHT) was supplied by Botanical Resources Australia, reagents were purchased from Sigma-Aldrich and solvents were purchased from Chem-Supply. THF was dried by distillation over sodium benzophenone ketyl, DCM was dried by distillation over calcium hydride and acetonitrile was dried by distillation over 4 Å molecular sieves. Thin layer chromatography (TLC) was performed using Chem-Supply silica gel 60 F_{254} TLC plates and visualised under UV light (254 nm) or permanganate stain. Column chromatography was undertaken using Sanpont silica gel of 230-400 mesh (0.040-0.063 mm) at atmospheric pressure.

The pyrethrum concentrate was separated by dry column vacuum chromatography (DCVC) using silica gel of 230-400 mesh (0.040-0.063 mm) and a gradient elution from 1% to 25% ethyl acetate in hexane to give the Pyrethrins I and Pyrethrins II subsets. Pyrethrin I (91% purity) was obtained by subjecting the Pyrethrins I subset to column chromatography on a 3-tiered glass column eluting in 8% ethyl acetate in hexane and pyrethrin II (91% purity) was obtained by repeated dry column vacuum chromatography (DCVC) of the Pyrethrins II subset. Individual jasmolins and cinerins were provided by CSIRO in >98% purity. For synthetic protocols, BHT was removed from pyrethrum concentrate by application to a short silica gel plug with hexane, then eluting the Pyrethrins off the plug with ethyl acetate.

All ^{1}H and ^{13}C NMR spectra were recorded on a Bruker 600 Avance III NMR spectrometer at 600 MHz and 150 MHz respectively. All spectra were recorded at 298 K using $CDCl_3$ or DMSO-d_6 as the solvent and internal lock. All spectra were referenced to the solvent peak ($CDCl_3$: ^{1}H = 7.26 ppm, ^{13}C = 77.0 ppm; DMSO-d_6: ^{1}H = 2.50 ppm, ^{13}C = 39.52 ppm) and were recorded as follows: 1. Chemical shift (ppm) (proton spectra are reported to two decimal places and carbon spectra are reported to one decimal place except when an additional digit is necessary to discern overlapping peaks), 2. Integration, 3. Multiplicity (s = singlet, d = doublet, t = triplet, q = quartet, quin = quintet, dd = doublet of doublets, dt = doublet of triplets, m = multiplet, brs = broad singlet, brd = broad doublet, * = multiplicity assigned based on homonuclear decoupling experiments (Supporting Information) and comparison to prior literature,[1] signals overlap due to similar magnitude coupling constants), 4. Coupling constant (Hz).

Homonuclear (^{1}H-^{1}H) correlation spectroscopy (COSY) and heteronuclear (^{1}H-^{13}C) correlation spectroscopy (HSQC, HMBC) were carried out for all new compounds (Supporting Information). Stereochemical configurations were assigned through nuclear Overhauser effect spectroscopy (NOESY). Variable temperature ^{1}H NMR spectra were obtained on a Bruker 600 Avance III NMR spectrometer at 600 MHz in DMSO-d_6 up to 358 K. Selective 1D correlation spectra (COSY, TOCSY, NOESY) were recorded on a Bruker 400 Avance III spectrometer at 400 MHz at 299 K using $CDCl_3$ as solvent and internal lock. ^{11}B NMR spectra were obtained on a Bruker 400 Avance III spectrometer at 128 MHz at 299 K using $CDCl_3$ as solvent.

High Performance Liquid Chromatography (HPLC) analysis was performed on an Agilent Technologies 1200 series HPLC system with a photodiode array detector at 223, 229 and 235 nm with a Phenomenex Phenosphere-Next C18 column (150 mm x 4.6 mm I.D., 5 µm). Solvent A was 1% acetic acid in water and solvent B was acetonitrile. The column was kept at 40 °C with a constant flow rate of 0.8 mL/min and a 10 µL injection. The solvent program was amended from Wang, *et al.*[2] and is as follows: 50% solvent A for 10 min followed by a linear gradient to 40% solvent A over 5 min. Solvent A was held at 40% for a further 10 min before a linear gradient to 35% solvent A over 5 min. 35% solvent A was held for 10 min after which a linear gradient to 20% solvent A was undertaken over 5 min. 20% solvent A was then held for an additional 5 min.

LC-MS analysis was conducted on a Shimadzu LCMS-2020 with a photodiode array detector at 254 nm and a single quadrupole mass spectrometer. Solvent A was 0.1% formic acid in water and solvent B was 0.1% formic acid in acetonitrile. The column was a Phenomenex Kinetex C18 column (100 mm x 2.1 mm I.D., 2.1 µm) maintained at 30 °C with a constant flow rate of 0.4 mL/min and a 1 µL injection. The solvent program was as follows: 30% solvent A for 0.5 min before a linear gradient to 5% solvent A over 5.5 min. Solvent A was held at 5% for 2 min before a linear gradient to 30% solvent A over 0.5 min. Solvent A was held at 30% for an additional 3.5 min. The mass spectrometer was operated with APCI with a mass range of 50-1000 *m/z*, nebulising gas flow of 1.5 mL/min., drying gas of 15 mL/min. and desolvation temperature was 250 °C. Alternate LC-MS analysis was conducted on a Waters Acquity UPLC coupled to a Waters Synapt HDMS. Solvent A was 0.1% formic acid in water and solvent B was methanol. The column was a Phenomenex Kinetex XB-C18 column (50 mm x 2.1 mm I.D., 2.6

μm) maintained at 30 °C with a constant flow rate of 0.2 mL/min and a 4 μL injection. The solvent program was as follows: 35% solvent A was held for 2 min before a linear gradient to 10% solvent A over 18 min. Solvent A was held at 10% for 1 min before returning to 35% over 1 min. Solvent A remained at 35% for a further 8 min. The Waters Synapt HDMS was operated using ESI with a mass range from 100-900 *m/z*, a capillary voltage of 2.5 kV and cone voltage of 40 V. The source temperature was 80 °C and desolvation temperature was 350 °C.

UltraPerformance Convergence Chromatography (UPCC) was utilised for chiral analysis on a Waters Acquity UPC^2 system equipped with photodiode array detection at 230 nm. The column was maintained at 40 °C with a constant flow rate of 1.2 mL/min, a 1 μL injection and convergence pressure of 2000 psi. The solvent program was as follows: 97% solvent A for 0.5 min followed by a linear gradient to 40% solvent A over 2.5 min. Solvent A was held at 40% for 3 min before a linear gradient to 97% solvent A over 0.1 min. Solvent A was CO_2 and solvent B was either ethanol: isopropanol: acetonitrile (1:1:1) with 20 mM ammonium acetate, methanol: isopropanol (1:1) with 0.2% v/v formic acid, ethanol: acetonitrile (1:1) with 0.2% v/v formic acid, or ethanol: isopropanol (1:1) with 0.2% v/v formic acid. The column was either a Waters Trefoil AMY1 (50 mm x 2.1 mm I.D., 2.5 μm), Waters Trefoil CEL1 (50 mm x 2.1 mm I.D., 2.5 μm), or Waters Trefoil CEL2 (50 mm x 2.1 mm I.D., 2.5 μm).

Fourier Transform Infrared Spectroscopy (FTIR) was recorded using a Perkin Elmer Spectrum100 spectrometer with an ATR diamond crystal attachment. All spectra are reported in wavenumbers ($\bar{\nu} = \text{cm}^{-1}$).

High resolution mass spectrometry (HRMS) was performed on a Perkin Elmer AxION Direct Sample Analysis (DSA) with an AxION®2 Time of Flight (ToF) mass spectrometer using Atmospheric Pressure Chemical Ionisation (APCI) in positive ion mode.

Optical rotations were recorded on a PolAAR 21 polarimeter referenced to the sodium D-line (589 nm) at 20 °C. Specific rotations are reported at the concentrations stated.

Melting points were obtained on a Sanyo Gallenkamp melting point apparatus.

Molecular modelling was undertaken using Spartan '16[3] on a Dell Optiplex 990 desktop computer with an Intel® Core™ i7-2600 CPU and 16 GB RAM. Geometry optimisations were carried out using a DFT method with a B3LYP hybrid functional and 6-31G* basis set. The

molecular orbitals were visualised with the Spartan '16 program[3] and HOMO-LUMO energy gaps were determined by the difference in the calculated SCF values.

Australian sheep blowfly (*L. cuprina)* larvae were prepared and used in insecticidal activity assays as detailed in published procedures.[4, 5] Specifically, a plug of cotton wool (~0.2 g) on top of 3 layers of filter paper (within a 70 mL plastic pot) was loaded with 4 mL of a solution of the compound in ethanol, and the solvent allowed to evaporate. Controls were prepared in the same manner, by loading the cotton wool plug with ethanol or a solution of BHT. On day 0 of the assay, a sheep-serum based medium was added to the cotton wool and 50 freshly hatched *L. cuprina* larvae were added. The plastic pots containing the larvae were incubated at 28 °C over a period of 4 days. The larvae were fed with 1 mL of nutrient medium on day 1, and 2 mL on days 2 and 3. Late on day 4, the larvae were transferred to larger pots with a layer of sand (a medium for pupation) and allowed to incubate further. On day 9, the resulting pupae were collected by sieving the sand and the bioactivity calculated by pupation rate: the number of collected pupae in assays with experimental compounds was expressed as a percentage of the average number of pupae in the control assays. All tested materials had a purity >90% and were prepared as solutions in hexane or acetone, stabilised with 5 wt% BHT and subsequently diluted for testing in ethanol. BHT controls exhibited no inhibition of pupation on *L. cuprina* larvae at concentrations up to 5 µmol/assay, ten times the amount present in the individual samples. Each assay was performed in duplicate.

The pupation rate dose-response data were analysed with GraphPad Prism® software. Non-linear regression was performed using a four-parameter logistic regression model with the 'variable slope' option to determine IC_{50} values for reduction in pupation, together with 95% confidence intervals.

7.2 Synthetic protocols

7.2.1 Reduction chemistry

Hydroboration-protonolysis of pyrethrins with 9-BBN

Pyrethrin I **5a** (117 mg, 0.357 mmol) was stirred in a solution of 9-BBN (0.65 mL, 0.5 M in THF, 0.3 mmol) under an atmosphere of nitrogen for 5 h. Acetic acid (200 µL, 3.49 mmol) was added and the resulting mixture refluxed for an hour. Residual acid was quenched with 10% sodium bicarbonate solution and the resulting mixture extracted with ethyl acetate. The

solution was dried (Na_2SO_4) and solvent removed *in vacuo* giving a pale yellow oil. The residue was purified by column chromatography (15% ethyl acetate in hexane) yielding the allylic alcohol **(4'*R*)-51a** (18 mg, 15%) and allylic ester **52a** (11 mg , 8%, dr 4:1 (*S:R*)).

Pyrethrin II **5b** (79 mg, 0.21 mmol) was subjected to the above procedure using 9-BBN (0.6 mL, 0.5 M in THF, 0.3 mmol) and acetic acid (200 µL, 3.49 mmol). Column chromatography (15% ethyl acetate in hexane) afforded the allylic alcohol **(4'*R*)-51b** (15 mg, 19%) and allylic ester **52b** (8 mg, 9%, dr 3.3:1(*S:R*)).

Reduction of pyrethrins with sodium borohydride

Sodium borohydride (90 mg, 2.4 mmol) was added to a solution of pyrethrin I **5a** (310 mg, 0.95 mmol) in methanolic THF (10% v/v, 5 mL) at 0 °C. The resulting mixture was stirred for 3 h with continued cooling. Water was added and the aqueous mixture was extracted with ethyl acetate. The ethyl acetate was dried (Na_2SO_4) and the solvent removed *in vacuo* giving a diastereomeric mixture of the allylic alcohol **51a** as a colourless oil (305 mg, 98%, dr 5.5:1 *(R:S)*). The individual diastereomers were isolated by silica gel column chromatography (15% ethyl acetate in hexane) giving **(4'*R*)-51a** (202 mg) and **(4'*S*)-51a** (45 mg).

Pyrethrin II **5b** (330 mg, 0.89 mmol) was subjected to the same procedure using sodium borohydride (86 mg, 2.3 mmol). The diastereomeric mixture of the allylic alcohol **51b** (330 mg, 99%, dr 4.5:1 *(R:S)*) was resolved by silica gel column chromatography (30% ethyl acetate in hexane) giving **(4'*R*)-51b** (163 mg) and **(4'*S*)-51b** (40 mg).

Stereoselective reduction of pyrethrins with L-selectride.

L-Selectride (1.0 M in THF, 0.5 mL, 0.5 mmol) was added to a solution of pyrethrin I **5a** (160 mg, 0.49 mmol) in dry THF 5 mL at 0 °C under an atmosphere of nitrogen. The mixture was allowed to stir with continued cooling for an additional hour. The reaction was quenched with water and extracted with ethyl acetate. The ethyl acetate was dried (Na_2SO_4) and the solvent

removed *in vacuo* giving a yellow oil. The oil was subjected to column chromatography (15% ethyl acetate in hexane) giving allylic alcohol **(4'*R*)-51a** (62 mg, 38%).

Pyrethrin II **5b** (150 mg, 0.3 mmol) was subjected to the same procedure detailed above. The resulting oil was subjected to column chromatography (30% ethyl acetate in hexane) giving allylic alcohol **(4'*R*)-51b** (30 mg, 20%).

(1S, 4R)-4-hydroxy-2-methyl-3-((2Z)-penta-2,4-dien-1-yl)cyclopent-2-en-1-yl (1R,3R)-2,2-dimethyl-3-(2-methylprop-1-enyl)cyclopropane-1-carboxylate **(4'*R*)-51a**

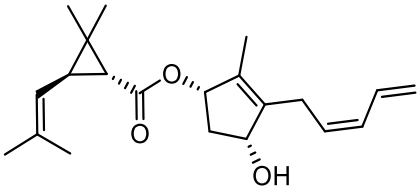

^{1}H NMR (600 MHz, $CDCl_3$) δ 6.75 (1H, ddd*, *J* = 10.1, 10.7, 16.9 Hz), 6.07 (1H, dd*, *J* = 10.7, 10.9 Hz), 5.42 (1H, dt, *J* = 10.9, 8.5 Hz), 5.35 (1H, m), 5.23 (1H, d, *J* = 16.7 Hz), 5.16 (1H, d, *J* = 10.1 Hz), 4.90 (1H, d, *J* = 7.7 Hz), 4.50 (1H, brs), 3.16 (1H, dd, *J* = 8.5, 14.9 Hz), 3.05 (1H, dd, *J* = 7.3, 14.9 Hz), 2.78 (1H, m), 2.04 (1H, m), 1.71 (3H, s), 1.70 (3H, s), 1.67 (1H, d, *J* = 8.1 Hz), 1.57 (3H, s), 1.54 (1H, m), 1.39 (1H, d, *J* = 5.3 Hz), 1.25 (3H, s), 1.12 (3H, s); ^{13}C NMR (150 MHz, $CDCl_3$) δ 172.6, 141.7, 135.7, 134.8, 131.8, 130.6, 128.3, 121.3, 118.3, 79.3, 75.8, 40.7, 35.0, 32.6, 28.7, 25.7, 24.8, 22.3, 20.6, 18.6, 11.8. $[\alpha]_D^{20}$ = 73.7 (c = 0.6, $CHCl_3$).

(1S, 4S)-4-hydroxy-2-methyl-3-((2Z)-penta-2,4-dien-1-yl)cyclopent-2-en-1-yl (1R,3R)-2,2-dimethyl-3-(2-methylprop-1-enyl)cyclopropane-1-carboxylate **(4'*S*)-51a**

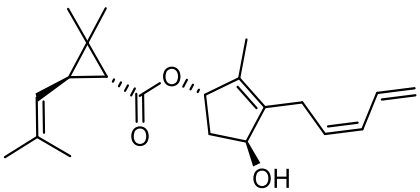

^{1}H NMR (600 MHz, $CDCl_3$) δ 6.75 (1H, ddd*, *J* = 10.1, 10.7, 16.7 Hz), 6.09 (1H, dd*, *J* = 10.7, 10.9 Hz), 5.69 (1H, d, *J* = 6.1 Hz), 5.45 (1H, dt, *J* = 10.9, 8.3Hz), 5.24 (1H, d, *J* = 16.7 Hz), 5.16 (1H, d, *J* = 10.1 Hz), 4.88 (1H, d, *J* = 7.7 Hz), 4.81 (1H, brs), 3.12 (1H, dd, *J* = 8.3, 14.9 Hz), 3.03 (1H, dd, *J* = 7.3, 14.9 Hz), 2.15 (1H, ddd, *J* = 3.2, 7.0, 14.9 Hz), 2.06 (1H, ddd, *J* = 3.2, 7.0, 14.9

Hz), 2.03 (1H, m), 1.70 (3H, s), 1.69 (6H, s), 1.49 (1H, d, *J* = 6.4 Hz), 1.36 (1H, d, *J* = 5.3 Hz), 1.24 (3H, s), 1.11 (3H, s); ^{13}C NMR (150 MHz, $CDCl_3$) δ 172.8, 142.1, 135.7, 135.3, 131.8, 130.7, 128.2, 121.2, 118.3, 81.1, 76.9, 41.2, 35.0, 32.6, 28.7, 25.7, 24.9, 22.3, 20.5, 18.6, 11.8. $[\alpha]_D^{20}$ = 286.7 (c = 0.5, $CHCl_3$).

FTIR ($\bar{\nu}$): 3424, 2921, 1719, 1421, 1378, 1282, 1195, 1158, 1081, 1023, 904, 852. HRMS calculated for $C_{21}H_{29}O_2$ $[M-OH]^+$: 313.2162, observed: 313.2162.

(1S,4R)-4-hydroxy-2-methyl-3-((2Z)-penta-2,4-dien-1-yl)cyclopent-2-en-1-yl (1R,3R)-3-((E)-3-methoxy-2-methyl-3-oxoprop-1-enyl)-2,2-dimethylcyclopropane-1-carboxylate **(4'*R*)-51b**

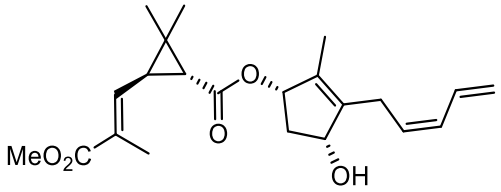

^{1}H NMR (600 MHz, $CDCl_3$) δ 6.75 (1H, ddd*, *J* = 10.1, 10.7, 16.8 Hz), 6.46 (1H, d, *J* = 9.6 Hz), 6.08 (1H, dd*, *J* = 10.7, 10.9 Hz), 5.42 (1H, dt, *J* = 10.9, 8.2Hz), 5.36 (1H, m), 5.54 (1H, d, *J* = 16.8 Hz), 5.17 (1H, d, *J* = 10.1 Hz), 4.51 (1H, brs), 3.73 (3H, s), 3.16 (1H, dd, *J* = 8.2, 14.9 Hz), 3.05 (1H, dd, *J* = 7.2, 14.9 Hz), 2.80 (1H, m), 2.20 (1H, dd, *J* = 5.2, 9.6 Hz), 1.93 (3H, s), 1.72 (1H, d, *J* = 5.2 Hz), 1.70 (3H, s), 1.69 (1H, d, *J* = 7.4 Hz), 1.57 (3H, s), 1.54 (1H, m), 1.30 (3H, s), 1.22 (3H, s); ^{13}C NMR (150 MHz, $CDCl_3$) δ 171.5, 168.4, 142.0, 139.6, 134.5, 131.8, 130.6, 129.6, 128.2, 118.4, 79.9, 75.8, 51.9, 40.7, 36.4, 32.7, 24.8, 22.8, 22.6, 20.6, 13.0, 11.8. $[\alpha]_D^{20}$ = 117.3 (c = 0.5, $CHCl_3$).

(1S,4S)-4-hydroxy-2-methyl-3-((2Z)-penta-2,4-dien-1-yl)cyclopent-2-en-1-yl (1R,3R)-3-((E)-3-methoxy-2-methyl-3-oxoprop-1-enyl)-2,2-dimethylcyclopropane-1-carboxylate **(4'*S*)-51b**

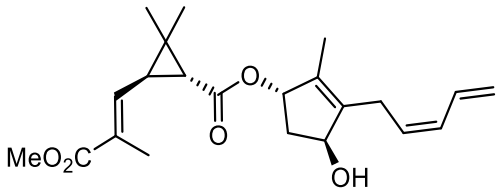

^{1}H NMR (600 MHz, $CDCl_3$) δ 6.75 (1H, ddd*, *J* = 10.1, 10.7, 16.8 Hz), 6.45 (1H, d, *J* = 9.7 Hz), 6.10 (1H, dd*, *J* = 10.7, 10.9 Hz), 5.70 (1H, d, *J* = 6.9 Hz), 5.45 (1H, dt, *J* =10.9, 8.2Hz), 5.26 (1H, d, *J* = 16.7 Hz), 5.17 (1H, d, *J* = 10.1 Hz), 4.82 (1H, brs), 3.72 (3H, s), 3.12 (1H, dd, *J* = 8.2, 14.9

Hz), 3.04 (1H, dd, *J* = 7.1, 14.9 Hz), 2.17 (2H, m), 2.06 (1H, ddd, *J* = 3.1, 6.9, 14.8 Hz), 1.93 (3H, s), 1.70 (4H, m), 1.54 (1H, d, *J* = 6.7 Hz), 1.29 (3H, s), 1.21 (3H, s); ^{13}C NMR (150 MHz, $CDCl_3$) δ 171.6, 168.4, 142.4, 139.7, 135.1, 131.7, 130.8, 129.6, 128.1, 118.5, 81.6, 76.9, 51.9, 41.2, 36.4, 32.7, 30.2, 24.9, 22.6, 20.6, 13.0, 11.9. $[\alpha]_D^{20} = -177.5$ (c = 0.4, $CHCl_3$).
FTIR ($\bar{\nu}$): 3489, 2924, 1713, 1642, 1434, 1261, 1222, 1176, 111, 1010, 940, 905, 831, 762. HRMS calculated for $C_{22}H_{29}O_4$ $[M-OH]^+$: 357.2060, observed: 357.2077.

General Procedure for the acylation of allylic alcohols

Acetic anhydride (1 mL, 11 mmol) and triethylamine (1 mL, 7 mmol) were added to a solution of the allylic alcohol **51** in dry DCM (5 mL) under a nitrogen atmosphere. The mixture was heated under reflux for 4.5 h. The resulting solution was allowed to cool to room temperature and washed with water. The organic layer was collected and dried (Na_2SO_4). The solvent was removed *in vacuo* yielding the allyl ester **52**.

(1S,4R)-4-acetoxy-2-methyl-3-((2Z)-penta-2,4-dien-1-yl)cyclopent-2-en-1-yl (1R,3R)-2,2-dimethyl-3-(2-methylprop-1-enyl)cyclopropane-1-carboxylate **(4'*R*)-52a**

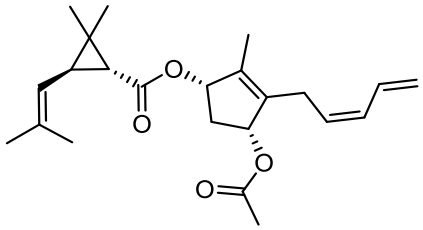

Yield: 110 mg, 85%. ^{1}H NMR (600 MHz, $CDCl_3$) δ 6.64 (1H, ddd*, *J* = 10.1, 10.7, 16.8 Hz), 6.05 (1H, dd*, *J* = 10.7, 10.9 Hz), 5.48 (1H, m), 5.44 (1H, m), 5.35 (1H, dt, *J* =10.9, 7.9 Hz), 5.23 (1H, d, *J* = 16.8 Hz), 5.14 (1H, d, *J* = 10.1 Hz), 4.90 (1H, d, *J* = 7.8 Hz), 3.04 (2H, m), 2.92 (1H, m), 2.05 (1H, m), 2.04 (3H, s), 1.74 (3H, s), 1.71 (3H, s), 1.70 (3H, s), 1.54 (1H, m), 1.41 (1H, d, *J* = 5.3 Hz), 1.25 (3H, s), 1.13 (3H, s); ^{13}C NMR (150 MHz, $CDCl_3$) δ 172.5, 170.9, 137.8, 137.6, 135.7, 131.6, 130.6, 127.8, 121.2, 118.3, 79.1, 77.7, 38.2, 34.9, 32.7, 28.8, 25.7, 25.0, 22.3, 21.3, 20.6, 18.6, 11.9. $[\alpha]_D^{20} = -12.5$ (c = 0.4, $CHCl_3$).

(1S,4S)-4-acetoxy-2-methyl-3-((2Z)-penta-2,4-dien-1-yl)cyclopent-2-en-1-yl (1R,3R)-2,2-dimethyl-3-(2-methylprop-1-enyl)cyclopropane-1-carboxylate **(4'*S*)-52a**

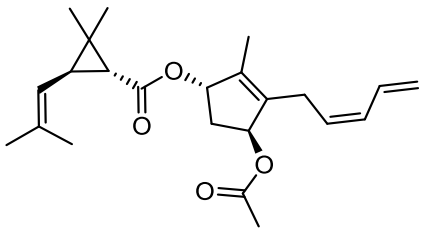

Yield: 68 mg, 56%. ^{1}H NMR (600 MHz, $CDCl_3$) δ 6.65 (1H, ddd*, *J* = 10.1, 10.7, 16.8 Hz), 6.06 (1H, dd*, *J* = 10.7, 10.9 Hz), 5.72 (1H, d, *J* = 6.9 Hz), 5.68 (1H, brs), 5.37 (1H, dt, *J* = 10.9, 8.2 Hz), 5.22 (1H, d, *J* = 16.8 Hz), 5.14 (1H, d, *J* =10.1 Hz), 4.88 (1H, d, *J* = 7.8 Hz), 3.01 (2H, m), 2.20 (1H, ddd, *J* = 3.0, 7.0 15.2 Hz), 2.12 (1H, ddd, *J* = 3.4, 7.0, 15.2 Hz), 2.04 (1H, m), 2.01 (3H, s), 1.73 (3H, s), 1.71 (3H, s), 1.70 (3H, s), 1.38 (1H, d, *J* = 5.3 Hz), 1.24 (3H, s), 1.12 (3H, s); ^{13}C NMR (150 MHz, $CDCl_3$) δ 172.7, 171.1, 138.4, 138.1, 135.7, 131.7, 130.6, 127.6, 121.2, 118.2, 80.6, 79.4, 38.6, 35.0, 32.7, 28.8, 25.7, 25.1, 22.3, 21.3, 20.5, 18.6, 11.9. $[\alpha]_D^{20}$ = 183.3 (c = 0.6, $CHCl_3$).

FTIR ($\bar{\nu}$): 2924, 1736, 1720, 1433, 1377, 1236, 1194, 1158, 1115, 1022, 997, 906. HRMS calculated for $C_{23}H_{33}O_4$ $[M+H]^+$: 373.2373, observed: 373.2382.

(1S,4R)-4-acetoxy-2-methyl-3-((2Z)-penta-2,4-dien-1-yl)cyclopent-2-en-1-yl (1R,3R)-3-((E)-3-methoxy-2-methyl-3-oxoprop-1-enyl)-2,2-dimethylcyclopropane-1-carboxylate **(4'*R*)-52b**

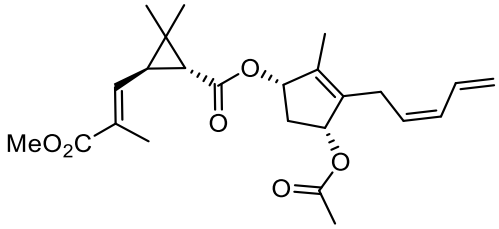

Yield: 158 mg, 91%. ^{1}H NMR (600 MHz, $CDCl_3$) δ 6.64 (1H, ddd*, *J* = 10.1, 10.7, 16.8 Hz), 6.45 (1H, d, *J* = 9.7 Hz), 6.05 (1H, dd*, *J* = 10.7, 10.9 Hz), 5.49 (1H, m), 5.44 (1H, m), 5.33 (1H, dt, *J* = 10.9, 7.9 Hz), 5.23 (1H, d, *J* = 16.8 Hz), 5.14 (1H, d, *J* = 10.1 Hz), 3.72 (3H, s), 3.04 (2H, m), 2.93 (1H, m), 2.19 (1H, dd, *J* = 5.3, 9.7 Hz), 2.04 (3H, s), 1.93 (3H, s), 1.73 (4H, m), 1.53 (1H, m), 1.29 (3H, s), 1.21 (3H, s); ^{13}C NMR (150 MHz, $CDCl_3$) δ 171.3, 170.8, 168.3, 139.6, 138.1, 137.2, 131.6, 130.6, 129.6, 127.6, 118.3, 79.6, 77.6, 51.9, 38.2, 36.2, 32.7, 30.3, 25.0, 22.5, 21.3, 20.6, 13.0, 11.9. $[\alpha]_D^{20}$ = 25.0 (c = 0.4, $CHCl_3$).

(1S,4S)-4-acetoxy-2-methyl-3-((2Z)-penta-2,4-dien-1-yl)cyclopent-2-en-1-yl (1R,3R)-3-((E)-3-methoxy-2-methyl-3-oxoprop-1-enyl)-2,2-dimethylcyclopropane-1-carboxylate **(4'*S*)-52b**

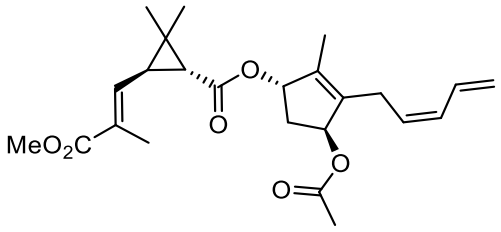

Yield: 44 mg, 46%. ^{1}H NMR (600 MHz, $CDCl_3$) δ 6.65 (1H, ddd*, *J* = 10.1, 10.7, 16.8 Hz), 6.45 (1H, d, *J* = 9.7 Hz), 6.07 (1H, dd*, *J* = 10.7, 10.9 Hz), 5.72 (1H, m), 5.67 (1H, m), 5.37 (1H, dt, *J* = 10.9, 7.9Hz), 5.23 (1H, d, *J* = 16.8 Hz), 5.14 (1H, d, *J* = 10.1 Hz), 3.72 (3H, s), 3.02 (2H, m), 2.19 (2H, m), 2.14 (1H, ddd, *J* = 3.4, 7.1, 15.4 Hz), 2.02 (3H, s), 1.93 (3H, s), 1.72 (3H, s), 1.70 (1H, d, *J* = 5.2 Hz), 1.29 (3H, s), 1.22 (3H, s); ^{13}C NMR (150 MHz, $CDCl_3$) δ 171.6, 171.1, 168.3, 139.6, 138.5, 138.0, 131.6, 130.7, 129.6, 127.5, 118.3, 81.7, 79.3, 51.9, 38.6, 36.3, 32.7, 30.4, 25.0, 22.5, 21.3, 20.5, 13.0, 11.9. $[\alpha]_D^{20} = -70.0$ (c = 0.4, $CHCl_3$).
FTIR ($\bar{\nu}$): 3668, 2970, 2924, 1715, 1643, 1434, 1381, 1259, 1222, 1174, 1150, 1111, 1050, 904, 804. HRMS calculated for $C_{22}H_{29}O_4$ $[M-OAc]^+$: 357.2060, observed: 357.2062.

Catalytic hydrogenation of the pyrethrins.

Pyrethrin I **5a** (100 mg, 0.305 mmol) in THF (2 mL) was stirred in the presence of palladium on carbon (10 wt% loading, 10 mg) under an atmosphere of hydrogen at room temperature. After 4 h, the mixture was filtered over Celite and the solvent removed *in vacuo* yielding **53a** as a colourless oil (83 mg, 83%).

(1S)-2-methyl-4-oxo-3-pentylcyclopent-2-en-1-yl (1R,3R)-2,2-dimethyl-3-(2-methylprop-1-enyl)cyclopropane-1-carboxylate **53a**

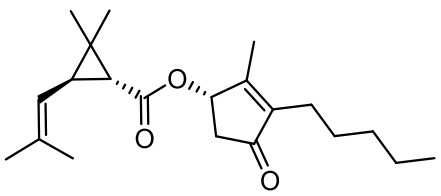

^{1}H NMR (600 MHz, $CDCl_3$) δ 5.65 (1H, brd, *J* = 6.2 Hz), 4.89 (1H, d, *J* = 7.7 Hz), 2.83 (1H, dd, *J* = 6.2, 18.7 Hz), 2.21 (1H, dd, *J* = 1.7, 18.7 Hz), 2.18 (2H, m), 2.08 (1H, m), 2.01 (3H, s), 1.71 (3H,

s), 1.69 (3H, s), 1.40-1.27 (7H, m), 1.26 (3H, s), 1.13 (3H, s), 0.88 (3H, t, *J* = 7.3 Hz); ^{13}C NMR (150 MHz, $CDCl_3$) δ 204.7, 172.5, 164.7, 144.4, 136.0, 121.0, 73.1, 42.3, 34.7, 33.1, 31.9, 29.2, 27.9, 25.7, 23.2, 22.6, 22.3, 20.5, 18.6, 14.1 (2 overlapping signals). FTIR ($\bar{\nu}$): 3675, 2971, 2922, 1713, 1655, 1420, 1380, 1282, 1235, 1192, 1151, 1114, 1065, 995, 964, 906, 849. HRMS calculated for $C_{21}H_{33}O_3$ $[M+H]^+$: 333.2424, observed: 333.2439. $[\alpha]_D^{20} = -27.4$ (c = 0.8, $CHCl_3$).

Pyrethrin II **1b** (136 mg, 0.366 mmol) was subjected to the procedure detailed above using palladium on carbon (1 wt% loading, 12 mg). Tetrahydropyrethrin **53b** was obtained as a colourless oil (133 mg, 97%).

(1S)-2-methyl-4-oxo-3-pentylcyclopent-2-en-1-yl (1R,3R)-3-((E)-3-methoxy-2-methyl-3-oxoprop-1-en-1-yl)-2,2-dimethylcyclopropane-1-carboxylate **53b**

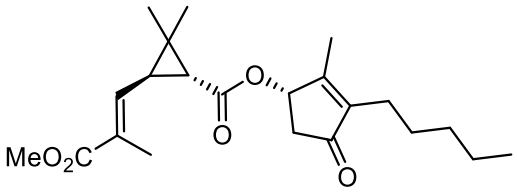

^{1}H NMR (600 MHz, $CDCl_3$) δ 6.45 (1H, d, *J* = 9.6 Hz), 5.64 (1H, brd, *J* = 6.3 Hz), 3.72 (3H, s), 2.84 (1H, dd, *J* = 6.3, 18.6 Hz), 2.22 (4H, m), 1.99 (3H, s), 1.84 (3H, s), 1.74 (1H, d, *J* = 5.2 Hz), 1.38 (2H, m), 1.30 (3H, s), 1.27 (4H, m), 1.23 (3H, s), 0.87 (3H, t, *J* = 6.9); ^{13}C NMR (150 MHz, $CDCl_3$) δ 204.5, 171.4, 168.3, 164.2, 144.6, 139.2, 129.9, 73.6, 52.0, 42.2, 36.0, 33.0, 31.9, 30.5, 27.9, 23.2, 22.6, 22.5, 20.6, 14.1, 13.0. FTIR ($\bar{\nu}$): 3675, 2954, 2928, 2872, 1710, 1649, 1435, 1385, 1260, 1221, 1173, 1148, 1055, 993, 831. HRMS calculated for $C_{22}H_{33}O_5$ $[M+H]^+$: 377.2323, observed: 377.2333. $[\alpha]_D^{20} = 15.2$ (c = 1.3, $CHCl_3$).

Isomerism of pyrethrins under catalytic transfer hydrogenation conditions

Pyrethrin I **5a** (110 mg, 0.335 mmol) was heated under reflux in dry THF (2 mL) in the presence of palladium on carbon (10 wt% loading, 15 mg) and formic acid (200 µL, 5.30 mmol) for 5 h under nitrogen. The mixture was allowed to cool, filtered over Celite and the solvent removed *in vacuo* yielding a pale yellow oil. The resulting mixture was purified by column

chromatography (10% ethyl acetate in hexane) giving *trans*-pyrethrin **34a** (10 mg, 9%) and a diastereomeric mixture of the isopyrethrins **25a** (17 mg, 15%).

(1S)-2-methyl-4-oxo-3-((E)-penta-2,4-dien-1-yl)cyclopent-2-en-1-yl (1R,3R)-2,2-dimethyl-3-(2-methylprop-1-enyl)cyclopropane-1-carboxylate **34a**

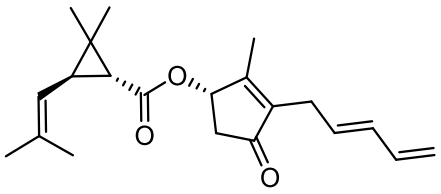

^{1}H NMR (600 MHz, $CDCl_3$) δ 6.27 (1H, ddd*, *J* = 10.1, 10.3, 16.9 Hz), 6.05 (1H, dd, *J* = 10.3, 15.2 Hz), 5.67 (1H, d, *J* = 6.3 Hz), 5.64 (1H, dt, *J* = 15.2, 6.8Hz), 5.12 (1H, d, *J* = 16.9 Hz), 5.00 (1H, d, *J* = 10.1 Hz), 4.90 (1H, d, *J* = 7.7 Hz), 3.00 (2H, d, *J* = 6.8 Hz), 2.87 (1H, dd, *J* = 6.3, 18.7 Hz), 2.24 (1H, dd, *J* = 1.32, 18.7 Hz), 2.08 (1H, m), 2.03 (3H, s), 1.72 (3H, s), 1.71 (3H, s), 1.40 (1H, d, *J* = 5.3 Hz), 1.26 (3H, s), 1.14 (3H, s); ^{13}C NMR (150 MHz, $CDCl_3$) δ 204.0, 172.5, 165.9, 141.7, 136.8, 136.1, 132.5, 129.6, 120.9, 116.2, 73.1, 42.2, 34.7, 33.1, 29.3, 26.2, 25.7, 22.3, 20.6, 18.6, 14.2. FTIR ($\bar{\nu}$): 3675, 2972, 2924, 1715, 1655, 1420, 1380, 1282, 1235, 1193, 1152, 1114, 1065, 1003, 963, 901, 849. HRMS calculated for $C_{21}H_{29}O_3$ $[M+H]^+$: 329.2111, observed: 329.2122. $[\alpha]_D^{20} = -44.7$ (c = 0.8, $CHCl_3$).

(S)-2-methyl-4-oxo-3-(penta-1,3-dien-1-yl)cyclopent-2-en-1-yl (1R,3R)-2,2-dimethyl-3-(2-methylprop-1-enyl)cyclopropane-1-carboxylate **25a**

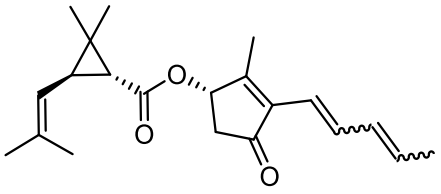

^{1}H NMR (600 MHz, $CDCl_3$) δ 7.64 (0.37H, dd, *J* = 11.4, 15.5 Hz), 7.29 (0.63H, dd, *J* = 10.7, 15.6 Hz), 6.09 (2H, m), 5.92 (0.63H, m), 5.67 (1.4H, m), 4.90 (1H, d, *J* =7.6 Hz), 2.90 (1H, m), 2.28 (1H, m), 2.09 (3H, s), 1.85 (2H, d, *J* = 7.1 Hz), 1.80 (3H, d, *J* = 6.7 Hz), 1.72 (3H, s), 1.71 (3H, s), 1.41 (2H, m), 1.26 (3H, s), 1.13 (3H, s) (some diastereomeric signals overlap); ^{13}C NMR (150 MHz, $CDCl_3$) δ 203.4, 172.5, 163.9, 163.4, 137.9, 136.2, 136.1, 133.3, 132.6, 131.0, 130.4, 130.2, 121.0, 119.7, 117.7, 72.7, 43.0, 34.8, 33.1, 30.5, 29.3, 25.7, 22.3, 20.6, 18.7, 14.4, 14.1

(some diastereomeric signals overlap). FTIR ($\bar{\nu}$): 2955, 2926, 1716, 1431, 1379, 1282, 1193, 1152, 1114, 994, 860. HRMS calculated for $C_{21}H_{29}O_3$ $[M+H]^+$: 329.2111, observed: 329.2122. $[\alpha]_D^{20} = -179.2$ (c = 0.5, $CHCl_3$).

Pyrethrin II **1b** (108 mg, 0.290 mmol) was treated following the above procedure using palladium on carbon (10 wt% loading, 12 mg) and formic acid (200 µL, 5.30 mmol). The isolated yellow oil was purified by column chromatography (20% ethyl acetate in hexane) giving **34b** (15 mg, 14%) and a diastereomeric mixture of **25b** (20 mg, 19%).

(1S)-2-methyl-4-oxo-3-((E)-penta-2,4-dien-1-yl)cyclopent-2-en-1-yl (1R,3R)-3-((E)-3-methoxy-2-methyl-3-oxoprop-1-en-1-yl)-2,2-dimethylcyclopropane-1-carboxylate **34b**

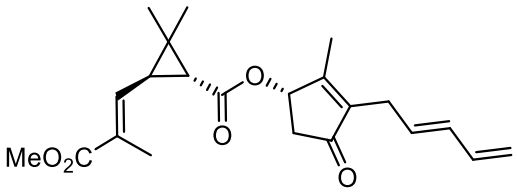

^{1}H NMR (600 MHz, $CDCl_3$) δ 6.46 (1H, d, *J* = 9.6 Hz), 6.26 (1H, ddd*, *J* = 10.1, 10.3, 16.9 Hz), 6.05 (1H, dd, *J* = 10.3, 15.1 Hz), 5.67 (1H, d, *J* = 6.2 Hz), 5.64 (1H, dt, *J* =15.2, 6.8 Hz), 5.11 (1H, d, *J* = 16.9 Hz), 4.99 (1H, d, *J* = 10.1 Hz), 3.72 (3H, s), 3.01 (2H, d, *J* = 6.8 Hz), 2.88 (1H, dd, *J* = 6.2, 18.7 Hz), 2.23 (2H, m), 2.03 (3H, s), 1.94 (3H, s), 1.74 (1H, d, *J* = 5.1 Hz), 1.30 (3H, s), 1.23 (3H, s); ^{13}C NMR (150 MHz, $CDCl_3$) δ 203.7, 171.4, 168.3, 165.4, 141.9, 139.1, 136.7, 132.5, 129.9, 129.5, 116.3, 73.5, 52.0, 42.1, 35.9, 33.1, 30.7, 26.2, 22.5, 20.6, 14.2, 13.0. FTIR ($\bar{\nu}$): 3662, 2952, 1709, 1649, 1435, 1383, 1340, 1260, 1221, 1173, 1147, 1111, 1055, 996, 904, 830. HRMS calculated for $C_{22}H_{29}O_5$ $[M+H]^+$: 373.2010, observed: 373.2022. $[\alpha]_D^{20} = 17.8$ (c = 0.5, $CHCl_3$).

(S)-2-methyl-4-oxo-3-(penta-1,3-dien-1-yl)cyclopent-2-en-1-yl (1R,3R)-3-((E)-3-methoxy-2-methyl-3-oxoprop-1-en-1-yl)-2,2-dimethylcyclopropane-1-carboxylate **25b**

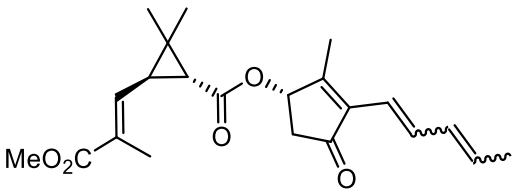

^{1}H NMR (600 MHz, $CDCl_3$) δ 7.71 (0.33H, dd, *J* = 11.5, 15.4 Hz), 7.35 (0.66H, dd, *J* = 10.7, 15.6 Hz), 6.46 (1H, d, *J* = 9.6 Hz), 6.09 (2H, m), 5.92 (0.66H, m), 5.66 (1.66H, m), 3.72 (3H, s), 2.90 (1H, m), 2.25 (2H, m), 2.08 (3H, s), 1.94 (3H, s), 1.84 (1H, d, *J* = 7.2 Hz), 1.80 (2H, d, *J* = 6.7 Hz), 1.74 (1H, m), 1.30 (3H, s), 1.24 (3H, s) (some diastereomeric signals overlap); ^{13}C NMR (150 MHz, $CDCl_3$) δ 203.1, 171.4, 168.2, 163.3, 162.8, 139.1, 138.1, 136.4, 133.5, 132.5, 131.1, 130.3, 129.9, 119.6, 117.6, 73.2, 51.9, 42.9, 36.0, 33.0, 30.7, 22.5, 20.6, 18.6, 14.3, 14.0, 13.0 (some diastereomeric signals overlap). FTIR ($\bar{\nu}$): 2952, 2928, 1710, 1643, 1435, 1385, 1260, 1221, 1173, 1147, 1111, 993, 830. HRMS calculated for $C_{22}H_{29}O_5$ $[M+H]^+$: 373.2010, observed: 373.2010. $[\alpha]_D^{20} = -56.9$ (c = 1.0, $CHCl_3$).

Reduction of pyrethrins by diimide-mediated transfer hydrogenation

Pyrethrin I **5a** (110 mg, 0.335 mmol) in THF (5 mL) was left to vigorously stir open to air in the presence of hydrazine monohydrate (800 mg, 16.0 mmol), copper(II) sulphate pentahydrate (8.5 mg, 0.034 mmol, 10 %mol) and acetic acid (20 mg, 0.33 mmol). The reaction was monitored by TLC (8% ethyl acetate in hexane) until all of the pyrethrin starting material was consumed (typically 7-8 h). The reaction mixture was filtered and subsequently diluted with brine water. The resulting solution was extracted with ethyl acetate and dried (Na_2SO_4). Solvent was removed *in vacuo* yielding a colourless oil (85 mg, 77% mass recovery) which was analysed by HPLC to be 68.0% jasmolin I **7a** and 24.7% tetrahydropyrethrin I **53a**. Characterisation was undertaken on the isolated mixture with signals assigned to jasmolin I by comparison to the natural ester.

*Jasmolin I **7a***

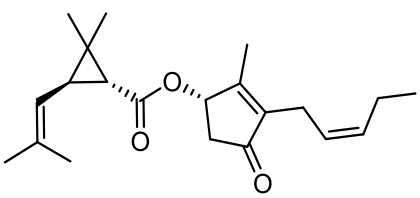

^{1}H NMR (600 MHz, $CDCl_3$) δ 5.65 (1H, brd, *J* = 6.4 Hz), 5.42 (1H, dt, *J* = 10.5, 7.3 Hz), 5.24 (1H, dt, *J* = 10.5, 7.3 Hz), 4.90 (1H, d, *J* = 7.7 Hz), 2.98 (2H, d, *J* = 7.3 Hz), 2.85 (1H, dd, *J* = 6.4, 18.7 Hz), 2.22 (1H, dd, *J* = 1.9, 18.7 Hz), 2.15 (2H, m), 2.08 (1H, m), 2.03 (3H, s), 1.73 (3H, s), 1.71 (3H, s), 1.41 (1H, m) 1.26 (3H, s), 1.14 (3H, s), 0.99 (3H, t, *J* = 7.5 Hz); ^{13}C NMR (150 MHz, $CDCl_3$) δ 204.1, 172.5, 165.0, 142.9, 136.0, 133.3, 124.1, 121.0, 73.1, 42.2, 34.7, 33.1, 29.2, 25.7, 22.2, 21.4, 20.7, 20.5, 18.6, 14.2, 14.2. FTIR ($\bar{\nu}$): 3675, 2965, 2928, 1714, 1655, 1447, 1420, 1380, 1282, 1235, 1193, 1152, 1114, 1046, 995, 850. HRMS calculated for $C_{21}H_{31}O_3$ $[M+H]^+$: 331.2268, observed: 331.2256. Isolated mixture $[\alpha]_D^{20} = -32.2$ (c = 0.9, $CHCl_3$) (natural jasmolin I $[\alpha]_D^{20} = -56.0$ (c = 0.5, $CHCl_3$)).

Pyrethrin II **5b** (145 mg, 0.390 mmol) in THF (5 mL) was subjected to the same procedure as above using hydrazine monohydrate (270 mg, 5.4 mmol), copper(II) sulphate pentahydrate (11 mg, 0.044 mmol, 10 %mol) and acetic acid (10 mg, 0.17 mmol). The reaction was monitored by TLC (25% ethyl acetate in hexane) until all of the pyrethrin starting material was consumed (typically 7-8 h). A colourless oil was obtained (120 mg, 83% mass recovery) which was analysed by HPLC to be 65.8% jasmolin II **7a** and 25.6% tetrahydropyrethrin II **53b**. Characterisation was undertaken on the isolated mixture with signals assigned to jasmolin II by comparison to the natural ester.

*Jasmolin II **7b***

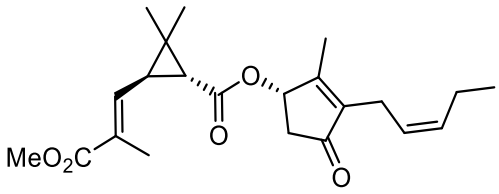

^{1}H NMR (600 MHz, $CDCl_3$) δ 6.45 (1H, d, *J* = 9.6 Hz), 5.64 (1H, d, *J* = 6.4 Hz), 5.42 (1H, dt, *J* = 10.6, 7.2 Hz), 5.23 (1H, dt, *J* = 10.6, 7.2Hz), 3.73 (3H, s), 2.97 (2H, d, *J* = 7.2 Hz), 2.86 (1H, dd, *J* = 6.4, 18.7 Hz), 2.23 (2H, m), 2.16 (2H, m), 2.03 (3H, s), 1.94 (3H, s), 1.74 (1H, d, *J* =5.2 Hz), 1.30 (3H, s), 1.23 (3H, s), 0.99 (3H, t, *J* = 7.5 Hz); ^{13}C NMR (150 MHz, $CDCl_3$) δ 203.87, 171.39, 168.28, 164.51, 143.17, 139.19, 133.42, 129.91, 123.94, 73.63, 51.97, 42.20, 35.95, 33.03, 30.69, 22.47, 21.37, 20.75, 20.56, 14.23, 14.17, 13.02. FTIR ($\bar{\nu}$): 3675, 2956, 1712, 1648, 1435, 1383, 1324, 1261, 1221, 1174, 1148, 1111, 1056, 995, 830, 762. HRMS calculated for $C_{22}H_{31}O_5$

$[M+H]^+$: 375.2166, observed: 375.2162. Isolated mixture $[\alpha]_D^{20}$ = 10.3 (c = 1.1, $CHCl_3$) (natural jasmolin II $[\alpha]_D^{20}$ = 8.0 (c=0.5, $CHCl_3$)).

Pyrethrum concentrate (HPLC analysis: 43.1% pyrethrin I **5a**, 36.2% pyrethrin II **5b**, 3.8% jasmolin I **7a**, 4.3% jasmolin II **7b**) (500 mg, ~1.36 mmol) in THF (5 mL) was left to vigorously stir open to air in the presence of hydrazine monohydrate (517 mg, 10.3 mmol), copper (II) sulphate (19 mg, 0.12 mmol, 10 %mol) and acetic acid (10 mg, 0.17 mmol). The reaction was left to stir at room temperature for 8 h before being filtered and diluted with brine. The resulting solution was extracted with ethyl acetate and dried (Na_2SO_4). Solvent was removed *in vacuo* yielding a pale yellow oil (HPLC analysis: 3.2% pyrethrin I **5a**, 1.8% pyrethrin II **5b**, 29.2% jasmolin I **7a**, 35.7% jasmolin II **7b**, 7.3% tetrahydropyrethrin I **53a**, 8.0% tetrahydropyrethrin II **53b**) (400 mg, 80% mass recovery).

7.2.2 Diels Alder chemistry

Cis-trans isomerism of pyrethrins

A solution of pyrethrin I **5a** or II **5b** (350 mg) in dry THF (3 mL) was irradiated with UV light (254 nm) for 16 h at room temperature. The solvent was removed *in vacuo* giving a mixture of *trans*-pyrethrin **55** with the starting material. The mixture was used without further purification.

Pyrethrin I (330 mg, 94%, 1: 1.3 *E:Z*; **34a**:**5a**)

Pyrethrin II (335 mg, 96%, 1: 2.2 *E:Z*; **34b**:**5b**)

Normal electron demand Diels-Alder with maleic anhydride

Maleic anhydride **59** (1.5 eq) was added to a solution of *trans*-pyrethrin **34** mixture (150 mg, 0.46 mmol. (pyrethrin I) or 0.40 mmol. (pyrethrin II)) in THF (5 mL). The resulting solution was refluxed for 8 h followed by solvent removal *in vacuo*. Attempted purification by column chromatography resulted in decomposition.

General procedure for the synthesis of 3,6-disubstituted tetrazines.

Amended from Li,[6] the aromatic nitrile (48 mmol), sulfur (1 g, 31 mmol) and hydrazine monohydrate (10 mL, 206 mmol) in ethanol (10 mL) were heated under reflux for 4 h. The reaction mixture was cooled to 0 °C and filtered. The solid was washed with cold ethanol and allowed to dry giving the dihydrotetrazine which was used without further purification.

The dihydrotetrazine was suspended in acetic acid (30 mL) and cooled to 0 °C. A solution of sodium nitrite (5 g, 73 mmol) in water (10 mL) was added dropwise with vigorous stirring to the suspension of dihydrotetrazine with continued cooling. The mixture was left to stir until no more gas was evolved and quenched with aqueous ammonium hydroxide solution (28-30% w/v) with continued cooling. The resulting slurry was filtered, washed with cold water and allowed to dry. Once dry, the tetrazine was recrystallised from ethanol.

3,6-bisphenyl-1,2,4,5-tetrazine **71**

Prepared as per general procedure using benzonitrile (1.9 g, 19 mmol), sulfur (0.5 g, 16 mmol), hydrazine monohydrate (5 mL, 103 mmol) in ethanol (5 mL). The resulting dihydrotetrazine was immediately oxidised in acetic acid (10 mL) with sodium nitrite (2.5 g, 36 mmol) in water (5 mL). Recrystallisation gave the desired tetrazine **71** as dark pink, needle-like crystals (1.07 g, 24%) m.p. 197 °C (lit. m.p. 196-198 °C).[7]

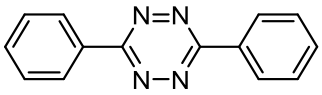

^{1}H NMR (600 MHz, $CDCl_3$) δ 8.66 (4H, dd, *J* =1.4, 7.9 Hz), 7.63 (6H, m); ^{13}C NMR (150 MHz, $CDCl_3$) δ 163.98, 132.67, 131.78, 129.29, 127.97. FTIR ($\bar{\nu}$): 3070, 1599, 1455, 1387, 1308, 1187, 1103, 1074, 999, 917, 764, 685. HRMS calculated for $C_{14}H_{11}N_4$ $[M+H]^+$: 235.0978, observed: 235.0981.

3,6-bis(2'-pyridyl)-1,2,4,5-tetrazine **72**

Prepared as per general procedure using 2-cyanopyridine (5 g, 48 mmol), sulfur (1 g, 31 mmol), hydrazine monohydrate (10 mL, 206 mmol) in ethanol (10 mL). The resulting dihydrotetrazine was immediately oxidised in acetic acid (30 mL) with sodium nitrite (5 g, 73 mmol) in water (5 mL). Recrystallisation from ethanol gave the desired tetrazine **72** as fine, dark red crystals (3.3 g, 29%) m.p. 223 °C (lit. m.p. 227 °C).[8]

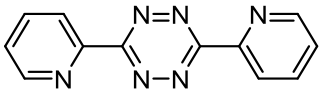

^{1}H NMR (600 MHz, $CDCl_3$) δ 9.01 (2H, d, *J* = 4.7 Hz), 8.77 (2H, d, *J* =7.9 Hz), 8.03 (2H, ddd, *J* = 1.7, 7.6, 7.9 Hz), 7.60 (2H, dd, *J* = 4.7, 7.6 Hz); ^{13}C NMR (150 MHz, $CDCl_3$) δ 163.87, 151.03, 150.08, 137.46, 126.57, 124.51. FTIR ($\bar{\nu}$): 3095, 3060, 1581, 1442, 1387, 1239, 1127, 1090, 992, 918, 796, 743, 731. HRMS calculated for $C_{12}H_9N_6$ $[M+H]^+$: 237.0883, observed: 237.0879.

3,6-bis(3'-pyridyl)-1,2,4,5-tetrazine **73**

Prepared as per general procedure using 3-cyanopyridine (5 g, 48 mmol), sulfur (1 g, 31 mmol), hydrazine monohydrate (10 mL, 206 mmol) in ethanol (10 mL). The resulting dihydrotetrazine was immediately oxidised in acetic acid (30 mL) with sodium nitrite (5 g, 73 mmol) in water (5 mL). Recrystallisation from ethanol gave the desired tetrazine **73** as purple, needle-like crystals (3.7 g, 32%) m.p. 203 °C (lit. m.p. 203-204 °C).[6]

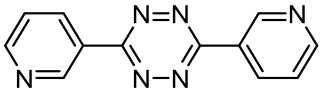

^{1}H NMR (600 MHz, $CDCl_3$) δ 9.87 (2H, s), 8.91 (4H, m), 7.59 (2H, dd, *J* =4.8, 7.9 Hz); ^{13}C NMR (150 MHz, $CDCl_3$) δ 163.42, 153.56, 149.48, 135.20, 127.58, 124.05. FTIR ($\bar{\nu}$): 3078, 3061, 1582, 1572, 1436, 1383, 1340, 1126, 1109, 1057, 1015, 916, 819, 700. HRMS calculated for $C_{12}H_9N_6$ $[M+H]^+$: 237.0883, observed: 237.0892.

3,6-bis(4'-pyridyl)-1,2,4,5-tetrazine **74**

Prepared as per general procedure using 4-cyanopyridine (5 g, 48 mmol), sulfur (1 g, 31 mmol), hydrazine monohydrate (10 mL, 206 mmol) in ethanol (10 mL). The resulting dihydrotetrazine was immediately oxidised in acetic acid (30 mL) with sodium nitrite (5 g, 73 mmol) in water (5 mL). Recrystallisation from ethanol gave desired tetrazine **74** as fine, magenta crystals (2.5 g, 22%) m.p. 254 °C (lit. m.p. (decomp.) 258 °C).[8]

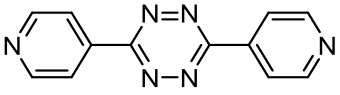

^{1}H NMR (600 MHz, $CDCl_3$) δ 8.96 (4H, dd, *J* =1.6, 4.4 Hz), 8.51 (4H, dd, *J* =1.6, 4.4 Hz); ^{13}C NMR (150 MHz, $CDCl_3$) δ 163.77, 151.31, 138.62, 121.38. FTIR ($\bar{\nu}$): 3032, 1588, 1558, 1495, 1410, 1385, 1262, 1217, 1111, 1054, 991, 917, 829, 714. HRMS calculated for $C_{12}H_9N_6$ $[M+H]^+$: 237.0883, observed: 237.0891.

Preparation of triaminoguanidine hydrochloride **76**

As detailed by Coburn,[9] hydrazine monohydrate (10.0 g, 200 mmol) was added to a suspension of guanidine hydrochloride **75** (5.0 g, 52 mmol) in 1,4-dioxane (30 mL). The resulting mixture was allowed to reflux for 2 h. The mixture was cooled to 0 °C, filtered and the resulting solid washed with 1,4-dioxane. The off-white solid was dried giving a near quantitative yield of triaminoguanidine hydrochloride **76** (7.0 g, 95%) m.p. 231 °C (lit. m.p. 230 °C).[9]

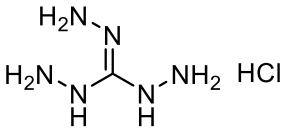

^{1}H NMR (600 MHz, DMSO-d_6) δ 8.58 (2H, brs), 4.49 (4H, s). ^{13}C NMR (150 MHz, DMSO-d_6) δ 159.51.

Synthesis of 3,6-bis(3',5'-dimethylpyrazol-1'-yl)-1,2 -dihydro-1,2,4,5-tetrazine **77**

As previously described by Coburn,[9] 2,4-pentandione (7.2 g, 72 mmol) was added dropwise to a suspension of triaminoguanidine hydrochloride **76** (5.0 g, 36 mmol) in water (30 mL). The resulting bright yellow solution was allowed to stir at room temperature before being heated at 70 °C for 4 h. The resulting yellow precipitate was collected by vacuum filtration and washed with water. Recrystallisation from ethanol yielded the dihydrotetrazine **77** as yellow, needle-like crystals (3.15 g, 33%) m.p. 150-152 °C (lit. m.p. 150 °C).[9]

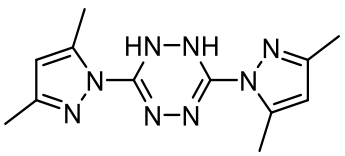

^{1}H NMR (600 MHz, $CDCl_3$) δ 8.04 (2H, s), 5.97 (2H, s), 2.49 (6H, s), 2.22 (6H, s); ^{13}C NMR (150 MHz, $CDCl_3$) δ 149.97, 145.77, 142.30, 109.88, 13.80, 13.47. FTIR ($\bar{\nu}$): 3248, 2981, 2930, 1676,

1567, 1467, 1404, 1381, 1361, 1295, 1147, 1059, 1027, 984, 966, 886, 787. HRMS calculated for $C_{12}H_{17}N_8$ $[M+H]^+$: 273.1571, observed: 273.1557.

Synthesis of 3,6-bis(3',5'-dimethylpyrazol-1'-yl)-1,2,4,5-tetrazine **78**

Dihydrotetrazine **77** (3.15 g, 11.6 mmol) was suspended in dichloromethane (40 mL) and cooled to 0 °C. With vigorous stirring, concentrated nitric acid (70% w/v) was added dropwise to the suspension with continued cooling until gas evolution ceased (approximately 2 mL). The resulting red suspension was left to stir with continued cooling for an additional 1 h. Collection of the precipitate by vacuum filtration and subsequent recrystallisation from acetone gave the desired tetrazine **78** as red, needle-like crystals (1.79 g, 57%) m.p. 225-227 °C (lit. m.p. 226 °C).[9]

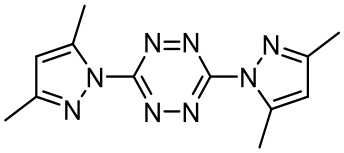

^{1}H NMR (600 MHz, $CDCl_3$) δ 6.18 (2H, s), 2.69 (6H, s), 2.38 (6H, s); ^{13}C NMR (150 MHz, $CDCl_3$) δ 159.31, 154.49, 143.79, 111.91, 14.68, 13.87. FTIR ($\bar{\nu}$): 3084, 2993, 2933, 1576, 1479, 1421, 1380, 1273, 1162, 1077, 1048, 1022, 968, 938, 845, 756. HRMS calculated for $C_{12}H_{15}N_8$ $[M+H]^+$: 271.1414, observed: 271.1422.

Preparation of 3,6-dihydrazinyl-1,2,4,5-tetrazine **79**

As prepared by Gong,[10] hydrazine monohydrate (0.6 g, 12 mmol) was slowly added to a solution of 3,6-bis(3',5'-dimethylpyrazol-1'-yl)-1,2,4,5-tetrazine **78** (1.0 g, 3.7 mmol) in acetonitrile (20 mL) at room temperature. The resulting dark red solution was then refluxed for 30 min. After the reaction mixture cooled to room temperature, the resulting maroon precipitate was filtered and washed with acetonitrile to give the desired tetrazine **79** (0.39 g, 74%) m.p. 148 °C (decomp.) (lit. m.p. 158-160 °C).[11]

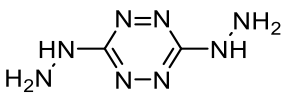

^{1}H NMR (600 MHz, DMSO-d_6) δ 8.37 (2H, s), 4.24 (4H, s); ^{13}C NMR (150 MHz, DMSO-d_6) δ 163.37. FTIR ($\bar{\nu}$): 3292, 3209, 3022, 2925, 1632, 1535, 1449, 1296, 1169, 1050, 1003, 935, 698.

Synthesis of 3,6-dichloro-1,2,4,5-tetrazine **80**

Hydrochloric acid (32% w/v) was added dropwise to trichloroisocyanuric acid (8.2 g, 35 mmol, 5 eq) generating chlorine gas that was gently bubbled through a stirring suspension of 3,6-dihydrazinyl-1,2,4,5-tetrazine **79** (1 g, 7 mmol) in dichloromethane (40 mL) at 0 °C. Once gas evolution ceased, the orange suspension was allowed to stir at room temperature for an additional 1 h. The solvent was gently removed *in vacuo* at ambient temperature and the orange residue purified by silica gel plug (DCM) giving the tetrazine **80** (0.72 g, 69%) m.p. 145-150 °C (lit. m.p. 144-147 °C (decomp.)).[12]

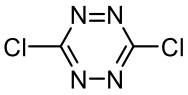

^{13}C NMR (150 MHz, $CDCl_3$) δ 168.11. FTIR ($\bar{\nu}$): 2931, 2295, 1732, 1454, 1371, 1257, 1236, 1156, 1064, 1025, 882, 834.

General procedure for the IEDDA of pyrethrins with 3,6-disubstituted tetrazines

3,6-disubsituted-1,2,4,5-tetrazine (1 eq) was added to a solution of pyrethrin I **5a** or II **5b** (150 mg, 0.46 mmol. (pyrethrin I) or 0.40 mmol. (pyrethrin II)) in dry THF (5 mL). The mixture was refluxed under an atmosphere of nitrogen for 8 or 24 h, as indicated. Once cooled to room temperature, DDQ (1 eq) was added and the mixture allowed to stir for 2 hr. The reaction was diluted with saturated sodium bicarbonate solution and extracted with dichloromethane. The organic extract was dried (Na_2SO_4) and the solvent removed *in vacuo* giving the crude IEDDA adduct. Each adduct was purified as described below.

(S)-3-((Z)-3-(3,6-diphenylpyridazin-4-yl)allyl)-2-methyl-4-oxocyclopent-2-en-1-yl (1R,3R)-2,2-dimethyl-3-(2-methylprop-1-en-1-yl)cyclopropane-1-carboxylate **88a**

Prepared as per general procedure using pyrethrin I **5a** (400 mg, 1.22 mmol), 3,6-bisphenyl-1,2,4,5-tetrazine **71** (285 mg, 1.22 mmol) and dry THF (10 mL). The reaction was heated under reflux for 24 h. The resulting mixture was purified by column chromatography (20% ethyl acetate in hexane) giving the pyridazine adduct **88a** (155 mg, 24%).

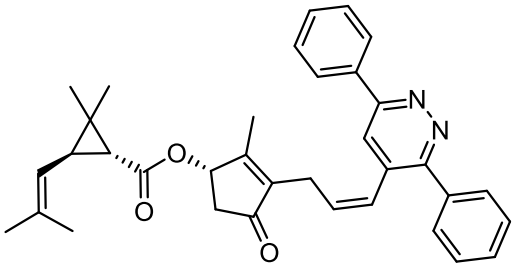

^{1}H NMR (600 MHz, $CDCl_3$) δ 8.26 (2H, d, *J* = 7.5 Hz), 8.18 (1H, s), 7.79 (2H, d, *J* = 7.9 Hz), 7.56 (2H, t, *J* = 7.5 Hz), 7.48 (4H, m), 6.41 (1H, d, *J* = 11.6 Hz), 5.83 (1H, dt, *J* =11.6, 7.4 Hz), 5.67 (1H, brd, *J* = 6.3 Hz), 4.90 (1H, d, *J* = 7.7 Hz), 3.25 (2H, d, *J* = 7.4 Hz), 2.91 (1H, dd, *J* = 6.3, 18.6 Hz), 2.27 (1H, dd, *J* = 1.2, 18.6 Hz), 2.09 (1H, m), 1.97 (3H, s), 1.73 (3H, s), 1.71 (3H, s), 1.40 (1H, d, *J* = 5.3 Hz), 1.26 (3H, s), 1.15 (3H, s); ^{13}C NMR (150 MHz, $CDCl_3$) δ 203.9, 172.2, 166.3, 158.3, 157.4, 141.0, 136.6, 136.2, 136.0, 134.0, 131.9, 130.0, 129.8, 129.2, 129.1, 128.3, 127.2, 126.9, 124.3, 120.7, 72.8, 42.1, 34.5, 33.1, 29.3, 25.6, 22.9, 20.4, 18.5, 14.2. FTIR ($\bar{\nu}$): 2927, 1713, 1655, 1567, 1529, 1427, 1380, 1339, 1153, 1114, 1085, 970. HRMS calculated for $C_{35}H_{37}N_2O_3$ $[M+H]^+$: 533.2799, observed: 533.2807. $[\alpha]_D^{20} = -37.7$ (c = 1.3, $CHCl_3$).

(S)-3-((Z)-3-(3,6-diphenylpyridazin-4-yl)allyl)-2-methyl-4-oxocyclopent-2-en-1-yl (1R,3R)-3-((Z)-3-methoxy-2-methyl-3-oxoprop-1-en-1-yl)-2,2-dimethylcyclopropane-1-carboxylate **88b**

Prepared as per general procedure using pyrethrin II (400 mg, 1.08 mmol), 3,6-bisphenyl-1,2,4,5-tetrazine **71** (253 mg, 1.08 mmol) and dry THF (10 mL). The reaction was heated under reflux for 24 h. The resulting mixture was purified by column chromatography (40% ethyl acetate in hexane) giving the pyridazine adduct **88b** (109 mg, 18%).

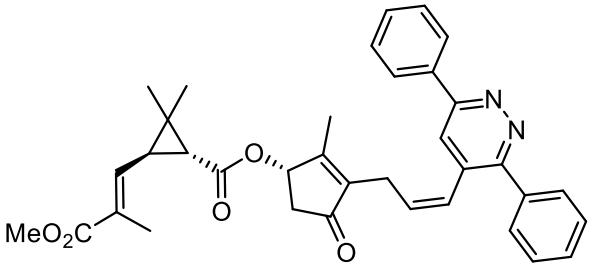

^{1}H NMR (600 MHz, $CDCl_3$) δ 8.26 (2H, d, *J* = 7.1 Hz), 8.17 (1H, s), 7.79 (2H, dd, *J* = 2.0, 8.0 Hz), 7.54 (2H, t, *J* = 7.1 Hz), 7.48 (4H, m), 6.45 (1H, d, *J* = 9.6 Hz), 6.41 (1H, d, *J* = 11.5 Hz), 5.82 (1H, dt, *J* =11.5, 7.4 Hz), 5.68 (1H, brd, *J* = 6.3 Hz), 3.74 (3H, s), 3.25 (2H, d, *J* = 7.4 Hz), 2.91 (1H, dd, *J* = 6.3, 18.7 Hz), 2.26 (1H, dd, *J* = 1.9, 18.7 Hz), 2.22 (1H, dd, *J* = 5.2, 9.6 Hz), 1.97 (3H, s), 1.94

(3H, s), 1.73 (1H, d, *J* = 5.2 Hz), 1.31 (3H, s), 1.25 (3H, s); ^{13}C NMR (150 MHz, $CDCl_3$) δ 203.6, 171.1, 168.1, 165.8, 158.2, 157.3, 141.2, 139.8, 136.6, 136.2, 133.9, 131.8, 130.0, 129.9, 129.8, 129.2, 128.2, 127.1, 127.0, 124.3, 73.2, 51.8, 42.0, 35.7, 33.0, 30.6, 22.9, 22.3, 20.4, 14.1. FTIR ($\bar{\nu}$): 2927, 1711, 1655, 1586, 1529, 1446, 1425, 1380, 1338, 1282, 1151, 1113, 1044, 1027, 970, 786. HRMS calculated for $C_{36}H_{37}N_2O_5$ $[M+H]^+$: 577.2697, observed: 577.2694. $[\alpha]_D^{20}$ = 8.3 (c = 0.9, $CHCl_3$).

(S)-3-((Z)-3-(3,6-di(pyridin-2-yl)pyridazin-4-yl)allyl)-2-methyl-4-oxocyclopent-2-en-1-yl (1R,3R)-2,2-dimethyl-3-(2-methylprop-1-en-1-yl)cyclopropane-1-carboxylate **87a**

Prepared as per general procedure using pyrethrin I **5a** (150 mg, 0.46 mmol), 3,6-(2'-pyridyl)-1,2,4,5-tetrazine **72** (108 mg, 0.46 mmol) and dry THF (5 mL). The reaction was heated under reflux for 8 h. The resulting brown solid was purified by trituration and subsequent precipitation from hexane giving the pyridazine adduct **87a** (90 mg, 37%).

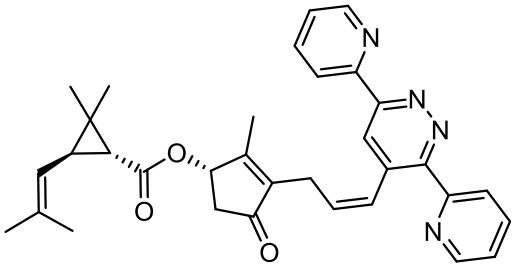

^{1}H NMR (600 MHz, $CDCl_3$) δ 8.73 (3H, m), 8.67 (1H, s), 8.19 (1H, d, *J* = 7.8 Hz), 7.89 (2H, m), 7.39 (2H, m), 6.92 (1H, d, *J* = 11.7 Hz), 5.86 (1H, dt, *J* = 11.7, 7.3Hz), 5.62 (1H, brd, *J* = 6.4 Hz), 4.88 (1H, d, *J* = 7.5 Hz), 3.17 (2H, d, *J* = 7.3 Hz), 2.83 (1H, dd, *J* = 6.4, 18.6 Hz), 2.20 (1H, d, *J* = 18.6 Hz), 2.06 (1H, m), 1.87 (3H, s), 1.72 (3H, s), 1.69 (3H, s), 1.37 (1H, d, *J* = 5.3 Hz), 1.24 (3H, s), 1.13 (3H, s); ^{13}C NMR (150 MHz, $CDCl_3$) δ 203.9, 172.4, 166.4, 157.9, 157.4, 155.9, 153.6, 149.7, 148.9, 141.6, 137.3, 136.9, 136.1, 135.8, 130.9, 127.0, 125.6, 124.9, 124.8, 123.8, 121.9, 120.9, 73.0, 42.1, 34.7, 33.1, 29.3, 25.7, 23.0, 22.3, 20.6, 18.7, 14.3. FTIR ($\bar{\nu}$): 3059, 2925, 1710, 1654, 1585, 1577, 1476, 1442, 1395, 1283, 1192, 1152, 1114, 1044, 992, 911, 794, 730. HRMS calculated for $C_{33}H_{35}N_4O_3$ $[M+H]^+$: 535.2704, observed: 535.2709. $[\alpha]_D^{20}$ = −9.3 (c = 0.4, $CHCl_3$).

(S)-3-((Z)-3-(3,6-di(pyridin-2-yl)pyridazin-4-yl)allyl)-2-methyl-4-oxocyclopent-2-en-1-yl (1R,3R)-3-((Z)-3-methoxy-2-methyl-3-oxoprop-1-en-1-yl)-2,2-dimethylcyclopropane-1-carboxylate **87b**

Prepared as per general procedure using pyrethrin II **5b** (150 mg, 0.40 mmol), 3,6-(2'-pyridyl)-1,2,4,5-tetrazine **72** (95 mg, 0.40 mmol) and dry THF (5 mL). The reaction was heated under reflux for 8 h and the resulting brown solid purified by trituration and subsequent precipitation from hexane giving the pyridazine adduct **87b** (108 mg, 46%).

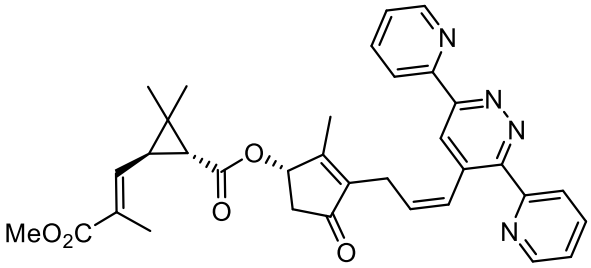

^{1}H NMR (600 MHz, $CDCl_3$) δ 8.77 (1H, d, *J* = 8.0 Hz), 8.74 (1H, d, *J* = 4.6 Hz), 8.70 (1H, d, *J* = 4.6 Hz), 8.60 (1H, s), 8.20 (1H, d, *J* = 7.9 Hz), 7.89 (2H, m), 7.40 (2H, m), 6.92 (1H, d, *J* = 11.6 Hz), 6.45 (1H, d, *J* = 9.6 Hz), 5.86 (1H, dt, *J* =11.6, 7.3 Hz), 5.60 (1H, brd, *J* = 6.2 Hz), 3.73 (3H, s), 3.18 (2H, d, *J* = 7.3 Hz), 2.84 (1H, dd, *J* = 6.2, 18.7 Hz), 2.20 (2H, m), 1.93 (3H, s), 1.87 (3H, s), 1.70 (1H, d, *J* = 5.2 Hz), 1.29 (3H, s), 1.23 (3H, s); ^{13}C NMR (150 MHz, $CDCl_3$) δ 203.4, 171.1, 168.1, 165.8, 157.7, 157.2, 155.7, 153.4, 151.0, 149.5, 148.7, 141.6, 138.9, 137.1, 136.7, 135.6, 130.6, 129.8, 127.0, 125.4, 124.7, 124.6, 123.7, 121.7, 73.3, 51.8, 41.9, 35.7, 32.9, 30.5, 22.8, 22.3, 20.4, 14.0, 12.6. FTIR ($\bar{\nu}$): 3054, 3003, 2953, 1710, 1655, 1641, 1578, 1475, 1429, 1396, 1265, 1225, 1177, 1149, 1111, 999, 941, 831, 796, 744. HRMS calculated for $C_{34}H_{35}N_4O_5$ $[M+H]^+$: 579.2602, observed: 579.2614. $[\alpha]_D^{20}$ = 37.5 (c = 0.4, $CHCl_3$).

(S)-3-((Z)-3-(3,6-di(pyridin-3-yl)pyridazin-4-yl)allyl)-2-methyl-4-oxocyclopent-2-en-1-yl (1R,3R)-2,2-dimethyl-3-(2-methylprop-1-en-1-yl)cyclopropane-1-carboxylate **89a**

Prepared as per general procedure using pyrethrin I **5a** (150 mg, 0.46 mmol), 3,6-(3'-pyridyl)-1,2,4,5-tetrazine **73** (108 mg, 0.46 mmol) and dry THF (5 mL). The reaction was heated under reflux for 24 h and solvent removed *in vacuo* without addition of DDQ. The subsequent mixture purified by column chromatography (5% methanol in dichloromethane) giving the adduct **89a** as a mixture of isomers (105 mg, 43%, d.r.1:2 (*E:Z*)).

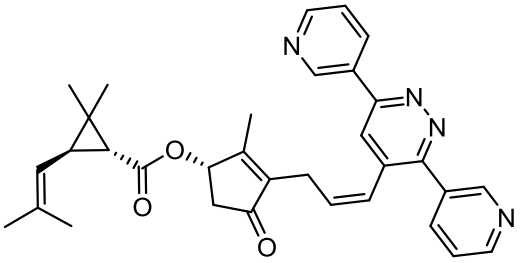

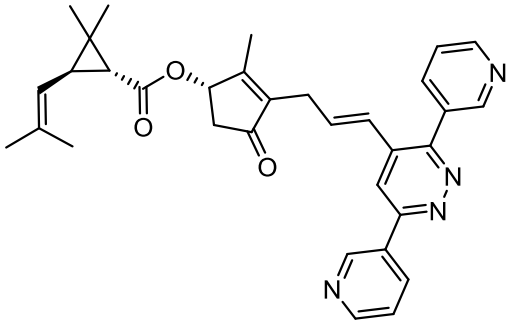

^{1}H NMR (600 MHz, $CDCl_3$) δ 9.50 (0.66H, brs), 9.31 (0.33H, brs), 9.21 (0.33H, brs), 9.02 (0.66H, brs), 8.94 (0.33H, brs), 8.76 (1H, m), 8.73 (0.66H, d, *J* = 4.7 Hz), 8.68 (0.66H, d, *J* = 7.8 Hz), 8.53 (0.33H, d, *J* = 7.8 Hz), 8.48 (0.66H, s), 8.39 (0.33H, d, *J* = 8.0 Hz), 8.21 (0.66H, d, *J* = 7.7 Hz), 8.09 (0.33H, d, *J* = 7.8 Hz), 7.93 (0.33H, s), 7.50 (2H, m), 6.58 (0.33H, dt, *J* = 15.8, 6.4Hz), 6.42 (0.33H, d, *J* = 15.8 Hz), 6.38 (0.66H, d, *J* = 11.5 Hz), 5.87 (0.66H, dt, *J* =11.5, 7.6Hz), 5.70 (1H, m), 4.91 (1H, d, *J* = 7.6 Hz), 3.27 (1H, d, *J* = 7.6 Hz), 3.23 (1H, d, *J* = 6.4 Hz), 2.91 (1H, m), 2.27 (1H, m), 2.09 (1H, m), 2.08 (1H, s), 2.05 (2H, s), 1.73 (3H, s), 1.71 (3H, s), 1.42 (0.66H, d, *J* = 5.3 Hz), 1.39 (0.33H, d, *J* = 5.3 Hz), 1.27 (2H, s), 1.26 (1H, s), 1.15 (2H, s), 1.14 (1H, s) (some diastereomeric signals overlap); ^{13}C NMR (150 MHz, $CDCl_3$) δ 204.06, 203.72, 172.21, 166.91, 166.77, 156.22, 156.07, 155.86, 155.72, 152.20, 151.14, 150.50, 150.47, 150.34, 148.98, 148.53, 148.19, 140.35, 139.99, 137.29, 137.13, 136.02, 135.23, 134.98, 134.88, 134.65, 134.61, 134.55, 133.29, 132.35, 132.07, 131.86, 131.72, 126.22, 126.07, 125.95, 124.58, 124.04, 123.88, 123.40, 123.36, 120.69, 120.16, 72.75, 42.06, 42.03, 34.46, 34.43, 33.16, 33.14, 29.30, 27.06, 25.55, 22.98, 22.08, 20.40, 20.38, 18.50, 14.21, 14.17 (some diastereomeric signals overlap). FTIR ($\bar{\nu}$): 2924, 1710, 1655, 1591, 1385, 1282, 1235, 1192, 1153, 1114, 1022, 812, 708. HRMS calculated for $C_{33}H_{35}N_4O_3$ $[M+H]^+$: 535.2704, observed: 535.2704. $[\alpha]_D^{20} = -48.5$ (c = 1.0, $CHCl_3$).

(S)-3-((Z)-3-(3,6-di(pyridin-3-yl)pyridazin-4-yl)allyl)-2-methyl-4-oxocyclopent-2-en-1-yl (1R,3R)-3-((Z)-3-methoxy-2-methyl-3-oxoprop-1-en-1-yl)-2,2-dimethylcyclopropane-1-carboxylate **89b**

Prepared as per general procedure using pyrethrin II **5b** (150 mg, 0.40 mmol), 3,6-(3'-pyridyl)-1,2,4,5-tetrazine **73** (95 mg, 0.40 mmol) and dry THF (5 mL). The reaction was heated under reflux for 24 h and solvent removed *in vacuo* without addition of DDQ. The subsequent

mixture was purified by column chromatography (5% methanol in dichloromethane) giving the adduct **89b** as a mixture of isomers (107 mg, 46 %, d.r.1:2.3 (*E:Z*)).

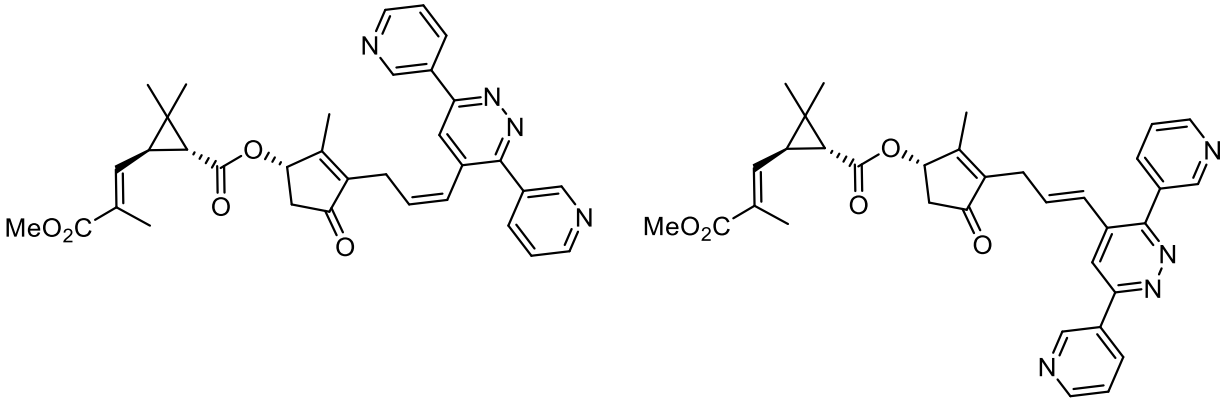

^{1}H NMR (600 MHz, $CDCl_3$) δ 9.49 (0.7H, brs), 9.31 (0.3H, brs), 9.21 (0.3H, brs), 9.01 (0.7H, brs), 8.93 (0.3H, brs), 8.76 (1H, m,), 8.73 (0.7H, d, *J* = 4.9 Hz), 8.68 (0.7H, d, *J* = 8.0 Hz), 8.53 (0.3H, d, *J* = 8.0 Hz), 8.46 (0.7H, s), 8.39 (0.3H, d, *J* = 8.0 Hz), 8.21 (0.7H, d, *J* = 7.8 Hz), 8.10 (0.3H, d, *J* = 7.8 Hz), 7.93 (0.3H, s), 7.48 (2H, m), 6.57 (0.3H, dt, *J* = 16.0, 6.3Hz), 6.46 (1H, m), 6.40 (1H, m), 5.87 (0.7H, dt, *J* = 11.5, 7.7Hz), 5.70 (1H, d, *J* = 5.9 Hz), 3.74 (3H, s), 3.26 (1.3H, m), 3.22 (0.7H, d, *J* = 6.3 Hz), 2.93 (1H, m), 2.25 (2H, m), 2.08 (0.7H, s), 2.05 (2.3H, s), 1.95 (3H, s), 1.76 (0.7H, d, *J* = 5.2 Hz), 1.71 (0.3H, d, *J* = 4.9 Hz), 1.32 (2.3H, s), 1.31 (0.7H, s), 1.24 (2.3H, s), 1.23 (0.7H, s) (some diastereomeric signals overlap); ^{13}C NMR (150 MHz, $CDCl_3$) δ 203.77, 203.44, 171.13, 168.08, 166.44, 166.29, 165.42, 156.21, 156.07, 155.83, 155.70, 152.20, 151.15, 150.47, 150.36, 148.98, 148.50, 148.18, 140.62, 140.24, 138.82, 138.79, 137.30, 137.13, 135.08, 134.94, 134.87, 134.61, 134.51, 133.14, 132.33, 132.06, 131.84, 131.71, 126.21, 126.16, 124.54, 124.03, 123.89, 123.41, 120.17, 73.20, 51.83, 41.97, 35.65, 33.08, 33.03, 30.70, 27.05, 22.99, 22.30, 20.40, 14.21, 14.16, 12.89 (some diastereomeric signals overlap). FTIR ($\bar{\nu}$): 2953, 1710, 1650, 1591, 1386, 1263, 1222, 1149, 1112, 1023, 758, 709. HRMS calculated for $C_{34}H_{35}N_4O_5$ $[M+H]^+$: 579.2602, observed: 579.2595. $[\alpha]_D^{20} = -10.8$ (c = 0.7, $CHCl_3$).

(S)-2-methyl-4-oxo-3-((Z)-3-(3-phenyl-6-(pyridin-4-yl)pyridazin-4-yl)allyl)cyclopent-2-en-1-yl (1R,3R)-2,2-dimethyl-3-(2-methylprop-1-en-1-yl)cyclopropane-1-carboxylate **90a**

Prepared as per general procedure using pyrethrin I **5a** (150 mg, 0.46 mmol), 3,6-(4'-pyridyl)-1,2,4,5-tetrazine **74** (108 mg, 0.46 mmol) and dry THF (5 mL). The reaction was heated under

reflux for 8 h and the subsequent mixture purified by careful column chromatography (1:2:97 TEA:MeOH:DCM) giving the pyridazine adduct **90a** (115 mg, 47%).

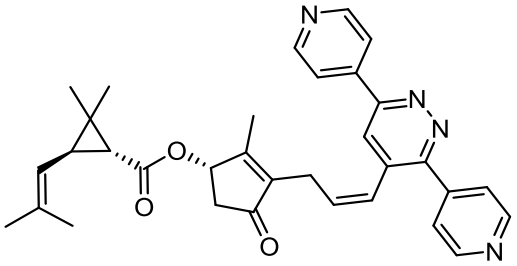

^{1}H NMR (600 MHz, $CDCl_3$) δ 8.85 (2H, d, *J* = 4.7 Hz), 8.78 (2H, d, *J* = 4.7 Hz), 8.61 (1H, s), 8.26 (2H, d, *J* = 4.8 Hz), 7.74 (2H, d, *J* = 4.8 Hz), 6.37 (1H, d, *J* = 11.6 Hz), 5.87 (1H, dt, *J* = 11.6, 7.6Hz), 5.72 (1H, d, *J* = 6.4 Hz), 4.91 (1H, d, *J* = 7.9 Hz), 3.26 (2H, d, *J* = 7.6 Hz), 2.95 (1H, dd, *J* = 6.4, 18.8 Hz), 2.31 (1H, d, *J* = 18.8 Hz), 2.11 (1H, m), 2.08 (3H, s), 1.73 (3H, s), 1.72 (3H, s), 1.41 (1H, d, *J* = 5.3 Hz), 1.27 (3H, s), 1.15 (3H, s); ^{13}C NMR (150 MHz, $CDCl_3$) δ 204.3, 172.3, 167.2, 157.3, 156.3, 151.0, 150.2, 143.9, 143.2, 140.3, 136.2, 134.8, 133.5, 125.9, 125.2, 124.2, 121.3, 120.8, 72.9, 42.2, 34.6, 33.3, 29.5, 25.7, 23.1, 22.2, 20.5, 18.6, 14.4. FTIR ($\bar{\nu}$): 3030, 2922, 1707, 1653, 1598, 1577, 1409, 1282, 1152, 1064, 992, 829. HRMS calculated for $C_{33}H_{35}N_4O_3$ $[M+H]^+$: 535.2704, observed: 535.2701. $[\alpha]_D^{20} = -40.9$ (c = 0.2, $CHCl_3$).

(S)-2-methyl-4-oxo-3-((Z)-3-(6-phenyl-3-(pyridin-4-yl)pyridazin-4-yl)allyl)cyclopent-2-en-1-yl (1R,3R)-3-((Z)-3-methoxy-2-methyl-3-oxoprop-1-en-1-yl)-2,2-dimethylcyclopropane-1-carboxylate **90b**

Prepared as per general procedure using pyrethrin II **5b** (150 mg, 0.40 mmol), 3,6-(4'-pyridyl)-1,2,4,5-tetrazine **74** (95 mg, 0.40 mmol) and dry THF (5 mL). The reaction was heated under reflux for 8 h and then was purified by careful column chromatography (1:4:95 TEA:MeOH:DCM) giving the pyridazine adduct **90b** (140 mg, 60%).

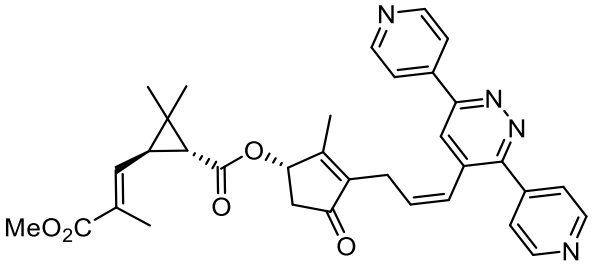

^{1}H NMR (600 MHz, $CDCl_3$) δ 8.83 (2H, d, *J* = 4.7 Hz), 8.77 (2H, d, *J* = 4.7 Hz), 8.60 (1H, s), 8.24 (2H, d, *J* = 4.8 Hz), 7.73 (2H, d, *J* = 4.8 Hz), 6.46 (1H, d, *J* = 9.6 Hz), 6.36 (1H, d, *J* = 11.5 Hz), 5.84 (1H, dt, *J* = 11.5, 7.8Hz), 5.71 (1H, d, *J* = 6.2 Hz), 3.72 (3H, s), 3.25 (2H, d, *J* = 7.8 Hz), 2.94 (1H, dd, *J* = 6.2, 18.7 Hz), 2.29 (1H, d, *J* = 18.7 Hz), 2.23 (1H, m), 2.06 (3H, s), 1.94 (3H, s), 1.73 (1H, d, *J* = 5.0 Hz), 1.31 (3H, s), 1.23 (3H, s); ^{13}C NMR (150 MHz, $CDCl_3$) δ 204.1, 171.3, 168.2, 166.8, 157.3, 156.3, 151.0, 150.2, 144.0, 143.2, 140.6, 138.9, 134.8, 133.4, 130.1, 126.0, 125.2, 124.2, 121.4, 73.3, 52.0, 42.2, 35.8, 33.2, 30.9, 23.1, 22.5, 20.6, 14.4, 13.0. FTIR ($\bar{\nu}$): 3031, 2952, 1706, 1649, 1598, 1578, 1434, 1410, 1385, 1262, 1221, 1174, 1148, 1111, 1056, 992, 915, 829, 729. HRMS calculated for $C_{34}H_{35}N_4O_5$ $[M+H]^+$: 579.2602, observed: 579.2593. $[\alpha]_D^{20}$ = −89.8 (c = 0.3, $CHCl_3$).

(S)-3-((Z)-3-(3,6-bis(3,5-dimethyl-1H-pyrazol-1-yl)pyridazin-4-yl)allyl)-2-methyl-4-oxocyclopent-2-en-1-yl (1R,3R)-2,2-dimethyl-3-(2-methylprop-1-en-1-yl)cyclopropane-1-carboxylate **91a**

Prepared as per general procedure using pyrethrin I **5a** (150 mg, 0.46 mmol), 3,6-bis(3',5'-dimethylpyrazol-1'-yl)-1,2,4,5-tetrazine **78** (125 mg, 0.46 mmol) and dry THF (5 mL). The reaction was heated under reflux for 8 h and subsequently purified by column chromatography (40% ethyl acetate in hexane) giving the pyridazine adduct **91a** (110 mg, 42%).

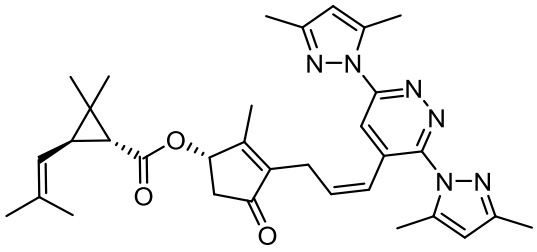

^{1}H NMR (600 MHz, $CDCl_3$) δ 8.29 (1H, s), 6.38 (1H, d, *J* = 11.7 Hz), 6.08 (1H, s), 6.02 (1H, s), 5.87 (1H, dt, *J* = 11.7, 7.4Hz), 5.65 (1H, d, *J* = 6.3 Hz), 4.89 (1H, d, *J* = 7.7 Hz), 3.26 (2H, d, *J* = 7.4 Hz), 2.86 (1H, dd, *J* = 6.3, 18.7 Hz), 2.77 (3H, s), 2.32 (3H, s), 2.31 (3H, s), 2.28 (3H, s), 2.22 (1H, d, *J* = 18.7 Hz), 2.08 (1H, m), 1.99 (3H, s), 1.72 (3H, s), 1.70 (3H, s), 1.38 (1H, d, *J* = 7.0 Hz), 1.25 (3H, s), 1.14 (3H, s); ^{13}C NMR (150 MHz, $CDCl_3$) δ 203.6, 172.4, 166.5, 156.3, 151.7, 150.5, 142.8, 141.9, 141.0, 136.0, 135.0, 123.2, 121.4, 120.8, 110.5, 107.2, 72.9, 42.0, 34.5, 33.1, 29.2, 25.6, 23.1, 22.1, 20.4, 18.5, 15.1, 14.3, 13.7, 13.7, 11.9. FTIR ($\bar{\nu}$): 2929, 1713, 1653, 1567,

1427, 1339, 1261, 1222, 1174, 1148, 1112, 970, 912, 738. HRMS calculated for $C_{33}H_{41}N_6O_3$ $[M+H]^+$: 569.3235, observed: 569.3240. $[\alpha]_D^{20}$ = 13.9 (c = 0.4, $CHCl_3$).

(S)-3-((Z)-3-(3,6-bis(3,5-dimethyl-1H-pyrazol-1-yl)pyridazin-4-yl)allyl)-2-methyl-4-oxocyclopent-2-en-1-yl (1R,3R)-3-((Z)-3-methoxy-2-methyl-3-oxoprop-1-en-1-yl)-2,2-dimethylcyclopropane-1-carboxylate **91b**

Prepared as per general procedure using pyrethrin II **5b** (150 mg, 0.40 mmol), 3,6-bis(3',5'-dimethylpyrazol-1'-yl)-1,2,4,5-tetrazine **78** (108 mg, 0.40 mmol) and dry THF (5 mL). The reaction was heated under reflux for 8 h and subsequently purified by column chromatography (40% ethyl acetate in hexane) giving the pyridazine adduct **91b** (110 mg, 45%).

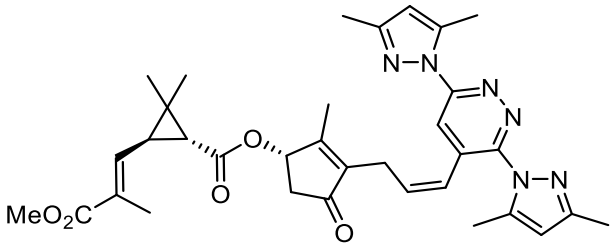

^{1}H NMR (600 MHz, $CDCl_3$) δ 8.28 (1H, s), 6.46 (1H, d, *J* = 9.6 Hz), 6.44 (1H, d, *J* = 11.7 Hz), 6.08 (1H, s), 6.02 (1H, s), 5.87 (1H, dt, *J* = 11.7, 7.4Hz), 5.65 (1H, d, *J* = 6.3 Hz), 3.74 (3H, s), 3.26 (2H, d, *J* = 7.4 Hz), 2.88 (1H, dd, *J* = 6.3, 18.8 Hz), 2.77 (3H, s), 2.32 (3H, s), 2.31 (3H, s), 2.28 (3H, s), 2.22 (2H, m), 1.99 (3H, s), 1.94 (3H, s), 1.29 (3H, s), 1.24 (1H, d, *J* = 7.0 Hz), 1.23 (3H, s); ^{13}C NMR (150 MHz, $CDCl_3$) δ 203.3, 171.1, 168.1, 166.0, 151.6, 150.4, 142.8, 141.8, 141.2, 138.9, 135.3, 134.1, 129.8, 123.3, 121.4, 110.5, 107.2, 73.3, 51.8, 41.9, 35.7, 32.9, 30.3, 29.7, 23.0, 22.3, 20.4, 15.0, 14.3, 13.7, 13.6, 12.9, 11.9. FTIR ($\bar{\nu}$): 2925, 1711, 1655, 1566, 1529, 1425, 1380, 1337, 1152, 1113, 969, 765. HRMS calculated for $C_{34}H_{41}N_6O_5$ $[M+H]^+$: 613.3133, observed: 613.3127. $[\alpha]_D^{20}$ = 13.3 (c = 0.8, $CHCl_3$).

(S)-3-((Z)-3-(3,6-dichloropyridazin-4-yl)allyl)-2-methyl-4-oxocyclopent-2-en-1-yl (1R,3R)-2,2-dimethyl-3-(2-methylprop-1-en-1-yl)cyclopropane-1-carboxylate **92a** and *(S)-3-(3-(3,6-dichloropyridazin-4-yl)propyl)-2-methyl-4-oxocyclopent-2-en-1-yl (1R,3R)-2,2-dimethyl-3-(2-methylprop-1-en-1-yl)cyclopropane-1-carboxylate* **93a**

Prepared as per general procedure using pyrethrin I **5a** (150 mg, 0.46 mmol), 3,6-dichloro-1,2,4,5-tetrazine **80** (70 mg, 0.46 mmol) and dry THF (5 mL). The reaction was heated under reflux for 8 h and the resulting mixture subjected to silica gel plug (50% ethyl acetate in hexane) giving a mixture of **92a** and **93a** (31% mass yield, 1:2.3; **92a**:**93a**).

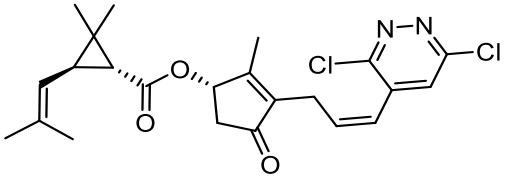

92a

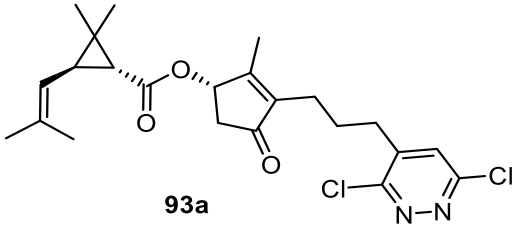

93a

^{1}H NMR (600 MHz, $CDCl_3$) δ 7.50 (0.3H, brs), 7.44 (0.7H, brs), 6.56 (0.6H, m), 5.72 (0.3H, d, *J* = 6.3 Hz), 5.67 (0.7H, d, *J* = 6.2 Hz), 4.90 (1H, d, *J* = 7.6 Hz), 3.26 (0.6H, m), 2.92 (0.3H, dd, *J* = 6.3, 18.6 Hz), 2.86 (0.7H, dd, *J* = 6.2, 18.6 Hz), 2.72 (1.4H, m), 2.32 (1.4H, m), 2.27 (1H, d, *J* = 18.6 Hz), 2.09 (0.9H, s), 2.04 (2.1H, s), 1.81 (1.4H, m), 1.72 (3H, s), 1.72 (3H, s), 1.41 (1H, d, *J* = 5.3 Hz), 1.26 (3H, s), 1.14 (3H, s); ^{13}C NMR (150 MHz, $CDCl_3$) δ 204.44, 172.25, 167.18, 166.01, 162.24, 156.87, 156.04, 155.99, 154.28, 150.85, 143.57, 142.38, 139.60, 138.12, 137.64, 136.07, 135.99, 129.07, 124.37, 123.19, 120.71, 120.65, 72.76, 42.04, 41.98, 34.48, 33.18, 33.09, 31.96, 29.24, 27.16, 25.65, 25.54, 22.53, 22.08, 20.39, 18.49, 14.23, 14.09 (some signals overlap).

(S)-3-((Z)-3-(3,6-dichloropyridazin-4-yl)allyl)-2-methyl-4-oxocyclopent-2-en-1-yl (1R,3R)-3-((E)-3-methoxy-2-methyl-3-oxoprop-1-en-1-yl)-2,2-dimethylcyclopropane-1-carboxylate **92b** and *(S)-3-(3-(3,6-dichloropyridazin-4-yl)propyl)-2-methyl-4-oxocyclopent-2-en-1-yl (1R,3R)-3-((E)-3-methoxy-2-methyl-3-oxoprop-1-en-1-yl)-2,2-dimethylcyclopropane-1-carboxylate* **93b**

Prepared as per general procedure using pyrethrin II **5b** (150 mg, 0.40 mmol), 3,6-dichloro-1,2,4,5-tetrazine **80** (60 mg, 0.40 mmol) and dry THF (5 mL). The reaction was heated under reflux for 8 h and the resulting mixture subjected to silica gel plug (50% ethyl acetate in hexane) giving a mixture of **92b** and **93b** (30% mass yield, 1:2.3; **92b**:**93b**).

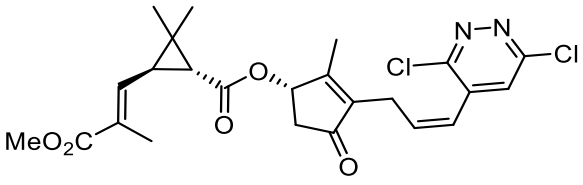

92b

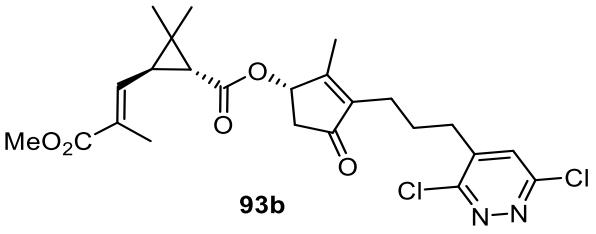

93b

^{1}H NMR (600 MHz, $CDCl_3$) δ 7.50 (0.3H, brs), 7.44 (0.7H, brs), 6.56 (0.6H, m), 6.45 (1H, d, *J* = 9.6 Hz), 5.72 (0.3H, d, *J* = 6.3 Hz), 5.67 (0.7H, d, *J* = 6.3 Hz), 3.73 (3H, s), 3.26 (0.6H, m), 2.93 (0.3H, dd, *J* = 6.3, 18.8 Hz), 2.88 (0.7H, dd, *J* = 6.3, 18.8 Hz), 2.72 (1.4H, m), 2.33 (1.4H, m), 2.23 (1H, m), 2.09 (0.9H, s), 2.04 (2.1H, s), 1.94 (3H, s), 1.81 (1.4H, m), 1.74 (1H, d, *J* = 5.2 Hz), 1.30 (3H, s), 1.24 (3H, s); ^{13}C NMR (150 MHz, $CDCl_3$) δ 204.16, 203.29, 171.16, 171.12, 168.09, 168.06, 166.71, 165.55, 156.85, 156.04, 155.98, 154.26, 143.54, 142.63, 139.86, 138.86, 138.75, 137.99, 137.61, 129.88, 129.82, 129.07, 124.38, 123.26, 73.22, 51.83, 41.95, 41.89, 35.69, 35.65, 33.07, 33.00, 31.97, 30.70, 30.65, 27.17, 25.61, 22.56, 22.29, 20.39, 14.20, 14.08, 12.87 (some signals overlap).

7.2.3 Mizoroki-Heck chemistry

General procedure for Mizoroki-Heck coupling of aryl iodides with pyrethrins

Pyrethrin **5** (150 mg, 0.46 mmol (pyrethrin I **5a**) or 0.40 mmol (pyrethrin II **5b**)) was added to a stirring mixture of silver acetate (1.5 eq), triphenylphosphine (7.5 mol%), palladium acetate (2.5 mol%) and aryl iodide (1.2 eq) in dry acetonitrile (5 mL) under nitrogen. The resulting mixture was allowed to stir at RT for 30 min before being refluxed for 16 h. The suspension was cooled to RT and filtered over Celite. The filtrate was diluted with HCl (1 M) and extracted with DCM. The organic fraction was dried (Na_2SO_4) and solvent removed *in vacuo*. The resulting mixture was purified by column chromatography (ethyl acetate in hexane) as stated to give the product.

Iodobenzene with pyrethrin I

Prepared as per general procedure using pyrethrin I **5a** (150 mg, 0.46 mmol), silver acetate (117 mg, 0.70 mmol), triphenylphosphine (9 mg, 0.03 mmol), palladium acetate (3 mg, 0.01 mmol) and iodobenzene (62 µL, 0.55 mmol) in dry acetonitrile (5 mL). The resulting mixture was purified by column chromatography (10% ethyl acetate in hexane) giving **111a** (48 mg, 26%) and **125a** (55 mg, 30%).

(S)-2-methyl-4-oxo-3-((2E,4E)-5-phenylpenta-2,4-dien-1-yl)cyclopent-2-en-1-yl (1R,3R)-2,2-dimethyl-3-(2-methylprop-1-en-1-yl)cyclopropane-1-carboxylate **111a**

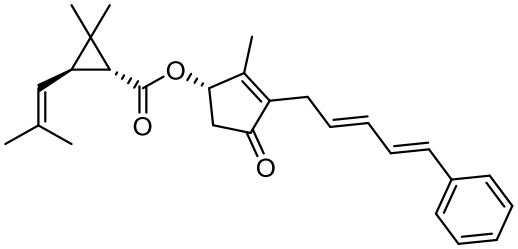

^{1}H NMR (600 MHz, $CDCl_3$) δ 7.34 (2H, d, *J* = 7.7 Hz), 7.29 (2H, dd, *J* = 7.3, 7.7 Hz), 7.19 (1H, t, *J* = 7.3 Hz), 6.71 (1H, dd, *J* = 10.5, 15.7 Hz), 6.46 (1H, d, *J* = 15.7 Hz), 6.21 (1H, dd, *J* = 10.5, 15.1 Hz), 5.75 (1H, dt, *J* =15.1, 6.9 Hz), 5.68 (1H, d, *J* = 6.3 Hz), 4.90 (1H, d, *J* = 7.8 Hz), 3.08 (2H, d, *J* = 6.8 Hz), 2.89 (1H, dd, *J* = 6.3, 18.7 Hz), 2.25 (1H, dd, *J* = 1.4, 18.7 Hz), 2.09 (1H, m), 2.06 (3H, s), 1.72 (3H, s), 1.71 (3H, s), 1.41 (1H, d, *J* = 5.3 Hz), 1.26 (3H, s), 1.14 (3H, s); ^{13}C NMR (150 MHz, $CDCl_3$) δ 203.91, 172.35, 165.78, 141.59, 137.35, 135.96, 131.96, 131.35, 129.45, 128.63, 128.60, 127.39, 126.25, 120.82, 72.97, 42.10, 34.59, 33.03, 29.19, 26.35, 25.58, 22.13, 20.44, 18.53, 14.15. FTIR ($\bar{\nu}$): 3024, 2925, 1714, 1656, 1447, 1421, 1380, 1282, 1235, 1193, 1152, 1114, 990, 848, 749, 692. HRMS calculated for $C_{27}H_{33}O_3$ $[M+H]^+$: 405.2424; observed: 405.2458. $[\alpha]_D^{20}$ = −34.0 (c= 0.5, $CHCl_3$).

(S)-2-methyl-4-oxo-3-((1E,3E)-5-phenylpenta-1,3-dien-1-yl)cyclopent-2-en-1-yl (1R,3R)-2,2-dimethyl-3-(2-methylprop-1-en-1-yl)cyclopropane-1-carboxylate **125a**

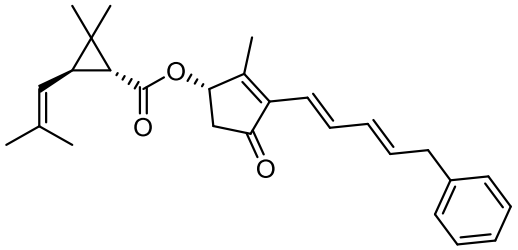

^{1}H NMR (600 MHz, $CDCl_3$) δ 7.38 (1H, dd, *J* = 10.4, 15.7 Hz), 7.29 (2H, dd, *J* = 7.3, 7.7 Hz), 7.20 (3H, m), 6.09 (3H, m), 5.68 (1H, d, *J* = 6.4 Hz), 4.91 (1H, d, *J* = 7.7 Hz), 3.47 (2H, d, *J* = 6.6 Hz), 2.90 (1H, dd, *J* = 6.4, 18.7 Hz), 2.27 (1H, dd, *J* = 1.9, 18.7 Hz), 2.08 (3H, s), 2.04 (1H, m), 1.72 (3H, s), 1.71 (3H, s), 1.41 (1H, d, *J* = 5.4 Hz), 1.26 (3H, s), 1.14 (3H, s); ^{13}C NMR (150 MHz, $CDCl_3$) δ 203.2, 172.4, 163.7, 139.8, 137.7, 136.4, 136.0, 135.7, 132.2, 128.7, 128.5, 126.2, 120.8, 118.8, 72.6, 42.8, 39.2, 34.6, 33.0, 29.2, 25.6, 20.5, 18.5, 14.2. FTIR ($\bar{\nu}$): 3026, 2925, 1714, 1637, 1585, 1494, 1452, 1421, 1380, 1282, 1235, 1193, 1152, 1114, 985, 849, 748, 699. HRMS calculated for $C_{27}H_{33}O_3$ $[M+H]^+$: 405.2424; observed: 405.2416. $[\alpha]_D^{20}$ = −96.0 (c = 0.5, $CHCl_3$).

Iodobenzene with pyrethrin II

Prepared as per general procedure using pyrethrin II **5b** (150 mg, 0.40 mmol), silver acetate (100 mg, 0.6 mmol), triphenylphosphine (9 mg, 0.03 mmol), palladium acetate (3 mg, 0.01 mmol) and 4-iodobenzene (54 µL, 0.48 mmol) in dry acetonitrile (5 mL). The resulting mixture was purified by column chromatography (20% ethyl acetate in hexane) giving **111b** (31 mg, 17%) and **125b** (31 mg, 17%).

(S)-2-methyl-4-oxo-3-((2E,4E)-5-phenylpenta-2,4-dien-1-yl)cyclopent-2-en-1-yl (1R,3R)-3-((E)-3-methoxy-2-methyl-3-oxoprop-1-en-1-yl)-2,2-dimethylcyclopropane-1-carboxylate **111b**

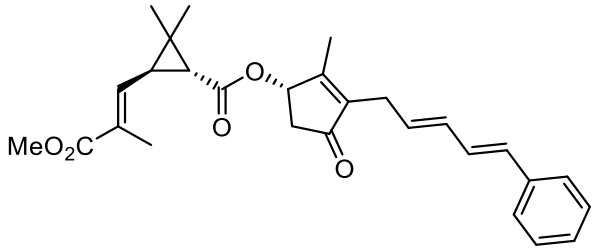

^{1}H NMR (600 MHz, $CDCl_3$) δ 7.35 (2H, d, *J* = 7.7 Hz), 7.29 (2H, dd, *J* = 7.3, 7.7 Hz), 7.20 (1H, t, *J* = 7.3 Hz), 6.71 (1H, dd, *J* = 10.4, 15.7 Hz), 6.47 (2H, m), 6.21 (1H, dd, *J* = 10.4, 15.1 Hz), 5.75 (1H, dt, *J* =15.1, 6.9Hz), 5.68 (1H, d, *J* = 6.2 Hz), 3.73 (3H, s), 3.08 (2H, d, *J* = 6.9 Hz), 2.90 (1H, dd, *J* = 6.2, 18.7 Hz), 2.24 (2H, m), 2.06 (3H, s), 1.95 (3H, s), 1.75 (1H, d, *J* = 5.2 Hz), 1.31 (3H, s), 1.24 (3H, s); ^{13}C NMR (150 MHz, $CDCl_3$) δ 203.59, 171.22, 168.11, 165.25, 141.82, 138.96, 137.28, 132.01, 131.39, 129.78, 129.46, 128.57, 128.55, 127.38, 126.22, 73.42, 51.82, 41.99, 35.77, 32.92, 30.58, 26.32, 22.32, 20.41, 14.11, 12.88. FTIR ($\bar{\nu}$): 3024, 2951, 1713, 1645, 1435, 1383, 1262, 1222, 1174, 1148, 1112, 992, 829, 750. HRMS calculated for $C_{28}H_{33}O_5$ $[M+H]^+$: 449.2323; observed: 449.2345. $[\alpha]_D^{20} = -36.7$ (c = 0.3, $CHCl_3$).

(S)-2-methyl-4-oxo-3-((1E,3E)-5-phenylpenta-2,4-dien-1-yl)cyclopent-2-en-1-yl (1R,3R)-3-((E)-3-methoxy-2-methyl-3-oxoprop-1-en-1-yl)-2,2-dimethylcyclopropane-1-carboxylate **125b**

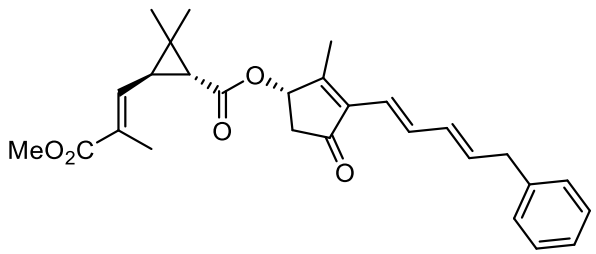

^{1}H NMR (600 MHz, $CDCl_3$) δ 7.39 (1H, dd, *J* = 10.3, 15.7 Hz), 7.29 (2H, dd, *J* = 7.3, 7.7 Hz), 7.20 (3H, m), 6.45 (1H, d, *J* = 9.7 Hz), 6.11 (2H, m), 6.07 (1H, m), 5.66 (1H, d, *J* = 6.4 Hz), 3.73 (3H, s), 3.47 (2H, d, *J* = 6.6 Hz), 2.91 (1H, dd, *J* = 6.4, 18.7 Hz), 2.26 (1H, dd, *J* = 2.0, 18.7 Hz), 2.22 (1H, m), 2.08 (3H, s), 1.94 (3H, s), 1.74 (1H, d, *J* = 5.3 Hz), 1.30 (3H, s), 1.23 (3H, s); ^{13}C NMR (150 MHz, $CDCl_3$) δ 202.9, 171.2, 168.1, 164.4, 163.1, 139.0, 136.6, 135.9, 132.2, 129.8, 128.7, 128.5, 126.2, 125.6, 118.6, 73.0, 51.8, 42.7, 42.0, 39.2, 35.8, 32.9, 30.6, 22.3, 20.4, 14.2. 12.8. FTIR ($\bar{\nu}$): 2952, 1712, 1643, 1435, 1384, 1263, 1222, 1174, 1148, 1112, 995, 830, 760, 700. HRMS calculated for $C_{28}H_{33}O_5$ $[M+H]^+$: 449.2323; observed: 449.2341. $[\alpha]_D^{20} = -33.3$ (c = 0.3, $CHCl_3$).

1-iodo-4-nitrobenzene with pyrethrin I

Prepared as per general procedure using pyrethrin I **5a** (150 mg, 0.46 mmol), silver acetate (117 mg, 0.70 mmol), triphenylphosphine (9 mg, 0.03 mmol), palladium acetate (3 mg, 0.01 mmol) and 1-iodo-4-nitrobenzene (136 mg, 0.55 mmol) in dry acetonitrile (5 mL). The resulting mixture was purified by column chromatography (15% ethyl acetate in hexane) giving **129a** (90 mg, 44%).

(S)-2-methyl-3-((2E,4E)-5-(4-nitrophenyl)penta-2,4-dien-1-yl)-4-oxocyclopent-2-en-1-yl (1R,3R)-2,2-dimethyl-3-(2-methylprop-1-en-1-yl)cyclopropane-1-carboxylate **129a**

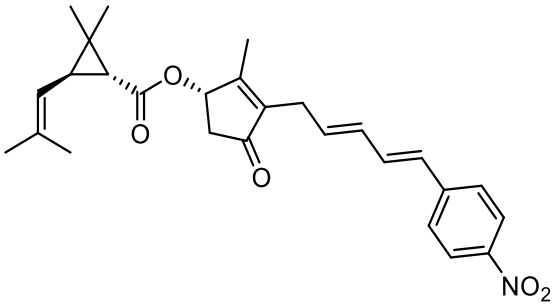

^{1}H NMR (600 MHz, $CDCl_3$) δ 8.14 (2H, d, *J* = 8.7 Hz), 7.45 (2H, d, *J* = 8.7 Hz), 6.85 (1H, dd, *J* = 10.5, 15.7 Hz), 6.50 (1H, d, *J* = 15.7 Hz), 6.25 (1H, dd, *J* = 10.5, 15.1 Hz), 5.90 (1H, dt, *J* =15.1, 6.9 Hz), 5.70 (1H, d, *J* = 6.2 Hz), 4.90 (1H, d, *J* = 6.8 Hz), 3.11 (2H, d, *J* = 6.9 Hz), 2.90 (1H, dd, *J* = 6.2, 18.7 Hz), 2.26 (1H, dd, *J* = 1.4, 18.7 Hz), 2.09 (1H, m), 2.06 (3H, s), 1.71 (3H, s), 1.70 (3H, s), 1.41 (1H, d, *J* = 5.2 Hz), 1.26 (3H, s), 1.14 (3H, s); ^{13}C NMR (150 MHz, $CDCl_3$) δ 203.8, 172.3, 166.1, 143.9, 141.1, 136.0, 134.8, 133.3, 133.2, 131.3, 129.5, 128.9, 126.6, 124.5, 124.1, 123.7, 120.8, 72.9, 42.1, 34.6, 33.1, 29.3, 26.5, 25.6, 22.1, 20.4, 18.5, 14.2. FTIR ($\bar{\nu}$): 2926,

1711, 1656, 1591, 1421, 1380, 1340, 1282, 1193, 1152, 1112, 991, 863, 849, 826, 747. HRMS calculated for $C_{27}H_{32}NO_5$ $[M+H]^+$: 450.2275; observed: 450.2303. $[\alpha]_D^{20}$= −55.6 (c = 0.9, $CHCl_3$).

1-iodo-4-nitrobenzene with pyrethrin II

Prepared as per general procedure using pyrethrin II **5b** (150 mg, 0.40 mmol), silver acetate (100 mg, 0.6 mmol), triphenylphosphine (9 mg, 0.03 mmol), palladium acetate (3 mg, 0.01 mmol) and 1-iodo-4-nitrobenzene (120 mg, 0.48 mmol) in dry acetonitrile (5 mL). The resulting mixture was purified by column chromatography (25% ethyl acetate in hexane) giving **129b** (62 mg, 31%).

(S)-2-methyl-3-((2E,4E)-5-(4-nitrophenyl)penta-2,4-dien-1-yl)-4-oxocyclopent-2-en-1-yl (1R,3R)-3-((E)-3-methoxy-2-methyl-3-oxoprop-1-en-1-yl)-2,2-dimethylcyclopropane-1-carboxylate **129b**

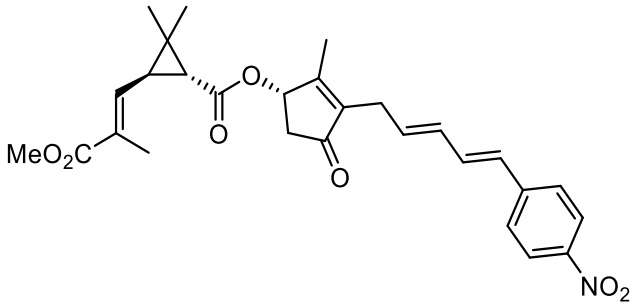

^{1}H NMR (600 MHz, $CDCl_3$) δ 8.15 (2H, d, *J* = 8.7 Hz), 7.46 (2H, d, *J* = 8.7 Hz), 6.85 (1H, dd, *J* = 10.4, 15.6 Hz), 6.50 (1H, d, *J* = 15.6 Hz), 6.46 (1H, d, *J* = 9.5 Hz), 6.25 (1H, dd, *J* = 10.4, 15.1 Hz), 5.90 (1H, dt, *J* =15.1, 6.8 Hz), 5.70 (1H, d, *J* = 6.3 Hz), 3.73 (3H, s), 3.12 (2H, d, *J* = 6.8 Hz), 2.91 (1H, dd, *J* = 6.3, 18.7 Hz), 2.24 (2H, m), 2.06 (3H, s), 1.95 (3H, s), 1.74 (1H, d, *J* = 5.2 Hz), 1.31 (3H, s), 1.24 (3H, s); ^{13}C NMR (150 MHz, $CDCl_3$) δ 203.51, 171.19, 168.12, 165.59, 146.60, 143.86, 151.31, 138.89, 133.10, 133.07, 131.37, 129.83, 128.97, 126.53, 124.08, 73.33, 51.84, 41.95, 35.73, 32.99, 30.63, 26.45, 22.32, 20.40, 14.12, 12.88. FTIR ($\bar{\nu}$): 2951, 2926, 1710, 1642, 1592, 1515, 1435, 1383, 1340, 1263, 1222, 1175, 1148, 1111, 992, 827, 748. HRMS calculated for $C_{28}H_{32}NO_7$ $[M+H]^+$: 494.2173; observed: 494.2182. $[\alpha]_D^{20}$= −23.3 (c = 0.6, $CHCl_3$).

1-iodo-3-nitrobenzene and pyrethrin I

Prepared as per general procedure using pyrethrin I **5a** (150 mg, 0.46 mmol), silver acetate (117 mg, 0.70 mmol), triphenylphosphine (9 mg, 0.03 mmol), palladium acetate (3 mg, 0.01 mmol) and 1-iodo-3-nitrobenzene (136 mg, 0.55 mmol) in dry acetonitrile (5 mL). The resulting mixture was purified by column chromatography (10% ethyl acetate in hexane) giving **130a** (60 mg, 30%) and **135a** (40 mg, 19%).

(S)-2-methyl-3-((1E,3E)-5-(3-nitrophenyl)penta-1,3-dien-1-yl)-4-oxocyclopent-2-en-1-yl (1R,3R)-2,2-dimethyl-3-(2-methylprop-1-en-1-yl)cyclopropane-1-carboxylate **130a**

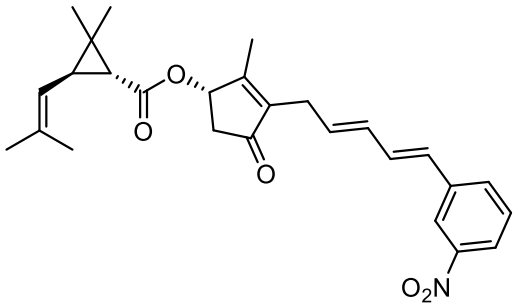

^{1}H NMR (600 MHz, $CDCl_3$) δ 8.19 (1H, brs), 8.04 (1H, dd, *J* = 1.9, 8.2 Hz), 7.63 (1H, d, *J* = 7.7 Hz), 7.45 (1H, dd, *J* = 7.7, 8.2Hz), 6.82 (1H, dd, *J* = 10.4, 15.7 Hz), 6.49 (1H, d, *J* = 15.7 Hz), 6.24 (1H, dd, *J* = 10.4, 15.1 Hz), 5.86 (1H, dt, *J* = 15.1, 6.9Hz), 5.70 (1H, d, *J* = 6.3 Hz), 4.91 (1H, d, *J* = 7.7 Hz), 3.11 (2H, d, *J* = 6.9 Hz), 2.90 (1H, dd, *J* = 6.3, 18.7 Hz), 2.27 (1H, dd, *J* = 1.9, 18.7 Hz), 2.09 (1H, m), 2.07 (3H, s), 1.72 (3H, s), 1.71 (3H, s), 1.42 (1H, d, *J* = 5.4 Hz), 1.26 (3H, s), 1.14 (31H, s); ^{13}C NMR (150 MHz, $CDCl_3$) 203.8, 172.3, 166.0, 148.7, 141.2, 139.2, 136.0, 132.3, 131.9, 131.6, 131.2, 129.5, 128.6, 121.8, 120.8, 120.6, 72.9, 42.1, 34.5, 33.1, 29.2, 26.4, 25.6, 22.1, 20.4, 18.5, 14.2. FTIR ($\bar{\nu}$): 2925, 2872, 1713, 1655, 1529, 1422, 1380, 1350, 1282, 1235, 1193, 1153, 1114, 991, 854, 822, 734. HRMS calculated for $C_{27}H_{32}NO_5$ $[M+H]^+$: 450.2275; observed: 450.2270. $[\alpha]_D^{20} = -44.8$ (c = 0.6, $CHCl_3$).

(S)-2-methyl-3-((1E,3E)-5-(3-nitrophenyl)penta-1,3-dien-1-yl)-4-oxocyclopent-2-en-1-yl (1R,3R)-2,2-dimethyl-3-(2-methylprop-1-en-1-yl)cyclopropane-1-carboxylate **135a**

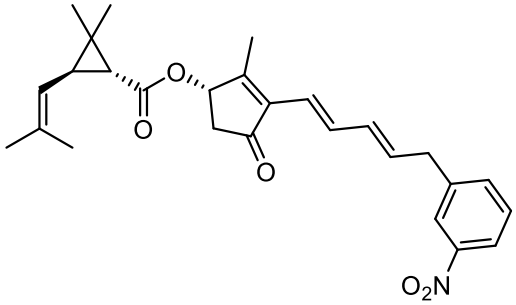

^{1}H NMR (600 MHz, $CDCl_3$) δ 8.09 (1H, d, *J* = 8.1 Hz), 8.06 (1H, brs), 7.52 (1H, d, *J* = 7.5 Hz), 7.47 (1H, dd, *J* = 7.5, 8.1 Hz), 7.41 (1H, dd, *J* = 10.4, 15.4 Hz), 6.17 (2H, m), 6.03 (1H, m), 5.68 (1H, d, *J* = 6.4 Hz), 4.91 (1H, d, *J* = 7.8 Hz), 3.57 (2H, d, *J* = 6.8 Hz), 2.91 (1H, dd, *J* = 6.4, 18.7 Hz), 2.28 (1H, dd, *J* = 1.9, 18.7 Hz), 2.10 (3H, s), 2.08 (1H, m), 1.72 (3H, s), 1.71 (3H, s), 1.41 (1H, d, *J* = 5.2 Hz), 1.26 (3H, s), 1.14 (3H, s); ^{13}C NMR (150 MHz, $CDCl_3$) δ 203.1, 172.3, 164.4, 148.5, 141.9, 137.4, 136.0, 135.0, 134.9, 134.0, 133.5, 129.4, 123.6, 121.5, 120.8, 119.8, 72.5, 42.8, 38.7, 34.6, 33.0, 29.2, 25.6, 22.1, 20.4, 18.5, 14.2. FTIR ($\bar{\nu}$): 2922, 2872, 1713, 1583, 1529, 1422, 1380, 1351, 1282, 1234, 1193, 1152, 1114, 1082, 996, 849, 805, 733. HRMS calculated for $C_{27}H_{32}NO_5$ $[M+H]^+$: 450.2275; observed: 450.2279. $[\alpha]_D^{20} = -128.9$ (c = 0.4, $CHCl_3$).

1-iodo-3-nitrobenzene and pyrethrin II

Prepared as per general procedure using pyrethrin II **5b** (150 mg, 0.40 mmol), silver acetate (100 mg, 0.6 mmol), triphenylphosphine (9 mg, 0.03 mmol), palladium acetate (3 mg, 0.01 mmol) and 1-iodo-3-nitrobenzene (120 mg, 0.48 mmol) in dry acetonitrile (5 mL). The resulting mixture was purified by column chromatography (20% ethyl acetate in hexane) giving **130b** (30 mg, 15%) and **135b** (21 mg, 11%).

(S)-2-methyl-3-((2E,4E)-5-(3-nitrophenyl)penta-2,4-dien-1-yl)-4-oxocyclopent-2-en-1-yl (1R,3R)-3-((E)-3-methoxy-2-methyl-3-oxoprop-1-en-1-yl)-2,2-dimethylcyclopropane-1-carboxylate **130b**

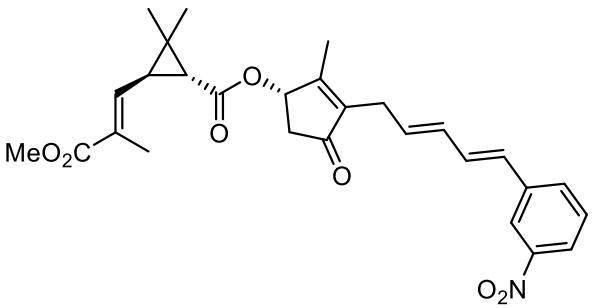

^{1}H NMR (600 MHz, $CDCl_3$) δ 8.20 (1H, brs), 8.04 (1H, d, *J* = 8.1 Hz), 7.64 (1H, d, *J* = 7.6 Hz), 7.46 (1H, dd, *J* = 7.6, 8.1 Hz), 6.82 (1H, dd, *J* = 10.4, 15.6 Hz), 6.50 (1H, d, *J* = 15.6 Hz), 6.46 (1H, d, *J* = 9.6 Hz), 6.24 (1H, dd, *J* = 10.4, 15.1 Hz), 5.87 (1H, dt, *J* =15.1, 6.9 Hz), 5.70 (1H, d, *J* = 6.4 Hz), 3.74 (3H, s), 3.11 (2H, d, *J* = 6.9 Hz), 2.91 (1H, dd, *J* = 6.4, 18.7 Hz), 2.24 (2H, m), 2.07 (3H, s), 1.96 (3H, s), 1.75 (1H, d, *J* = 5.2 Hz), 1.32 (3H, s), 1.25 (3H, s); ^{13}C NMR (150 MHz, $CDCl_3$) δ 203.5, 171.2, 168.1, 165.5, 148.7, 141.4, 139.2, 138.9, 132.1, 131.9, 131.5, 131.2, 129.8, 129.5, 128.7, 121.8, 120.6, 73.4, 51.8, 42.0, 35.8, 24.0, 30.6, 26.4, 22.3, 20.4, 14.1, 12.9. FTIR ($\bar{\nu}$): 2957, 2925, 1712, 1644, 1529, 1435, 1383, 1351, 1263, 1222, 1175, 1148, 1112, 992, 823, 735. HRMS calculated for $C_{28}H_{32}NO_7$ $[M+H]^+$: 494.2173; observed: 494.2187. $[\alpha]_D^{20}$= −20.0 (c = 0.3, $CHCl_3$).

(S)-2-methyl-3-((1E,3E)-5-(3-nitrophenyl)penta-1,3-dien-1-yl)-4-oxocyclopent-2-en-1-yl (1R,3R)-3-((E)-3-methoxy-2-methyl-3-oxoprop-1-en-1-yl)-2,2-dimethylcyclopropane-1-carboxylate **135b**

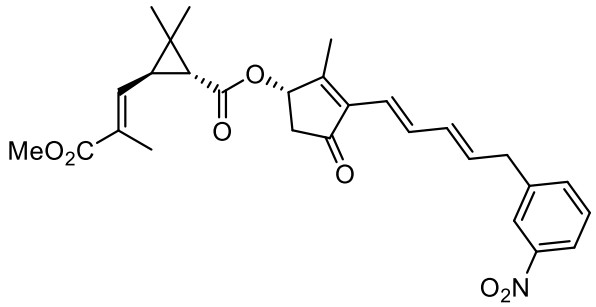

^{1}H NMR (600 MHz, $CDCl_3$) δ 8.08 (1H, d, *J* = 8.1 Hz), 8.06 (1H, brs), 7.51 (1H, d, *J* = 7.6 Hz), 7.47 (1H, dd, *J* = 7.6, 8.1 Hz), 7.42 (1H, dd, *J* = 10.6, 15.6 Hz), 6.46 (1H, d, *J* = 9.7 Hz), 6.17 (2H, m), 6.04 (1H, m), 5.68 (1H, d, *J* = 6.5 Hz), 3.74 (3H, s), 3.58 (2H, d, *J* = 6.9 Hz), 2.92 (1H, dd, *J* = 6.5, 18.7 Hz), 2.28 (1H, dd, *J* = 1.9, 18.7 Hz), 2.23 (1H, m), 2.10 (3H, s), 1.95 (3H, s), 1.75 (1H, d, *J* = 5.3 Hz), 1.31 (3H, s), 1.24 (3H, s); ^{13}C NMR (150 MHz, $CDCl_3$) δ 202.8, 171.2, 168.1, 163.8, 141.8, 138.9, 137.6, 135.2, 134.9, 134.1, 133.4, 129.8, 129.4, 123.5, 123.3, 121.5, 119.6, 73.0, 51.8, 43.0, 38.7, 35.8, 32.9, 30.6, 22.3, 20.4, 14.2, 12.9. FTIR ($\bar{\nu}$): 2957, 2925, 2854, 1712, 1642, 1529, 1435, 1385, 1351, 1262, 1222, 1174, 1148, 1112, 996, 825, 734. HRMS calculated for $C_{28}H_{32}NO_7$ $[M+H]^+$: 494.2173; observed: 494.2175. $[\alpha]_D^{20}$= −105.0 (c = 0.2, $CHCl_3$).

1-iodo-2-nitrobenzene and pyrethrin I

Prepared as per general procedure using pyrethrin I **5a** (150 mg, 0.46 mmol), silver acetate (117 mg, 0.70 mmol), triphenylphosphine (9 mg, 0.03 mmol), palladium acetate (3 mg, 0.01 mmol) and 1-iodo-2-nitrobenzene (136 mg, 0.55 mmol) in dry acetonitrile (5 mL). The resulting mixture was purified by column chromatography (15% ethyl acetate in hexane) giving **131a** (61 mg, 30%) and **136a** (15 mg, 7%).

(S)-2-methyl-3-((2E,4E)-5-(2-nitrophenyl)penta-2,4-dien-1-yl)-4-oxocyclopent-2-en-1-yl (1R,3R)-2,2-dimethyl-3-(2-methylprop-1-en-1-yl)cyclopropane-1-carboxylate **131a**

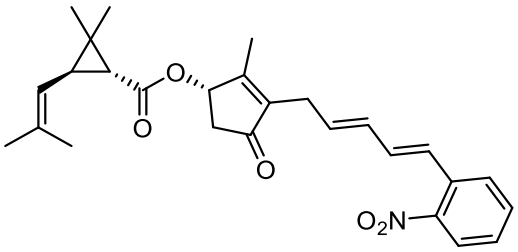

^{1}H NMR (600 MHz, $CDCl_3$) δ 7.88 (1H, d, *J* = 8.2 Hz), 7.61 (1H, d, *J* = 8.0 Hz), 7.53 (1H, dd, *J* = 8.0, 7.7 Hz), 7.34 (1H, dd, *J* = 8.2, 7.7 Hz), 6.94 (1H, d, *J* = 15.5 Hz), 6.71 (1H, dd, *J* = 10.4, 15.5 Hz), 6.25 (1H, dd, *J* = 10.4, 15.1 Hz), 5.89 (1H, dt, *J* = 15.1, 6.7 Hz), 5.70 (1H, d, *J* = 6.3 Hz), 4.91 (1H, d, *J* = 7.1 Hz), 3.09 (2H, d, *J* = 6.7 Hz), 2.90 (1H, dd, *J* = 6.3, 18.7 Hz), 2.26 (1H, d, *J* = 18.7 Hz), 2.10 (1H, m), 2.07 (3H, s), 1.72 (3H, s), 1.71 (3H, s), 1.43 (1H, d, *J* = 5.3 Hz), 1.27 (3H, s), 1.15 (3H, s); ^{13}C NMR (150 MHz, $CDCl_3$) δ 203.8, 172.3, 166.1, 147.8, 141.1, 135.9, 133.8, 132.8, 132.7, 132.7, 131.4, 127.7, 125.5, 124.7, 120.8, 72.9, 42.1, 35.5, 33.0, 29.2, 26.4, 25.5, 22.1, 20.4, 18.5, 14.1. FTIR ($\bar{\nu}$): 2925, 2857, 1713, 1656, 1604, 1523, 1442, 1421, 1345, 1282, 1235, 1193, 1152, 1114, 991, 859, 783, 742. HRMS calculated for $C_{27}H_{32}NO_5$ $[M+H]^+$: 450.2275; observed: 450.2284. $[\alpha]_D^{20} = -28.3$ (c = 0.6, $CHCl_3$).

(S)-2-methyl-3-((1E,3E)-5-(2-nitrophenyl)penta-1,3-dien-1-yl)-4-oxocyclopent-2-en-1-yl (1R,3R)-3-((E)-3-methoxy-2-methyl-3-oxoprop-1-en-1-yl)-2,2-dimethylcyclopropane-1-carboxylate **136a**

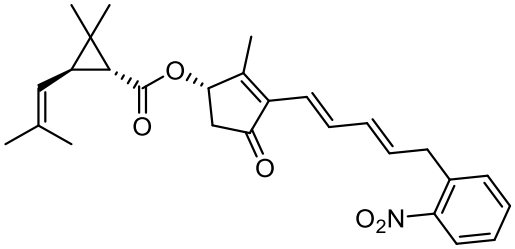

^{1}H NMR (600 MHz, $CDCl_3$) δ 7.93 (1H, d, *J* = 8.2 Hz), 7.54 (1H, dd, *J* = 7.5, 8.0 Hz), 7.36 (3H, m), 6.15 (2H, m), 6.03 (1H, m), 5.67 (1H, d, *J* = 6.4 Hz), 4.90 (1H, d, *J* = 7.9 Hz), 3.76 (2H, d, *J* = 6.8 Hz), 2.89 (1H, dd, *J* = 6.4, 18.7 Hz), 2.27 (1H, dd, *J* = 2.2, 18.7 Hz), 2.08 (3H, s), 2.07 (1H, m), 1.72 (3H, s), 1.70 (3H, s), 1.40 (1H, d, *J* = 5.4 Hz), 1.25 (3H, s), 1.13 (3H, s); ^{13}C NMR (150 MHz, $CDCl_3$) δ 203.1, 172.3, 164.2, 137.4, 135.9, 135.1, 134.8, 133.4, 133.3, 133.1, 131.9, 127.4, 124.8, 120.8, 119.6, 72.5, 42.7, 36.1, 34.6, 33.0, 29.1, 25.5, 22.1, 20.4, 14.2. FTIR ($\bar{\nu}$): 2925, 2860, 1713, 1608, 1583, 1526, 1421, 1379, 1350, 1282, 1234, 1193, 1152, 1114, 1081, 1064, 995, 857, 786, 745. HRMS calculated for $C_{28}H_{32}NO_7$ $[M+H]^+$: 450.2275; observed: 450.2268. $[\alpha]_D^{20}$= −133.3 (c = 0.2, $CHCl_3$).

1-iodo-2-nitrobenzene and pyrethrin II

Prepared as per general procedure using pyrethrin II **5b** (150 mg, 0.40 mmol), silver acetate (100 mg, 0.6 mmol), triphenylphosphine (9 mg, 0.03 mmol), palladium acetate (3 mg, 0.01 mmol) and 1-iodo-2-nitrobenzene (120 mg, 0.48 mmol) in dry acetonitrile (5 mL). The resulting mixture was purified by column chromatography (25% ethyl acetate in hexane) giving **131b** (40 mg, 20%) and **136b** (24 mg, 12%).

(S)-2-methyl-3-((2E,4E)-5-(2-nitrophenyl)penta-2,4-dien-1-yl)-4-oxocyclopent-2-en-1-yl (1R,3R)-3-((E)-3-methoxy-2-methyl-3-oxoprop-1-en-1-yl)-2,2-dimethylcyclopropane-1-carboxylate **131b**

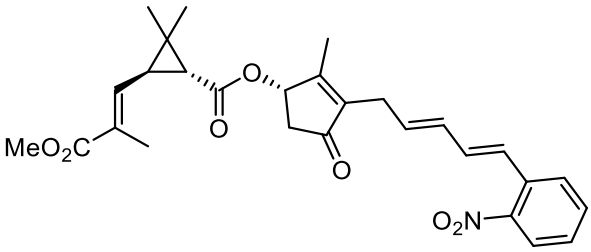

^{1}H NMR (600 MHz, $CDCl_3$) δ 7.88 (1H, d, *J* = 8.1 Hz), 7.61 (1H, d, *J* = 8.1 Hz), 7.53 (1H, dd, *J* = 7.4, 8.1 Hz), 7.34 (1H, dd, *J* = 7.4, 8.1 Hz), 6.94 (1H, d, *J* = 15.5 Hz), 6.71 (1H, dd, *J* = 10.4, 15.5

Hz), 6.46 (1H, d, *J* = 9.6 Hz), 6.25 (1H, dd, *J* = 10.4, 15.2 Hz), 5.88 (1H, dt, *J* =15.2, 6.8 Hz), 5.70 (1H, d, *J* = 6.3 Hz), 3.73 (3H, s), 3.10 (2H, d, *J* = 6.8 Hz), 2.91 (1H, dd, *J* = 6.3, 18.8 Hz), 2.25 (2H, m), 2.07 (3H, s), 1.95 (3H, s), 1.76 (1H, d, *J* = 5.2 Hz), 1.32 (3H, s), 1.24 (3H, s); ^{13}C NMR (150 MHz, $CDCl_3$) δ 203.56, 171.21, 168.11, 165.65, 141.41, 138.94, 133.71, 132.83, 132.52, 131.47, 129.80, 127.69, 127.67, 125.55, 124.67, 73.39, 51.82, 41.98, 35.75, 32.97, 30.62, 26.38, 22.32, 20.42, 14.14, 12.89. FTIR ($\bar{\nu}$): 2952, 2926, 1712, 1643, 1523, 1435, 1345, 1264, 1222, 1175, 1149, 1112, 992, 830, 743. HRMS calculated for $C_{28}H_{32}NO_7$ $[M+H]^+$: 494.2173; observed: 494.2180. $[\alpha]_D^{20}$= −20.8 (c = 0.2, $CHCl_3$).

(S)-2-methyl-3-((1E,3E)-5-(2-nitrophenyl)penta-1,3-dien-1-yl)-4-oxocyclopent-2-en-1-yl (1R,3R)-3-((E)-3-methoxy-2-methyl-3-oxoprop-1-en-1-yl)-2,2-dimethylcyclopropane-1-carboxylate **136b**

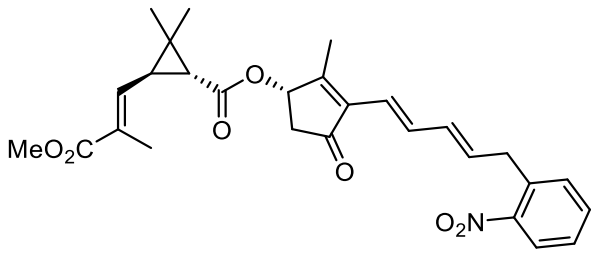

^{1}H NMR (600 MHz, $CDCl_3$) δ 7.87 (1H, d, *J* = 8.0 Hz), 7.47 (1H, dd, *J* = 7.7, 8.0 Hz), 7.31 (3H, m), 6.46 (1H, d, *J* = 10.5 Hz), 6.15 (2H, m), 6.04 (1H, m), 5.67 (1H, d, *J* = 6.5 Hz), 3.77 (2H, d, *J* = 6.8 Hz), 3.73 (3H, s), 2.92 (1H, dd, *J* = 6.5, 18.7 Hz), 2.27 (1H, dd, *J* = 2, 18.7 Hz), 2.09 (3H, s), 1.94 (3H, s), 1.74 (1H, d, *J* = 5.3 Hz), 1.30 (3H, s), 1.23 (3H, s); ^{13}C NMR (150 MHz, $CDCl_3$) δ 202.8, 171.2, 168.1, 163.8, 141.8, 138.9, 137.6, 135.1, 134.9, 134.1, 133.4, 129.4, 123.5, 121.5, 119.6, 72.9, 51.8, 42.7, 38.7, 35.8, 32.9, 30.6, 22.3, 20.4, 14.2, 12.9. FTIR ($\bar{\nu}$): 2954, 2926, 1712, 1526, 1435, 1348, 1263, 1222, 1148, 1112, 996, 744. HRMS calculated for $C_{28}H_{32}NO_7$ $[M+H]^+$: 494.2173; observed: 494.2191. $[\alpha]_D^{20}$= −38.1 (c = 0.2, $CHCl_3$).

4-iodoanisole and pyrethrin I

Prepared as per general procedure using pyrethrin I **5a** (150 mg, 0.46 mmol), silver acetate (117 mg, 0.70 mmol), triphenylphosphine (9 mg, 0.03 mmol), palladium acetate (3 mg, 0.01 mmol) and 4-iodoanisole (129 mg, 0.55 mmol) in dry acetonitrile (5 mL). The resulting mixture

was purified by column chromatography (10% ethyl acetate in hexane) giving **132a** (15 mg, 8%) and **137a** (25 mg, 13%).

(S)-3-((2E,4E)-5-(4-methoxyphenyl)penta-2,4-dien-1-yl)-2-methyl-4-oxocyclopent-2-en-1-yl (1R,3R)-2,2-dimethyl-3-(2-methylprop-1-en-1-yl)cyclopropane-1-carboxylate **132a**

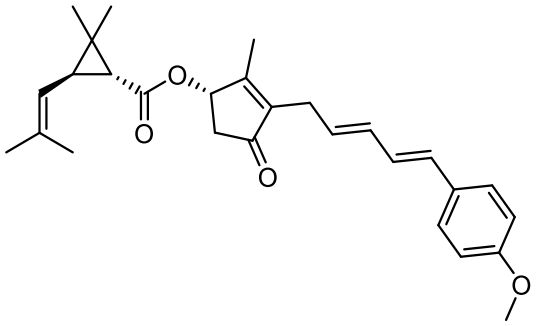

^{1}H NMR (600 MHz, $CDCl_3$) δ 7.29 (2H, d, *J* = 8.7 Hz), 6.83 (2H, d, *J* = 8.7 Hz), 6.58 (1H, dd, *J* = 10.3, 15.6 Hz), 6.41 (1H, d, *J* = 15.6 Hz), 6.19 (1H, dd, *J* = 10.3, 15.1 Hz), 5.68 (2H, m), 4.90 (1H, d, *J* = 7.6 Hz), 3.79 (3H, s), 3.06 (2H, d, *J* = 6.8 Hz), 2.88 (1H, dd, *J* = 6.3, 18.7 Hz), 2.25 (1H, dd, *J* = 1.6, 18.7 Hz), 2.09 (1H, m), 2.05 (3H, s), 1.72 (3H, s), 1.71 (3H, s), 1.41 (1H, d, *J* = 5.3 Hz), 1.26 (3H, s), 1.14 (3H, s); ^{13}C NMR (150 MHz, $CDCl_3$) δ 203.9, 172.3, 165.6, 159.1, 141.7, 135.9, 132.1, 130.9, 130.2, 128.4, 127.4, 126.6, 120.8, 114.1, 73.0, 55.3, 42.1, 34.6, 33.0, 29.2, 26.3, 25.6, 22.1, 20.4, 18.5, 14.1. FTIR ($\bar{\nu}$): 2927, 1713, 1656, 1604, 1510, 1442, 1421, 1381, 1282, 1251, 1193, 1152, 1116, 1033, 989, 828, 760. HRMS calculated for $C_{28}H_{35}O_4$ $[M+H]^+$: 435.2530; observed: 435.2527. $[\alpha]_D^{20} = -26.7$ (c = 0.2, $CHCl_3$).

(S)-3-((1E,3E)-5-(4-methoxyphenyl)penta-1,3-dien-1-yl)-2-methyl-4-oxocyclopent-2-en-1-yl (1R,3R)-2,2-dimethyl-3-(2-methylprop-1-en-1-yl)cyclopropane-1-carboxylate **137a**

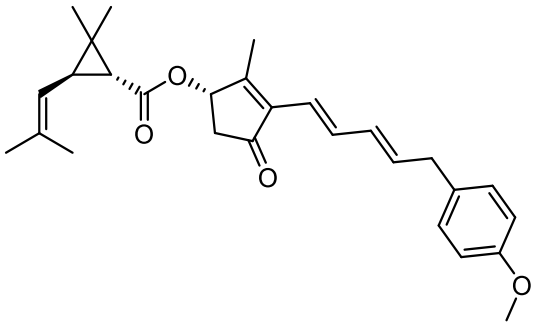

^{1}H NMR (600 MHz, $CDCl_3$) δ 7.38 (1H, dd, *J* = 10.3, 15.7 Hz), 7.09 (2H, d, *J* = 8.5 Hz), 6.84 (2H, d, *J* = 8.5 Hz), 6.10 (2H, m), 6.03 (1H, m), 5.67 (1H, d, *J* = 6.3 Hz), 4.90 (1H, d, *J* = 7.6 Hz), 3.79

(3H, s), 3.41 (2H, d, *J* = 6.5 Hz), 2.90 (1H, dd, *J* = 6.3, 18.7 Hz), 2.28 (1H, dd, *J* = 2.0, 18.7 Hz), 2.08 (4H, m), 1.72 (3H, s), 1.71 (3H, s), 1.40 (1H, d, *J* = 5.4 Hz), 1.26 (3H, s), 1.14 (3H, s); ^{13}C NMR (150 MHz, $CDCl_3$) δ 203.2, 172.3, 163.6, 158.1, 137.7, 136.9, 135.9, 135.7, 131.9, 131.8, 129.6, 120.8, 118.6, 113.9, 72.5, 55.3, 42.7, 38.3, 34.6, 33.0, 29.1, 25.5, 22.1, 20.4, 18.5, 14.2. FTIR ($\bar{\nu}$): 2927, 1714, 1611, 1584, 1511, 1421, 1380,1300, 1282, 1246, 1193, 1152, 1114, 1082, 995, 846, 819. HRMS calculated for $C_{28}H_{35}O_4$ $[M+H]^+$: 435.2530; observed: 435.2537. $[\alpha]_D^{20}$= −112.0 (c = 0.3, $CHCl_3$).

4-iodoanisole and pyrethrin II

Prepared as per general procedure using pyrethrin II **5b** (150 mg, 0.40 mmol), silver acetate (100 mg, 0.6 mmol), triphenylphosphine (9 mg, 0.03 mmol), palladium acetate (3 mg, 0.01 mmol) and 4-iodoanisole (112 mg, 0.48 mmol) in dry acetonitrile (5 mL). The resulting mixture was purified by column chromatography (20% ethyl acetate in hexane) giving **132b** (24 mg, 13%) and **137b** (28 mg, 15%).

(S)-3-((2E,4E)-5-(4-methoxyphenyl)penta-2,4-dien-1-yl)-2-methyl-4-oxocyclopent-2-en-1-yl (1R,3R)-3-((E)-3-methoxy-2-methyl-3-oxoprop-1-en-1-yl)-2,2-dimethylcyclopropane-1-carboxylate **132b**

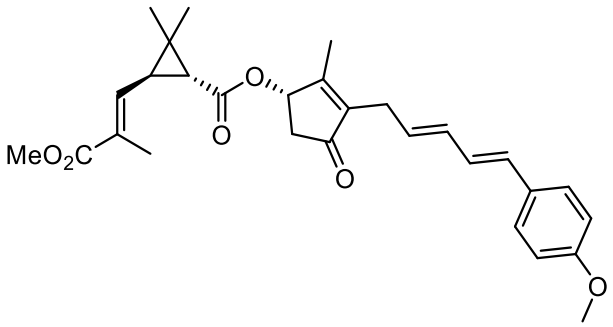

^{1}H NMR (600 MHz, $CDCl_3$) δ 7.28 (2H, d, *J* = 8.5 Hz), 6.83 (2H, d, *J* = 8.5 Hz), 6.57 (1H, dd, *J* = 10.4, 15.6 Hz), 6.46 (1H, d, *J* = 9.7 Hz), 6.42 (1H, d, *J* = 15.6 Hz), 6.19 (1H, dd, *J* = 10.4, 15.2 Hz), 5.68 (2H, m), 3.79 (3H, s), 3.73 (3H, s), 3.07 (2H, d, *J* = 6.7 Hz), 2.89 (1H, dd, *J* = 6.2, 18.7 Hz), 2.23 (2H, m), 2.05 (3H, s), 1.94 (3H, s), 1.75 (1H, d, *J* = 5.2 Hz), 1.31 (3H, s), 1.24 (3H, s); ^{13}C NMR (150 MHz, $CDCl_3$) δ 203.6, 171.2, 168.1, 165.2, 159.1, 142.0, 139.0, 132.2, 130.9, 129.8, 128.2, 127.4, 126.6, 114.1, 73.4, 55.3, 51.8, 42.0, 35.8, 32.9, 30.6, 26.3, 22.3, 20.4, 14.1, 12.9. FTIR ($\bar{\nu}$): 2951, 1712, 1646, 1605, 1510, 1436, 1383, 1252, 1222, 1175, 1149, 1112, 1034, 991,

828, 761. HRMS calculated for $C_{29}H_{35}O_6$ $[M+H]^+$: 479.2428; observed: 479.2442. $[\alpha]_D^{20}$= −29.2 (c = 0.2, $CHCl_3$).

(S)-3-((1E,3E)-5-(4-methoxyphenyl)penta-1,3-dien-1-yl)-2-methyl-4-oxocyclopent-2-en-1-yl (1R,3R)-3-((E)-3-methoxy-2-methyl-3-oxoprop-1-en-1-yl)-2,2-dimethylcyclopropane-1-carboxylate **137b**

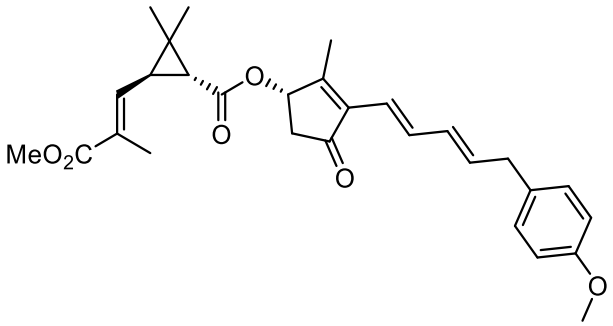

^{1}H NMR (600 MHz, $CDCl_3$) δ 7.39 (1H, dd, *J* = 10.2, 15.6 Hz), 7.10 (2H, d, *J* = 8.5 Hz), 6.84 (2H, d, *J* = 8.5 Hz), 6.46 (1H, d, *J* = 9.5 Hz), 6.09 (3H, m), 5.67 (1H, d, *J* = 6.4 Hz), 3.79 (3H, s), 3.74 (3H, s), 3.41 (2H, d, *J* = 6.5 Hz), 2.91 (1H, dd, *J* = 6.4, 18.7 Hz), 2.26 (1H, dd, *J* = 1.9, 18.7 Hz), 2.22 (1H, m), 2.08 (3H, s), 1.95 (3H, s), 1.74 (1H, d, *J* = 5.3 Hz), 1.31 (3H, s), 1.23 (3H, s); ^{13}C NMR (150 MHz, $CDCl_3$) δ 202.9, 171.2, 163.0, 158.1, 139.0, 137.8, 137.1, 135.9, 131.8, 131.7, 129.8, 129.6, 118.5, 113.9, 73.0, 55.3, 51.8, 42.7, 38.3, 35.8, 32.9, 30.5, 22.3, 20.4, 14.2, 12.9. FTIR ($\bar{\nu}$): 2951, 1641, 1610, 1511, 1435, 1385, 1247, 1222, 1148, 1112, 996, 828. HRMS calculated for $C_{29}H_{35}O_6$ $[M+H]^+$: 479.2428; observed: 479.2442. $[\alpha]_D^{20}$= −90.0 (c = 0.2, $CHCl_3$).

3-iodoanisole and pyrethrin I

Prepared as per general procedure using pyrethrin I **5a** (150 mg, 0.46 mmol), silver acetate (117 mg, 0.70 mmol), triphenylphosphine (9 mg, 0.03 mmol), palladium acetate (3 mg, 0.01 mmol) and 3-iodoanisole (129 mg, 0.55 mmol) in dry acetonitrile (5 mL). The resulting mixture was purified by column chromatography (10% ethyl acetate in hexane) giving **133a** (16 mg, 8%) and **138a** (36 mg, 18%).

(S)-3-((2E,4E)-5-(3-methoxyphenyl)penta-2,4-dien-1-yl)-2-methyl-4-oxocyclopent-2-en-1-yl (1R,3R)-2,2-dimethyl-3-(2-methylprop-1-en-1-yl)cyclopropane-1-carboxylate **133a**

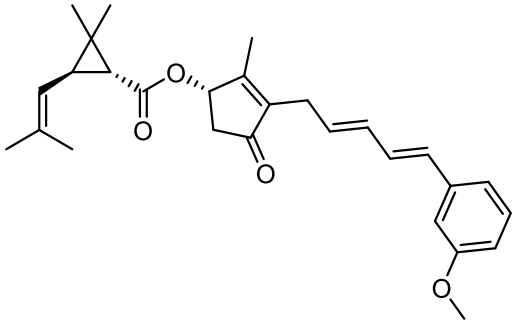

^{1}H NMR (600 MHz, $CDCl_3$) δ 7.20 (1H, dd, *J* = 7.7, 8.2 Hz), 6.95 (1H, d, *J* = 7.7 Hz), 6.88 (1H, brs), 6.75 (1H, dd, *J* = 2.5, 8.2 Hz), 6.69 (1H, dd, *J* = 10.4, 15.7 Hz), 6.43 (1H, d, *J* = 15.7 Hz), 6.20 (1H, dd, *J* = 10.4, 15.1 Hz), 5.76 (1H, dt, *J* = 6.8, 15.1 Hz), 5.69 (1H, d, *J* = 6.2 Hz), 4.90 (1H, d, *J* = 7.7 Hz), 3.80 (3H, s), 3.07 (2H, d, *J* = 6.9 Hz), 2.88 (1H, dd, *J* = 6.2, 18.7 Hz), 2.26 (1H, dd, *J* = 1.7, 18.7 Hz), 2.09 (1H, m), 2.05 (3H, s), 1.72 (3H, s), 1.71 (3H, s), 1.42 (1H, d, *J* = 5.5 Hz), 1.26 (3H, s), 1.14 (3H, s); ^{13}C NMR (150 MHz, $CDCl_3$) δ 203.9, 172.3, 165.8, 159.8, 141.5, 138.8, 135.9, 131.8, 131.2, 129.8, 129.5, 128.9, 120.8, 119.0, 113.1, 111.4, 72.9, 55.2, 42.1, 34.5, 33.0, 29.2, 26.3, 25.5, 22.1, 20.4, 18.5, 14.1. FTIR ($\bar{\nu}$): 2952, 1713, 1655, 1596, 1577, 1488, 1433, 1380, 1263, 1193, 1154, 1114, 1044, 990, 849, 777, 688. HRMS calculated for $C_{28}H_{35}O_4$ $[M+H]^+$: 435.2530; observed: 435.2544. $[\alpha]_D^{20} = -120.0$ (c = 0.2, $CHCl_3$).

(S)-3-((1E,3E)-5-(3-methoxyphenyl)penta-1,3-dien-1-yl)-2-methyl-4-oxocyclopent-2-en-1-yl (1R,3R)-2,2-dimethyl-3-(2-methylprop-1-en-1-yl)cyclopropane-1-carboxylate **138a**

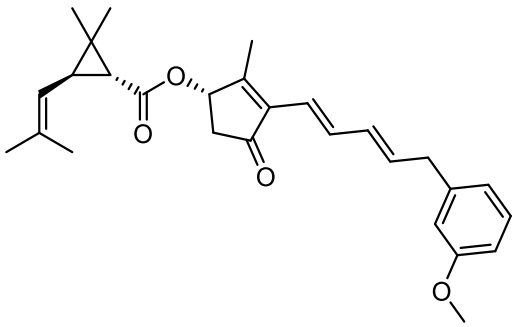

^{1}H NMR (600 MHz, $CDCl_3$) δ 7.38 (1H, dd, *J* = 10.5, 15.8 Hz), 7.21 (1H, dd, *J* = 7.7, 8.2 Hz), 6.76 (2H, m), 6.73 (1H, brs), 6.17 (2H, m), 6.05 (1H, m), 5.67 (1H, d, *J* = 6.4 Hz), 4.91 (1H, d, *J* = 7.7 Hz), 3.79 (3H, s), 3.45 (2H, d, *J* = 6.8 Hz), 2.90 (1H, dd, *J* = 6.4, 18.7 Hz), 2.27 (1H, dd, *J* = 2.2, 18.7 Hz), 2.09 (3H, s), 2.07 (1H, m), 1.72 (3H, s), 1.71 (3H, s), 1.40 (1H, d, *J* = 5.3 Hz), 1.26 (3H, s), 1.14 (3H, s); ^{13}C NMR (150 MHz, $CDCl_3$) δ 203.2, 172.3, 163.7, 159.8, 141.4, 137.6, 136.1, 135.9, 135.6, 132.3, 129.4, 121.0, 120.8, 118.8, 114.3, 111.6, 72.5, 55.2, 42.7, 39.2, 34.6, 33.0,

29.1, 22.1, 20.4, 18.5, 14.2. FTIR ($\bar{\nu}$): 2926, 1714, 1600, 1585, 1489, 1435, 1379, 1281, 1258, 1235, 1193, 1152, 1114, 1049, 995, 850, 778, 695. HRMS calculated for $C_{28}H_{35}O_5$ $[M+H]^+$: 435.2530; observed: 435.2527. $[\alpha]_D^{20} = -125.7$ (c = 0.4, $CHCl_3$).

3-iodoanisole and pyrethrin II

Prepared as per general procedure using pyrethrin II **5b** (150 mg, 0.40 mmol), silver acetate (100 mg, 0.6 mmol), triphenylphosphine (9 mg, 0.03 mmol), palladium acetate (3 mg, 0.01 mmol) and 3-iodoanisole (112 mg, 0.48 mmol) in dry acetonitrile (5 mL). The resulting mixture was purified by column chromatography (20% ethyl acetate in hexane) giving **133b** (17 mg, 7%) and **138b** (26 mg, 13%).

(S)-3-((2E,4E)-5-(3-methoxyphenyl)penta-2,4-dien-1-yl)-2-methyl-4-oxocyclopent-2-en-1-yl (1R,3R)-3-((E)-3-methoxy-2-methyl-3-oxoprop-1-en-1-yl)-2,2-dimethylcyclopropane-1-carboxylate **133b**

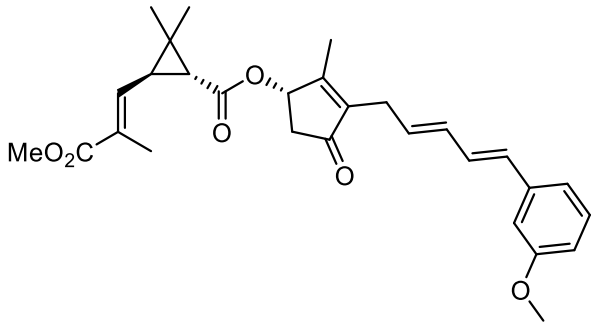

^{1}H NMR (600 MHz, $CDCl_3$) δ 7.14 (1H, dd, *J* = 7.6, 8.1 Hz), 6.89 (1H, d, *J* = 7.6 Hz), 6.82 (1H, brs), 6.70 (1H, dd, *J* = 2.2, 8.1 Hz), 6.63 (1H, dd, *J* = 10.4, 15.6 Hz), 6.38 (2H, m), 6.14 (1H, dd, *J* = 10.4, 15.1 Hz), 5.68 (1H, dt, *J* = 15.1, 6.8 Hz), 5.61 (1H, d, *J* = 6.4 Hz), 3.74 (3H, s), 3.66 (3H, s), 3.01 (2H, d, *J* = 6.8 Hz), 2.83 (1H, dd, *J* = 6.4, 18.8 Hz), 2.16 (2H, m), 1.99 (3H, s), 1.88 (3H, s), 1.69 (1H, d, *J* = 5.2 Hz), 1.24 (3H, s), 1.17 (3H, s); ^{13}C NMR (150 MHz, $CDCl_3$) δ 203.6, 171.2, 168.1, 165.3, 159.8, 141.8, 139.0, 131.9, 131.3, 129.7, 129.5, 128.9, 119.0, 113.1, 111.4, 73.4, 55.2, 51.8, 42.0, 35.8, 32.9, 30.6, 26.3, 22.3, 20.4, 14.1, 12.9. FTIR ($\bar{\nu}$): 2952, 1712, 1647, 1597, 1434, 1383, 1263, 1222, 1156, 1112, 1049, 991, 689. HRMS calculated for $C_{29}H_{35}O_6$ $[M+H]^+$: 479.2428; observed: 479.2443. $[\alpha]_D^{20} = -117.6$ (c = 0.2, $CHCl_3$).

(S)-3-((1E,3E)-5-(3-methoxyphenyl)penta-1,3-dien-1-yl)-2-methyl-4-oxocyclopent-2-en-1-yl (1R,3R)-3-((E)-3-methoxy-2-methyl-3-oxoprop-1-en-1-yl)-2,2-dimethylcyclopropane-1-carboxylate **138b**

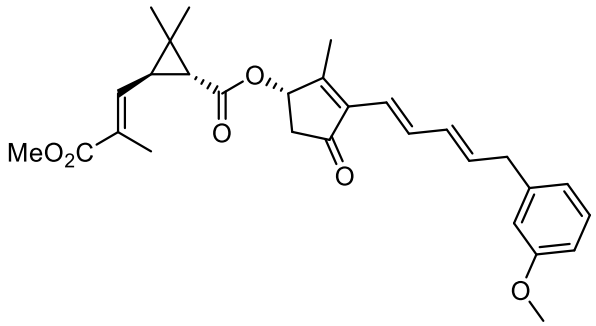

^{1}H NMR (600 MHz, $CDCl_3$) δ 7.32 (1H, dd, *J* = 10.4, 15.7 Hz), 7.14 (1H, dd, *J* = 7.7, 8.2 Hz), 6.70 (2H, m), 6.66 (1H, brs), 6.39 (1H, d, *J* = 9.4 Hz), 6.05 (2H, m), 5.98 (1H, m), 5.61 (1H, d, *J* = 6.4 Hz), 3.72 (3H, s), 3.66 (3H, s), 3.38 (2H, d, *J* = 6.7 Hz), 2.84 (1H, dd, *J* = 6.4, 18.7 Hz), 2.20 (1H, dd, *J* = 2.0, 18.7 Hz), 2.16 (1H, m), 2.02 (3H, s), 1.88 (3H, s), 1.68 (1H, d, *J* = 5.3 Hz), 1.24 (3H, s), 1.16 (3H, s); ^{13}C NMR (150 MHz, $CDCl_3$) δ 202.9, 171.2, 168.1, 159.7, 139.0, 137.8, 136.3, 135.8, 132.2, 129.7, 129.4, 121.0, 118.7, 114.3, 111.6, 73.0, 55.2, 51.8, 42.7, 39.2, 35.8, 32.9, 30.5, 22.3, 20.4, 14.2, 12.9. FTIR ($\bar{\nu}$): 2951, 1713, 1641, 1600, 1489, 1435, 1385, 1260, 1222, 1149, 1112, 1051, 995, 830, 761, 695. HRMS calculated for $C_{29}H_{35}O_4$ $[M+H]^+$: 479.2428; observed: 479.2447. $[\alpha]_D^{20}$= −134.8 (c = 0.2, $CHCl_3$).

4-iodobenzotrifluoride and pyrethrin I

Prepared as per general procedure using pyrethrin I **5a** (150 mg, 0.46 mmol), silver acetate (117 mg, 0.70 mmol), triphenylphosphine (9 mg, 0.03 mmol), palladium acetate (3 mg, 0.01 mmol) and 4-iodobenzotrifluoride (80 µL, 0.55 mmol) in dry acetonitrile (5 mL). The resulting mixture was purified by column chromatography (10% ethyl acetate in hexane) giving **134a** (27 mg, 13%)

(S)-2-methyl-4-oxo-3-((2E,4E)-5-(4-(trifluoromethyl)phenyl)penta-2,4-dien-1-yl)cyclopent-2-en-1-yl (1R,3R)-2,2-dimethyl-3-(2-methylprop-1-en-1-yl)cyclopropane-1-carboxylate **134a**

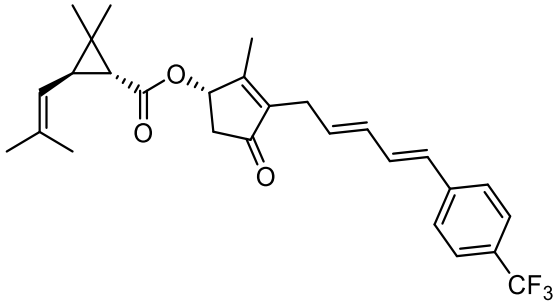

^{1}H NMR (600 MHz, $CDCl_3$) δ 7.53 (2H, d, *J* = 8.3 Hz), 7.43 (2H, d, *J* = 8.3 Hz), 6.77 (1H, dd, *J* = 10.5, 15.7 Hz), 6.47 (1H, d, *J* = 15.7 Hz), 6.22 (1H, dd, *J* = 10.5, 15.1 Hz), 5.83 (1H, dt, *J* =15.1, 6.8Hz), 5.68 (1H, d, *J* = 6.3 Hz), 4.90 (1H, d, *J* = 7.7 Hz), 3.08 (2H, d, *J* = 6.8 Hz), 2.89 (1H, dd, *J* = 6.3, 18.7 Hz), 2.26 (1H, dd, *J* = 1.7, 18.7 Hz), 2.09 (1H, m), 2.06 (3H, s), 1.72 (3H, s), 1.71 (3H, s), 1.41 (1H, d, *J* = 5.3 Hz), 1.26 (3H, s), 1.14 (3H, s); ^{13}C NMR (150 MHz, $CDCl_3$) δ 203.82, 172.30, 165.90, 141.29, 140.81, 135.97, 131.56, 131.47, 131.02, 129.70, 126.25, 125.54, 125.52, 120.77, 72.91, 42.06, 34.54, 33.04, 29.20, 26.37, 25.56, 22.11, 20.41, 18.50, 14.13. FTIR ($\bar{\nu}$): 2926, 1713, 1656, 1610, 1417, 1381, 1324, 1282, 1235, 1192, 1154, 1121, 1067, 1015, 989, 831. HRMS calculated for $C_{28}H_{32}F_3O_3$ $[M+H]^+$: 473.2298; observed: 473.2309. $[\alpha]_D^{20}$= −40.7 (c = 0.3, $CHCl_3$).

4-iodobenzotirfluoride and pyrethrin II

Prepared as per general procedure using pyrethrin II **5b** (150 mg, 0.40 mmol), silver acetate (100 mg, 0.6 mmol), triphenylphosphine (9 mg, 0.03 mmol), palladium acetate (3 mg, 0.01 mmol) and 4-iodobenzotrifluoride (70 µL, 0.48 mmol) in dry acetonitrile (5 mL). The resulting mixture was purified by column chromatography (20% ethyl acetate in hexane) giving **134b** (30 mg, 14%)

(S)-2-methyl-4-oxo-3-((2E,4E)-5-(4-(trifluoromethyl)phenyl)penta-2,4-dien-1-yl)cyclopent-2-en-1-yl (1R,3R)-3-((E)-3-methoxy-2-methyl-3-oxoprop-1-en-1-yl)-2,2-dimethylcyclopropane-1-carboxylate **134b**

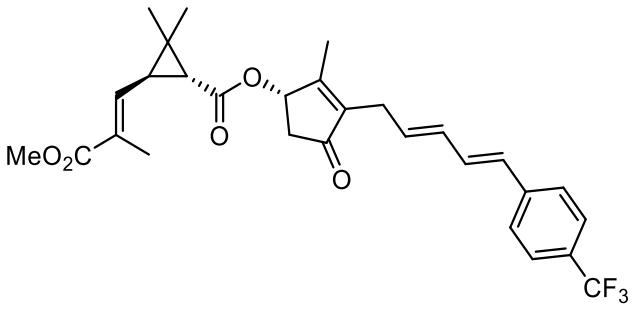

^{1}H NMR (600 MHz, $CDCl_3$) δ 7.54 (2H, d, *J* = 8.2 Hz), 7.44 (2H, d, *J* = 8.2 Hz), 6.78 (1H, dd, *J* = 10.4, 15.7 Hz), 6.47 (2H, m), 6.23 (1H, dd, *J* = 10.4, 15.1 Hz), 5.83 (1H, dt, *J* = 15.1, 6.9 Hz), 5.70 (1H, d, *J* = 6.3 Hz), 3.74 (3H, s), 3.09 (2H, d, *J* = 6.9 Hz), 2.90 (1H, dd, *J* = 6.3, 18.7 Hz), 2.24 (2H, m), 2.07 (3H, s), 1.95 (3H, s), 1.74 (1H, d, *J* = 5.2 Hz), 1.32 (3H, s), 1.25 (3H, s); ^{13}C NMR (150 MHz, $CDCl_3$) δ 203.54, 171.21, 168.11, 165.42, 141.55, 140.77, 138.92, 131.54, 131.39, 130.96, 129.81, 129.77, 126.26, 125.54, 125.51, 73.37, 51.83, 41.97, 35.75, 32.97, 30.61, 26.37, 22.32, 20.41, 14.11, 12.88. FTIR ($\bar{\nu}$): 2957, 2929, 1713, 1645, 1613, 1436, 1384, 1325, 1263, 1222, 1165, 1112, 1067, 991, 831, 760. HRMS calculated for $C_{29}H_{32}F_3O_5$ $[M+H]^+$: 517.2196; observed: 517.2203. $[\alpha]_D^{20}$= −8.0 (c = 0.3, $CHCl_3$).

7.2.4 Model compound

Dianion alkylation of ethyl acetoacetate **187**

Ethyl acetoacetate **187** (5.0 g, 38 mmol) was slowly added to a suspension of sodium hydride (2.1 g, 60 %wt in mineral oil, 52 mmol) in dry THF (30 mL) at −15 °C under an atmosphere of N_2. After 15 min, *n*-butyl lithium (16 mL, 2.5 M in hexanes, 40 mmol.) was slowly added at −78 °C and the mixture was left to stir for an additional 20 min. Propargyl bromide (4.6 mL, 80 % wt in toluene, 41.4 mmol.) was slowly added to the mixture with continued cooling and over 1.5 h the reaction mixture was allowed to warm to room temperature. The reaction was quenched with saturated ammonium chloride solution (20 mL), acidified with hydrochloric acid (1 M) and extracted with ethyl acetate. The ethyl acetate was washed with saturated sodium chloride solution. The organic fraction was dried (Na_2SO_4) and the solvent removed *in vacuo* yielding a dark brown liquid. The mixture was distilled by Kugelrohr short path distillation yielding **188** as a colourless liquid (110 °C at 0.8 mmHg) (4.98 g, 76%).

Ethyl 3-oxohept-6-ynoate **188**

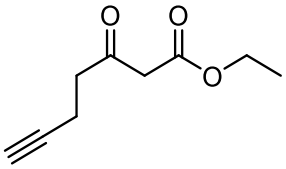

^{1}H NMR (600 MHz, $CDCl_3$) δ 4.20 (2H, q, *J* = 7.1 Hz), 3.46 (2H, s,), 2.81 (2H, t, *J* = 7.4 Hz), 2.47 (2H, td, *J* = 7.4, 2.6 Hz), 1.95 (1H, t, *J* = 2.6 Hz), 1.27 (3H, t, *J* = 7.1 Hz); ^{13}C NMR (150 MHz, $CDCl_3$) δ 200.7, 167.0, 82.6, 69.1, 61.6, 49.4, 41.7, 14.2, 13.0. FTIR ($\bar{\nu}$): 3287, 2984, 2934, 2120, 1739, 1715, 1410, 1367, 1316, 1190, 1083, 1031, 641. HRMS calculated for $C_9H_{13}O_3$ $[M+H]^+$: 169.0859, observed: 169.0854.

Altered decarboxylative aldol addition

Ethyl 3-oxohept-6-ynoate **188** (4.25 g, 25.3 mmol) was slowly added to a solution of sodium hydroxide (15 mL, 10 %wt) cooled over an ice bath. The reaction mixture was left for 6 h at room temperature before being cooled to 0 °C and acidified to pH 5 with hydrochloric acid (1 M). With continued cooling, sodium dithionite (0.9 g, 5.2 mmol) and toluene (15 mL) were added followed by the slow addition of methylglyoxal (6.0 g, 40 %wt in water, 33 mmol). After complete addition of the methylglyoxal solution, the mixture was allowed to warm to room temperature and was left to slowly stir overnight. The aqueous layer was saturated with sodium chloride and the toluene layer collected. The aqueous layer was extracted with ethyl acetate and the organic fractions combined. The combined organic extract was dried (Na_2SO_4) and the solvent removed *in vacuo* yielding a dark brown, viscous oil. Short path distillation by Kugelrohr under vacuum was used to remove the undesired by-product **184** (100 °C at 0.8 mmHg) leaving **174** a viscous orange liquid (2.5 g, 66%) which was used without further purification.

3-hydroxy-8-nonyne-2,5-dione **174**

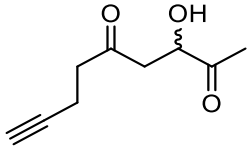

^{1}H NMR (600 MHz, $CDCl_3$) δ 4.36 (1H, dd, *J* = 3.8, 6.4 Hz), 2.97 (1H, dd, *J* = 3.8, 16.9 Hz), 2.84 (1H, dd, *J* = 6.4, 16.9 Hz), 2.73 (2H, t, *J* = 7.1 Hz), 2.45 (2H, td, *J* =7.1, 2.6 Hz), 2.26 (3H, s), 1.95 (1H, t, *J* = 2.6 Hz); ^{13}C NMR (150 MHz, $CDCl_3$) δ 209.1, 207.0, 82.7, 73.8, 69.1, 45.5, 42.4, 25.5,

12.9. FTIR ($\bar{\nu}$): 3440, 3285, 2924, 2118, 1709, 1631, 1360, 1093, 639. HRMS calculated for $C_9H_{12}O_3$ $[M+H]^+$: 169.0859, observed: 169.0856.

Altered cyclisation by aldol condensation

3-hydroxy-8-nonyne-2,5-dione **174** (2.3 g, 14 mmol) was slowly added to a sodium hydroxide solution (15 mL, 10 %wt) and toluene (10 mL) over an ice-salt bath. The mixture was left to stir with continued cooling for 1.5 h before being acidified with concentrated hydrochloric acid (32%). The mixture was extracted with ethyl acetate and dried (Na_2SO_4). The solvent was removed *in vacuo* and the resulting viscous liquid was distilled under vacuum (150 °C at 0.8 mmHg) giving **175** as a yellow oil (1.47 g, 72%).

4-hydroxy-3-methyl-2-(2-propyn-1-yl)-2-cyclopenten-1-one **175**

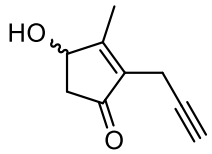

^{1}H NMR (600 MHz, $CDCl_3$) δ 4.74 (1H, brd, *J* = 6.1 Hz), 3.11 (2H, m), 2.80 (1H, dd, *J* = 6.1, 18.4 Hz), 2.30 (1H, dd, *J* = 1.9, 18.4 Hz), 2.22 (3H, s), 1.96 (1H, t, *J* = 2.7 Hz);^{13}C NMR (150 MHz, $CDCl_3$) δ 203.5, 170.8, 136.7, 79.8, 71.8, 69.0, 44.1, 14.0, 12.5. FTIR ($\bar{\nu}$): 3398, 3287, 2120, 1693, 1649, 1382, 1277, 1190, 1050, 1011, 943. HRMS calculated for $C_9H_{11}O_2$ $[M+H]^+$: 151.0754, observed: 151.0751.

Modified Sonogashira coupling chain extension

A solution of 4-hydroxy-3-methyl-2-(2-propyn-1-yl)-2-cyclopenten-1-one **175** (741 mg, 4.94 mmol) and triethylamine (2.5 mL, 18 mmol) in vinyl bromide solution (12 mL, 1.0 M in THF, 12 mmol) was deoxygenated with argon over 40 min. Under an atmosphere of argon, tetrakis(triphenylphosphine)palladium(0) (252 mg, 0.218 mmol, 5 mol.%) and copper(I) iodide (94 mg, 0.49 mmol, 10 mol.%) were added with stirring. The resulting mixture was left to stir at room temperature over 17 h. The mixture was poured over cooled hydrochloric acid (1 M) and extracted with ethyl acetate. The ethyl acetate solution was dried (Na_2SO_4) and

solvent removed *in vacuo* yielding a viscous, brown oil. The mixture was purified by silica gel plug (DCM → DCM:EtOAc (1:1) → EtOAc) yielding **155** as an amber oil (537 mg, 62%).

4-hydroxy-3-methyl-2-(4-penten-2-yn-1-yl)- 2-cyclopenten-1-one **155**

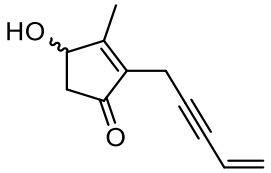

^{1}H NMR (600 MHz, $CDCl_3$) δ 5.73 (1H, ddt, *J* = 17.5, 11.1, 2.2 Hz), 5.55 (1H, dd, *J* = 2.2, 17.5 Hz), 5.39 (1H, dd, *J* = 2.2, 11.1 Hz), 4.75 (1H, brd, *J* = 6.2 Hz), 3.24 (2H, m), 2.82 (1H, dd, *J* = 6.2, 18.4 Hz), 2.30 (1H, dd, *J* = 2.0, 18.4 Hz), 2.22 (3H, s); ^{13}C NMR (150 MHz, $CDCl_3$) δ 203.4, 170.3, 137.2, 126.5, 117.3, 86.1, 79.8, 71.9, 44.2, 14.0, 13.4. FTIR ($\bar{\nu}$): 3406, 2920, 1701, 1651, 1382, 1052. HRMS calculated for $C_{11}H_{13}O_2$ $[M+H]^+$: 177.0910, observed: 177.0910.

Alkyne semi-reduction

Activated zinc (330 mg, 5.04 mmol) was added to a mixture of 4-hydroxy-3-methyl-2-(4-penten-2-yn-1-yl)- 2-cyclopenten-1-one **155** (600 mg, 3.41 mmol) in *n*-propanol:water (1:1, 10 mL). The resulting suspension was refluxed for 1.5 h and filtered to remove residual zinc. The mixture was diluted with water (10 mL) and extracted with ethyl acetate. The ethyl acetate was dried (Na_2SO_4) and solvent was removed *in vacuo* giving (*Z*)-pyrethrolone **21** as a mixture with starting material and over-reduction products (550 mg, 11% by ^{1}H NMR). Characterisation was undertaken on the isolated mixture with signals assigned to (*Z*)-pyrethrolone **21** by comparison to literature spectroscopic data.[13]

(*Z*)-*Pyrethrolone* **21**

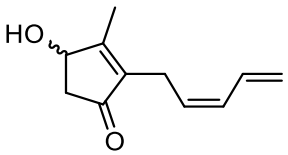

^{1}H NMR (600 MHz, $CDCl_3$) δ 6.75 (1H, ddd*, *J* = 10.1, 10.7, 16.8 Hz), 6.03 (1H, m), 5.36 (1H, m), 5.22 (1H, d, *J* = 16.8 Hz), 5.16 (1H, d, *J* = 10.1 Hz), 4.74 (1H, brs), 3.09 (2H, d, *J* = 7.8 Hz), 2.79 (1H, dd, *J* = 6.1, 18.2 Hz), 2.29 (1H, dd, *J* = 2.2, 18.2 Hz), 2.09 (3H, s); ^{13}C NMR (150 MHz, $CDCl_3$) δ 203.4, 170.4, 140.4, 131.8, 130.3, 127.3, 118.3, 71.9, 44.4, 21.8, 13.9.

7.3 References

1. Bramwell, A. F.; Crombie, L.; Hemesley, P.; Pattenden, G., Nuclear Magnetic Resonance Spectra of the Natural Pyrethrins and Related Compounds. *Tetrahedron* **1969,** *25*, 1727-1741.
2. Wang, I.-H.; Subramanian, V.; Moorman, R.; Burleson, J.; Ko, J., Direct determination of pyrethrins in pyrethrum extracts by reversed-phase high-performance liquid chromatography with diode-array detection. *J. Chromatogr. A* **1997,** *766*, 277-281.
3. *Spartan '16 for Windows*, Wavefunction Inc.: 18401 Von In Karman Avenue, Suite 370, Irvine, CA 92612 U.S.A.
4. Bagnall, N. H.; Hines, B. M.; Lucke, A. J.; Gupta, P. K.; Reid, R. C.; Fairlie, D. P.; Kotze, A. C., Insecticidal activities of histone deacetylase inhibitors against a dipteran parasite of sheep, *Lucilia cuprina*. *Int. J. Paristol. Drugs Drug Resist.* **2017,** *7*, 51-60.
5. Kotze, A. C.; Bagnall, N. H.; Ruffell, A. P.; Pearson, R., Cloning, recombinant expression and inhibitor profiles of dihydrofolate reductase from the Australian sheep blow fly, *Lucilia cuprina*. *Med. Vet. Entomol.* **2014,** *28* (3), 297-306.
6. Li, C.; Ge, H.; Yin, B.; She, M.; Liu, P.; Li, X.; Li, J., Novel 3,6-unsymmetrically disubstituted-1,2,4,5-tetrazines S-induced one-pot synthesis, properties and theoretical study. *RSC Adv.* **2015,** *5*, 12277-12286.
7. Haddadin, M. J.; Zadeh, E. H. G., A novel method for the synthesis of 3,5-disubstituted-(NH)-1,2,4-triazoles from 3,6-diaryl-1,2,4,5-tetrazines. *Tetrahedron Lett.* **2010,** *51* (13), 1654-1656.
8. Bakkali, H.; Marie, C.; Ly, A.; Thobie-Gautier, C.; Graton, J.; Pipelier, M.; Sengmany, S.; Leonel, E.; Nedelec, J.-Y.; Evain, M.; Dubreuil, D., Funtionalized 2,5-Dipyridinylpyrroles by Electrochemical Reduction of 3,6-Dipyridinylpyridazine Precursors. *Eur. J. Org. Chem* **2008,** *2008* (12), 2156-2166.
9. Coburn, M. D.; Buntain, G. A.; Harris, B. W.; Hiskey, M. A.; Lee, K. Y.; Ott, D. G., An Improved Synthesis of 3,6-Diamino-1,2,4,5-tetrazine. II. From Triaminoguanidine and 2,4-Pentanedione. *J. Heterocyclic Chem.* **1991,** *28*, 2049-2050.
10. Gong, Y.-H.; Miomandre, F.; Meallet-Renault, R.; Badre, S.; Galmiche, L.; Tang, J.; Audebert, P.; Clavier, G., Synthesis and Physical Chemistry of *s*-Tetrazines: Which Ones are Fluorescent and Why? *Eur. J. Org. Chem* **2009,** *2009* (35), 6121-6128.

11. Rao, B. V.; Dhokale, S.; Rajamohanan, P. R.; Hotha, S., A tetrazine templated method for the synthesis of ternary conjugates. *Chem. Commun.* **2013,** *49* (92), 10808-10810.
12. Bagge, R. E.; Mauldin, T. C.; Boday, D. J.; Kobilka, B. M.; Loy, D. A., Transforming Polybutadiene with Tetrazine Click Chemistry into Antioxidant Foams That Fluoresce with Oxidation. *Chem. Mater.* **2017,** *29* (18), 7953-7960.
13. Matsuo, N.; Takagaki, T.; Watanabe, K.; Ohno, N., The First Practical Synthesis of (S)-Pyrethrolone, an Alcohol Moiety of Natural Pyrethrins I and II. *Biosci. Biotech. Biochem.* **1993,** *57* (4), 693-694.